RELIABILITY ASPECTS OF RELEVATION TRANSFORMS WITH SPECIAL EMPHASIS TO EXTREME MODELS

Thesis submitted to the University of Calicut

for the award of the degree of

DOCTOR OF PHILOSOPHY

IN

STATISTICS

under the Faculty of Science

by

ANAND. R

under the guidance of

Prof. (Dr.) C. CHANDRAN

and

Dr. DILEEPKUMAR. M

DEPARTMENT OF STATISTICS

UNIVERSITY OF CALICUT

KERALA - 673 635

INDIA

MAY 2026

DEPARTMENT OF STATISTICS

UNIVERSITY OF CALICUT

.....

CERTIFICATE

I hereby certify that the thesis entitled **"Reliability Aspects of Relevation Transforms with Special Emphasis to Extreme Models"** is a bona fide record of the research work carried out by **Mr. Anand R.**, Research Scholar, Department of Statistics, University of Calicut, under my supervision and guidance for the award of the degree of Doctor of Philosophy in Statistics of the University of Calicut. The work reported in this thesis does not form part of any other thesis or dissertation submitted previously for the award of any degree or diploma of any university or institution. It is also certified that the contents of this thesis have been checked using an anti-plagiarism database, and no unacceptable similarity has been detected.

University of Calicut

Date: 6/4/26

Dr. Dileepkumar M

Co-guide

Dr. DILEEP KUMAR M
Assistant Professor
Dept. of Statistics
University of Calicut
Calicut University P.O., 673 635

Prof. (Dr.) C. Chandran

Supervising Guide

Dr. C CHANDRAN
Professor (Retd)
Dept. of Statistics
University of Calicut, Kerala, India- 673 635

DECLARATION

I, Anand R., hereby declare that the thesis entitled **"Reliability Aspects of Relevation Transforms with Special Emphasis to Extreme Models"**, submitted to the University of Calicut for the award of the degree of Doctor of Philosophy in Statistics, is a bona fide record of the research work carried out by me under the guidance and supervision of Dr. C. Chandran, Senior Professor (Retd.), and Dr. Dileepkumar M., Assistant Professor, Department of Statistics, University of Calicut. The contents of this thesis have been subjected to plagiarism checking using *iThenticate* software at the C. H. M. K. Library, University of Calicut, and the similarity index has been found to be within the permissible limits. I further declare that this thesis does not contain any AI-generated content.

Anand. R

University of Calicut

Date: 6/4/26

Dr. Dileepkumar. M

Co-guide

Dr. DILEEP KUMAR M
Assistant Professor
Dept. of Statistics
University of Calicut
Calicut University P.O., 673 635

Prof. (Dr.) C. Chandran

Supervising Guide

Dr. C CHANDRAN
Professor (Retd)
Dept. of Statistics
University of Calicut, Kerala, India- 673 635

DEPARTMENT OF STATISTICS

UNIVERSITY OF CALICUT

.....

CERTIFICATE

Certified that no corrections/suggestions were recommended by the adjudicators of the Ph.D. thesis entitled **"Reliability Aspects of Relevation Transforms with Special Emphasis to Extreme Models"** submitted by **Mr. Anand R**, Research Scholar, Department of Statistics, University of Calicut, under my supervision and guidance, and that the contents in the thesis and the soft copy are one and the same.

University of Calicut

Date: 3/9/26

Dr. Dileepkumar M
Co-guide

Dr. DILEEP KUMAR M
Assistant Professor
Dept. of Statistics
University of Calicut
Calicut University P.O., 673 635

Prof. (Dr.) C. Chandran
Supervising Guide

Dr. C CHANDRAN
Professor (Retd)
Dept. of Statistics
University of Calicut, Kerala, India- 673 635

UNIVERSITY OF CALICUT

CERTIFICATE ON PLAGIARISM CHECK

1.	Name of the Research Scholar	ANAND R	
2.	Title of thesis / dissertation	RELIABILITY ASPECTS OF RELEVATION TRANSFORMS WITH SPECIAL EMPHASIS TO EXTREME MODELS	
3.	Name of the Supervisor	Prof. (Dr.). C. Chandran Dr. Dileepkumar. M	
4.	Department/Institution	Research Scholar, Department of Statistics, University of Calicut	
5.	Similar content (%) identified	Non Core **Introduction/ Theoretical overview/Review of literature/ Materials & Methods/ Methodology**	Core **Analysis/Result/Discussion / Summary/Conclusion/ Recommendations**
		8	**6**
	Acceptable maximum limit (%)	10	10
6.	Software used	iThenticate	
7.	Date of verification	04.04.2026	

Report on plagiarism check, specifying included/excluded items with % of similarity to be attached.

U.H. MOHAMMED KOYA LIBRARY P.O. CALICUT UNIVERSITY UNIVERSITY OF CALICUT

SEEMA M.V.
Assistant Librarian
University of Calicut
Malappuram - 673 635

Checked by (with name , designation & signature) Seema

Name and signature of the Researcher Anand. R

Name and signature of the Supervisor. 04/04/2026.

6/4/26

Dr. DILEEP KUMAR M
Assistant Professor
Dept. of Statistics
University of Calicut
Calicut University P.O., 673 635

The Doctoral Committee* has verified the report on plagiarism check with the contents of the thesis, as summarized above and appropriate measures have been taken to ensure originality of the Research accomplished herein.

DR. C CHANDRAN
Professor (Retd)
Dept. of Statistics
University of Calicut, Kerala, India- 673 635

Name & Signature of the HoD/~~HoI~~ (Chairperson of the Doctoral Committee)

06.04.2026

Dr. Krishnarani SD

THE HEAD
DEPARTMENT OF STATISTICS
UNIVERSITY OF CALICUT
KERALA - 673 635

DEPARTMENT OF STATISTICS * KERALA - 673635 *

**In case of languages like Malayalam, Tamil etc..on which no software is available for plagiarism check, a manual check shall be made by the Doctoral Committee, for which an additional certificate has to be attached.*

Acknowledgments

First and foremost, I would like to express my sincere and heartfelt gratitude to my supervising guide, Dr. C. Chandran, Senior Professor (Retd.), Department of Statistics, University of Calicut, for his profound knowledge, insightful direction, and unwavering support that have played a pivotal role in the successful completion of this work. I am deeply thankful for his patience, constructive feedback, and for instilling in me a disciplined and rigorous approach to research.

Words fall short in expressing my deepest gratitude to my co-guide, Dr. Dileepkumar M., Assistant Professor, Department of Statistics, University of Calicut. His unwavering faith in my abilities, remarkable willingness to be available at any time, and his invaluable role in shaping not only my understanding of the subject but also my perspective on life have been truly inspiring.

I extend my sincere thanks to Dr. Krishnarani. S. D, Head of the Department; Dr. Manoharan. M, Senior Professor (Retd.); Dr. Jayakumar. K, Senior Professor (Retd.); the guest faculties, and the non-teaching staffs of the Department.

I owe my deepest gratitude to Dr. N. Unnikrishnan Nair, Former Vice Chancellor, CUSAT, whose inspiring guidance and suggestions throughout the course of this work have been instrumental in shaping this thesis in its present form.

I also express my sincere gratitude to my teacher, Dr. P. G. Sankaran, Former Vice Chancellor, CUSAT, for his insightful contributions that have significantly enhanced the quality of this thesis.

I would like to thank Dr. Muhammed Anvar. P, Head of the Department, Department of Statistical Sciences, Kannur University for taking me in as a research scholar under the ASPIRE research award.

I wish to express my deep respect and gratitude to my former teachers, Mrs. Sudha Nath, Mr. Shajeeb Usman and Mr. Sasi Kumar whose early guidance laid the foundation for my passion for research.

I would like to express my sincere gratitude to all my friends and fellow research scholars in my department for their valuable discussions and continuous support throughout this journey. I also extend my heartfelt thanks to the families of Chandran Sir and Dileep Sir for their warmth, affection, and care.

I am forever grateful to my family for their invaluable support, without which this research could not have been completed. I also wish to remember with love and gratitude my grandparents, Ammuma and Thathi, whose unconditional love continues to be a source of strength and inspiration.

A heartfelt thanks to my childhood friend and life partner, Greeshma, my constant companion, for always being there for me. Your have been my greatest source of strength throughout this journey. I am also deeply grateful for your valuable contribution as a co-author in my work, which has added meaningfulness to the thesis.

Last but not the least, I express my sincere thanks to science itself for continually inspiring curiosity, discovery, and the enduring pursuit of knowledge.

Abstract

This thesis investigates the reliability properties and theoretical developments of the relevation and reversed relevation transforms, with emphasis on their applications in reliability theory and extreme value analysis. The study examines these transforms under modified proportional hazards and proportional reversed hazards frameworks, analyzing their aging characteristics, stochastic ordering properties, and characterization results. It introduces multi-phase auto-relevation and reversed auto-relevation transforms, establishing their connections with stochastic processes such as the non-homogeneous Poisson process. Several new distributional models, including generalizations of the exponential, log-logistic, Fréchet, and half-logistic distributions, are developed and analyzed in terms of reliability behavior, tail properties, and applicability to both complete and censored data. The work further incorporates quantile-based formulations and information measures to provide deeper structural insights, with applications in risk assessment and stress–strength reliability analysis using real data. In the context of extreme value theory, the truncated generalized extreme value distribution and its reversed auto-relevation version are studied. Parameter estimation of the generalized extreme value distribution is addressed through regression-based methods, supported by a review of existing techniques and the construction of bootstrap confidence intervals, with performance evaluated via simulation studies. Overall, the thesis provides a comprehensive framework for relevation transform based reliability modeling, combining theoretical advancements with practical applicability.

Keywords: Relevation transform, Reversed relevation transform, Reliability analysis, Aging properties, Stochastic orders, Extreme value distributions.

പഠനസംഗ്രഹം

ഈ പ്രബന്ധം, വിശ്വാസ്യതാ സിദ്ധാന്തത്തിലും അത്യന്ത മൂല്യ വിശകലനത്തിലും ഉള്ള അവയുടെ പ്രയോഗങ്ങളിൽ ഊന്നൽ നൽകിക്കൊണ്ട്, റെലിവേഷൻ പരിവർത്തനം, വിപരീത റെലിവേഷൻ പരിവർത്തനം എന്നിവയുടെ വിശ്വാസ്യതാ ഗുണങ്ങളെയും സൈദ്ധാന്തിക വികസനങ്ങളെയും അന്വേഷിക്കുന്നു. പരിഷ്കരിച്ച ആനുപാതിക അപകട ചട്ടക്കൂടുകളുടെയും ആനുപാതിക വിപരീത അപകട ചട്ടക്കൂടുകളുടെയും കീഴിൽ ഈ പരിവർത്തനങ്ങളുടെ സ്വഭാവം പരിശോധിച്ച്, അവയുടെ പ്രായമാകൽ സവിശേഷതകൾ, സ്റ്റോക്കാസ്റ്റിക് ക്രമീകരണ ഗുണങ്ങൾ, സ്വഭാവരൂപീകരണ ഫലങ്ങൾ എന്നിവയെ പഠനം വിശകലനം ചെയ്യുന്നു. മൾട്ടി- ഫേസ് സ്വയം-റെലിവേഷൻ പരിവർത്തനം, വിപരീത സ്വയം- റെലിവേഷൻ പരിവർത്തനം എന്നിവയെ പരിചയപ്പെടുത്തി, ഏകതാനമല്ലാത്ത പോയ്സ്സൺ പ്രക്രിയ പോലുള്ള സ്റ്റോക്കാസ്റ്റിക് പ്രക്രിയകളുമായുള്ള അവയുടെ ബന്ധങ്ങളെ ഈ പഠനം സ്ഥാപിക്കുന്നു. നിലവിൽ, എക്സ്പോണെൻഷ്യൽ, ലോഗ്-ലോജിസ്റ്റിക്, ഫ്രെഷെ, അർദ്ധ-ലോജിസ്റ്റിക് വിതരണങ്ങളുടെ സാമാന്യവൽക്കരണങ്ങൾ ഉൾപ്പെടെ നിരവധി പുതിയ വിതരണ മാതൃകകൾ വികസിപ്പിക്കപ്പെട്ടിട്ടുണ്ട്, വിശ്വാസ്യതാ സ്വഭാവം, വാൽ ഗുണങ്ങൾ, പൂർണ്ണവും സെൻസർ ചെയ്തതുമായ ഡാറ്റയ്ക്കുള്ള പ്രയോഗക്ഷമത എന്നിവയുടെ അടിസ്ഥാനത്തിൽ അവ വിശകലനം ചെയ്യപ്പെടുന്നും ഉണ്ട്. ഈ പഠനം, യഥാർത്ഥ ഡാറ്റ ഉപയോഗിച്ചുള്ള അപകടസാധ്യതാ വിലയിരുത്തലിലും സമ്മർദ്ദ–ശക്തി വിശ്വാസ്യതാ വിശകലനത്തിലും ഉള്ള പ്രയോഗങ്ങളോടൊപ്പം, ക്വാണ്ടൈൽ അധിഷ്ഠിത രൂപീകരണങ്ങളും വിവരമാനങ്ങളുമുപയോഗിച്ച് കൂടുതൽ ആഴത്തിലുള്ള ഘടനാപരമായ ഉൾക്കാഴ്ചകൾ കൂട്ടിച്ചേർക്കുന്നു. അത്യന്ത മൂല്യ സിദ്ധാന്തത്തിന്റെ പശ്ചാത്തലത്തിൽ, വെട്ടിച്ചുരുക്കിയ സാമാന്യവൽക്കരിച്ച അത്യന്ത മൂല്യ വിതരണത്തെയും അതിന്റെ വിപരീത സ്വയം-റെലിവേഷൻ പതിപ്പിനെയും പഠനവിധേയമാക്കുന്നു. സാമാന്യവത്കൃത അത്യന്തമൂല്യ വിതരണത്തിന്റെ പരാമീറ്റർ നിർണ്ണയം നിലവിലുള്ള സാങ്കേതിക വിദ്യകളുടെ അവലോകനവും ബൂട്ട്സ്ട്രാപ്പ് വിശ്വാസ ഇടവേളകളുടെ നിർമ്മിതിയും ഉൾക്കൊള്ളുന്ന റിഗ്രഷൻ അധിഷ്ഠിത രീതികളിലൂടെ അഭിസംബോധന ചെയ്യപ്പെടുന്നു; കൂടാതെ സിമുലേഷൻ പഠനങ്ങളിലൂടെ പ്രകടനം വിലയിരുത്തപ്പെടുന്നു. ആകെത്തുകയിൽ, ഈ പ്രബന്ധം സൈദ്ധാന്തിക പുരോഗതികളെ പ്രയോഗക്ഷമതയുമായി സംയോജിപ്പിച്ച്, റെലിവേഷൻ പരിവർത്തനാധിഷ്ഠിത വിശ്വാസ്യതാ മോഡലിംഗിനായി സമഗ്രമായ ഒരു ചട്ടക്കൂട് അവതരിപ്പിക്കുന്നു.

സൂചകപദങ്ങൾ: റെലിവേഷൻ പരിവർത്തനം, വിപരീത റെലിവേഷൻ പരിവർത്തനം, വിശ്വാസ്യത പഠനം, പ്രായാധീന സ്വഭാവ സവിശേഷതകൾ അത്യന്തമൂല്യ വിതരണങ്ങൾ

Contents

Acronyms **xix**

List of Figures **xxiii**

List of Tables **xxvii**

1 Introduction **1**

1.1 Overview of relevation transforms 2

1.2 Overview of extreme value theory 6

1.3 Motivation of the study 9

1.4 Objectives of the study 9

1.5 Significance of the study 10

1.6 Basic concepts 11

1.6.1 Reliability measures 12

1.6.2 Aging properties 17

1.6.3 Stochastic orders 18

1.6.4 Distortion function 19

1.6.5 Information measures 21

1.7 Statistical inference 23

1.8 Model selection criteria 24

1.9 Overview of the thesis 27

2 Modified proportional hazards relevation transform **29**

2.1 Introduction 29

2.2 Modified proportional hazards model 30
2.3 Censoring 32
2.4 Modified proportional hazards relevation transform 33
2.5 Aging properties 38
2.6 Stochastic orders 42
2.7 Modified proportional hazards relevated exponential distribution . 44
2.7.1 Parameter estimation 45
2.7.2 Simulation and real data applications for complete sample 48
2.7.3 Simulation and real data applications for censored sample 52
2.8 Modified proportional hazards relevated Weibull model 55
2.8.1 Parameter estimation 57
2.8.2 Real data analysis 57
2.9 Summary of the chapter 59

3 Multi-phase auto-relevation transform 61
3.1 Introduction 61
3.2 Auto-relevation transform 62
3.3 Multi-phase auto-relevation transform 64
3.4 Stochastic orders 71
3.5 Auto-relevation process 73
3.6 Models characterized by special properties 81
3.7 Summary of the chapter 88

4 Auto-relevated log-logistic distribution: Properties and applications 89
4.1 Introduction 89
4.2 Log-logistic distribution 90
4.3 Auto-relevated log-logistic model 92
4.4 Reliability properties 97
4.5 Parameter estimation 101
4.6 Simulation study 102
4.7 Tail behavior 103

4.8 Risk assessment measures of the ARLL distribution 108
4.8.1 Value at Risk 108
4.8.2 Tail Value at Risk 109
4.9 Real data analysis 111
4.9.1 Risk analysis 113
4.10 Summary of the chapter 116

5 Proportional reversed hazards reversed relevation transform 119
5.1 Introduction 119
5.2 Proportional reversed hazards model 120
5.3 Proportional reversed hazard reversed relevation transform 121
5.4 Reliability properties 124
5.5 Aging properties 127
5.6 Stochastic orders 129
5.7 Information measures 133
5.8 Quantile based representation 136
5.9 Applications based on Fréchet model 137
5.9.1 Parameter estimation 138
5.9.2 Real data analysis 139
5.10 Summary of the chapter 141

6 The reversed auto-relevation transform 143
6.1 Introduction 143
6.2 Reversed auto-relevation transform 144
6.2.1 Characterization based on truncated moments 151
6.2.2 Distorted representation 153
6.3 Aging properties 154
6.4 Stochastic orders 159
6.5 Stress-strength reliability 165
6.6 Quantile based properties 167
6.7 Entropy and inaccuracy measures 172
6.8 Applications based on truncated Gumbel model 179

6.8.1 Estimation of parameters . . . 181
6.8.2 Real data application . . . 182
6.9 Summary of the chapter . . . 183

7 Multi-phase reversed auto-relevation transform 185
7.1 Introduction . . . 185
7.2 Multi-phase RART . . . 186
7.3 Aging properties . . . 191
7.4 Stochastic orders . . . 200
7.5 Summary of the chapter . . . 203

8 RART based GEVD and parameter estimation 205
8.1 Truncated GEVD . . . 206
8.2 RART truncated GEVD . . . 208
8.3 Review of literature on parameter estimation of GEVD . . . 210
8.4 Estimation techniques . . . 211
8.4.1 Method of moments . . . 212
8.4.2 Maximum likelihood . . . 212
8.4.3 Probability weighted moments . . . 213
8.4.4 L-Moments . . . 214
8.4.5 Method of maximum product spacing . . . 215
8.5 Regression method of estimation for GEVD . . . 216
8.5.1 Regression method in truncated GEVD . . . 220
8.6 Bootstrap confidence interval . . . 221
8.7 Simulation study . . . 222
8.8 Real data analysis . . . 225
8.9 Summary of the chapter . . . 227

9 Conclusions and recommendations for future research 229
9.1 Summary of the thesis . . . 229
9.2 Future scope and recommendations . . . 230

Publications 233

Presentations **235**

Bibliography **237**

Acronyms

AD	Anderson-Darling
AI	aging intensity
ARLL	auto-relevated log-logistic
ART	auto-relevation transform
CDF	cumulative distribution function
CRE	cumulative residual entropy
CTE	cumulative Tsallis past entropy
CvM	Cramér-von Mises
DD	decreasing density
DHR	decreasing hazard rate
DHRA	decreasing hazard rate average
DLOR	decreasing log-odds rate
DLR	decreasing likelihood ratio
DMIT	decreasing mean inactivity time
DMRL	decreasing mean residual life
DRHR	decreasing reversed hazard rate
ECDF	empirical cumulative distribution function
EVT	extreme value theory
GEVD	generalized extreme value distribution
GMD	Gini's mean difference
GPD	generalized Pareto distribution
GRRP	generalized reversed relevated power

GRRT	generalied reversed relevation transform
ID	increasing density
IHR	increasing hazard rate
IHRA	increasing hazard rate average
ILOR	increasing log-odds rate
ILR	increasing likelihood ratio
IMIT	increasing mean inactivity time
IMRL	increasing mean residual life
IRHR	increasing reversed hazard rate
KL	Kullback-Leibler
KRI	key risk indicators
KS	Kolmogorov-Smirnov
LL	log-logistic
LM	l-moment
LMRQ	linear mean residual quantile
MIT	mean inactivity time
ML	maximum likelihood
MLE	maximum likelihood estimate
MLE-PL	MLE re-parametrized profile likelihood
MOM	method of moments
MOOP	mean of order P
MPHM	modified proportional hazards model
MPHRE	modified proportional hazards relevated exponential
MPHRT	modified proportional hazards relevation transform
MPHRW	modified proportional hazards relevated Weibull
MPRHM	modified proportional reversed hazards model
MPS	maximum product spacing
MRL	mean residual life
MSE	mean squared error
NBU	new better than used
NBUHR	new better than used hazard rate

NHPP	non-homogeneous Poisson process
NWU	new worse than used
NWUHR	new worse than used hazard rate
P-P plot	probability-probability plot
PHM	proportional hazards model
PHR	periodic hazard rate
POM	proportional odds model
PORT-VaR	peak over random threshold value-at-risk
PRHM	proportional reversed hazards model
PRHRR-F	proportional reversed hazards reversed relevated Fréchet
PRHRRT	proportional reversed hazards reversed relevation transform
PWM	probability weighted moment
Q-Q plot	quantile-quantile plot
RAI	reversed aging intensity
RART	reversed auto-relevation transform
RART-HL	reversed auto-relevated half-logistic
RARTG	reversed auto-relevated truncated Gumbel
SE	standard error
TG	truncated Gumbel
TGEVD	truncated GEVD
TMV	true mean value
TVaR	tail value at risk
TVP	tail variance premium
UBT	upside-down bathtub
VaR	value at risk

List of Figures

2.1 Hazard plots of rescaled beta and MPHRT rescaled beta. 40
2.2 Hazard plots of Pareto type-II and MPHRT Pareto type-II. . . . 41
2.3 Hazard plots of MPHRE model. 45
2.4 Q-Q plot of the MPHRE models. 52
2.5 Hazard plots of MPHRW model. 56
2.6 Q-Q plot of the MPHRW model for the two datasets. 59

3.1 Hazard plots of n^{th} phase auto-relevated exponential model 66
3.2 Hazard plots of second phase auto-relevated Weibull model 69
3.3 Plot of $l_2(u)$ against u 70
3.4 Hazard plots for various parameters of generalized gamma model. 77

4.1 Density plots of ARLL for various parameter combinations. . . . 93
4.2 Plots of Galton's skewness and Moor's kurtosis 96
4.3 Hazard plots of ARLL for different parameters 98
4.4 Odds function plots of ARLL and LL model 99
4.5 LOR plots of ARLL and LL models 100
4.6 Survival function plots of ARLL and LL model 107
4.7 Q-Q plot and histogram and density plot for dataset I. 112
4.8 Q-Q plot and histogram and density plot for dataset II. 113
4.9 The plots of MOOP, Bias, and MSE for different orders P. 115
4.10 Histograms of peaks over VaR for different confidence levels. . . . 116

4.11 Model based VaR versus CL (top left), number of peaks over VaR versus CL (top right), VaR and TVaR versus CL (bottom left), and histogram of claims with fitted density (bottom right). 116

5.1 Plots of $h_{X[Y]}(x)$ for two parameter values. 130
5.2 Plots of $h_{X[Y]}(x)$ for two parameter values. 130
5.3 Plots of $h_W(x)$ for various parameter combinations. 139
5.4 Histogram and density plots for the dataset I. 140
5.5 Histogram and density plots for the dataset II. 141
5.6 Q-Q plots for both datasets. 142

6.1 Hazard plots of Pareto type-I and RART Pareto type-I. 156
6.2 Plots of hazard rates RART Weibull for different values of α. . . . 157
6.3 Plots of hazard rates of HL and RART-HL distribution. 158
6.4 Hazard plots of $X[X]$ and $Y[Y]$ 162
6.5 Plot of $p(u)$. 163
6.6 Plots of $qh_X(u)$ and $qh_Y(u)$ for different parameters. 171
6.7 Plots of $h_X(x)$ and $h_{X[X]}(x)$ for various parameter combinations. . 181
6.8 Q-Q plots for the dataset 182

7.1 Hazard plots for different values of n. 189
7.2 Plot of histogram of Z superimposed with the density curve of Y, for different sample sizes 192
7.3 Plot of $\Delta_n(x)$ for different values of n 193
7.4 Plots of hazard rate for the n^{th} phase RART Burr type-XII model for various values of n 194
7.5 Plots of $h(x)$ and $B_n(x)$ for different values of n for the n^{th} phase RART-HL model 195
7.6 Hazard plots for different values of n for n^{th} phase RART-HL model 195
7.7 Q-Q plot and histogram of the RART-HL model for dataset I and dataset II. 197
7.8 Plots of $l_2(u)$, $l_3(u)$ and $l_4(u)$ for different values of n. 200

8.1 Hazard plot of RART-TGEVD 208
8.2 Goodness of fit plots for GEVD using regression estimates. 226
8.3 Goodness of fit plots for TGEVD using regression estimates. . . . 226

List of Tables

2.1 Aging classes preserved under the MPHRT 40
2.2 Bias and MSE of MLE-PL, AD, CvM and MPS estimators of the MPHRE model parameters 50
2.3 Goodness of fit measures for dataset I. 51
2.4 Goodness of fit measures for dataset II. 52
2.5 Bias and MSE for censored samples when $\alpha = 2$ and $\lambda = 2$. 53
2.6 Bias and MSE for censored samples when $\alpha = 1$ and $\lambda = 0.75$. . . 54
2.7 Goodness of fit measures of censored dataset I. 54
2.8 Goodness of fit measures of censored dataset II. 55
2.9 Goodness of fit measures for dataset I. 58
2.10 Goodness of fit measures for dataset II. 58

3.1 Models for NHPP and their expected aging. 81

4.1 Values of S and K for varying β. 96
4.2 Bias and MSE of the estimators of the ARLL model parameters. . 103
4.3 Summary statistics of the datasets 112
4.4 Goodness of fit measures for dataset I. 112
4.5 Goodness of fit measures for dataset II. 113
4.6 MOOP Analysis for different orders P 114
4.7 Model based VaR, TVaR, N_{PORT} and empirical characteristics of peaks over VaR. 115

5.1 Aging classes preserved under PRHRRT 129

5.2 Estimates, KS statistics and p-values for the dataset I. 140
5.3 Estimates, KS statistics and p-values for the dataset II. 141

6.1 Characterizations based on reversed hazard rate. 147
6.2 Fit measures and goodness of fit for floods data. 182

7.1 Some lifetime models and their n^{th} stage RART form 188
7.2 Some lifetime models and their n^{th} stage RART form 190
7.3 Goodness of fit measures for dataset I. 197
7.4 Goodness of fit measures for dataset II. 197

8.1 MSEs of the estimates of GEVD 223
8.2 Absolute biases of the estimates of GEVD 223
8.3 MSE and absolute biases of the estimates of TGEVD using regression method 224
8.4 Descriptive statistics for the considered data. 225
8.5 Estimates and confidence intervals using regression method and the MLE for the crude oil data for GEVD. 226

Chapter 1

Introduction

Reliability theory employs probabilistic methods to model failures, predict system behavior, and evaluate the likelihood of successful system operation over time. It plays a vital role in ensuring the safety, performance, and durability of systems in areas such as engineering, consumer products, infrastructure, healthcare, and finance. Many reliability problems focus on system lifetime modeling under different design configurations aimed at improving system performance, efficiency, and safety. In engineering reliability, the study of redundant system lifetimes is of significant technical interest. In active redundancy, a standby component that has been operating under a milder environment is designed to replace the primary component and assume the workload upon its failure. Such a framework arises in many practical reliability settings. For example, in high-precision machinery manufacturing, a failed gear is often replaced by an aged gear, since introducing a new gear may create synchronization issues and compromise system performance. Similarly, in military and aerospace applications, if a wing flap on a fighter jet fails after 2,000 flight hours, it is replaced by a wing flap from a grounded aircraft having comparable operating time. In electrical systems, failed transformers are commonly replaced by aged units rather than new ones to ensure compatibility and stable operation.

In this context, the concept of the relevation transform was introduced by Krakowski (1973) and has since received considerable attention in the

literature. It has been applied in various areas such as repair and replacement strategies in production processes, characterization of probability distributions, evolution of cumulative entropies, sequential order statistics, and stochastic comparisons of systems. Moreover, the dual concept of the relevation transform, known as the reversed relevation transform, was introduced by Di Crescenzo and Toomaj (2015) and has since been applied in deriving distributions of sequences of random variables as well as in entropy related studies. Despite their theoretical importance, the reliability properties of systems modeled through the relevation and reversed relevation transforms have not been extensively explored, particularly in the context of extreme value distributions.

Building on the concepts of the relevation and reversed relevation transforms, this thesis investigates their reliability properties with particular emphasis on lifetime characteristics and system comparisons. In addition, their applicability to extreme value distributions is explored, leading to the construction of new extreme lifetime models capable of capturing complex behaviors. These contributions enhance the usefulness of relevation transforms in modeling extreme lifetimes and comparing reliability systems under diverse probabilistic settings. The next section presents an overview of the relevation transforms along with a detailed review of the related literature.

1.1 Overview of relevation transforms

In reliability engineering, modeling system lifetimes under redundancy is of central interest. As mentioned earlier, Krakowski (1973) introduced the relevation transform, and it is defined as follows:

Definition 1.1. Let X denote the lifetime of a component with survival function $\bar{F}_X(\cdot)$. Suppose that Y, independent of X, denotes the lifetime of the redundancy with survival function $\bar{F}_Y(\cdot)$. Then, the system lifetime $Y\nu X$, representing the lifetime of Y, given that the redundancy outlives the primary component,

i.e., $Y\nu X \stackrel{d}{=} \{Y \mid Y > X\}$, has the survival function

$$\bar{F}_{Y\nu X}(x) = \bar{F}_Y(x) + \bar{F}_X(x) \int_0^x \frac{1}{\bar{F}_X(t)}\, d\bar{F}_Y(t), \quad x \geq 0, \tag{1.1}$$

which is called the relevation transform of X and Y.

Since its inception, relevation transform has evoked interest from researchers in different areas of statistics. Grosswald et al. (1980) provided characterizations of the exponential distribution based on the relevation transform. The concept of the dependent relevation transform was first introduced by Johnson and Kotz (1981), and further developments were presented by Fang et al. (2023). Applications of n-fold recursive relevation transform in reliability contexts were considered by Baxter (1982). Shanthikumar and Baxter (1985) established closure properties of reliability measures in the relevation framework and the results were later improved by Lau and Rao (1990). Belzunce et al. (2001) established the relationship between the relevation transform and record values. The quantile-based relevation transform was introduced by Dileepkumar et al. (2018). Moreover, the load-sharing and minimal repair policy models arise as two particular cases of the relevation transform under the proportional hazards and identical distribution assumptions for the redundancy, respectively. The reliability properties and applications of the load-sharing and minimal repair policy models are discussed in Sankaran and Dileepkumar (2019) and Dileepkumar and Sankaran (2021), respectively. Recently, Dileepkumar and Sankaran (2024) studied the reliability properties of the relevation transform when the redundancy is assumed to be a proportional odds model of the primary component.

Over the past four decades, numerous researchers have contributed to the development of the theory of relevation transform from a stochastic process perspective. Gupta and Kirmani (1988) demonstrated that the study of the relevation transform is fundamentally equivalent to the analysis of record values, through the non-homogeneous Poisson process. Pellerey et al. (2000) analyzed

the epoch times and inter-arrival times of a non-homogeneous Poisson process and extended it to introduce the relevation counting process. Motivated by this, Kapodistria and Psarrakos (2012) derived the weighted tail distribution of a sequence of random variables using the relevation transform. A comparative study based on the stochastic process arising from a policy based on relevation and replacement by a new one was provided by Belzunce et al. (2021). The relevation transform can also model a repair policy. When a failed system is repaired by replacing or fixing some components, the system retains the age at failure, but its underlying distribution changes due to the altered components. Thus, the relevation transform represents not only a replacement policy but also a repair policy similar to minimal repair, where the system's age remains unchanged while its failure characteristics are modified. Belzunce et al. (2019) considered the problem of optimal allocation of a relevation within a system to enhance its overall reliability, focusing particularly on the cases of load-sharing and minimal repair policies. The minimal repair strategies in coherent systems using the framework of the relevation transform were studied by Navarro et al. (2019). The problem of allocating a single relevation resource within coherent systems was addressed by Wu et al. (2022). Zhang and Zhang (2023) investigated the problem of allocating relevations to two nodes in a coherent system with independent components, aiming to improve the system's overall reliability. Li and Li (2024) examined the application of relevation redundancy to coherent systems consisting of homogeneous components. Recently, Kumar et al. (2026) investigated the allocation of relevations to one or two nodes in a coherent system comprising independent components, with the objective of improving system reliability.

While the relevation transform describes the residual lifetime behavior of redundant systems, its dual concept focuses on the analysis of past lifetimes. Motivated by this perspective, Di Crescenzo and Toomaj (2015) introduced the reversed relevation transform, defined as follows:

Definition 1.2. Let X denote the lifetime of a component with cumulative distribution function (CDF) $F_X(\cdot)$. Suppose we randomly inspect the status of

the component and let Y denote the random inspection time with CDF $F_Y(\cdot)$. Then the CDF of the random variable $X[Y]$, which denotes the lifetime of X given that it is less than the random inspection time Y (*i.e.* $X \mid X \leq Y$) is given by

$$F_{X[Y]}(x) = F_Y(x) + F_X(x) \int_x^\infty \frac{1}{F_X(t)}\, dF_Y(t), \quad x \geq 0, \tag{1.2}$$

which is called the reversed relevation transform of X and Y.

The above expression can be derived as follows.

$$\begin{aligned}
F_{X[Y]}(x) &= P(X \leq x \big| X \leq Y) \\
&= \int_0^\infty P(X \leq x \big| X \leq t)\, dF_Y(t) \\
&= \int_0^x \frac{P(X \leq x, X \leq t)}{P(X \leq t)}\, dF_Y(t) + \int_x^\infty \frac{P(X \leq x, X \leq t)}{P(X \leq t)}\, dF_Y(t) \\
&= \int_0^x \frac{P(X \leq t)}{P(X \leq t)}\, dF_Y(t) + \int_x^\infty \frac{P(X \leq x)}{P(X \leq t)}\, dF_Y(t) \\
&= F_Y(x) + F_X(x) \int_x^\infty \frac{1}{F_X(t)}\, dF_Y(t).
\end{aligned}$$

The reversed relevation transform provides a mathematical description of the past lifetime of a system, given that failure is observed before the inspection epoch. For example, critical infrastructure such as bridges or dams is often inspected periodically rather than continuously due to cost and accessibility constraints, and an inspection conducted at a given time can reveal whether the structure may have been operating unsafely for some period beforehand. Similarly, pipelines carrying water, gas, or oil are typically examined using robotic inspection tools deployed at random times, which may detect corrosion or damage that has already compromised the system. These scenarios illustrate the importance of the reversed relevation transform in assessing past failure behavior and supporting informed decisions in safety evaluation and environmental risk management.

Following its introduction, the reversed relevation transform has gained considerable attention in the study of entropy and past lifetime analysis. Di Crescenzo and Toomaj (2015) studied various properties of a sequence of random variables formed by the repeated application of the reversed relevation transform. Kayal (2016) introduced a generalized form of cumulative entropy, leveraging the concept of the reversed relevation transform. Further, Di Crescenzo and Toomaj (2017) demonstrated a correspondence between the distribution of the n-fold recursive relevation transform and the distribution of lower record values. They also investigated the relationship between generalized cumulative entropy and the n-fold recursive relevation transform. Results related to certain entropy measures and the reversed relevation transform were discussed in Di Crescenzo et al. (2018). Nair et al. (2019) presented results which connect the proportional reversed hazards model and certain entropy measures with the reversed relevation transform.

Although the relevation and reversed relevation transforms have been widely studied from a distributional and theoretical perspective, their reliability aspects have not been explored in sufficient depth. Moreover, their potential applications in modeling extreme lifetimes remain largely unexplored. This motivates the need to link the relevation framework with reliability theory extreme value distributions, which provides suitable tools for analyzing extreme events and tail behavior. Accordingly, a brief overview of extreme value theory is presented next to facilitate the development of relevation-based extreme lifetime models in the subsequent chapters.

1.2 Overview of extreme value theory

Classical extreme value theory studies the distributional properties of the statistics $M_n = \max(X_1, \ldots, X_n)$ and $m_n = \min(X_1, \ldots, X_n)$ of independent and identically distributed random variables $X_1, \ldots, X_n$. The pioneering works on the distributional aspects of extremes were carried out by Fréchet (1927) and

Fisher and Tippett (1928). In their seminal work, Fisher and Tippett (1928) derived the well-known three types of limiting distributions of extremes, also known as the type-I, type-II and type-III extreme value distributions. These three models for extremes can be briefly described as follows. Let $(X_1, \ldots, X_n)$ be independent and identically distributed random variables. If the asymptotic distribution of M_n under proper normalization exists, *i.e.*, if

$$P\left(\frac{M_n - b_n}{a_n} \leq x\right) \xrightarrow{w} G(x), \tag{1.3}$$

for sequences of constants $\{a_n > 0\}$ and $\{b_n\}$ and a non-degenerate CDF $G(\cdot)$, then $G(\cdot)$ belongs to one of the following three families:

$$\begin{aligned}
&\text{Type-I} : G_1(x) = \exp\left(-\exp\left(-\frac{x-\mu}{\sigma}\right)\right), \qquad -\infty < x < \infty \\
&\text{Type-II} : G_2(x) = \begin{cases} 0, & x \leq \mu \\ \exp\left(-\left(\frac{x-\mu}{\sigma}\right)^{-\xi}\right), & \text{for some } \xi > 0,\ x > \mu \end{cases} \\
&\text{Type-III} : G_3(x) = \begin{cases} \exp\left(-\left(-\left(\frac{x-\mu}{\sigma}\right)^{-\xi}\right)\right), & \text{for some } \xi < 0,\ x \leq \mu \\ 1, & x > \mu. \end{cases}
\end{aligned} \tag{1.4}$$

When $\mu = 0$ and $\sigma = 1$, the type-I, type-II, and type-III distributions in (1.4) are the standard extreme value distributions. A complete theoretical framework for this result was later established by Gnedenko (1943). For a given dataset, type-I, type-II, and type-III extreme value distributions are fitted and the best-fitting model is used for further analysis of extremes. Von Mises (1936) and Jenkinson (1955) unified these three families of distributions into a single family known as the generalized extreme value distribution (GEVD), by incorporating a new parameter in the model. The GEVD proposed by Von Mises (1936) and Jenkinson (1955) has distribution function

$$G(x) = \exp\left(-\left(1 - \xi\left(\frac{x-\mu}{\sigma}\right)\right)^{1/\xi}\right), \tag{1.5}$$

where $-\infty < \mu < \infty$ is the location parameter, $\sigma > 0$ is the scale parameter, and $-\infty < \xi < \infty$ is the shape parameter. Also, $x < \mu + \frac{\xi}{\sigma}$, when $\xi > 0$, $x > \mu + \frac{\xi}{\sigma}$, when $\xi < 0$, and $x \in \mathbb{R}$, when $\xi = 0$. The distribution function $G(\cdot)$ given in equation (1.5) is the three parameter GEVD. The case $\xi = 0$, is interpreted as $\lim_{\xi \to 0} G(x)$ which is the type-I extreme value distribution or Gumbel distribution. For $\xi > 0$, $G(\cdot)$ is the type-II extreme value distribution or Fréchet distribution, and for $\xi < 0$, $G(\cdot)$ is the type-III extreme value distribution or reverse Weibull distribution. The practical advantage of GEVD is that the type of extreme value distribution is determined from the data through the estimation of the shape parameter ξ. Detailed theoretical aspects of the above results, its consequences and practical applications can be seen in Leadbetter et al. (1983), Resnick (1987) and Embrechts et al. (1997). Practical applications of model (1.5) in hydrology were discussed in Jenkinson (1955) and a recent review on model (1.5) can be seen in Coles et al. (2001). Moreover, the National Environment Research Council in 1975, recommended the use of GEVD in flood-related studies in the United States. The development of the theory of extremes and reliability has led to the creation of new models that better fit real-life situations. One such contribution was by Aryal and Tsokos (2009), wherein the transmuted extreme value distribution was introduced into the literature, whose properties and applications were later developed by Otiniano et al. (2019). The q-generalized extreme value distribution was proposed by Provost et al. (2018), wherein its applications in predicting the reliability of systems were illustrated. Zaid et al. (2022) derived some important information measures of the extreme value and the q-generalized extreme value distributions.

While extreme value theory provides powerful tools for modeling rare events and tail behavior, its integration with reliability-based transforms such as the relevation and reversed relevation transforms remains limited. In particular, there has been no systematic investigation of the reliability characteristics of systems governed by extreme value distributions under these transformations. These gaps naturally motivate the present study.

1.3 Motivation of the study

Over the years, various aspects of relevation transforms have been extensively studied, as discussed in the previous section. However, their reliability properties remain comparatively less explored, as reflected in the practical scenarios outlined earlier. This gap provides a strong motivation for the present study. By addressing this aspect, the study aims to enhance the understanding of the reliability properties of these transforms and encourage further exploration of their structural features. Moreover, while classical reliability models primarily focus on average lifetime behavior, many contemporary datasets in engineering and finance exhibit extreme shocks and pronounced tail behavior. To adequately capture such behavior, we employ extreme value theory (EVT) to demonstrate the applicability and relevance of the relevation transforms in modeling systems subject to rare but impactful events. Extreme value distributions provide flexible models for systems operating under extreme conditions. EVT focuses on modeling extreme deviations from typical behavior, particularly the tail behavior of distributions, making it a powerful framework for analyzing rare events such as catastrophic system failures, natural calamities, or extreme stock market variations. By analyzing the reliability behavior of relevation transforms under extreme value distributions, this study addresses the aforementioned gap. Based on these motivations, the objectives of the present study are formulated.

1.4 Objectives of the study

1. To study the reliability, aging, and stochastic ordering properties of relevation transforms.

2. To analyze the reliability aspects of auto-relevation and reversed auto-relevation transforms.

3. To extend auto-relevation and reversed auto-relevation transforms to a

multi-phase framework and investigate their reliability characteristics.

4. To investigate various aspects of the non-homogeneous Poisson process based on the auto-relevation process.

5. To develop new models based on relevation transforms with applications to extreme value theory.

6. To propose a new method for estimating the parameters of the generalized extreme value distribution.

7. To evaluate the performance of parameter estimators for the proposed models.

8. To demonstrate the applicability of the proposed models through simulation and real data analysis.

1.5 Significance of the study

The present study is significant in strengthening the theoretical understanding and practical applicability of the relevation transforms within reliability analysis. A major contribution lies in the systematic investigation of reliability, aging, and stochastic ordering properties of these transforms, providing deeper insight into the behavior of lifetime distributions. In particular, the extension of auto-relevation and reversed auto-relevation transforms to a multi-phase framework offers a realistic modeling approach for systems undergoing successive stages of operation, especially under imperfect repair conditions. This facilitates a better understanding of the evolution of system reliability and degradation over time. The study also contributes by examining the preservation of aging classes and stochastic orderings, which are essential for comparing system performance across phases and for establishing structural reliability properties. These results enhance the interpretability and applicability of the models in practical reliability assessment and decision-making. In addition, new models based on extreme

value distributions are derived and analyzed, further enhancing the modeling capability and flexibility of the proposed framework. These models provide useful alternatives for capturing diverse lifetime behaviors and tail characteristics, thereby complementing the reliability structures developed in this study. Overall, the results contribute to a comprehensive approach for analyzing reliability behavior in complex systems, particularly under multi-phase and imperfect repair settings, with potential applications in maintenance planning, survival analysis, extreme value theory, and risk assessment.

1.6 Basic concepts

Understanding the behavior of systems over time and modeling their lifetime characteristics are fundamental problems in reliability theory. The study of lifetime distributions and related quantities such as hazard rates, odds rates, and aging properties provides important insights into system performance and failure mechanisms. In this context, relevation and reversed relevation transforms have emerged as useful tools, offering alternative perspectives for analyzing system behavior, failure dynamics, and redundancy structures. This section introduces the key concepts and preliminaries required for the developments in the subsequent chapters. These ideas form the theoretical foundation for the models and results presented throughout the thesis.

Survival function

The survival function represents the probability that the system under consideration survives beyond a time x. It is the complement of CDF and provides a measure of reliability over time. The survival function of a random variable X is denoted by $\bar{F}_X(\cdot)$ and is defined as

$$\bar{F}_X(x) = P(X > x) = 1 - F_X(x), \tag{1.6}$$

where $F_X(\cdot)$ is the CDF of X. Note that the survival function is a non-increasing and right-continuous function and for a non-negative random variable X, $\bar{F}_X(0) = 1$ and $\bar{F}_X(\infty) = 0$.

Quantile function

A quantile function $Q_X(u)$ of a random variable X with distribution function $F_X(x)$ is a real-valued function $Q : [0, 1] \to \mathbb{R}$, defined as

$$Q_X(u) = \inf\{x : F_X(x) \geq u\}, \quad 0 \leq u \leq 1. \tag{1.7}$$

For $-\infty < x < \infty$ and $0 < u < 1$, the following implication holds:

$$F_X(x) \geq u \quad \text{if and only if} \quad Q_X(u) \leq x.$$

Note that, the quantile function $Q_X(u)$ uniquely characterizes the underlying distribution of X. The quantile density function of X is defined by

$$q_X(u) = Q'_X(u). \tag{1.8}$$

For more details on quantile functions and its properties one may refer Gilchrist (2000) and Nair et al. (2013).

1.6.1 Reliability measures

Reliability measures provide quantitative descriptions of lifetime behavior and failure mechanisms of components or systems. They are essential for assessing performance, predicting failures, and comparing different systems under uncertainty. Some fundamental reliability measures used in reliability analysis are discussed in this section.

Hazard rate

The hazard rate, also referred to as failure rate, measures the instantaneous risk of failure of an item at time x, given that the item has survived up to the time x. The hazard rate of a random variable X, denoted by $h_X(\cdot)$ is defined as

$$h_X(x) = \frac{f_X(x)}{\bar{F}_X(x)} = \frac{d}{dx}\left(-\log \bar{F}_X(x)\right), \tag{1.9}$$

where $f_X(\cdot)$ is the density function of X. By integrating (1.9) over $(0, x)$, we get the corresponding survival function as

$$\bar{F}_X(x) = \exp\left(-\int_0^x h_X(t)\, dt\right). \tag{1.10}$$

This identity shows that the underlying distribution can be characterized through the hazard rate. Note that the term $H_X(x) = \int_0^x h_X(t)\, dt$ is the cumulative hazard rate of X.

Reversed hazard rate

Reversed hazard is the dual concept of the hazard rate which measures the probability of instantaneous failure in the past, *i.e.*, the probability that the failure of an item has occurred at time x, given that the item has failed before time x.

$$\lambda_X(x) = \frac{f_X(x)}{F_X(x)} = \frac{d}{dx}\left(\log F_X(x)\right). \tag{1.11}$$

Now, by integrating (1.11) over (x, ∞), we get the CDF as

$$F_X(x) = \exp\left(-\int_x^\infty \lambda_X(t)\, dt\right) = \exp\left(-\Lambda_X(x)\right). \tag{1.12}$$

Here also, we observe that the underlying distribution can be characterized by the above identity (1.12). The term $\Lambda_X(x) = \int_x^\infty \lambda_X(t)\, dt$ is the cumulative reversed hazard rate of X.

Odds ratio

The concept of odds ratio is well-known in epidemiological research, serving as a measure of the approximate relative risk of an event, such as disease or death, with or without a specific factor. If we define X as an individual's lifespan, there are two types of odds ratios; odds to survival ($\phi_X(\cdot)$) and odds to failure ($\theta_X(\cdot)$), where

$$\phi_X(x) = \frac{\bar{F}_X(x)}{F_X(x)} \quad \text{and} \quad \theta_X(x) = \frac{F_X(x)}{\bar{F}_X(x)}, \tag{1.13}$$

and

$$F_X(x) = \frac{1}{1+\phi_X(x)} = \frac{\theta_X(x)}{1+\theta_X(x)}, \quad \text{for } x > 0. \tag{1.14}$$

Note that $\phi_X(x)$ is decreasing and $\theta_X(x)$ is increasing in x. For more details on properties and applications of odds ratios, one could refer to Bennett (1983), Zimmer et al. (1998), Navarro et al. (2008), Lando et al. (2022), and the references therein.

Odds rate and log odds rate

As an alternative to the well-known hazard rate, Lando et al. (2022) introduced and studied characterizations of distributions based on the odds rate. The odds rate can be used as an indicator of aging, and it has wider practical applicability than the hazard rate based on survival bounds and tolerance limits. The odds rate function defined by Lando et al. (2022) is given as

$$\theta'_X(x) = \frac{d}{dx}\left(\theta_X(x)\right) = \frac{f_X(x)}{\left(\bar{F}_X(x)\right)^2}. \tag{1.15}$$

In engineering contexts, component reliability and non-monotonic hazard rates often require alternative indicators beyond the hazard rate. The log-odds (LO) and log-odds rate (LOR) functions serve as useful indicators in addressing these challenges. Zimmer et al. (1998) and Wang et al. (2003) introduced a new way to model continuous time to failure using LOR. These models were found to be similar to those based on the hazard rate. The LO function of the random

variable X is defined by

$$LO_X(x) = \log\left(\frac{F_X(x)}{\bar{F}_X(x)}\right).$$

Mathematically, the LOR function is defined as

$$LOR_X(x) = \frac{d}{dx}\left(LO_X(x)\right) = \frac{f_X(x)}{F_X(x)\bar{F}_X(x)}. \tag{1.16}$$

Mean residual life

The mean residual life (MRL) of a random variable X, denoted by $m_X(\cdot)$, represents the expected remaining lifetime of a system or component, given that it has already survived up to a certain time x. It is defined as

$$m_X(x) = \frac{1}{\bar{F}_X(x)}\int_x^\infty \bar{F}_X(t)\,dt = E(X - x \mid X > x).$$

More details are available in Bryson and Siddiqui (1969) and Muth (1977).

Mean inactivity time

The mean inactivity time (MIT) of a random variable X, denoted by $\mu_X(\cdot)$, is the dual concept of MRL and represents the expected past lifetime of a system or component, given that it fails before a stipulated time x. It is defined as

$$\mu_X(x) = \frac{1}{F_X(x)}\int_0^x F_X(t)\,dt = E(x - X \mid X < x).$$

For more details one may refer to Ruiz and Jorge (1996) and Chandra and Roy (2001).

Aging intensity and reversed aging intensity

Another measure of aging is the aging intensity (AI) function introduced by Jiang et al. (2003). It is defined as the ratio between the instantaneous hazard failure and the average risk over time. The average risk over time of a random

variable X is defined as

$$\frac{H_X(x)}{x} = \frac{1}{x}\int_0^x h_X(t)\,dt,$$

where $H_X(\cdot)$ is the cumulative hazard rate. Now, for a non-negative random variable X, the AI function is defined as

$$L_X(x) = \frac{h_X(x)}{H_X(x)/x} = -\frac{x f_X(x)}{\bar{F}_X(x)\log \bar{F}_X(x)}. \tag{1.17}$$

The AI function $L_X(x) = 1$, when the hazard rate is constant. It exceeds 1 when the hazard rate is increasing, and falls below 1 when the hazard rate is decreasing. A higher value of $L_X(x)$ indicates a stronger aging tendency, while a lower value reflects a stronger anti-aging effect.

Later, Rezaei and Khalaf (2014) introduced the dual concept of AI function called reversed aging intensity (RAI). It is defined as the ratio of instantaneous reversed hazard rate to its baseline value. The baseline value of the reversed hazard rate is

$$\frac{\Lambda_X(x)}{x} = \frac{1}{x}\int_x^\infty \lambda_X(t)\,dt.$$

The RAI function for a random variable X, written as $\tilde{L}_X(\cdot)$, is defined as

$$\tilde{L}_X(x) = \frac{x\lambda_X(x)}{\Lambda_X(x)}. \tag{1.18}$$

A higher reversed aging intensity implies a higher instantaneous reversed hazard rate, a smaller accumulation of failures beyond the time point x, and a greater likelihood that the unit has survived up to time x. This corresponds to a weaker tendency of aging.

The reliability measures discussed above provide fundamental insights to the characteristics of lifetime models. To gain deeper insight into the temporal behavior of systems and how reliability evolves with age, we next consider aging properties which capture monotonic and structural features of these measures over time.

1.6.2 Aging properties

Understanding aging properties is crucial for assessing the long-term performance and reliability of systems and for implementing maintenance strategies. Let X be an absolutely continuous lifetime random variable. Then we have the following aging properties:

(i) Increasing (decreasing) hazard rate (*i.e.*, IHR (DHR)) if the hazard rate $h_X(x)$ is increasing (decreasing) in x.

(ii) Increasing (decreasing) hazard rate average (*i.e.*, IHRA (DHRA)) if $\frac{1}{x}\int_0^x h_X(u)\,du$ is increasing (decreasing) in x.

(iii) New better (worse) than used (*i.e.*, NBU (NWU)) if $\bar{F}_X(x+t) \leq (\geq)\ \bar{F}_X(x)\bar{F}_X(t)$, for all $x, t > 0$.

(iv) New better (worse) than used in hazard rate (*i.e.*, NBUHR (NWUHR)) if $h_X(0) \leq (\geq)\, h_X(x)$, for all $x > 0$.

(v) Increasing (decreasing) reversed hazard rate (*i.e.*, IRHR (DRHR)) if $\lambda_X(x)$ is increasing (decreasing) in x.

(vi) Increasing (decreasing) likelihood ratio (*i.e.*, ILR (DLR)) if $f_X(x)$ is log-concave (log-convex) in x.

(vii) Increasing (decreasing) log-odds rate (ILOR (DLOR)) if the log-odds rate function $LOR_X(x)$ is increasing (decreasing) in x.

(viii) Decreasing (increasing) mean residual life (*i.e.*, DMRL (IMRL)) if the mean residual life function $m_X(x)$ is decreasing (increasing) in x.

(ix) Decreasing (increasing) mean inactivity time (*i.e.*, DMIT (IMIT)) if the mean inactivity time function $\mu_X(x)$ is decreasing (increasing) in x.

(x) Increasing (decreasing) density (*i.e.*, ID (DD)) if the density function $f_X(x)$ is increasing (decreasing) on its support.

For more details on aging properties and their applications, one may refer Barlow and Proschan (1975), Lai and Xie (2006), Navarro (2022) and Breneman et al. (2022).

1.6.3 Stochastic orders

Stochastic orders provide a systematic framework for understanding the relative behaviors and properties of lifetime distributions, making them essential in various fields including reliability analysis and risk assessment. Let X and Y be two absolutely continuous lifetime random variables. Then we have the following stochastic ordering relations.

(i) X is said to be smaller than Y in the usual stochastic order, denoted $X \leq_{st} Y$, if and only if $\bar{F}_X(x) \leq \bar{F}_Y(x)$ for all x.

(ii) X is smaller than Y in the hazard rate order, denoted $X \leq_{hr} Y$, if and only if $\frac{\bar{F}_Y(x)}{\bar{F}_X(x)}$ is increasing in x.

(iii) X is smaller than Y in the likelihood ratio order, denoted $X \leq_{lr} Y$, if and only if $\frac{f_Y(x)}{f_X(x)}$ is increasing over the union of their supports.

(iv) X is smaller than Y in the increasing convex order, denoted $X \leq_{icx} Y$, if and only if $\int_x^\infty \bar{F}_X(t)\,dt \leq \int_x^\infty \bar{F}_Y(t)\,dt$ for all x.

(v) X is smaller than Y in the reversed hazard rate order, denoted $X \leq_{rhr} Y$, if $\frac{F_Y(x)}{F_X(x)}$ is increasing in x.

(vi) X is smaller than Y in the mean residual life order, denoted $X \leq_{mrl} Y$, if $m_X(x) \leq m_Y(x)$ for all x.

(vii) X is smaller than Y in the mean inactivity time order, denoted $X \leq_{mit} Y$, if $\mu_X(x) \leq \mu_Y(x)$ for all x.

(viii) X is smaller than Y in the star order, denoted $X \leq_* Y$, if and only if $Q_Y(F_X(x))$ is star-shaped in x.

(ix) X is smaller than Y in NBU, denoted $X \leq_{nbu} Y$, if $\bar{F}_X(x+y) \leq \bar{F}_X(x)\bar{F}_Y(y)$.

(x) X is smaller than Y in the odds rate order, denoted $X \leq_{or} Y$, if $\theta'_X(x) \leq \theta'_Y(x)$ for all $x > 0$.

(xi) X is smaller than Y in the LOR order, denoted $X \leq_{lor} Y$, if $l_X \leq l_Y$, $u_X \leq u_Y$, and $LOR_X(x) \geq LOR_Y(x)$ for all $x \in (l_Y, u_X)$, where l_X, l_Y and u_X, u_Y are lower and upper bounds of the random variables X and Y.

(xii) X is smaller than Y in the relative hazard rate order, denoted $X \leq_{rh} Y$, if and only if $\frac{h_X(x)}{h_Y(x)}$ is increasing in $x > 0$.

(xiii) X is smaller than Y in the relative reversed hazard rate order, denoted $X \leq_{rrh} Y$, if and only if $\frac{\lambda_X(x)}{\lambda_Y(x)}$ is decreasing in $x > 0$.

(xiv) X is smaller than Y in the excess wealth order, denoted $X \leq_{ew} Y$, if and only if $\int_p^1 Q_X(u)\,du \leq \int_p^1 Q_Y(u)\,du$, for all $p \in (0,1)$.

(xv) X is said to be smaller than Y in the total time on test transform order, denoted $X \leq_{ttt} Y$, if and only if $\int_0^{F_X^{-1}(p)} F_X(t)\,dt \leq \int_0^{F_Y^{-1}(p)} F_Y(t)\,dt$ for all $p \in (0,1)$.

(xvi) X is said to be smaller than Y in the dispersive order, denoted $X \leq_{disp} Y$, if and only if $F_X^{-1}(q) - F_X^{-1}(p) \leq F_Y^{-1}(q) - F_Y^{-1}(p)$ for all $0 < p < q < 1$.

More properties and applications of stochastic orders can be seen in Shaked and Shanthikumar (2007), Belzunce et al. (2016) and Kochar (2022).

1.6.4 Distortion function

The concept of distortion functions, introduced by Denneberg (1990), has gained wide applications in the areas of actuarial science, risk theory, reliability theory and survival analysis. A distortion function, denoted as $q(\cdot)$, is a non-decreasing function defined from $[0,1]$ to $[0,1]$ with $q(0) = 0$ and $q(1) = 1$.

This concept has given rise to the notion of distortion random variables in the literature. Suppose we have two lifetime random variables, denoted as X and Y, with corresponding survival functions $\bar{F}_X(\cdot)$ and $\bar{F}_Y(\cdot)$ respectively. We can say that Y serves as the distortion random variable for X when the relationship $\bar{F}_Y(x) = q(\bar{F}_X(x))$ holds true, where $q(\cdot)$ represents a distortion function. The importance of distorted random variables in reliability studies has been pointed out by various researchers, such as Wang (1996), Sordo and Suárez-Llorens (2011), Navarro et al. (2013, 2014, 2016), Sordo et al. (2015) and Navarro (2022). Motivated by these developments, it is of interest to examine how the application of a distortion function influence aging properties and stochastic ordering relations between lifetime distributions. When two survival functions are connected through a distortion function, it is natural to inquire whether key aging and stochastic ordering concepts are preserved under such transformations. The following results from Wang et al. (2003), Navarro et al. (2014) and Navarro et al. (2025) show the preservation of various aging classes between two random variables X and Y, which are connected through a distortion function $q(\cdot)$.

Result 1: If $l_1(u) = \frac{u\,q'(u)}{q(u)}$ is decreasing (increasing) in $(0,1)$ and, X is IHR (DHR), then Y is IHR (DHR); and if Y is DHR (IHR), then X is DHR (IHR).

Result 2: If $l_2(u) = \frac{u\,q'(1-u)}{1-q(1-u)}$ is decreasing in $(0,1)$ and X is DRHR, then Y is DRHR; and if $l_2(u)$ is increasing in $(0,1)$ and Y is DRHR, then X is DRHR.

Result 3: If $l_3(u) = \frac{u\,q''(u)}{q'(u)}$ is increasing in $(0,1)$ and X is DLR, then Y is DLR.

Result 4: If $q(u\,v) \leq (\geq)\ q(u)\,q(v)$ for $u, v \in (0,1)$ and X is NBU (NWU), then Y is NBU (NWU).

Result 5: If $q(u^a) \leq (\geq)\ (q(u))^a$ for $u \in (0,1)$ and $0 < a < 1$ and X is IHRA (DHRA), then Y is IHRA (DHRA).

Result 6: If $l_4(u) = \frac{u(1-u)\,q'(u)}{q(u)(1-q(u))}$ is decreasing (increasing) in $(0,1)$ and X is ILOR (DLOR), then Y is ILOR (DLOR).

Result 7: If $q(u)$ is concave (convex) on $(0,1)$ and X is ID (DD) then Y is ID (DD).

Similarly, the results in Navarro et al. (2013) and Kayid and Almohsen (2024)

establish conditions under which stochastic ordering relationships between random variables X and Y and their corresponding distorted random variables X_D and Y_D, under a common distortion function $q(\cdot)$.

Result 8: $X_D \leq_{lr} (\geq_{lr}) X$ if and only if $\frac{q'(u)}{q_1'(u)}$ is increasing (decreasing) in $u \in (0,1)$, where $q_1(u) = u$ denotes the identity distortion function.

Result 9: If $X \leq_{st} Y$, then $X_D \leq_{st} Y_D$.

Result 10: If $X \leq_{hr} Y$ and $\frac{u\,q'(u)}{q(u)}$ is decreasing in $(0,1)$, then $X_D \leq_{hr} Y_D$.

Result 11: If $X \leq_{rhr} Y$ and $\frac{(1-u)\,q'(u)}{1-q(u)}$ is increasing in $(0,1)$, then $X_D \leq_{rhr} Y_D$.

Result 12: If $X \leq_{lr} Y$ and $\frac{u\,q''(u)}{q'(u)}$ is non-negative and decreasing in $(0,1)$, then $X_D \leq_{lr} Y_D$.

Result 13: If $X \leq_{icx} Y$ and $q(u)$ is concave on $(0,1)$, then $X_D \leq_{icx} Y_D$.

Result 14: If $X \leq_{ttt} Y$ and $q(u)$ is convex on $(0,1)$, then $X_D \leq_{ttt} Y_D$, and if $X_D \leq_{ttt} Y_D$ and $q(u)$ is concave on $(0,1)$, then $X \leq_{ttt} Y$.

Result 15: $X \leq_{disp} Y$ if and only if $X_D \leq_{disp} Y_D$.

Result 16: If $X \leq_{ew} Y$ and $q(u)$ is concave on $(0,1)$, then $X_D \leq_{ew} Y_D$.

Result 17: If $X \leq_{hr} Y$ and $X \leq_{rrh} Y$ and $l_5(u) = \frac{w(u)}{u\,w'(u)}$ and $\frac{-u\,\log(u)\,l_5'(u)}{l_5(u)}$ are non-decreasing functions of $u \in (0,1)$, where $w(u) = 1 - q(1-u)$, then $X_D \leq_{rrh} Y_D$.

In the subsequent chapters, these results are systematically employed to analyze and establish the aging behavior and ordering properties of the proposed models.

1.6.5 Information measures

Information theory provides a framework for quantifying uncertainty and is used to analyze the amount of uncertainty or randomness associated with a random variable. Measuring and quantifying uncertainty is crucial in various real-life scenarios. Shannon (1948) introduced Shannon entropy of a random variable X as

$$H_X = -\int_0^\infty f_X(x) \log f_X(x)\, dx. \tag{1.19}$$

Kerridge (1961) generalized the idea of uncertainty and introduced a measure called Kerridge inaccuracy measure, for a discrete setup. It was later extended by Nath (1968) to the continuous case. Let X and Y be two continuous lifetime random variables, with density functions $f_X(\cdot)$ and $f_Y(\cdot)$ respectively. Then, the Kerridge inaccuracy measure or the differential entropy is given by

$$H_{X,Y} = -\int_0^\infty f_X(x) \log f_Y(x)\, dx. \tag{1.20}$$

A cumulative version of the Shannon entropy called cumulative entropy (ζ) was introduced by Di Crescenzo and Longobardi (2009) for estimating the uncertainty in past lifetimes, which is defined by

$$\zeta_X = -\int_0^\infty F_X(x) \log F_X(x)\ dx. \tag{1.21}$$

Di Crescenzo and Longobardi (2009) also introduced a dynamic version of the cumulative entropy given by

$$\zeta_X(x) = \int_0^x \frac{F_X(t)}{F_X(x)} \left(-\log\left(\frac{F_X(t)}{F_X(x)}\right)\right) dt. \tag{1.22}$$

An alternate measure of uncertainty is the extropy, introduced into the literature by Lad et al. (2015) as a dual of entropy. Since then, many researchers have introduced various extropy measures with widespread applications in the field of economics, risk analysis and forecast distributions. Jahanshahi et al. (2020) introduced the survival extropy of a random variable X as

$$S_X = -\frac{1}{2}\int_0^\infty \bar{F}_X^2(x)\, dx. \tag{1.23}$$

Most recently Abdul Sathar and Dhanya (2021) proposed the dynamic version of the survival extropy, defined as

$$S_X(x) = -\frac{1}{2\bar{F}_X^2(x)}\int_x^\infty \bar{F}_X^2(t)\, dt, \quad x \geq 0.$$

In the forthcoming chapters, we develop results based on various information measures in the context of relevation transforms. The next section outlines the statistical and methodological framework employed for data analysis, beginning with inference techniques followed by model selection criteria.

1.7 Statistical inference

Statistical inference refers to the process of drawing conclusions about a population based on the information obtained from a sample. It provides a systematic framework for estimating population parameters, testing hypotheses, and making predictions from observed data. Statistical inference plays a central role in data-driven scientific studies by enabling reliable conclusions to be drawn from incomplete or noisy data. In the next subsection, we discuss the method of maximum likelihood estimation

1.7.1 Method of maximum likelihood estimation

One of the most widely used frequentist methods for parameter estimation is the maximum likelihood estimation introduced by Fisher (1912). Let $\underline{X} = (x_1, x_2, \ldots, x_n)$ denote a random sample of size n drawn from a population with density function $f(\cdot \mid \boldsymbol{\theta})$ and CDF $F(\cdot \mid \boldsymbol{\theta})$, where $\boldsymbol{\theta} = (\theta_1, \theta_2, \ldots, \theta_k)$ is a vector of k unknown parameters such that $\boldsymbol{\theta} \in \Theta \subseteq \mathbb{R}^k$. The likelihood function based on the observed sample $\underline{X}$ is denoted by $L(\boldsymbol{\theta})$ and is defined as

$$L(\boldsymbol{\theta}) = L(\boldsymbol{\theta} \mid \underline{x}) = f(\underline{X} \mid \boldsymbol{\theta}) = \prod_{i=1}^{n} f(x_i \mid \boldsymbol{\theta}).$$

Then the maximum likelihood estimate (MLE) of $\boldsymbol{\theta}$, say $\hat{\boldsymbol{\theta}}$, is the value of the parameter for which the likelihood function attains its maximum value, *i.e.*,

$$L(\hat{\boldsymbol{\theta}} \mid \underline{X}) \geq L(\boldsymbol{\theta} \mid \underline{X}) \implies L(\hat{\boldsymbol{\theta}} \mid \underline{X}) = \sup_{\boldsymbol{\theta} \in \Theta} L(\boldsymbol{\theta} \mid \underline{X}).$$

For analytical convenience, inference is typically based on the log-likelihood function. The asymptotic properties of the MLE make it particularly useful for interval estimation of the unknown parameters. Under standard regularity conditions, the MLE is asymptotically normally distributed with mean equal to the true parameter value and covariance matrix given by the inverse of the Fisher information matrix. That is, for sufficiently large n, we have

$$\hat{\boldsymbol{\theta}} \sim N\left(\boldsymbol{\theta}, \frac{1}{nI(\boldsymbol{\theta})}\right),$$

where $I(\boldsymbol{\theta})$ is the Fisher information matrix defined as $I(\boldsymbol{\theta}) = -E\left[\frac{\partial^2 l(\boldsymbol{\theta})}{\partial\theta_i \partial\theta_j}\right]$, $i, j = 1, 2, \ldots, k$. Using this, the $100(1-\alpha)\%$ confidence interval for θ is defined as

$$\hat{\boldsymbol{\theta}} \pm z_{\alpha/2}\sqrt{Var(\hat{\boldsymbol{\theta}})},$$

where $z_{\alpha/2}$ denotes the upper $(\alpha/2)^{\text{th}}$ percentile of the standard normal distribution, and $Var(\hat{\boldsymbol{\theta}}) \approx I(\hat{\boldsymbol{\theta}})^{-1}$ evaluated at $\boldsymbol{\theta} = \hat{\boldsymbol{\theta}}$. It should be noted that closed-form expressions for the estimators may not always be obtainable from the likelihood equations. In such cases, numerical methods are employed to compute the corresponding estimators.

1.8 Model selection criteria

In statistical modeling, choosing an appropriate probability distribution is essential, as it affects the accuracy of inference and prediction. The selected model should adequately represent the underlying data and provide reliable conclusions. Model selection approaches are broadly classified into two categories: graphical techniques and formal statistical tests. Graphical methods offer visual insight into the agreement between empirical data and the proposed theoretical model, whereas formal statistical tests provide quantitative measures for assessing model adequacy. These criteria help determine the suitability of a model based on observed data. In the following subsections, some commonly

used model selection techniques are discussed.

Empirical CDF plot

The empirical cumulative distribution function (ECDF) plot is a non-parametric graphical tool used to describe the distributional characteristics of a dataset. Let $X_{(1)} \leq X_{(2)} \leq \cdots \leq X_{(n)}$ denote the ordered statistics of a sample of size n. The ECDF is defined as

$$\widehat{F}_n(x) = \begin{cases} 0, & x < X_{(1)}, \\ \dfrac{k}{n}, & X_{(k)} \leq x < X_{(k+1)}, \quad k = 1, 2, \ldots, n-1, \\ 1, & x \geq X_{(n)}. \end{cases}$$

The ECDF is a step function that increases by $\frac{1}{n}$ at each observed data point and represents the proportion of data points less than or equal to x. To assess the goodness of fit of a theoretical model, the ECDF is commonly plotted together with the CDF. A close agreement between the two curves across the data range indicates a good fit.

Probability-probability plot

The probability-probability plot (P-P plot) is a graphical technique used to evaluate the goodness of fit between a theoretical distribution and an observed dataset. It compares the empirical probabilities obtained from the ECDF with the corresponding probabilities from the theoretical CDF. In constructing a P-P plot, empirical probabilities are plotted against the corresponding theoretical probabilities obtained from the fitted model. If the proposed model fits the data well, the plotted points lie close to the 45° reference line. Points lying above the diagonal suggest underestimation by the model, whereas points below indicate overestimation.

Quantile-quantile plot

The quantile-quantile plot (Q-Q plot) is another widely used graphical technique for assessing the adequacy of a candidate distribution. Unlike the P-P plot, the Q-Q plot compares the quantiles of the empirical distribution with the corresponding quantiles of the theoretical distribution. In constructing a Q–Q plot, the sample quantiles obtained from the ordered data are plotted against the corresponding theoretical quantiles of the fitted distribution. A close alignment of points along the 45° reference line indicates a good fit of the model to the data.

Kolmogorov-Smirnov (KS) test

The Kolmogorov-Smirnov (KS) test is a widely used non-parametric statistical test for assessing the goodness of fit of a theoretical distribution. Let $X_1, X_2, \ldots, X_n$ be an independent random sample of size n drawn from a population with CDF $F(\cdot)$, and let $\widehat{F}_n(\cdot)$ denote the corresponding ECDF. The KS test statistic, denoted by D, is defined as

$$D = \sup_x \left| \widehat{F}_n(x) - F(x) \right|.$$

A smaller value of D indicates a closer agreement between the empirical and theoretical distributions. The associated p-value of the test is used to determine whether the proposed model provides an adequate fit to the observed data. Since the model parameters are estimated from the data, the standard p-value for the KS test is not valid. Therefore, the p-values are obtained using a parametric bootstrap procedure. Specifically, 1000 bootstrap samples are generated from the fitted model to approximate the null distribution of the KS test statistic. The p-value is then computed as the proportion of bootstrap KS statistics that are less than the observed KS statistic. The null hypothesis states that the sample follows the specified distribution $F(\cdot)$. If the computed p-value is less than the chosen significance level α, the null hypothesis is rejected.

1.9 Overview of the thesis

This thesis focuses on the reliability aspects of the relevation and reversed relevation transforms. The chapters are structured to ensure a logical progression from fundamental concepts to advanced theoretical developments and practical applications in reliability theory and extreme value analysis. The thesis is organized into nine chapters. The introductory chapter outlines the basic concepts used in this thesis, the background and motivation for the study, along with its significance and key objectives.

Chapter 2 studies the relevation transform under the modified proportional hazards assumption, focusing on its reliability properties and applications. Various aging and stochastic ordering characteristics are analyzed, and the practical applicability of the model is illustrated through a new generalization of the exponential distribution. Its suitability for both censored and complete data is demonstrated via simulation and real data analysis.

Chapter 3 investigates the multi-phase auto-relevation transform and its associated reliability properties. The preservation of aging and stochastic ordering properties are established, and the framework is extended through its connection with the non-homogeneous Poisson process. Several characterization results based on the non-homogeneous Poisson process are also derived.

Chapter 4 introduces the auto-relevated log-logistic distribution, obtained by applying the auto-relevation transform to the log-logistic distribution. Its reliability properties and tail characteristics are analyzed. The applicability of the model is illustrated through real data with emphasis on extreme risk assessment.

Chapter 5 examines the reversed relevation transform under the proportional reversed hazards assumption. The preservation of aging and stochastic ordering properties is studied, along with results based on information measures. A quantile-based formulation is developed, and a new generalization of the Fréchet distribution is proposed and analyzed.

Chapter 6 investigates the reversed auto-relevation transform, highlighting its reliability properties, characterization results, and preservation of aging classes and stochastic orders. It extends the study of the reversed auto-relevation transform by developing its quantile representation and analyzing information measures. Its practical applicability is also demonstrated using a real dataset.

Chapter 7 studies the multi-phase reversed auto-relevation transform, deriving its reliability measures and analyzing its aging behavior. Characterization results are established, and the model is illustrated through a new generalization of the half-logistic distribution with real data applications. The preservation of aging classes and stochastic orders across phases are also examined.

Chapter 8 investigates the truncated GEVD and examines its aging properties. The reversed auto-relevated form of the truncated GEVD is also introduced, and its aging behavior along with other properties are analyzed. The chapter further addresses parameter estimation for the GEVD using a regression-based approach. A comprehensive review of existing estimation techniques is provided, followed by the development of bootstrap confidence intervals. The performance of the estimators are evaluated through simulation studies, and the practical applicability of the models are illustrated using real datasets.

Finally, we incorporate the conclusions of the study along with recommendations for future research in Chapter 9.

Chapter 2

Modified proportional hazards relevation transform

2.1 Introduction

As discussed earlier, the relevation transform provides a systematic framework for modeling system lifetimes in the presence of redundancy. In this setting, the lifetime of a redundant component may be related to that of the primary component through various probabilistic structures. The proportional hazards model (PHM) and proportional odds model (POM) are two widely studied families in reliability and survival analysis, as they allow the hazard rate or odds function of a baseline distribution to be modified through a proportionality parameter, thereby capturing different aging behaviors and failure mechanisms.

Motivated by the Marshall–Olkin extension of a baseline distribution, Balakrishnan et al. (2018) introduced the modified proportional hazards model (MPHM), which generalize the classical PHM and POM frameworks and include them as special cases. In this chapter, we focus on the MPHM within the framework of the relevation transform and investigate various properties and applications of it.

The remainder of this chapter is structured as follows: Section 2.2 provides a brief overview of the modified proportional hazards model. Section 2.3 introduces

the concept of censoring. Section 2.4 presents the proposed model and its reliability properties. The preservation of different aging classes are studied in Section 2.5 and those of various stochastic orders in Section 2.6. In Section 2.7, a new generalization of the exponential distribution is introduced and a Monte Carlo simulation study and real data applications are discussed. Another model based on the Weibull distribution is also proposed in Section 2.8, along with its applications using real datasets. Finally, Section 2.9 concludes the chapter.

2.2 Modified proportional hazards model

Two commonly used models for comparing the lifetimes or failure times of systems or components are the PHM and the POM. These models provide flexible frameworks for describing relationships between failure mechanisms. Let X and Y be two random variables with hazard rates $h_X(\cdot)$ and $h_Y(\cdot)$ respectively. Then, Y is said to be the PHM of X with proportionality constant θ, if

$$h_Y(x) = \theta h_X(x), \quad \theta > 0. \tag{2.1}$$

This can be equally expressed as

$$\bar{F}_Y(x) = (\bar{F}_X(x))^\theta, \quad \theta > 0, \tag{2.2}$$

where $\bar{F}_X(\cdot)$ and $\bar{F}_Y(\cdot)$ are the respective survival functions of X and Y. More details on PHM can be found in Lawless (2003) and Kalbfleisch and Prentice (2011). To further characterize the distributional behavior of X, we now consider the POM, which is based on the odds function $\phi_X(\cdot)$ defined in (1.13). Suppose X and Y are two random variables with CDF $F_X(\cdot)$ and $F_Y(\cdot)$ respectively, satisfying the identity

$$\phi_Y(x) = \alpha\, \phi_X(x), \tag{2.3}$$

where $\alpha > 0$, is a constant. Then Y is said to be the POM of X, with proportionality constant α. The POM defined in (2.3) can be equivalently

written as

$$\frac{\bar{F}_Y(x)}{F_Y(x)} = \alpha \, \frac{\bar{F}_X(x)}{F_X(x)}, \quad x > 0.$$

This gives

$$\bar{F}_Y(x) = \frac{\alpha \bar{F}_X(x)}{F_X(x) + \alpha \bar{F}_X(x)} \quad \text{or equivalently,} \quad F_Y(x) = \frac{F_X(x)}{\alpha + F_X(x)(1-\alpha)}. \tag{2.4}$$

The concept of POM was introduced by McCullagh (1977) for comparing categorical data. It was later extended by Bennett (1983) for analyzing survival data as an alternative to the PHM. In the POM, hazard rates converge over time as opposed to the PHM where they hold a constant ratio to one another. This was pointed out by Bennett (1983), Rossini and Tsiatis (1996) and Kirmani and Gupta (2001), and thus found out that the POM is a better model than the PHM in certain situations where the constant hazard ratio is unreasonable. More details on POM can be seen in Pettitt (1984) and Collett (2015). A thorough review on the POM and its applications was carried out by Huang et al. (2022).

As mentioned earlier, Balakrishnan et al. (2018) introduced the MPHM in which the PHM and POM appear as special cases. They have provided results on important reliability aspects of the MPHM. The random variable Y is said to be the MPHM of X if

$$\bar{F}_Y(x) = \frac{\alpha \left(\bar{F}_X(x)\right)^{\lambda}}{1 + (\alpha - 1)\left(\bar{F}_X(x)\right)^{\lambda}}, \quad \alpha > 0, \ \lambda > 0. \tag{2.5}$$

Note that, when $\alpha = 1$, (2.5) becomes the PHM, when $\lambda = 1$, (2.5) becomes the POM and when $\alpha = \lambda = 1$, then $\bar{F}_X(x) = \bar{F}_Y(x)$. Recently, Sankaran and Dileepkumar (2019) and Dileepkumar and Sankaran (2024) studied reliability properties of the relevation transform, when the redundancy is assumed to be a PHM and POM of the primary component respectively. The MPHM is a versatile framework that simultaneously incorporates features of both the PHM and POM. This unified framework allows for the analysis of systems where the redundancy behavior cannot be adequately captured by either PHM or POM alone, thereby providing a more realistic representation of complex repairable

systems. We now turn our attention to another concept called censoring.

2.3 Censoring

In many life-testing experiments, censoring is a common occurrence that arises when the exact time of an event of interest such as system failure, death, or equipment breakdown is not fully observed for all experimental units. This typically results from practical limitations such as time or budget constraints, limited resources, loss to follow-up, or it may be intentionally introduced as part of a planned strategy to enhance testing efficiency. Censoring plays a vital role across various fields, including medical and clinical trials, engineering and reliability analysis, and actuarial science.

Progressive type-II censoring

In certain life-testing experiments, it may become necessary to withdraw some units that are still functioning during the course of the study. For instance, when testing the reliability of an electronic device, a manufacturer might need to reassign some operational units to meet urgent production demands. Traditional censoring schemes, such as type-I and type-II censoring, do not allow for the removal of active units once the experiment has begun. To overcome this limitation, the concept of progressive censoring was introduced, which permits the removal of active units at various points during the experiment. To incorporate the benefits of both type-II censoring and progressive censoring, the progressive type-II censoring scheme was developed. It is defined as follows: Consider an experiment that begins with N identical units, where the lifetimes of n failed units are completely observed. At the time of the first failure, R_1 units are randomly removed from the remaining $N-1$ units. At the second failure, R_2 units are removed from the remaining $N-R_1-2$ units. This procedure continues sequentially. At the time of the n^{th} failure, all remaining units, denoted by R_n, are withdrawn, and the experiment terminates. Furthermore, when $N = n$ and

$R_1 = \cdots = R_n = 0$, it corresponds to a complete sampling scheme. A detailed algorithm for implementing progressive type-II censoring is given in Balakrishnan and Sandhu (1995). For more detailed discussions on censoring schemes and their applications, refer to Balakrishnan and Aggarwala (2000) and Balakrishnan and Cramer (2014).

2.4 Modified proportional hazards relevation transform

In this section, we derive a special case of the relevation transform based on the MPHM, termed the modified proportional hazards relevation transform (MPHRT). The resulting model is described in the following proposition.

Proposition 2.1. Let X be a random variable with survival function $\bar{F}_X(\cdot)$. Suppose that Y is the MPHM of X and that X and Y are independent. Then, the survival function of MPHRT random variable Z is

$$\bar{F}_Z(x) = \frac{\lambda \bar{F}_X(x) + (\alpha(\lambda-1)-\lambda)\,(\bar{F}_X(x))^\lambda}{(\lambda-1)\left(1+(\alpha-1)(\bar{F}_X(x))^\lambda\right)}, \quad \alpha > 0,\ \lambda > 0. \tag{2.6}$$

Proof. Since Y is the MPHM of X, it follows from the relevation transform in (1.1) and the MPHM relation in (2.5) that

$$\begin{aligned}
\bar{F}_Z(x) &= \bar{F}_X(x) + \frac{\alpha\left(\bar{F}_X(x)\right)^\lambda}{1-(1-\alpha)\left(\bar{F}_X(x)\right)^\lambda}\int_0^x \left(\frac{\alpha+\left(\bar{F}_X(t)\right)^{-\lambda}-1}{\alpha}\right) f_X(t)\,dt \\
&= \bar{F}_X(x) + \frac{\left(\bar{F}_X(x)\right)^\lambda\left((\alpha-1)F_X(x) + \frac{\left(\bar{F}_X(x)\right)^{1-\lambda}-1}{\lambda-1}\right)}{1-(1-\alpha)\left(\bar{F}_X(x)\right)^\lambda} \\
&= \frac{\lambda\bar{F}_X(x) + (\alpha(\lambda-1)-\lambda)\,(\bar{F}_X(x))^\lambda}{(\lambda-1)\left(1+(1-\alpha)(\bar{F}_X(x))^\lambda\right)},
\end{aligned}$$

which completes the proof. □

Remark 2.1. When $\alpha = 1$, (2.6) becomes

$$\bar{F}_Z(x) = \frac{\left(\bar{F}_X(x)\right)^\lambda - \lambda \bar{F}_X(x)}{1-\lambda}, \quad \lambda > 0, \tag{2.7}$$

which is the proportional hazards relevation transform, discussed in Sankaran and Dileepkumar (2019).

Remark 2.2. The case when $\lambda = 1$ is treated as the limit when λ tends to 1, in which case (2.6) reduces to

$$\bar{F}_Z(x) = \frac{\bar{F}_X(x)\left(\alpha - \log\left(\bar{F}_X(x)\right)\right)}{\alpha - (\alpha-1)F_X(x)}, \quad \alpha > 0, \tag{2.8}$$

which corresponds to the proportional odds relevation transform, studied by Dileepkumar and Sankaran (2024).

Remark 2.3. When $\alpha = \lambda = 1$, (2.6) becomes

$$\bar{F}_Z(x) = \bar{F}_X(x)\left(1 - \log\left(\bar{F}_X(x)\right)\right), \tag{2.9}$$

which is the auto-relevation transform discussed in Dileepkumar and Sankaran (2021).

The density function of MPHRT is given by

$$f_Z(x) = \left(\frac{\lambda\left(1 - ((\alpha+\lambda-\alpha\lambda-1)F_X(x)+1)\left(\bar{F}_X(x)\right)^{\lambda-1}\right)}{(\lambda-1)\left(1+(\alpha-1)\left(\bar{F}_X(x)\right)^\lambda\right)^2} \right) f_X(x). \tag{2.10}$$

Note that, from the above relation, $f_Z(x)$ can be expressed as a weighted function of $f_X(x)$, *i.e.*,

$$f_Z(x) = \frac{w(x)}{E(w(x))} f_X(x), \tag{2.11}$$

where $w(x) = \frac{(1+(\alpha+\lambda-\alpha\lambda-1)F_X(x))\left(\bar{F}_X(x)\right)^{\lambda-1}-1}{\left(1+(\alpha-1)\left(\bar{F}_X(x)\right)^\lambda\right)^2}$, and $E(w(X)) = \frac{1-\lambda}{\lambda}$. From (2.6)

and (2.10), the hazard rate of Z can be obtained as

$$h_Z(x) = \left(\frac{\lambda}{1 + (\alpha - 1)\left(\bar{F}_X(x)\right)^{\lambda}} - \frac{\lambda(\lambda - 1)}{(\alpha(\lambda - 1) - \lambda)\left(\bar{F}_X(x)\right)^{\lambda - 1} - \lambda} \right) h_X(x). \tag{2.12}$$

The reversed hazard rate of Z can be written as

$$\lambda_Z(x) = \left(\frac{\lambda F_X(x)\left(((\alpha + \lambda - \alpha\lambda - 1)F_X(x) + 1)\left(\bar{F}_X(x)\right)^{\lambda - 1} - 1\right)}{\left(\left(\bar{F}_X(x)\right)^{\lambda} + \lambda F_X(x) - 1\right)\left(1 + (\alpha - 1)\left(\bar{F}_X(x)\right)^{\lambda}\right)} \right) \lambda_X(x). \tag{2.13}$$

Another measure of aging is the odds ratio, and in the following proposition, we provide expressions connecting the odds ratios of the baseline and MPHRT models.

Proposition 2.2. Let X and Y be two continuous random variables and Z be the corresponding relevation random variable. Then, Y is the MPHM of X if and only if

$$\text{(i)} \quad \theta_Z(x) = \left(\frac{\left(\bar{F}_X(x)\right)^{\lambda} + \lambda F_X(x) - 1}{\left(\lambda + (\alpha(\lambda - 1) - \lambda)\left(\bar{F}_X(x)\right)^{\lambda - 1}\right) F_X(x)} \right) \theta_X(x). \tag{2.14}$$

$$\text{(ii)} \quad \phi_Z(x) = \left(\frac{\left(\lambda + (\alpha(\lambda - 1) - \lambda)\left(\bar{F}_X(x)\right)^{\lambda - 1}\right) F_X(x)}{\left(\bar{F}_X(x)\right)^{\lambda} + \lambda F_X(x) - 1} \right) \phi_X(x), \tag{2.15}$$

where $\theta_Z(\cdot)$ is the odds to failure and ϕ_Z is the odds to survival of Z.

Proof. Since Z is the MPHRT random variable of X, we have

$$\begin{aligned}
\theta_Z(x) &= \frac{F_Z(x)}{\bar{F}_Z(x)} \\
&= \frac{\frac{\left(\bar{F}_X(x)\right)^{\lambda} + \lambda F_X(x) - 1}{(\alpha - 1)(\lambda - 1)\left(\bar{F}_X(x)\right)^{\lambda} + \lambda - 1}}{\frac{\lambda \bar{F}_X(x) + (\alpha(\lambda - 1) - \lambda)(\bar{F}_X(x))^{\lambda}}{(\lambda - 1)\left(1 + (1 - \alpha)(\bar{F}_X(x))^{\lambda}\right)}} \\
&= \left(\frac{\left(\bar{F}_X(x)\right)^{\lambda} + \lambda F_X(x) - 1}{\left(\lambda + (\alpha(\lambda - 1) - \lambda)\left(\bar{F}_X(x)\right)^{\lambda - 1}\right) F_X(x)} \right) \theta_X(x),
\end{aligned}$$

which proves (i). Similarly, we have

$$\begin{aligned}\phi_Z(x) &= \frac{\bar{F}_Z(x)}{F_Z(x)} \\ &= \frac{\frac{\lambda\bar{F}_X(x)+(\alpha(\lambda-1)-\lambda)(\bar{F}_X(x))^\lambda}{(\lambda-1)\left(1+(1-\alpha)(\bar{F}_X(x))^\lambda\right)}}{\frac{\left(\bar{F}_X(x)\right)^\lambda+\lambda F_X(x)-1}{(\alpha-1)(\lambda-1)\left(\bar{F}_X(x)\right)^\lambda+\lambda-1}} \\ &= \left(\frac{\left(\lambda+(\alpha(\lambda-1)-\lambda)\left(\bar{F}_X(x)\right)^{\lambda-1}\right)F_X(x)}{\left(\bar{F}_X(x)\right)^\lambda+\lambda F_X(x)-1}\right)\phi_X(x),\end{aligned}$$

which proves (ii). □

An alternative reliability measure is the odds rate and in the next proposition, we derive an expression for the odds rate of the MPHRT random variable.

Proposition 2.3. Let X and Y be two continuous random variables and Z be the corresponding relevation random variable. Then, Y is the MPHM of X if and only if

$$\theta'_Z(x) = \left(\frac{(\lambda-1)\lambda\left(\left(\bar{F}_X(x)\right)^\lambda\left(1+(\alpha+\lambda-\alpha\lambda-1)F_X(x)\right)-\bar{F}_X(x)\right)}{\bar{F}_X(x)\left(\lambda+(\alpha\lambda-\alpha-\lambda)\left(\bar{F}_X(x)\right)^{\lambda-1}\right)^2}\right)\theta'_X(x), \tag{2.16}$$

where $\theta'_Z(\cdot)$ is the odds rate of Z.

Proof. Since Z is the MPHRT random variable, from (1.15), we have

$$\begin{aligned}\theta'_Z(x) &= \frac{f_Z(x)}{\left(\bar{F}_Z(x)\right)^2} \\ &= \frac{(\lambda-1)\lambda f_X(x)\left(F_X(x)\left(\alpha(\lambda-1)\left(\bar{F}_X(x)\right)^\lambda-\lambda\left(\bar{F}_X(x)\right)^\lambda+\left(\bar{F}_X(x)\right)^\lambda-1\right)-\left(\bar{F}_X(x)\right)^\lambda+1\right)}{\bar{F}_X(x)\left(\alpha\left(\bar{F}_X(x)\right)^\lambda+\lambda\left(-\alpha\left(\bar{F}_X(x)\right)^\lambda+\left(\bar{F}_X(x)\right)^\lambda-1\right)+\lambda F_X(x)\right)^2} \\ &= \left(\frac{(\lambda-1)\lambda\left(\left(\bar{F}_X(x)\right)^\lambda\left(1+(\alpha+\lambda-\alpha\lambda-1)F_X(x)\right)-\bar{F}_X(x)\right)}{\bar{F}_X(x)\left(\lambda+(\alpha\lambda-\alpha-\lambda)\left(\bar{F}_X(x)\right)^{\lambda-1}\right)^2}\right)\theta'_X(x),\end{aligned}$$

which complete the proof. □

We now have the following proposition wherein an expression connecting the LOR of the baseline and MPHRT random variable has been provided.

Proposition 2.4. Let Z be the MPHRT random variable of X. Then, we have

$$LOR_Z(x) = \left(\frac{\lambda(\lambda-1)(F_X(x))^2}{\left(\bar{F}_X(x)\right)^{\lambda} + \lambda F_X(x) - 1} - \frac{\lambda(\lambda-1)F_X(x)}{((\alpha-1)\lambda-\alpha)\left(\bar{F}_X(x)\right)^{\lambda-1} + \lambda} \right) LOR_X(x). \tag{2.17}$$

Proof. Since Z is the MPHRT random variable of X, from (1.16), we have

$$LOR_Z(x) = \frac{f_Z(x)}{F_Z(x)\bar{F}_Z(x)}.$$

Then, from (2.10), we have

$$\begin{aligned} LOR_Z(x) &= \left(\frac{(\lambda-1)\lambda F_X(x) f_X(x)}{\bar{F}_X(x)\left(\left(\bar{F}_X(x)\right)^{\lambda} + \lambda F_X(x) - 1\right)} - \frac{(\lambda-1)\lambda f_X(x)}{((\alpha-1)\lambda-\alpha)\left(\bar{F}_X(x)\right)^{\lambda} - \lambda F_X(x) + \lambda} \right) \\ &= \left(\frac{\lambda(\lambda-1)F_X^2(x)}{\left(\bar{F}_X(x)\right)^{\lambda} + \lambda F_X(x) - 1} - \frac{\lambda(\lambda-1)F_X(x)}{((\alpha-1)\lambda-\alpha)\left(\bar{F}_X(x)\right)^{\lambda-1} + \lambda} \right) LOR_X(x), \end{aligned}$$

which completes the proof. □

The relations established from (2.12) through (2.17) often facilitate the study of the characteristics of MPHRT model, even in the absence of direct access to $F_Z(\cdot)$, which in some cases makes these properties difficult to establish.

Next, we move on to the concept of distortion function discussed in Chapter 1. From (2.6), we observe that the survival functions of Z and X can be connected through a distortion function, which is given in the following proposition.

Proposition 2.5. Let X and Y be two continuous random variables such that Y is the MPHM of X. Then, the MPHRT random variable $Z = Y\nu X$, is a distorted form of X with distortion function

$$q(u) = \frac{\lambda u + (\alpha(\lambda-1) - \lambda)u^{\lambda}}{(\lambda-1)\left((1-\alpha)u^{\lambda} + 1\right)}, \quad u \in (0,1). \tag{2.18}$$

Proof. Since Z is the MPHRT of X, from (2.6) we have

$$\bar{F}_Z(x) = q(\bar{F}_X(x)), \quad \text{where } q(u) = \frac{\lambda u + (\alpha(\lambda-1) - \lambda)u^{\lambda}}{(\lambda-1)\left((1-\alpha)u^{\lambda} + 1\right)},$$

is the underlying distortion function for $u \in (0,1)$. This completes the proof. □

Now we derive the preservation of various aging and stochastic ordering properties for the MPHRT using the above distortion relation in the upcoming sections.

2.5 Aging properties

We examine the aging characteristics of the MPHRT random variable Z in relation to those of the baseline variable X. For this, as mentioned earlier we employ the distortion function $q(\cdot)$ given in (2.18). Now, based on the results listed in Section 1.6.4 of Chapter 1, the following proposition provides conditions under which common aging classes are preserved for the MPHRT.

Proposition 2.6. Let Z be the MPHRT random variable of X with distortion function given in (2.18). Then, we have the following results:

(i) If X is IHR, then Z is also IHR, for $\alpha \leq 2$ and $\lambda \leq 2$.

(ii) If Z is DRHR, then X is also DRHR, for $\alpha > \lambda$ and $0.5 \leq \lambda \leq 1$.

(iii) If X is NBU, then Z is also NBU, for $\alpha > \lambda$ and $\lambda \geq 0.5$.

(iv) If X is IHRA, then Z is also IHRA, for $\alpha > \lambda$ and $\lambda \geq 0.5$.

(v) If X is DLOR, then Z is also DLOR, for $\alpha > \lambda$ and $\lambda \leq 2$.

Proof. To prove (i), from Result 1, we only need to show that $l_1(u) = \frac{uq'(u)}{q(u)}$ is decreasing for $u \in (0,1)$. We have

$$l_1(u) = \lambda \left(\frac{u(1-\lambda)}{((\alpha-1)\lambda - \alpha)u^\lambda + \lambda u} + \frac{1}{(\alpha-1)u^\lambda + 1} \right).$$

Then

$$\begin{aligned} l_1'(u) &= \lambda \left(\frac{1-\lambda}{((\alpha-1)\lambda-\alpha)u^\lambda + \lambda u} - \frac{(\alpha-1)\lambda u^{\lambda-1}}{((\alpha-1)u^\lambda+1)^2} - \frac{(u-\lambda u)\left(\lambda + \lambda((\alpha-1)\lambda-\alpha)u^{\lambda-1}\right)}{(((\alpha-1)\lambda-\alpha)u^\lambda + \lambda u)^2} \right) \\ &< 0, \quad \text{for } \alpha \leq 2 \text{ and } \lambda \leq 2, \end{aligned}$$

which proves (i).

For proving (ii), from Result 2 we only need to show that $l_2(u) = \frac{u\,q'(1-u)}{1-q(1-u)}$ is increasing for $u \in (0,1)$. We have

$$l_2(u) = \frac{\lambda u\left(\frac{1}{(\alpha-1)(1-u)^{\lambda}+1} - \frac{(\lambda-1)u}{(1-u)^{\lambda}+\lambda u-1}\right)}{u-1}.$$

Then

$$\begin{aligned} l_2'(u) &= \frac{\lambda\left(-\frac{(\lambda-1)^2\lambda u^3}{\left((1-u)^{\lambda}+\lambda u-1\right)^2} + \frac{\lambda u}{\left((\alpha-1)(1-u)^{\lambda}+1\right)^2} - \frac{\lambda u+1}{(\alpha-1)(1-u)^{\lambda}+1} + \frac{(\lambda-1)u((\lambda-1)u+2)}{(1-u)^{\lambda}+\lambda u-1}\right)}{(u-1)^2} \\ &> 0, \quad \text{for } \alpha > \lambda \text{ and } 0.5 \le \lambda \le 1, \end{aligned}$$

which proves (ii).

For the distortion function $q(\cdot)$ given in (2.18), it is evident that $q(u\,v) \le q(u)\,q(v)$ and $q(u^a) \ge (q(u))^a$, for $0 \le a \le 1$, $\alpha > \lambda$ and $\lambda \ge 0.5$. Thus, from Result 4 and Result 5, the proof of (iii) and (iv) follows.

From Result 6, the DLOR property is preserved when $l_4(u) = \frac{u(1-u)q'(u)}{q(u)(1-q(u))}$ is increasing for $u \in (0,1)$. We have

$$l_4(u) = \lambda(\lambda-1)(u-1)\left(\frac{1}{\lambda+(\alpha(\lambda-1)-\lambda)u^{\lambda-1}} + \frac{u-1}{\lambda+u^{\lambda}-\lambda u-1}\right).$$

Then

$$\begin{aligned} l_4'(u) &= \lambda(\lambda-1)\left(\frac{1}{\lambda+(\alpha(\lambda-1)-\lambda)u^{\lambda-1}} + \frac{u-1}{\lambda+u^{\lambda}-\lambda u-1}\right) \\ &\quad + \lambda(\lambda-1)(u-1)\left(\frac{1}{\lambda+u^{\lambda}-\lambda u-1} + \frac{\lambda(u-1)\left(u-u^{\lambda}\right)}{u\left(\lambda+u^{\lambda}-\lambda u-1\right)^2} - \frac{(\lambda-1)(\alpha(\lambda-1)-\lambda)u^{\lambda}}{\left((\alpha(\lambda-1)-\lambda)u^{\lambda}+\lambda u\right)^2}\right) \\ &> 0, \quad \text{for } \alpha > \lambda \text{ and } \lambda \le 2. \end{aligned}$$

which proves (v). □

These results are summarized in Table 2.1. To illustrate the preservation results established in the above proposition, we present the following examples.

Example 2.1. Consider a random variable X following rescaled beta distribution, with CDF $F_X(x) = 1-(1-\frac{x}{\sigma})^{\beta}$, $0 < x < \sigma$, β, $\sigma > 0$, and hazard rate

Table 2.1: Aging classes preserved under the MPHRT

Aging classes	Parameter range
IHR	$\alpha \leq 2, \quad \lambda \leq 2$
DRHR	$\alpha > \lambda, \quad 0.5 \leq \lambda \leq 1$
NBU	$\alpha > \lambda, \quad \lambda \geq 0.5$
IHRA	$\alpha > \lambda, \quad \lambda \geq 0.5$
DLOR	$\alpha > \lambda, \quad \lambda \leq 2$

$h_X(x) = \frac{\beta}{\sigma - x}$. Note that the hazard rate of rescaled beta has IHR behavior for all values of x. From (2.12) hazard rate of the MPHRT rescaled beta has the form

$$h_Z(x) = \frac{\beta\lambda\left(1-\frac{x}{\sigma}\right)^{\beta-1}\left(\frac{\left(1-\frac{x}{\sigma}\right)^{-\beta}}{(\alpha-1)\left(\left(1-\frac{x}{\sigma}\right)^{\beta}\right)^{\lambda}+1} + \frac{1-\lambda}{(\alpha(\lambda-1)-\lambda)\left(\left(1-\frac{x}{\sigma}\right)^{\beta}\right)^{\lambda}+\lambda\left(1-\frac{x}{\sigma}\right)^{\beta}}\right)}{\sigma}.$$

From Figure 2.1, observe that the IHR property is preserved under the formation of MPHRT for $\alpha \leq 2$ and $\lambda \leq 2$. For other values of α and λ, the IHR property is in general not preserved.

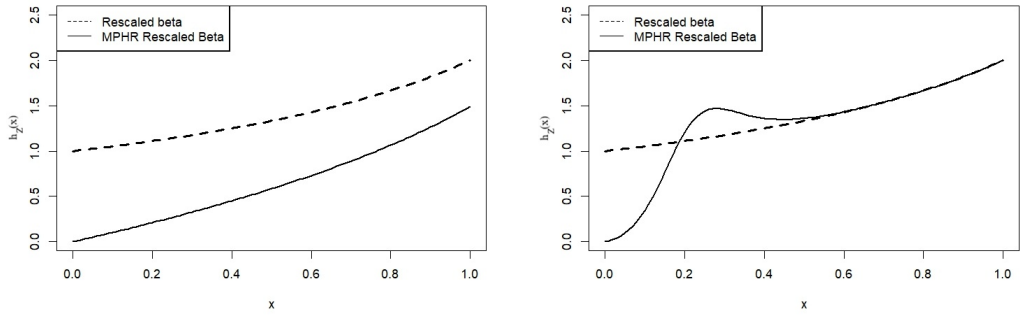

(a) $\beta = 2, \sigma = 2, \alpha = 1.5, \lambda = 1.5$. **(b)** $\beta = 2, \sigma = 2, \alpha = 15, \lambda = 15$.

Figure 2.1: Hazard plots of rescaled beta and MPHRT rescaled beta.

Example 2.2. Let X be a Pareto type-II random variable with survival function $\bar{F}_X(x) = \left(\frac{x+\gamma}{\gamma}\right)^{\beta}$, $x > 0$, $\gamma, \beta > 0$ and hazard rate $h_X(x) = \frac{\beta}{\gamma + x}$. The Pareto type-II distribution is always DHR. Now, the hazard rate of the MPHRT Pareto

type-II random variable is

$$h_Z(x) = \frac{\beta\lambda\left(\frac{1-\lambda}{(\alpha(\lambda-1)-\lambda)\left(\left(\frac{\gamma+x}{\gamma}\right)^{-\beta}\right)^{\lambda-1}+\lambda} + \frac{1}{(\alpha-1)\left(\left(\frac{\gamma+x}{\gamma}\right)^{-\beta}\right)^{\lambda}+1}\right)}{\gamma+x}.$$

We observe from Figure 2.2 that in general the DHR property is not preserved under the formation of MPHRT. Moreover, the hazard rate of the transformed model tends to indicate non-monotonic failure patterns as well, emphasizing the flexibility of the proposed transformation.

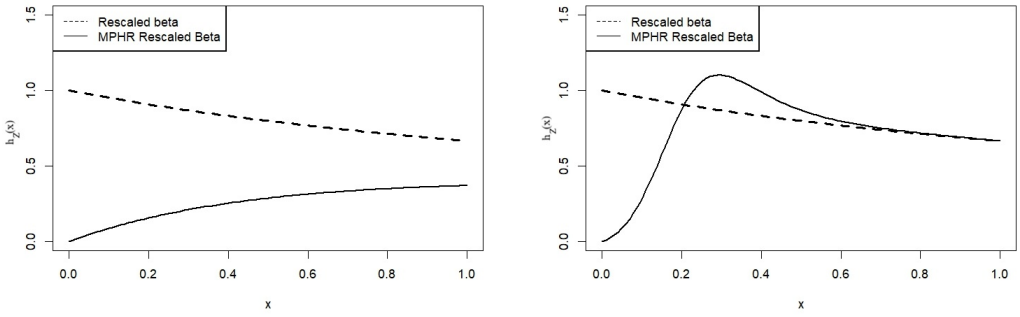

(a) $\beta = 2, \gamma = 2, \alpha = 1.5, \lambda = 1.5$. **(b)** $\beta = 2, \gamma = 2, \alpha = 15, \lambda = 15$.

Figure 2.2: Hazard plots of Pareto type-II and MPHRT Pareto type-II.

Remark 2.4. As noted earlier, when $\alpha = 1$ the MPHRT model given in (2.6) reduces to the PHRT model (Sankaran and Dileepkumar (2019)). As a direct consequence of Proposition 2.6, the following aging properties are preserved in the PHRT model: IHR, IHRA, NBU and NBUHR.

Remark 2.5. Similarly, when $\lambda = 1$, the MPHRT model given in (2.6) reduces to the PORT model (Dileepkumar and Sankaran (2024)). As an immediate consequence of Proposition 2.6, the PORT model preserves the following aging properties: IHRA, NBU and NBUHR, along with IHR for $\alpha > 1$.

2.6 Stochastic orders

Now we investigate the preservation of stochastic ordering relations in the MPHRT model. As mentioned earlier, using the distortion relation between Z and X given in (2.18), we establish the following proposition in light of the results listed in Section 1.6.4 Chapter 1.

Proposition 2.7. Let X be a non-negative continuous random variable and Z be the corresponding MPHRT random variable. Then $Z \geq_{lr} X$, for $\alpha > 0$ and $\lambda \leq 1$.

Proof. Since Z is the MPHRT of X, by recalling Result 8, we only need to show that $\frac{q'(u)}{q_1'(u)}$ is decreasing in $u \in (0,1)$, where $q_1(u) = u$ is the identity distortion function. From (2.18), we have

$$\begin{aligned}\frac{d}{du}\left(\frac{q'(u)}{q_1'(u)}\right) &= \frac{d}{du}\left(\frac{\lambda\left(u - u^{\lambda}(\alpha+\lambda-\alpha\lambda+u(\alpha-1)(\lambda-1))\right)}{u(\lambda-1)\left(1+(\alpha-1)u^{\lambda}\right)^2}\right)\\ &= \frac{\lambda\, u^{\lambda-2}\left(\alpha\lambda^2-2\alpha\lambda+\alpha-\lambda^2+\lambda+(\alpha-1)u^{\lambda}\left(\alpha+(\alpha-1)\lambda^2(u-1)+\lambda(u-\alpha u+1)\right)\right)}{(\lambda-1)\left((\alpha-1)u^{\lambda}+1\right)^3}\\ &\quad - \frac{\lambda\, u^{\lambda-2}\left(\alpha\lambda^2 u-\alpha\lambda u+\lambda^2 u+\lambda u\right)}{(\lambda-1)\left((\alpha-1)u^{\lambda}+1\right)^3}.\end{aligned}$$

which is less than 0 for $\alpha > 0$ and $\lambda \leq 1$. Thus $\frac{q'(u)}{q_1'(u)}$ is decreasing in $u \in (0,1)$, for $\alpha > 0$ and $\lambda \leq 1$, which completes the proof. □

Based on the findings outlined in Shaked and Shanthikumar (2007) and Navarro et al. (2013), we have the following implications in the case of MPHRT transform for $\alpha > 0$ and $\lambda \leq 1$:

$$\begin{array}{ccccccc} & & Z \geq_{mrl} X & & Z \geq_{ew} X & & \\ & & \Uparrow & & \Uparrow & & \\ Z \geq_{lr} X & \Longrightarrow & Z \geq_{hr} X & \Longrightarrow & Z \geq_{or} X & \Longrightarrow & Z \geq_{st} X \Longrightarrow Z \geq_{icx} X \\ \Downarrow & & & & & & \Downarrow \\ Z \geq_{rhr} X & \Longrightarrow & Z \geq_{mit} X & & Z \geq_{su} X & \Longleftarrow & Z \geq_{*} X \end{array}$$

Remark 2.6. From Proposition 2.7, we have $Z \geq_{lr} X$, for $\alpha > 0$ and $\lambda \leq 1$. In similar lines we can show that $Z \geq_{lr} Y$, where Y is the MPHM of X.

In the upcoming proposition, we consider the stochastic order relations between two MPHRT random variables.

Proposition 2.8. Let X and Y be two random variables with survival functions $\bar{F}_X(\cdot)$ and $\bar{F}_Y(\cdot)$. Suppose Z_X and Z_Y are the corresponding MPHRT random variables respectively. Then, the following properties hold:

(i) If $X \leq_{st} Y$, then $Z_X \leq_{st} Z_Y$.

(ii) If $X \leq_{disp} Y$, then $Z_X \leq_{disp} Z_Y$.

(iii) If $X \leq_{hr} Y$, then $Z_X \leq_{hr} Z_Y$, for $\alpha < 1$ and $\lambda > 0$.

(iv) If $X \leq_{icx} Y$, then $Z_X \leq_{icx} Z_Y$, for $\alpha < 1$ and $\lambda > 0$.

(v) If $Z_X \leq_{ttt} Z_Y$, then $X \leq_{ttt} Y$, for $\alpha < 1$ and $\lambda > 0$.

(vi) If $X \leq_{ew} Y$, then $Z_X \leq_{ew} Z_Y$, for $\alpha < 1$ and $\lambda > 0$.

Proof. Since Z_X and Z_Y are MPHRT random variables, they have a common distortion function. Now, proof of (i) and (ii) directly follow from Result 9 and Result 15 respectively.

To prove (iii), again from Result 10 we only need to show that $\frac{u\,q'(u)}{q(u)}$ is decreasing in $(0,1)$. We have

$$\frac{u\,q'(u)}{q(u)} = -\frac{\lambda\left((\alpha-1)(\lambda-1)u^{\lambda+1} + (\alpha(\lambda-1)-\lambda)u^{\lambda} + u\right)}{\left((\alpha-1)u^{\lambda}-1\right)\left((\alpha(\lambda-1)-\lambda)u^{\lambda}+\lambda u\right)},$$

whose first derivative is obtained as

$$\begin{aligned}
&\frac{\lambda}{\left((\alpha-1)u^{\lambda}-1\right)^2\left((\alpha(\lambda-1)-\lambda)u^{\lambda}+\lambda u\right)^2}\Bigg(-\left((\alpha-1)u^{\lambda}-1\right)\left((\alpha(\lambda-1)-\lambda)u^{\lambda}+\lambda u\right)\\
&\quad\times\left(\lambda(\alpha(\lambda-1)-\lambda)u^{\lambda-1}+(\alpha-1)(\lambda^2-1)u^{\lambda}+1\right)\\
&+(\alpha-1)\lambda u^{\lambda-1}\left((\alpha-1)(\lambda-1)u^{\lambda+1}+(\alpha(\lambda-1)-\lambda)u^{\lambda}+u\right)\left((\alpha(\lambda-1)-\lambda)u^{\lambda}+\lambda u\right)\\
&+\left((\alpha-1)u^{\lambda}-1\right)\left((\alpha-1)(\lambda-1)u^{\lambda+1}+(\alpha(\lambda-1)-\lambda)u^{\lambda}+u\right)\left(\lambda+\lambda(\alpha(\lambda-1)-\lambda)u^{\lambda-1}\right)\Bigg)\\
&<0, \quad \text{for } \alpha<1,\ \lambda>0,
\end{aligned}$$

which proves (ii).

The proofs of (iv), (v), and (vi) are also direct due to Result 13, Result 14 and, Result 16 and the fact that the function $q(u)$ given in (2.18) is concave for $\alpha < 1$ and $\lambda > 0$. □

Proposition 2.9. Let Z be the MPHRT of X. Then, $Z \geq_{or} X$ for $\alpha > 0$ and $\lambda \leq 4$.

Proof. To prove this, it suffices to show that $\frac{\theta'_Z(x)}{\theta'_X(x)} \leq 1$. From the definition of odds rate given in (1.15), we have

$$\frac{\theta'_Z(x)}{\theta'_X(x)} = \frac{\lambda(\lambda-1)\left(\left(\bar{F}_X(x)\right)^{\lambda-1}\left((\alpha-1)(\lambda-1)F_X(x)-1\right)+1\right)}{\left((\alpha+\lambda-\alpha\lambda)\left(\bar{F}_X(x)\right)^{\lambda-1}-\lambda\right)^2} \leq 1,$$

for all $x > 0$, $\alpha > 0$ and $\lambda \leq 4$. □

We now introduce new lifetime models based on the proposed transform, by taking the exponential and Weibull distributions as baseline models, and illustrate their practical applicability in the subsequent sections.

2.7 Modified proportional hazards relevated exponential distribution

In this section we introduce a new lifetime model based on the proposed transform and illustrate its practical applicability. For this, we consider the standard exponential distribution as baseline and propose a new modified proportional hazards relevated exponential (MPHRE) distribution. Let X be a random variable following standard exponential distribution with survival function $\bar{F}_X(x) = \exp(-x)$, $x > 0$. Now, from (2.6) we have

$$\bar{F}_Z(x) = \frac{\mathrm{e}^{-x}\left(\lambda + (\alpha(\lambda-1)-\lambda)\,\mathrm{e}^{-(\lambda-1)x}\right)}{(\lambda-1)\left(1+(\alpha-1)\,\mathrm{e}^{-\lambda x}\right)}, \quad x > 0,\ \alpha, \lambda > 0, \tag{2.19}$$

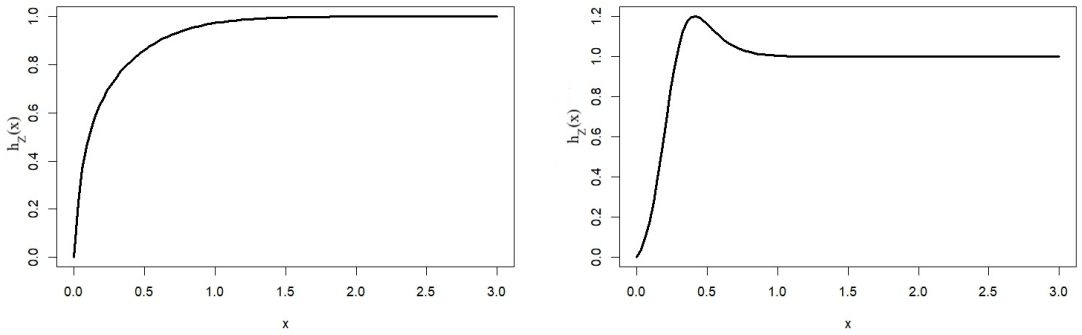

(a) $\alpha = 0.5$, $\lambda = 5$. **(b)** $\alpha = 10$, $\lambda = 10$.

Figure 2.3: Hazard plots of MPHRE model.

which is the survival function of the proposed MPHRE model. The corresponding hazard rate can be obtained from (2.12) as

$$h_Z(x) = \frac{\lambda \left((\mathrm{e}^x - 1) \left(\alpha(\lambda - 1) - \lambda \right) \mathrm{e}^{-\lambda x} - \mathrm{e}^{-\lambda x} + 1 \right)}{\left((\alpha - 1)\ \mathrm{e}^{-\lambda x} + 1 \right) \left(\lambda + \left(\alpha(\lambda - 1) - \lambda \right) \mathrm{e}^{-(\lambda - 1)x} \right)}. \tag{2.20}$$

From Figure 2.3 we observe that the proposed model incorporates the increasing and upside-down bathtub (UBT) shapes for the hazard rate while the baseline exponential only has the constant hazard rate. This shows the flexibility of the proposed model.

2.7.1 Parameter estimation

Let $X_1, X_2, \ldots, X_n$ be a random sample of size n from the MPHRE distribution with parameters (α, λ), and $\underline{x} = (x_1, x_2, \ldots, x_n)$ denote the corresponding observed values. Then, the log-likelihood function can be obtained as

$$L(\alpha, \lambda \mid \underline{x}) = \sum_{i=1}^{n} \left(x_i(-1 + \lambda) + \log \lambda + \log A_i - 2 \log B_i - \log(1 - \lambda) \right),$$

where $A_i = \lambda - 1 + \mathrm{e}^{x_i \lambda} + \alpha\, \mathrm{e}^{x_i} (\alpha(-1 + \lambda) - \lambda) - \alpha\lambda$, and $B_i = \alpha - 1 + \mathrm{e}^{x_i \lambda}$. Initial attempts to estimate the parameters of the MPHRE model using the method of MLE did not yield satisfactory results. The optimization of the

log-likelihood function frequently failed to converge, and even in cases where convergence was achieved, the resulting estimates often deviated substantially from the true parameter values. Furthermore, the MLE method exhibited strong sensitivity to the choice of initial values, leading to unstable and unreliable parameter estimates. These issues were also reflected in the inconsistency of the resulting bias and MSE across simulation studies. In view of these limitations, an alternative approach to the standard MLE method is adopted. Initially, the parameters α and λ are re-parameterized in the log-likelihood function to improve numerical stability, and the corresponding estimates are then obtained using an iterative profile likelihood estimation procedure. For comparison purposes, we evaluate the parameter estimates using the Anderson-Darlin method, the Cramér-von Mises method, and the method of maximum product spacing. A brief outline of these methods is presented below, and a detailed simulation study comparing their efficiencies is provided in Subsection 2.7.2.

Re-parameterized profile likelihood method

The profile likelihood method of estimation, proposed by Cox and Hinkley (1974), is commonly employed in situations where the MLE method encounters difficulties or fails to produce reliable estimates. Since the proposed model exhibits certain specification issues, the parameters are first transformed using the following re-parameterization in the log-likelihood function as $\alpha = e^{\theta_1}$ and $\lambda = e^{\theta_2}$, where $\theta_1, \theta_2 \in \mathbb{R}$. The estimation is then carried out using an iterative profile likelihood procedure. Initially, the profile likelihood estimate of θ_2 is obtained by fixing θ_1. Using this estimate of θ_2, the profile likelihood estimate of θ_1 is subsequently determined. The procedure is repeated alternately for the parameters until the differences between successive estimates $\mid \theta_1^{(n)} - \theta_1^{(n-1)} \mid$ and $\mid \theta_2^{(n)} - \theta_2^{(n-1)} \mid$ is less than a pre-specified small tolerance level. Finally, the estimates of α and λ are obtained by applying the inverse transformation to the estimated values of θ_1 and θ_2.

Anderson-Darling method

The Anderson-Darling (AD) estimation was proposed by Anderson and Darling (1952) as an alternative procedure for detecting departures of sample distributions from normality. It is known for its rapid convergence to its asymptotic distribution (Anderson and Darling (1954)). The AD estimators of the MPHRT are defined as the values of α and λ that minimize

$$A(\alpha,\lambda) = -n - \frac{1}{n}\sum_{i=1}^{n}(2i-1)\left(\log F_Z(x_{i:n} \mid \alpha,\lambda) + \log(1 - F_Z(x_{n+1-i:n} \mid \alpha,\lambda))\right), \tag{2.21}$$

where $x_{i:n}$ is the i^{th} order statistic of a random sample of size n from MPHRE distribution.

Cramér-von Mises method

The Cramér-von Mises (CvM) minimum distance estimators are obtained by minimizing the distance between the theoretical CDF and the empirical CDF. Macdonald (1971) provided empirical evidence that these estimators generally possess smaller bias compared with other minimum distance estimators. The CvM estimators for the MPHRT are defined as the values of α and λ that minimize

$$C(\alpha,\lambda) = \frac{1}{12n} + \sum_{i=1}^{n}\left(F_Z(x_{i:n} \mid \alpha,\lambda) - \frac{2i-1}{2n}\right)^2, \tag{2.22}$$

where $x_{i:n}$ is the i^{th} order statistic of a random sample of size n from MPHRE distribution.

Method of maximum product spacing

An estimation technique using Kullback-Leibler (KL) information, called the maximum product spacing (MPS) estimator was suggested by Cheng and Amin (1983) and was later developed independently by Ranneby (1984). It was proved by Ranneby (1984) that, when the MLE breaks down or when the likelihood is unbounded or when the MLE gives absurd results, the MPS method can be used as an alternative and consistent estimators can be obtained. Let $(X_1, \ldots, X_n)$ be

a random sample from a distribution, with CDF $F(\cdot \mid \underline{\theta})$, where $\underline{\theta}$ is the vector of parameters. Let $x_{(1)}, \ldots, x_{(n)}$ be the corresponding order statistics. Define $D_i(\underline{\theta})$ as

$$D_i(\underline{\theta}) = F(x_{(i)} \mid \underline{\theta}) - F(x_{(i-1)} \mid \underline{\theta}), \quad i = 1, \ldots, n+1,$$

where $F(x_0 \mid \underline{\theta}) = 0$ and $F(x_{(n+1)} \mid \underline{\theta}) = 1$. For MPHRE, $D_i(\alpha, \lambda)$ can be written from (2.19) as

$$D_i(\alpha, \lambda) = F_Z(x_{(i)} \mid \alpha, \lambda) - F_Z(x_{(i-1)} \mid \alpha, \lambda), \qquad i = 1, \ldots, n+1. \tag{2.23}$$

The MPS estimates of the parameters of MPHRE are obtained by maximizing the geometric mean of the spacing given in (2.23), with respect to each parameter. The geometric mean, $P(\alpha, \lambda)$ of this spacing is

$$P(\alpha, \lambda) = \left[\prod_{i=1}^{n+1} D_i(\alpha, \lambda) \right]^{\frac{1}{n+1}}.$$

Maximizing $P(\alpha, \lambda)$ is equivalent to maximizing $\log P(\alpha, \lambda) = R(\alpha, \lambda)$, given by

$$R(\alpha, \lambda) = \frac{1}{n+1} \sum_{i=1}^{n+1} \log D_i(\alpha, \lambda). \tag{2.24}$$

Hence, the MPS estimates can be obtained as the values of α and λ which maximizes $R(\alpha, \lambda)$. Numerical methods can be used in the case when the direct method dose not yield the solution.

2.7.2 Simulation and real data applications for complete sample

A Monte Carlo simulation study was conducted to evaluate the performance of the proposed MPHRE model. Since the quantile function of (2.19) does not admit a closed-form expression, random samples were generated using the acceptance–rejection method. For each simulated dataset, parameter estimation

was carried out using the AD, CvM, MPS, and the modified maximum likelihood estimation procedure based on the re-parameterized profile likelihood (MLE-PL) approach. To assess the precision and consistency of the estimators, the bias and MSE were calculated. The simulation was conducted for four different sets of parameters and sample sizes of 20, 50, 100, 250, and 500 to examine the effect of increasing sample size on the quality of the estimators. The reported results are based on 1000 replications, and all numerical computations were carried out using the R statistical software.

From Table 2.2, it is observed that the bias and MSE of the estimators generally decrease as the sample size increases, indicating the consistency of the methods. Among the estimators, the MPS method provides comparatively smaller bias and MSE values across most cases, showing better estimation accuracy. The AD and CvM methods exhibit moderate performance and improve with increasing sample size, whereas the MLE-PL estimator generally produces relatively larger bias and MSE values. Overall, the results indicate that the MPS method performs best for estimating the parameters of the MPHRE model. Moreover, the model is computationally efficient and easy to implement, making it practical for real-world applications. Next, we analyze the application of the proposed model in real life scenarios. For this we consider two reliability datasets. We fit the data using the proposed MPHRE model and compare it with some competing alternatives; exponential, Weibull, generalized exponential (Gupta and Kundu (1999)) and Weibull exponential (Oguntunde et al. (2015)). The distribution function of the competing models considered are given below:

(i) Exponential: $F_X(x) = 1 - \mathrm{e}^{-\frac{x}{\alpha}}, \quad \alpha > 0,\, x > 0.$

(ii) Weibull: $F_X(x) = 1 - \mathrm{e}^{-\left(\frac{x}{\alpha}\right)^{\beta}}, \quad \alpha,\, \beta > 0,\, x > 0.$

(iii) Generalized exponential : $F_X(x) = \left(1 - \mathrm{e}^{-\alpha\, x}\right)^{\beta}, \quad \alpha,\, \beta > 0,\, x > 0.$

(iv) Weibull exponential: $F_X(x) = 1 - \mathrm{e}^{-\alpha\,(\mathrm{e}^{\gamma\, x} - 1)^{\beta}}, \;\; \alpha,\, \beta,\, \gamma > 0,\, x > 0.$

The first dataset, studied by Barlow and Campo (1975) consists of the ordered failure times (in hours) of 107 right rear brakes on D9G-66A Caterpillar Tractors.

Table 2.2: Bias and MSE of MLE-PL, AD, CvM and MPS estimators of the MPHRE model parameters

Original values	n	MLE-PL				ADE				CvM				MPS			
		α		λ		α		λ		α		λ		α		λ	
		Bias	MSE	Bias	MSE	Bias	MSE	Bias	MSE	Bias	MSE	Bias	MSE	Bias	MSE	Bias	MSE
$\alpha = 1$ $\lambda = 0.75$	20	-0.33669	1.05478	0.06575	0.09805	0.24033	1.27296	0.03005	0.07203	0.25325	1.41033	0.02303	0.08181	-0.07164	0.83031	-0.07466	0.12073
	50	0.24249	0.68669	0.04772	0.04042	-0.21253	1.02654	0.01509	0.03495	0.23890	1.20364	0.01906	0.03702	0.07161	0.25756	-0.04630	0.03973
	100	-0.19518	0.44448	-0.03100	0.02223	0.04961	0.77170	-0.01035	0.02258	-0.16146	0.88175	-0.01342	0.02467	-0.02902	0.16234	-0.01715	0.01863
	250	0.08472	0.13700	-0.01332	0.00848	0.02135	0.29110	-0.00070	0.00856	-0.07952	0.43044	0.01061	0.01170	-0.01423	0.08850	0.00713	0.00852
	500	0.02768	0.05143	-0.00217	0.00363	-0.01525	0.09956	-0.00034	0.00326	-0.04182	0.14478	-0.00887	0.00445	0.00739	0.04857	0.00281	0.00354
$\alpha = 2$ $\lambda = 2$	20	-0.26271	1.87337	-0.16760	0.60571	-0.38445	1.65800	-0.15946	0.63229	-0.32754	1.74967	-0.13720	0.65394	-0.68858	0.99905	-0.31784	0.82262
	50	-0.09638	1.38439	-0.05755	0.33931	0.20635	1.38847	-0.06040	0.30981	0.21658	1.56016	-0.02913	0.32415	-0.29217	0.37560	0.02984	0.27243
	100	-0.03808	0.82736	-0.04602	0.16981	0.16320	1.16330	0.03530	0.17318	0.18482	1.42214	0.02731	0.19728	0.20595	0.30307	0.05453	0.17798
	250	0.06843	0.50693	0.00218	0.07705	0.11908	0.84393	0.01400	0.10576	-0.11766	0.93590	0.00799	0.09765	0.10215	0.28505	-0.00499	0.08307
	500	0.01162	0.31767	-0.00247	0.04176	-0.07100	0.43790	-0.00025	0.04590	0.06290	0.47231	0.01038	0.04415	-0.08406	0.22022	-0.00378	0.04630
$\alpha = 1.5$ $\lambda = 2.5$	20	-0.40355	0.98242	-0.43611	0.96361	0.25726	1.46430	-0.33181	1.01453	0.25768	1.73732	-0.29267	0.88616	-0.26908	0.90923	-0.44003	0.31704
	50	-0.12536	0.84501	-0.11366	0.54695	0.22720	1.35311	0.06874	0.71181	-0.25056	1.50404	-0.08774	0.63464	-0.17701	0.35138	0.13903	0.29717
	100	0.06388	0.65540	-0.02499	0.38976	-0.18981	1.26176	0.03595	0.46767	0.14558	1.30912	0.05414	0.39642	0.10913	0.34047	-0.07388	0.24834
	250	0.17172	0.46803	0.05490	0.17495	0.09623	0.82931	0.02072	0.26242	-0.12281	0.92163	0.03601	0.24523	0.09915	0.23680	0.03033	0.15911
	500	0.06946	0.27560	0.01433	0.10144	-0.07269	0.27978	0.01510	0.10648	0.03993	0.43047	0.01169	0.11732	-0.04090	0.19066	-0.00138	0.09947
$\alpha = 2.5$ $\lambda = 3$	20	-0.48220	1.46737	0.51599	1.04612	-0.87781	2.39361	-0.61371	1.33943	-0.82524	2.46792	-0.65413	1.30005	-0.97355	0.91528	-0.87111	0.77599
	50	0.33455	1.26824	0.25360	0.60036	-0.42967	1.69746	0.27553	0.73935	-0.52455	1.80108	-0.29191	0.76797	0.27775	0.33337	0.10590	0.30009
	100	0.14136	0.68267	-0.07366	0.35662	-0.27611	1.35588	-0.12081	0.43879	-0.26882	1.54843	-0.17062	0.51480	0.22736	0.32449	0.08884	0.27184
	250	-0.05996	0.57940	-0.04437	0.18014	0.05055	0.92118	-0.01680	0.23655	0.13736	0.91619	0.00321	0.23165	-0.12148	0.31116	-0.01003	0.18634
	500	-0.03411	0.42939	-0.01953	0.11222	-0.00126	0.63473	0.02198	0.12781	0.06363	0.80529	0.01810	0.13228	0.06631	0.27699	0.00022	0.12987

For the convenience of our study, we have converted the hourly data into daily data. We fit the data using the proposed MPHRE model and compare it with some competing alternatives.

Table 2.3: Goodness of fit measures for dataset I.

Model	Parameter estimates (SE)			KS statistic	p-value
MPHRE	$\alpha = 0.0015$ (0.0001)	$\lambda = 1.7343$ (0.1381)		0.0424	0.9905
Weibull	$\alpha = 1.4854$ (0.1101)	$\lambda = 93.2626$ (6.3878)		0.0489	0.9604
Weibull exponential	$\alpha = 4.1156$ (1.0781)	$\beta = 1.2488$ (0.0939)	$\gamma = 0.0029$ (0.0004)	0.0598	0.8387
Generalized exponential	$\alpha = 1.9806$ (0.2805)	$\beta = 0.0176$ (0.0019)		0.0731	0.6176
Exponential	$\lambda = 0.0119$ (0.0007)			0.1667	0.0052

Table 2.3 presents the goodness of fit measures along with the parameter estimates and their bootstrap standard error (SE). From the results, it can be observed that the proposed MPHRE model provides a better fit to the data compared with the competing models, as indicated by the smallest KS statistic and the largest p-value among the considered distributions. The Q-Q plot shown in Figure 2.4 a further supports this observation by illustrating the close agreement between the empirical and theoretical quantiles.

We now consider another dataset, which consists of the failure time of 50 components (in 1000 hours) studied in (Murthy et al. (2004)). We fit the data with the proposed model and compare the goodness of fit measures with some competing alternatives. The goodness of fit results are provided in Table 2.4 along with the parameter estimates and bootstrap standard errors. From the table, it can be observed that the proposed MPHRE model provides the best fit among the models considered, as it yields the smallest KS statistic and the largest p-value. This observation is further supported by the Q-Q plot given in Figure 2.4 b.

Table 2.4: Goodness of fit measures for dataset II.

Model	Parameter estimates (SE)	KS statistic	p-value
MPHRE	$\alpha = 0.0007$ $\lambda = 0.8577$ (0.0255) (0.4488)	0.0761	0.9340
Weibull exponential	$\alpha = 3.5182$ $\beta = 0.8691$ $\gamma = 0.1217$ (4.8902) (0.1581) (0.1445)	0.0818	0.8915
Exponential	$\lambda = 0.5977$ (0.0816)	0.0907	0.8050
Weibull	$\alpha = 0.9764$ $\lambda = 1.6571$ (0.1412) (0.1112)	0.0948	0.7599
Generalized exponential	$\alpha = 0.9039$ $\beta = 0.5600$ (0.2086) (0.1022)	0.1004	0.6945

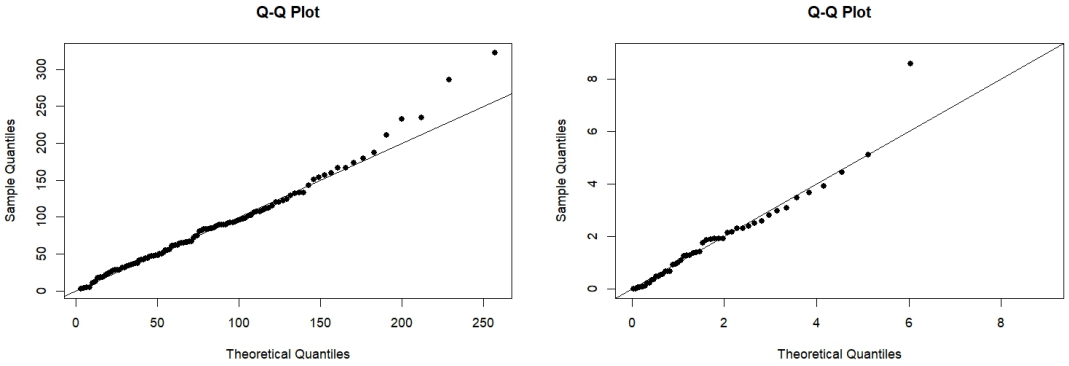

(a) Q-Q plot of dataset I. **(b)** Q-Q plot of dataset II.

Figure 2.4: Q-Q plot of the MPHRE models.

2.7.3 Simulation and real data applications for censored sample

We further illustrate the applicability of the proposed model in the presence of censored data. Specifically, progressive type-II right censored samples are considered, and a simulation study is conducted to assess the efficiency of the resulting parameter estimates. For each sample size, three distinct censoring schemes are applied, representing varying degrees of censoring severity. Specifically, scenarios involving 10 defective units from 50 samples, 20 from 100, 25 from 250, and 30 from 500 samples were explored using varying censoring patterns. For comparison, the bias and MSE corresponding to each censoring scheme were also reported. Table 2.5 and Table 2.6 presents the simulation results for different

sample sizes and censoring schemes, showing the bias and MSE for the estimates of two sets of parameter values for α and λ. The results demonstrate that both bias and MSE generally decrease with increasing sample size, indicating improved estimator performance. Additionally, less severe censoring schemes tend to yield more accurate and stable estimates, reinforcing the sensitivity of the estimation procedure to the amount and structure of censoring. In the next phase of our

Table 2.5: Bias and MSE for censored samples when $\alpha = 2$ and $\lambda = 2$.

(n, m)	Scheme	α		λ	
		Bias	MSE	Bias	MSE
(50,40)	$(3, 1^{*17}, 0^{*74})$	0.55525	0.36981	0.07703	0.27317
	$(1^{*10}, 0^{*30})$	-0.50388	0.39812	0.07038	0.26791
	$(1^{*6}, 2^{*2}, 0^{*32})$	-0.53908	0.37788	-0.06319	0.26544
(100,80)	$(3, 1^{*17}, 0^{*74})$	-0.31907	0.32664	-0.05747	0.22466
	$(1^{*20}, 0^{*60})$	0.29410	0.32365	0.05960	0.20423
	$(1^{*10}, 2^{*5}, 0^{*65})$	0.35987	0.34092	0.05286	0.23412
(250,225)	$(5, 1^{*20}, 0^{*204})$	0.15973	0.29583	-0.02564	0.09149
	$(1^{*25}, 0^{*200})$	-0.11093	0.26576	0.03808	0.10100
	$(1^{*15}, 2^{*5}, 0^{*205})$	-0.19132	0.27281	-0.02072	0.10030
(500,470)	$(8, 1^{*22}, 0^{*447})$	-0.04465	0.22883	-0.01187	0.04222
	$(1^{*30}, 0^{*440})$	0.00865	0.19003	-0.00356	0.04248
	$(1^{*10}, 2^{*10}0^{*450})$	-0.04347	0.21237	0.01378	0.04135

analysis, we examine the performance of the proposed model under progressive type-II censoring schemes using the same datasets described earlier. Progressive censoring is often encountered in reliability studies when it is not feasible to observe all units until failure. To replicate such real-life testing conditions, we construct suitable progressive censoring schemes for the datasets and apply our estimation procedure accordingly. This allows us to evaluate the robustness and flexibility of the proposed model in handling censored data scenarios, which are common in practice due to time or cost constraints.

The goodness of fit measures for different censoring schemes corresponding to the two datasets are provided in Table 2.7 and Table 2.8. In both cases, censoring schemes with gradual removal of units or mixed patterns with small

Table 2.6: Bias and MSE for censored samples when $\alpha = 1$ and $\lambda = 0.75$.

(n, m)	Scheme	α		λ	
		Bias	MSE	Bias	MSE
(50,40)	$(2, 1^{*8}, 0^{*31})$	0.26186	0.33701	0.06350	0.05624
	$(1^{*10}, 0^{*30})$	-0.26796	0.32476	-0.06458	0.05244
	$(1^{*6}, 2^{*2}, 0^{*32})$	-0.2466	0.33097	0.07322	0.05151
(100,80)	$(3, 1^{*17}, 0^{*62})$	-0.17735	0.21709	0.04937	0.03384
	$(1^{*20}, 0^{*60})$	0.23250	0.20474	-0.04449	0.02629
	$(1^{*10}, 2^{*5}, 0^{*65})$	-0.24016	0.22308	0.06479	0.02870
(250,225)	$(5, 1^{*20}, 0^{*204})$	0.09305	0.10619	0.02047	0.00980
	$(1^{*25}, 0^{*200})$	-0.09086	0.11073	0.02939	0.00900
	$(1^{*15}, 2^{*5}, 0^{*205})$	-0.08551	0.10445	-0.02313	0.00847
(500,470)	$(8, 1^{*22}, 0^{*447})$	-0.06107	0.05066	-0.01908	0.00451
	$(1^{*30}, 0^{*440})$	-0.03207	0.05263	-0.01418	0.00434
	$(1^{*10}, 2^{*10}0^{*450})$	0.04215	0.05869	0.01893	0.00392

Table 2.7: Goodness of fit measures of censored dataset I.

(n, m)	Scheme	Parameter estimates		KS statistic	p-value
		α	λ		
(107,102)	$(5, 0^{101})$	7.2408	0.0267	0.0701	0.6686
	$(1^{*5}, 0^{*97})$	6.9686	0.0264	0.0678	0.7079
	$(1, 2^{*2}, 0^{*99})$	7.0637	0.0264	0.0695	0.6787
(107,97)	$(10, 0^{*96})$	9.4946	0.0283	0.1040	0.1968
	$(1^{*10}, 0^{*87})$	8.3559	0.0272	0.0954	0.2841
	$(1^{*4}, 2^{*3}, 0^{*90})$	8.5029	0.0273	0.0976	0.2597

early removals, resulted in stable parameter estimates, low KS statistics, and high p-values, indicating a good agreement between the model and the observed data. On the other hand, more concentrated censoring patterns, tended to increase the variability in parameter estimates and yielded higher KS statistics and lower p-values, reflecting a reduced goodness of fit. This effect was more noticeable at higher levels of censoring, where early removals contributed to information loss. Nevertheless, even under these conditions, the model provided acceptable fits for most schemes, demonstrating its flexibility. Overall, the findings align with the trends observed in the simulation study and highlight the robustness of

Table 2.8: Goodness of fit measures of censored dataset II.

(n,m)	Scheme	Parameter estimates		KS statistic	p-value
		α	λ		
(50,46)	$(4,0^{45})$	0.0008	0.8462	0.0762	0.9334
	$(1^{*4},0^{*42})$	0.0007	0.8330	0.0762	0.9335
	$(1,2,0^{*42})$	0.0007	0.8391	0.0762	0.9335
(50,44)	$(6,0^{*43})$	0.2458	0.8514	0.1301	0.3654
	$(1^{*6},0^{*38})$	0.0007	0.8193	0.0762	0.9335
	$(1^{*2},2^{*2},0^{*40})$	0.0007	0.8282	0.0762	0.9335

the proposed model in practical reliability applications involving progressively censored data.

2.8 Modified proportional hazards relevated Weibull model

Among the three types of extreme value distributions discussed in Chapter 1, the type-III extreme value distribution, *i.e.*, the Weibull model plays an important role in providing insights into lifetime scenarios. In this section, we propose a new lifetime model based on the MPHRT using the Weibull distribution as the baseline. Let X be a Weibull random variable, with CDF

$$F_X(x) = 1 - \exp(-x^a), \quad x > 0,\, a > 0. \tag{2.25}$$

Applying the Weibull model in the proposed transform, we obtain the modified proportional hazards relevated Weibull (MPHRW) distribution. The corresponding survival function can be obtained from (2.6) as

$$\bar{F}_Z(x) = \frac{\mathrm{e}^{-x^a}\left((\alpha(\lambda-1)-\lambda)\left(\mathrm{e}^{-x^a}\right)^{\lambda-1}+\lambda\right)}{(\lambda-1)\left((\alpha-1)\left(\mathrm{e}^{-x^a}\right)^{\lambda}+1\right)}, \quad x > 0,\, \lambda,\, \alpha,\, a > 0. \tag{2.26}$$

The density function and hazard rate is given as

$$f_Z(x) = \frac{a\lambda x^{a-1}\left(\left(\mathrm{e}^{-x^a}\right)^{\lambda}\left(\alpha(-\lambda)+(\alpha-1)(\lambda-1)\mathrm{e}^{-x^a}+\alpha+\lambda\right)-\mathrm{e}^{-x^a}\right)}{(1-\lambda)\left((\alpha-1)\left(\mathrm{e}^{-x^a}\right)^{\lambda}+1\right)^2}, \tag{2.27}$$

and

$$h_Z(x) = \frac{a\lambda x^{a-1}\left((\alpha(\lambda-1)-\lambda)\left(\mathrm{e}^{x^a}-1\right)\mathrm{e}^{-\lambda x^a}-\mathrm{e}^{-\lambda x^a}+1\right)}{\left((\alpha-1)\,\mathrm{e}^{-\lambda x^a}+1\right)\left((\alpha(\lambda-1)-\lambda)\,\mathrm{e}^{-(\lambda-1)x^a}+\lambda\right)}. \tag{2.28}$$

In Figure 2.5, we plot the hazard rate of the MPHRW model. We observe that, the transformed model incorporates IHR, DHR and the non-monotonic UBT shape in comparison with the monotonic shapes of the Weibull model.

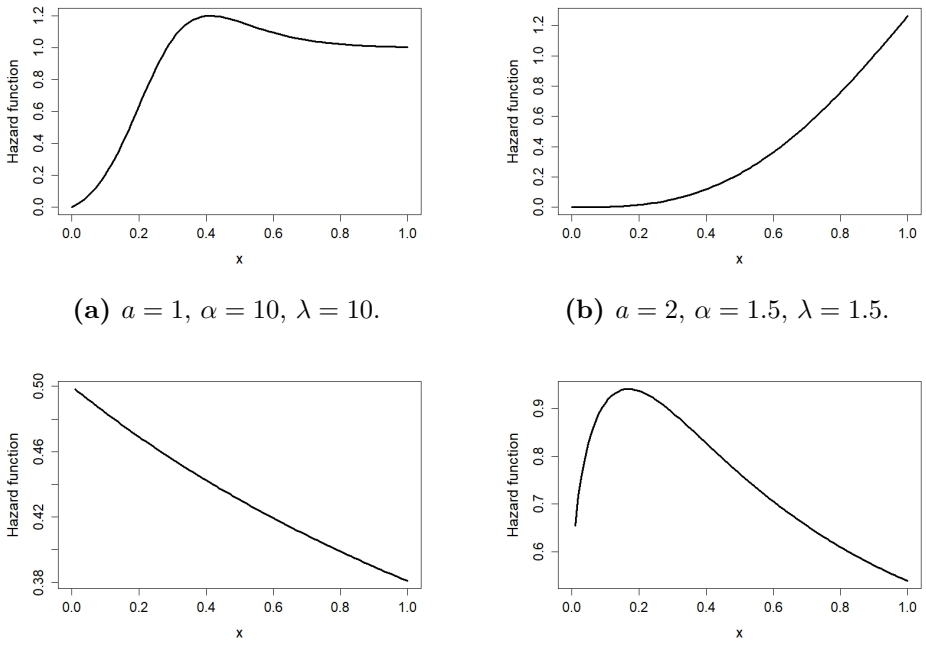

(a) $a = 1$, $\alpha = 10$, $\lambda = 10$. **(b)** $a = 2$, $\alpha = 1.5$, $\lambda = 1.5$.

(c) $a = 0.5$, $\alpha = 2$, $\lambda = 2$. **(d)** $a = 0.5$, $\alpha = 5$, $\lambda = 5$.

Figure 2.5: Hazard plots of MPHRW model.

Note that, the observations from the Figure 2.5 aligns with the findings in Proposition 2.6.

2.8.1 Parameter estimation

Let $X_1, X_2, \ldots, X_n$ be a random sample of size n from the MPHRW distribution with parameters (a, α, λ), and $\underline{x} = (x_1, x_2, \ldots, x_n)$ denote the corresponding observed values. Then, the log-likelihood function can be obtained from (2.27) as

$$L(a, \alpha, \lambda \mid \underline{x}) = \sum_{i=1}^{n} \left(\log a + \log \lambda + (a-1)\log x_i + \log A_i - \log(1-\lambda) - 2\log B_i\right),$$

where $A_i = \mathrm{e}^{-\lambda x_i^a}\Big[\alpha(-\lambda)+(\alpha-1)(\lambda-1)\mathrm{e}^{-x_i^a}+\alpha+\lambda\Big]-\mathrm{e}^{-x_i^a}$, $B_i = (\alpha-1)\mathrm{e}^{-\lambda x_i^a}+1$. The corresponding derivatives are

$$\frac{\partial L}{\partial a} = \sum_{i=1}^{n}\left[\frac{1}{a} + \log x_i + \frac{1}{A_i}\frac{\partial A_i}{\partial a} - \frac{2}{B_i}\frac{\partial B_i}{\partial a}\right],$$
$$\frac{\partial L}{\partial \alpha} = \sum_{i=1}^{n}\left[\frac{1}{A_i}\frac{\partial A_i}{\partial \alpha} - \frac{2}{B_i}\frac{\partial B_i}{\partial \alpha}\right],$$

and

$$\frac{\partial L}{\partial \lambda} = \sum_{i=1}^{n}\left[\frac{1}{\lambda} + \frac{1}{1-\lambda} + \frac{1}{A_i}\frac{\partial A_i}{\partial \lambda} - \frac{2}{B_i}\frac{\partial B_i}{\partial \lambda}\right].$$

Equating these equations to zero yields the likelihood equations corresponding to the parameters. As closed-form solutions are not available, the MLE are obtained through numerical techniques.

2.8.2 Real data analysis

We now move on to the application of the proposed model in real life scenarios. For this we consider two datasets. The first data concerns with application in reliability analysis. It consists of the failure times of 18 electronic devices initially reported in Wang (2000). We fit the data using the proposed MPHRW model and compare it with the corresponding baseline Weibull model. The KS statistic and p-value are given in Table 2.9.

Table 2.9: Goodness of fit measures for dataset I.

Model	Parameter estimates	KS statistic	p-value
MPHRW	$a = 0.7365$ $\alpha = 6.2381$ $\lambda = 0.0519$	0.1028	0.9806
Weibull	$\alpha = 1.1452$ $\lambda = 179.6586$	0.1129	0.9560

From Table 2.9 we can infer that proposed MPHRW model is better when compared to the baseline Weibull model, making it a better choice in these scenarios. The Q-Q plot given in Figure 2.6 a reiterates the fact that the proposed model fits the data well.

We now consider an extreme data in order to showcase the applicability of the MPHRW model in extreme scenarios. For this, we consider the thirty years of annual extreme wind speed data for Jacksonville, Florida, with storm types classified according to Changery's methodology, reported in Kinnison (1983). The wind speeds have been adjusted to represent values in miles per hour at a height of 10 meters. To show the efficiency of the proposed model when compared to the baseline Weibull model, we provide the KS statistic and p-value, in Table 2.10.

Table 2.10: Goodness of fit measures for dataset II.

Model	Parameter estimates	KS statistic	p-value
MPHRW	$a = 1.3626$ $\alpha = 426.4520$ $\lambda = 0.0319$	0.1020	0.9139
Weibull	$\alpha = 4.8020$ $\lambda = 52.2204$	0.1751	0.3168

Table 2.10 indicates that the proposed MPHRW model fits the extreme data better than the usual Weibull model. Moreover, the Q-Q plot given in Figure 2.6 b also indicates that the proposed model fits the data well.

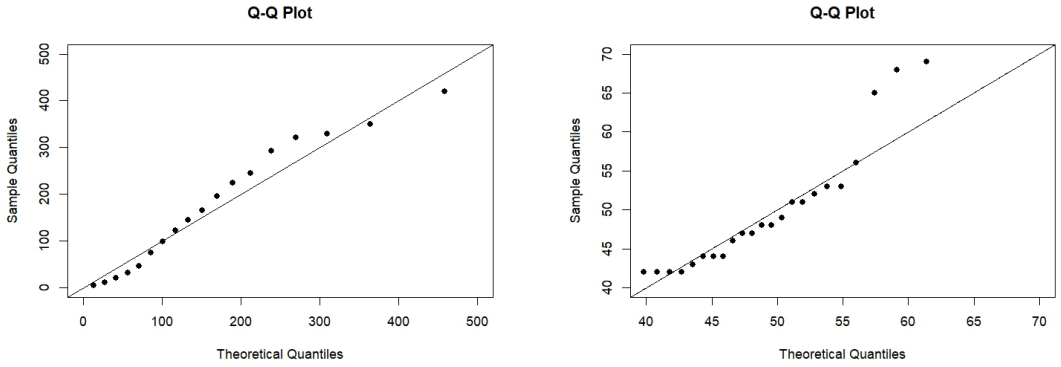

(a) Q-Q plot of dataset I.

(b) Q-Q plot of dataset II.

Figure 2.6: Q-Q plot of the MPHRW model for the two datasets.

2.9 Summary of the chapter

In this chapter, we have introduced and analyzed a new reliability model based on the relevation transform under the modified proportional hazards framework. Theoretical investigations into the model's aging characteristics, stochastic orderings, and hazard rate flexibility have been presented, along with the proposal of a generalized exponential distribution to demonstrate its structural advantages. A detailed Monte Carlo simulation study confirmed the consistency and accuracy of the parameter estimates under both complete and progressively censored samples. Furthermore, real data analyses illustrated the model's practical applicability and robustness under varying censoring schemes. A new generalization of Weibull model is also proposed and its properties and real data applications based on a reliability and extreme data are analyzed.

Chapter 3

Multi-phase auto-relevation transform

3.1 Introduction

As discussed in Chapter 1, the relevation transform was introduced both as a method for generating new lifetime distributions and as a framework for modeling replacement strategies following component failure in manufacturing systems. In this chapter, we focus on a special case, called the auto-relevation transform, which arises when the primary and redundant components are identically distributed. We further extend this concept to a multi-phase setting and develop results based on reliability properties and their connection with the Poisson process.

We discuss various reliability aspects of the distribution at the n^{th} stage of replacements. Among these, the most important one is to know how the aging characteristics like hazard rate, mean residual life, etc., change over time across different phases, in terms of various aging notions. When the baseline distribution of lifetimes is known from the information available from the initial phase, our results help the analyst to understand what would happen in the successive phases. Often replacement or repair strategies are adopted by industries to improve the reliability of their products. Two important methods applied in such circumstances are (i) to replace the failed unit by a new unit with

the same life distribution resulting in a renewal process and (ii) to replace the failed unit by means of another one with the same age resulting in the minimal repair strategy and the accompanying process is a non-homogeneous Poisson process (NHPP). The properties of the NHPP and its intensity function play a crucial role in the second case. To address this, we develop characterization results with relevance to various practical applications.

The remainder of the chapter is as follows: A brief overview of auto-relevation transform is provided in Section 3.2. The multi-phase auto-relevation transform and its aging properties are explored in Section 3.3. Stochastic ordering results based on distortion relation are provided in Section 3.4. In Section 3.5, we delve into the analysis of the non-homogeneous Poisson process based on the ART, called the auto-relevation process. Various characterization results based on the auto-relevation process are derived in Section 3.6. The chapter is concluded in Section 3.7.

3.2 Auto-relevation transform

The auto-relevation transform (ART) is obtained as a special case of the relevation transform given in (1.1) when X and Y are identically distributed with survival function $\bar{F}(\cdot)$. The survival function of ART is given by

$$A(x) = \bar{F}(x)\left(1 - \log \bar{F}(x)\right). \tag{3.1}$$

A physical interpretation of the ART is as follows: when a component fails at age x and is instantaneously replaced by another component of the same age, the total lifetime of the resulting unit follows the ART. Since its inception, the ART has evoked considerable interest in different areas such as, repair (replacement) strategies in production processes, characterization of probability distributions, aging properties of devices, evolution of cumulative entropies, sequential order statistics, stochastic comparisons of reliability systems, etc. Dimitrov et al. (1997) provided a characterization that, for two independent and identically

distributed exponential random variables X and Y, the random variable $X\nu Y$ has the same distribution as $X + Y$. They have also applied the transform in case of problems related to periodic random environments and queuing theory. Baxter (1982) has extended the ART to find the survival function of the time to n^{th} failure when the above replacement is applied recursively and found that the number of failures in $(0, t]$ is a NHPP. From a practical standpoint, industrial systems rarely operate without interruptions, and immediate replacement or repair upon failure is essential for continuous functioning. Consequently, when each replacement involves a new component having the same age and life distribution as the failed one, the relevation process implied by (3.1) must be applied recursively. This naturally leads to the framework of multi-phase auto-relevation, in which successive applications of (3.1) are required to obtain the distribution of failure times at different stages of system operation. In this direction, Krakowski (1973) derived the survival function of (3.1) at its n^{th} phase and investigated some properties of the resulting distribution.

Following this, the NHPP under this scheme and other results associated with this were studied by several authors. Sordo and Psarrakos (2017) who discussed the allocation of relevation in redundancy problems by comparing inter-failure times consequent on replacement and the study of the role of relevation policies in Arriaza et al. (2018) and Zhang and Zhao (2019) are two major developments. When one looks at the state of the process at time t two important factors that have relevance are the age and the residual life of the unit that is working at the juncture. Considerable amount of literature is available on these notions in the renewal process and the roles they play in different fields. Kirmani and Gupta (1989) have shown that the residual life has the same expression as the conventional concept available in reliability literature and derived a crucial relationship between the intensity (hazard) rate and the mean age at repair. We have explored this relationship further to determine the life distribution from it and also to characterize several distributions whose hazard rates generate some useful models of NHPP. We now move on to the multi-phase auto-relevation transform and delve into its reliability properties.

3.3 Multi-phase auto-relevation transform

Let $\bar{F}_n(\cdot)$ be the survival function of the time to failure of a unit at the n^{th} phase of a system, given that at each phase, the failed component is replaced by one of equal age and with the same life distribution $\bar{F}(\cdot)$. Then

$$\bar{F}_n(x) = \begin{cases} 1 - K(x), & n = 0 \\ \bar{F}(x), & n = 1 \\ \bar{F}_{n-1}(x)\nu\bar{F}(x), & n \geq 2, \end{cases}$$

where $K(\cdot)$ is the step down Heaviside function. It is shown in Krakowski (1973) that

$$\bar{F}_n(x) = \bar{F}(x) \sum_{r=0}^{n-1} \frac{(-\log \bar{F}(x))^r}{r!}, \quad n = 1, 2, \ldots, \tag{3.2}$$

is the survival function of the n^{th} phase ART. We denote by X_n the random variable with survival function (3.2), by $f_n(\cdot)$ its density function and by $f(\cdot)$ and $\bar{F}(\cdot)$ the density and survival functions of X. The hazard rates of X and X_n are $h(x) = -\frac{d \log \bar{F}(x)}{dx} = \frac{f(x)}{\bar{F}(x)}$ and $h_n(x) = -\frac{d \log \bar{F}_n(x)}{dx}$ with corresponding cumulative hazard rates $H(x) = \int_0^x h(t)\, dt = -\log \bar{F}(x)$ and $H_n(x) = -\log \bar{F}_n(x)$, respectively. From (3.2), we have

$$\bar{F}_n(x) = \bar{F}(x) \sum_{r=0}^{n-1} \frac{H^r(x)}{r!} \qquad f_n(x) = \frac{H^{n-1}(x) f(x)}{(n-1)!}.$$

It has been noted in Gupta and Kirmani (1988) and Psarrakos and Navarro (2013) that the above density function is equivalent to that of the n^{th} upper record value of a sequence of independent and identically distributed random variables. For brevity, writing $S_n(x) = \sum_{r=0}^{n-1} \frac{H^r(x)}{r!}$, $n = 1, 2, \ldots$, we have $S_1(x) = 1$, $S_2(x) = 1 + H(x)$ and

$$\bar{F}_n(x) = \bar{F}(x) S_n(x), \tag{3.3}$$

$$f_n(x) = (S_n(x) - S_{n-1}(x))\, f(x), \text{ for } n = 1, 2, \ldots, \tag{3.4}$$

where $S_n(x) - S_{n-1}(x) = \frac{H^{n-1}(x)}{(n-1)!} \geq 0$, so that $\{S_n(x),\, n = 1, 2, \ldots\}$ is an increasing sequence and $S'_n(x) = S'_{n-1}(x)h(x)$, where prime denote derivative. Further

$$\begin{aligned} h_n(x) &= \frac{H^{n-1}(x)h(x)}{S_n(x)} \\ &= \left(\frac{S_n(x) - S_{n-1}(x)}{S_n(x)}\right) h(x) \\ &= \left(1 - \frac{S_{n-1}(x)}{S_n(x)}\right) h(x), \quad n = 2, 3, \ldots. \end{aligned} \tag{3.5}$$

Specializing for the phase 2, the results are

$$\bar{F}_2(x) = (1 + H(x))\, \bar{F}(x), \quad h_1(x) = h(x), \quad h_2(x) = \frac{H(x)h(x)}{1 + H(x)}. \tag{3.6}$$

It follows from (3.5) that $\{h_n(x),\, n = 1, 2, \ldots\}$ is a decreasing sequence of hazard rates justifying the relevation strategy for replacement.

One of the points of interest in reliability theory is to assess the reliability of the unit in the n^{th} phase as it progresses through the different phases in the operation. That is, to determine whether the operation has enhanced or reduced the probability of successful working of the system. This aspect is generally done by comparing certain functions that characterize the life distributions like the hazard rate, mean residual life function, etc. A second aspect is whether the behavior of the functions of the baseline distribution has undergone changes over time. We will examine these two aspects using the identity obtained in (3.2) through (3.6). Among the various reliability concepts considered for the analysis, the hazard rate plays a pivotal role and the manner in which it behaves during the different phases is of primary concern. From (3.5), we have

$$h'_n(x) = \left(1 - \frac{S_{n-1}(x)}{S_n(x)}\right) h'(x) - h(x)\frac{d}{dx}\left(\frac{S_{n-1}(x)}{S_n(x)}\right). \tag{3.7}$$

But

$$\frac{d}{dx}\left(\frac{S_n(x)}{S_{n-1}(x)}\right) = \frac{d}{dx}\left(\frac{\sum_{r=0}^{n-1}\frac{H^r(x)}{r!}}{\sum_{r=0}^{n-2}\frac{H^r(x)}{r!}}\right).$$

The sign of the above derivative is determined by

$$\begin{aligned}\left(\sum_{r=0}^{n-2}\frac{H^r(x)}{r!}\right)\frac{H^{n-2}(x)h(x)}{(n-2)!} &- \left(\sum_{r=0}^{n-3}\frac{H^r(x)}{r!}\right)\frac{H^{n-1}h(x)}{(n-1!)} \\ &= \frac{h(x)H^{n-2}(x)}{(n-2)!}\left(\sum_{r=0}^{n-2}\left(\frac{1}{r!}-\frac{1}{(r-1)!(n-1)}\right)H^r(x)\right) \\ &= \frac{h(x)H^{n-2}(x)}{(n-2)!}\left(\sum_{r=0}^{n-2}\frac{1}{(r-1)!}\left(\frac{1}{r}-\frac{1}{n-1}\right)H^r(x)\right).\end{aligned}$$

Since $r \leq n-1$, we have $\frac{1}{r} \geq \frac{1}{n-1}$. Consequently, $\frac{d}{dx}\left(\frac{S_n(x)}{S_{n-1}(x)}\right) \geq 0$, which implies that $\frac{S_n(x)}{S_{n-1}(x)}$ is increasing in x, and hence its reciprocal $\frac{S_{n-1}(x)}{S_n(x)}$ is decreasing in x. Therefore, if X is IHR, so that $h'(x) \geq 0$, it follows that $h'_n(x) \geq 0$, and consequently X_n also possesses the IHR property. Similarly, from (3.7) we observe that if X_n is DHR, then X is also DHR. Also, if X has no-aging, *i.e.*, when X is exponential with parameter λ, the distribution of X_n is gamma with

$$f_n(x) = \frac{\lambda^n \mathrm{e}^{-\lambda x}x^{n-1}}{\Gamma(n)} \quad \text{and} \quad h_n(x) = \frac{\lambda(\lambda x)^{n-1}}{\sum_{r=0}^{n-1}\frac{(n-1)!(\lambda x)^r}{r!}}. \tag{3.8}$$

It is well known that (3.8) is IHR for $n > 1$ and no-aging for $n = 1$. Figure 3.1 provides plot of $h_n(x)$ for various values of n and λ.

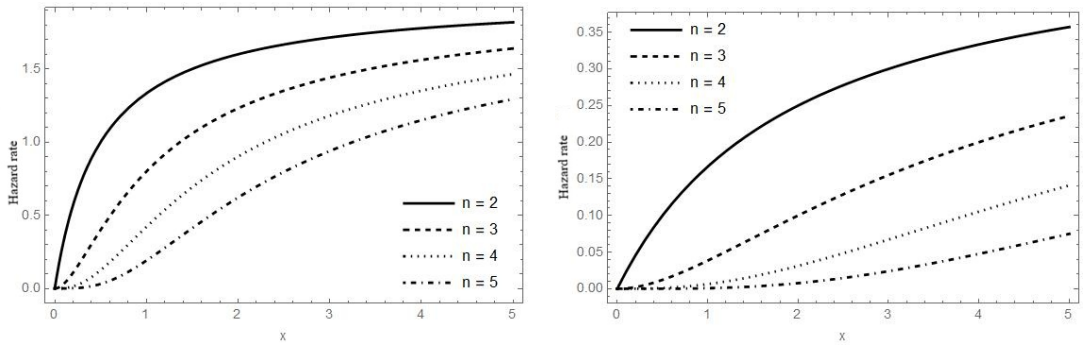

(a) $\lambda = 2$ **(b)** $\lambda = 0.5$

Figure 3.1: Hazard plots of n^{th} phase auto-relevated exponential model

In general, from (3.7), we have the DHR property is not preserved from X to X_n. To resolve this if it is assumed that X is DHR, then from (3.7) the necessary conditions for X_n to have DHR is

$$\left(1-\frac{S_{n-2}(x)}{S_{n-1}(x)}\right)h'(x) \leq h(x)\frac{d}{dx}\left(\frac{S_{n-2}(x)}{S_{n-1}(x)}\right), \quad \text{for } x>0,$$

or equivalently

$$\frac{d}{dx}\left(\log(B(x)h(x)\right) \leq 0, \tag{3.9}$$

where $B(x) = 1-\frac{S_{n-2}(x)}{S_{n-1}(x)}$. It is worth noting that in cases where the inequality (3.9) is not satisfied, the hazard rate $h_n(x)$ may exhibit different possible behaviors, even when the baseline hazard $h(x)$ is decreasing. These situations are illustrated in the following example.

Example 3.1. Let X follow a Weibull distribution with density

$$f(x) = \lambda x^{\lambda-1}\exp(-x^{\lambda}), \qquad x>0,\ \lambda>0,$$

so that $H(x) = x^{\lambda}$, $\bar{F}(x) = \exp(-x^{\lambda})$ and $h(x) = \lambda x^{\lambda-1}$. Consider X_2, the second phase auto-relevated Weibull distribution. Its survival and hazard rates are

$$\bar{F}_2(x) = \exp(-x^{\lambda})\big(1+x^{\lambda}\big), \qquad h_2(x) = \frac{\lambda x^{2\lambda-1}}{1+x^{\lambda}}. \tag{3.10}$$

For $\lambda = 1.5$, we have $\bar{F}(x) = \exp(-x^{1.5})$ and $h(x) = 1.5\,x^{0.5}$, which is IHR. For $n=2$, we have $\bar{F}_2(x) = \exp(-x^{1.5})(1+x^{1.5})$, and $h_2(x) = \frac{1.5\,x^2}{1+x^{1.5}}$. Observe that $h_2(x)$ is also increasing on $(0,\infty)$. Hence the IHR property is preserved. Next, consider $\lambda = 0.75$. Here we have X is DHR and the respective survival and hazard rates of the second phase are

$$\bar{F}_2(x) = \exp(-x^{0.75})(1+x^{0.75}) \quad \text{and} \quad h_2(x) = \frac{0.75\,x^{0.5}}{1+x^{0.75}}.$$

Differentiating $h_2(x)$, we observe that the sign of $h_2'(x)$ depends on

$$A(x) = \frac{0.375}{x^{0.25}} - 0.1875\,x^{0.5},$$

and $A(x) = 0$ at $x = 2.5198$, which is the turning point of a UBT hazard rate, presented in Figure 3.2. Hence the DHR property is not preserved. To further examine the aging behavior of the model (3.10), consider the Glaser's function $\eta_2(x) = \frac{f_2'(x)}{f_2(x)}$, where $f_2(\cdot)$ is the density of X_2. From (3.10), we have $\eta_2(x) = \frac{\lambda\left(2+x^\lambda\right)-1}{x}$, and

$$\eta_2'(x) = \frac{\lambda^2 x^\lambda - \lambda\left(x^\lambda - 2\right) - 1}{x^2}.$$

If $\lambda > 1$, then $\eta_2'(x) > 0$ for all $x > 0$, and hence, by Glaser's criterion, X_2 is IHR. If $\frac{1}{2} < \lambda < 1$, solving $\eta_2'(x) = 0$ yields a unique critical point

$$x_0 = \left(\frac{1-2\lambda}{(\lambda-1)\lambda}\right)^{1/\lambda},$$

with $\eta_2''(x_0) < 0$, implying that the hazard rate of X_2 has a UBT shape, with change point $\left(\frac{1-2\lambda}{\lambda-1}\right)^{1/\lambda}$. Finally, for $0 < \lambda \leq \frac{1}{2}$, we have $\eta_2'(x) < 0$ for all $x > 0$, and hence X_2 is DHR. Accordingly, although the IHR property is preserved under the second-phase auto-relevation mechanism, the DHR property is not retained in general. In particular, the shape of the hazard rate of X_2 depends critically on the parameter λ; it may exhibit an increasing, decreasing, or non-monotonic shape. These distinct behaviors are depicted in Figure 3.2.

Another concept of central importance is that of distortion functions, which were introduced and discussed in Chapter 1. Building on this framework, the following proposition presents a distorted representation of $F_n(\cdot)$ in terms of the baseline distribution function $F(\cdot)$.

Proposition 3.1. Let X_n be the n^{th} phase ART random variable corresponding to X with respective CDFs $F_n(x)$ and $F(x)$. Then X_n has a distorted representation of X with distortion function

$$q(u) = u \sum_{r=0}^{n-1} \frac{(-\log u)^r}{r!} \quad 0 < u < 1. \tag{3.11}$$

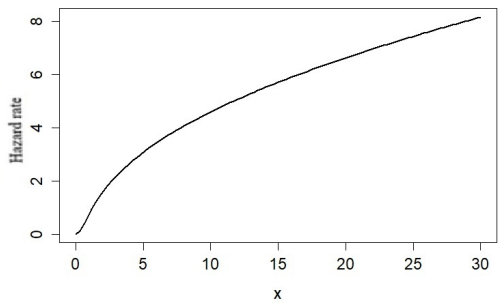

(a) $\lambda = 1.5$

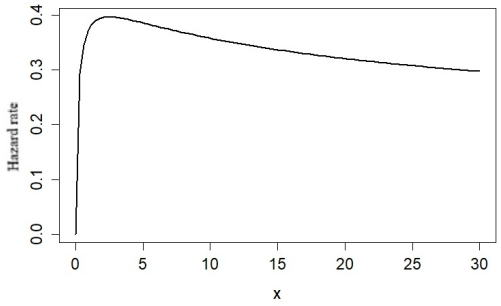

(b) $\lambda = 0.75$

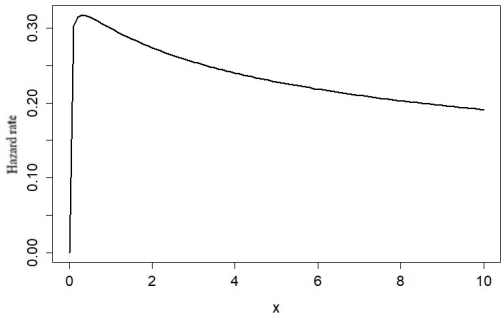

(c) $\lambda = 0.6$

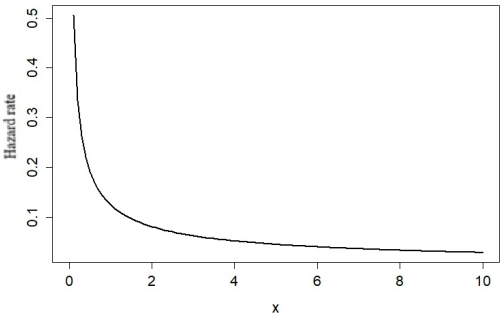

(d) $\lambda = 0.25$

Figure 3.2: Hazard plots of second phase auto-relevated Weibull model

Proof. From (3.2), the survival function of X_n is

$$\bar{F}_n(x) = \bar{F}(x) \sum_{r=0}^{n-1} \frac{(-\log(\bar{F}(x)))^r}{r!} = q(\bar{F}(x)),$$

where $q(u) = u \sum_{r=0}^{n-1} \frac{(-\log u)^r}{r!}$, which completes the proof. □

Observe that the function $q(u)$ is concave in u. In addition to the hazard rate class, several other important aging notions play an important role in reliability analysis. In the following theorem, we establish the preservation of the DRHR and ID classes using the distortion relation between X and X_n.

Proposition 3.2. If X_n is the n^{th} phase ART random variable of X, then for $n > 1$, we have the following:

(i) X is DRHR, then X_n is DRHR.

(ii) X is ID, then X_n is ID.

Proof. (i) From Result 2, we observe that the monotonic decrease of $l_2(u) = \frac{u\,q'(1-u)}{1-q(1-u)}$ in $(0,1)$ is sufficient to establish the result. We have

$$l_2(u) = -\frac{u(-\log(1-u))^{n-1}}{\Gamma(n) - \Gamma(n, -\log(1-u))}.$$

Denote $\Gamma(n) - \Gamma(n,t) = \gamma(n,t)$, where $t = -\log(1-u)$. Note that $\gamma(n,t)$ is the lower incomplete gamma function. Since $\frac{d}{dt}(\gamma(n,t)) = t^{n-1}\mathrm{e}^{-t} > 0$, $\gamma(n,t)$ is increasing. Even though the numerator $u\,t^{n-1}$ and the denominator $\gamma(n,t)$ of $l_2(u)$ are increasing, the denominator grows at a faster rate. Hence, $l_2(u)$ is decreasing for $u \in (0,1)$ for $n \geq 1$. The plot of $l_2(u)$ for various values of n is given in Figure 3.3. This completes the proof of (i).

(ii) From Result 7, the proof of (ii) holds, since $q(u)$ is concave in u. □

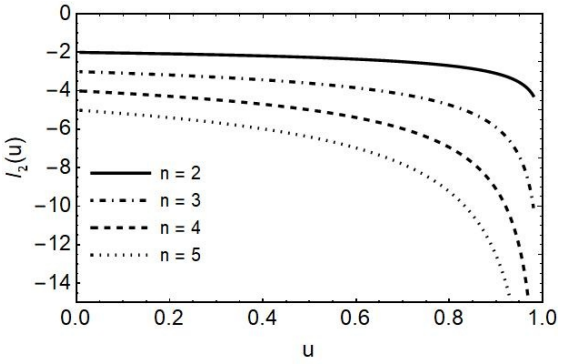

Figure 3.3: Plot of $l_2(u)$ against u

Proposition 3.3. Let X_n be the n^{th} phase ART random variable of X. Then

(i) X_n is always NBUHR, provided $f(0) = 0$.

(ii) X_n is DMRL if X is DMRL and

$$\frac{1}{\bar{F}(x)} \int_x^\infty \bar{F}(t)(S_n(t) - 1)\,dt,$$

is decreasing.

Proof. (i) From (3.5), and $S_n(0) = 1$, $n = 2, 3, \ldots$, we have $h_n(x) \geq 0 = h_n(0)$ and so X_n is NBUHR.

(ii) The mean residual life function of X_n is

$$\begin{aligned} m_n(x) &= \frac{1}{\bar{F}_n(x)} \int_x^\infty \bar{F}_n(t)\, dt \\ &= \frac{1}{\bar{F}_n(x)} \int_x^\infty \bar{F}(t) S_n(t)\, dt \\ &= \frac{1}{\bar{F}(x) S_n(x)} \int_x^\infty \left(\bar{F}(t) + \sum_{r=1}^{n-1} \bar{F}(t) \frac{H^r(t)}{r!} \right) dt \\ &= \frac{1}{S_n(x)} \left(m(x) + \frac{1}{\bar{F}(x)} \int_x^\infty \sum_{r=1}^{n-1} \bar{F}(t) \frac{H^r(t)}{r!} \right) dt. \end{aligned}$$

Since $S_n(x)$ is increasing in x, we conclude that $m_n(x)$ is decreasing whenever the second term in the braces is decreasing. The role of mean residual life in relating the relevation transform with measures of uncertainty will be discussed in Section 3.6. □

3.4 Stochastic orders

Stochastic orderings provide a systematic framework for comparing lifetime distributions at different stages of system operation and are widely used in reliability analysis, survival modeling, and risk assessment. In this section, several stochastic orders are further investigated using distortion functions, with the objective of examining and establishing ordering relationships between the random variables X and X_n, building on the results presented Section 1.6.4 in Chapter 1.

Proposition 3.4. Let X be a non-negative continuous random variable and X_n be the corresponding n^{th} phase ART random variable. Then $X_n \geq_{lr} X$, for $n > 1$.

Proof. Recalling Result 8, from 3.11 we have

$$\frac{q'(u)}{q_1'(u)} = \frac{(-\log(u))^{n-1}}{\Gamma(n)},$$

and

$$\frac{d}{du}\left(\frac{q'(u)}{q_1'(u)}\right) = -\frac{(n-1)(-\log(u))^{n-2}}{u\Gamma(n)} < 0, \quad \text{for } n > 1,$$

which completes the proof. □

Based on the findings outlined in Shaked and Shanthikumar (2007), Navarro et al. (2013), we have the following implications.

$$\begin{array}{ccccccccc} & & X_n \geq_{mrl} X & & & & X_n \geq_{ew} X & & \\ & & \Uparrow & & & & \Uparrow & & \\ X_n \geq_{lr} X & \Longrightarrow & X_n \geq_{hr} X & \Longrightarrow & X_n \geq_{or} X & \Longrightarrow & X_n \geq_{st} X & \Longrightarrow & X_n \geq_{icx} X \\ \Downarrow & & & & & & & & \Downarrow \\ X_n \geq_{rhr} X & \Longrightarrow & X_n \geq_{mit} X & & & & X_n \geq_{su} X & \Longleftarrow & X_n \geq_{*} X \end{array}$$

Proposition 3.5. Let X and Y be two random variables with survival functions $\bar{F}_X(\cdot)$ and $\bar{F}_Y(\cdot)$ respectively. Suppose X_n and Y_n are the corresponding n^{th} phase ART random variables. Then, for $n > 1$ the following properties hold:

(i) If $X \leq_{st} Y$, then $X_n \leq_{st} Y_n$.

(ii) If $X \leq_{disp} Y$, then $X_n \leq_{disp} Y_n$.

(iii) If $X \leq_{hr} Y$, then $X_n \leq_{hr} Y_n$.

(iv) If $X \leq_{icx} Y$, then $X_n \leq_{icx} Y_n$.

(v) If $X_n \leq_{ttt} Y_n$, then $X \leq_{ttt} Y$.

(vi) If $X \leq_{ew} Y$, then $X_n \leq_{ew} Y_n$.

Proof. Proof of (i) and (ii) directly follow from Result 9 and Result 15.

To prove (iii), from Result 10, we have

$$\frac{u\ q'(u)}{q(u)} = \frac{u(-\log(u))^{n-1}}{\Gamma(n, -\log(u))},$$

whose first derivative is obtained as

$$-\frac{(-\log(u))^{n-2}\left(u(-\log(u))^n+(n+\log(u)-1)\Gamma(n,-\log(u))\right)}{\Gamma(n,-\log(u))^2}>0, \quad \text{for } n>1,$$

which proves (iii).

The proofs of (iv), (v), and (vi) follow directly from Results 13, 14, and 16, respectively. □

3.5 Auto-relevation process

Assume that there is an arbitrarily large collection of units whose lifetimes X_n, $n = 1, 2, \ldots$ are independent and identically distributed with survival function $\bar{F}(\cdot)$ and hazard rate $h(\cdot)$. The operation of the system of units is such that (i) a unit of the system starts functioning at time $t = 0$ with all other units follow a hot standby (ii) when the unit in operation fails it is replaced by another item of the same age selected from the units still working (iii) again a similar replacement is made when the second item fails and so on, repeating the process. The above replacement procedure is equivalent to the repairing and restoring the failed unit immediately to its old condition at the time of failure and is categorized as a minimal repair process. Obviously, this process is equivalent to the auto-relevation process. If $N(t)$ denotes the number of failures in the interval $(0, t]$, then Baxter (1982) has shown that

$$P(N(t)=n)=\frac{\bar{F}(t)H^n(t)}{n!}, \quad n=0,1,2,\ldots, \tag{3.12}$$

so that $\{N(t), t > 0\}$ is a NHPP, with intensity rate $h(t)$ satisfying $H(t) = \int_0^t h(x)\,dx$ and $\bar{F}(t) = \mathrm{e}^{-H(t)}$. The interest of the researcher is noted more on the time and sequence of failures or on the inter-failure times than on $N(t)$, the number of failures during the process. The existing literature do not throw light on more information about the properties of the distribution of X_n and Y_n than their means. However the higher moments are also essential, especially

when estimation or testing of the mean and variance of the characteristics are considered. Therefore, we evaluate these two quantities at first and point out their use in certain well known NHPP models. Further new results concerning the process can also be seen in Section 3.6. The s^{th} moment of failure time at the n^{th} phase is

$$\begin{aligned} E(X_n^s) &= \int_0^\infty t^s \frac{H^{n-1}(t)f(t)}{(n-1)!}\,dt \\ &= \int_0^\infty \left(\frac{s\,t^{s-1}H^{n-1}(t)}{(n-1)!} + \frac{t^s H^{n-2}(t)h(t)}{(n-2)!} \right) \bar{F}(t)\,dt \\ &= \int_0^\infty \frac{s\,t^{s-1}H^{n-1}(t)}{(n-1)!}\bar{F}(t)\,dt + \int_0^\infty t^s \frac{H^{n-2}(t)}{(n-2)!} f(t)\,dt \\ &= E(X_{n-1}^s) + \frac{s}{(n-1)!}\int_0^\infty t^{s-1}H^{n-1}(t)\bar{F}(t)\,dt. \end{aligned} \tag{3.13}$$

When $s = 1$, we have the expression for the mean time to failure at the n^{th} phase given in Baxter (1982) and (Beichelt (1993)) as

$$E(X_n) = E(X_{n-1}) + \int_0^\infty \frac{H^{n-1}(t)}{(n-1)!}\bar{F}(t)\,dt. \tag{3.14}$$

The time between the $(n-1)^{th}$ and n^{th} failure, $Y_n = X_n - X_{n-1}$, $n = 1, 2, \ldots,$ with $X_0 = 0$ has distribution function (Beichelt and Tittmann (1991)) as

$$G_n(t) = \int_0^\infty \frac{\bar{F}(t+u)}{\bar{F}(u)} f_{n-1}(u)\,du, \tag{3.15}$$

so that

$$\bar{G}_n(t) = \int_0^\infty \frac{H^{n-1}(u)}{(n-1)!} f(t+u)\,du.$$

We have

$$\begin{aligned} E(Y_n^s) &= \int_0^\infty y^s g_n(y)\,dy \\ &= s\int_0^\infty y^{s-1}\bar{G}_n(y)\,dy \\ &= s\int_0^\infty\int_0^\infty \left(y^{s-1}\frac{\bar{F}(y+u)}{\bar{F}(u)}\,dy\right) g_{n-1}(u)\,dy \\ &= s\int_0^\infty E((X-u)^{s-1} \mid X>u)\, g_{n-1}(u)\,du \\ &= s\int_0^\infty m_X^{s-1}(y)\, g_{n-1}(y)\,dy, \quad s\geq 2, \end{aligned} \tag{3.16}$$

where $m_X^r(y) = E((X-y)^r \mid X > y)$ of the random variable X_n is the r^{th} moment of its residual life. The integral (3.16) is interpreted as the expected value of $(s-1)^{th}$ moment of residual life X with respect to the distribution of Y_n given in (3.15). Note that, from (3.14), we have

$$E(Y_n) = E(X_n) - E(X_{n-1)}) = \int_0^\infty \frac{H^{n-1}(t)}{(n-1)!}\bar{F}(t)\,dt. \tag{3.17}$$

Example 3.2. Power law process: The power law process is a very popular model belonging to the NHPP used to represent the times of occurrence of recurrent events in a variety of fields such as reliability, economics, information sciences, finance, etc. It is NHPP with power function for its intensity function, $H(t) = (\lambda t)^\alpha$, so that the survival function is Weibull with

$$f(t) = \alpha\,\lambda^\alpha\, t^{\alpha-1} \exp -(\lambda\, t)^\alpha,$$

and

$$\bar{F}(t) = \exp\left(-(\lambda\, t)^\alpha\right), \quad \lambda,\, \alpha > 0,\, t > 0. \tag{3.18}$$

The probability density function of the failure time at the n^{th} phase is

$$f_n(t) = \frac{\alpha\,\lambda}{\Gamma(n)}(\lambda\,t)^{n\alpha-1}\exp\left(-(\lambda\,t)^{\alpha}\right), \quad n = 1, 2, \ldots. \tag{3.19}$$

The distribution (3.19) remains valid when n is a positive real number. Note that (3.19) was introduced by Amoroso (1925) as a generalized gamma distribution and a comprehensive study of its properties is available in Bondesson (1992). It contains the gamma distribution when $\alpha = 1$, the Weibull when $n = 1$, the exponential when $n = 1$ and $\alpha = 1$ and the log-normal law as a limiting case when $n \to \infty$. The survival function of X_n is

$$\bar{F}_n(t) = \frac{\Gamma_{(\lambda\,t)^{\alpha}}(n)}{\Gamma(n)},$$

where $\Gamma_a(p) = \int_a^{\infty} \mathrm{e}^{-y} y^{p-1}\,dy$, is the incomplete gamma function. One can see that the hazard rate $h(t)$ is in terms of incomplete gamma function and is difficult to analytically examine its nature. However the use of Glaser function $\eta(x) = \frac{-f'(x)}{f(x)}$ is applicable in this case to distinguish the shape of the hazard rate as (i) IHR if $\alpha > 1$, $n \geq \frac{1}{\alpha}$, (ii) DHR if $\alpha \leq 1$, $n \leq \frac{1}{\alpha}$ (iii) bathtub shaped if $\alpha > 1$, $n\alpha < 1$ and (iv) UBT shaped if $\alpha < 1$, $n\alpha > 1$. Further, we have

$$E\left(X_n^r\right) = \frac{\Gamma\left(\frac{r}{\alpha} + n\right)}{\lambda^r \Gamma(n)}, \quad r > -n\alpha,$$

and in particular $E(X) = \frac{\Gamma\left(n+\frac{1}{\alpha}\right)}{\lambda\Gamma(n)}$. Also $E\left(Y_n\right) = \frac{\Gamma\left(n+\frac{1}{\alpha}-1\right)}{\lambda\,\alpha\,\Gamma(n)}$. See Figure 3.4 for the hazard rate shapes.

Example 3.3. Log-linear model: In this example, we consider a log-linear model for the intensity rate specified by $h(t) = \mathrm{e}^{a_0+bt}$ or equivalently by $h(t) = a\,\mathrm{e}^{bt}$, $a = \mathrm{e}^{a_0}$. The case when $b = 0$ leads to the exponential distribution. This is a classical model suggested by Lewis and Shedler (1976) and since then attained much popularity, see for example Jokiel-Rokita and Skoliński (2021), Yarmohammadi et al. (2022) and their references. In this case, the intensity

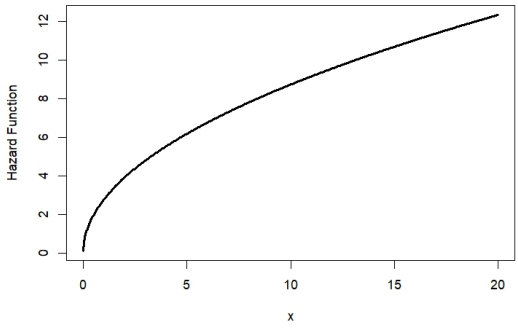

(a) $\lambda = 1.5$, $\alpha = 1.5$ and $n = 1$.

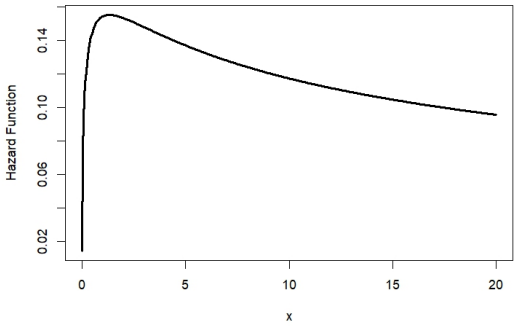

(b) $\lambda = 1.5$, $\alpha = 0.5$ and $n = 3$.

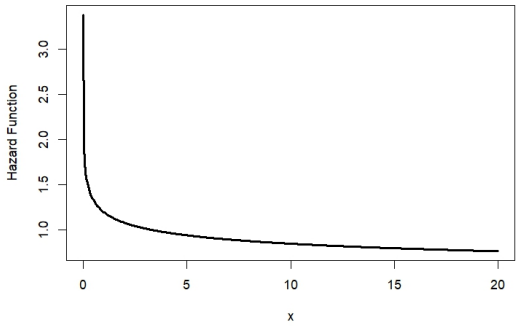

(c) $\lambda = 0.5$, $\alpha = 0.85$ and $n = 1$.

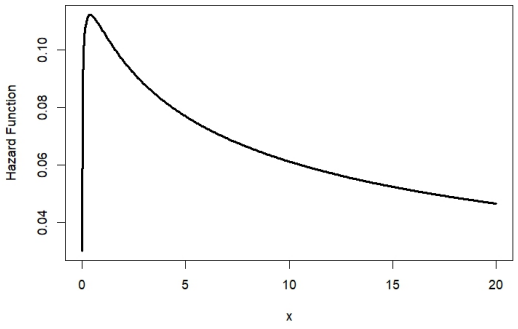

(d) $\lambda = 5$, $\alpha = 0.35$ and $n = 4$.

Figure 3.4: Hazard plots for various parameters of generalized gamma model.

function is of the form

$$H(t) = \frac{a}{b}\left(\mathrm{e}^{bt} - 1\right) = c\left(\mathrm{e}^{bt} - 1\right), \quad \text{where } c = \frac{a}{b}.$$

Hence the survival function is

$$\bar{F}(t) = \exp\left(-c\left(\mathrm{e}^{bt} - 1\right)\right), \quad t \geq 0,\, c,\, b > 0,$$

with density

$$f(t) = b\,c \exp\left(bt - c\left(\mathrm{e}^{bt} - 1\right)\right), \quad n = 1, 2, \ldots.$$

The corresponding functions of X_n are

$$f_n(t) = \frac{b\,c^n\left(\mathrm{e}^{bt}-1\right)^{n-1}}{(n-1)!}\exp\left(bt - c\left(\mathrm{e}^{bt}-1\right)\right),$$

and

$$\begin{aligned}\bar{F}_n(t) &= \frac{b\,c^n}{(n-1)!}\int_t^\infty \left(\mathrm{e}^{bt}-1\right)^{n-1}\exp\left(bt - c\left(\mathrm{e}^{bt}-1\right)\right)\,dt \\ &= \frac{1}{\Gamma(n)}\Gamma_{\left(\mathrm{e}^{bt}-1\right)}(n).\end{aligned}$$

The corresponding hazard rate can be obtained as $h(t) = b\,c\,\mathrm{e}^{bt}$, which is an increasing function. Hence $\bar{F}_n(t)$ is also IHR. Further

$$E(X_n^s) = E(X_{n-1}^s) + \frac{s}{(n-1)!}\int_0^\infty t^{s-1}c^{n-1}\left(\mathrm{e}^{bt}-1\right)^{n-1}\exp\left(-c\left(\mathrm{e}^{bt}-1\right)\right)dt,$$

to be found recursively and

$$\begin{aligned}E(Y_n) &= \frac{1}{(n-1)!}\int_0^\infty c^{n-1}\left(\mathrm{e}^{bt}-1\right)^{n-1}\exp\left(-c\left(\mathrm{e}^{bt}-1\right)\right)dt \\ &= \frac{1}{(n-1)!}\int_0^\infty \frac{\mathrm{e}^{-y}y^{n-1}}{b\,(y+c)}\,dy.\end{aligned}$$

Two other important functionals associated with the NHPP are the age and residual life of the unit, that is, $a(t)$ the time elapsed since the last minimal repair before and $r(t)$, the time from t until the next minimal repair. Obviously $a(t) = t - X_{N(t)}$ and $r(t) = X_{N(t)+1} - t$. Kirmani and Gupta (1989) have considered various properties for $a(t)$ and $r(t)$ and among them established that the joint distribution of $a(t)$ and $r(t)$ has survival function

$$\bar{F}(u,v) = \frac{\bar{F}(t+v)}{\bar{F}(t-u)}, \quad 0 < u < t,\ v > 0,$$

with marginals

$$\bar{F}_1(u) = P(a(t) > u) = \frac{\bar{F}(t)}{\bar{F}(t-u)}, \quad 0 \le u < t, \tag{3.20}$$

$$\bar{F}_2(v) \;=\; P(r(t) > v) = \frac{\bar{F}(t+v)}{\bar{F}(t)}, \quad v \geq 0, \tag{3.21}$$

and also that $a(t)$ and $r(t)$ are independent. In the following discussions it is assumed that $H(t) \to \infty$ as $t \to \infty$ and $\bar{F}(t) = \exp(-H(t))$ is the survival function of X_1, the time until first failure, to provide a connection between the results in Section 3.3 and the present one. The distribution of $a(t)$ is discontinuous at t with $P(a(t) = t) = \bar{F}(t)$. It is of interest to know the expected age at t to answer the question, how long a unit observed to be working at time t has been working since the last minimal repair. Kirmani and Gupta (1989) have established a relation between the expected age at time t, which is given as

$$\psi(t) = E(a(t)) = \int_0^t \frac{\bar{F}(t)}{\bar{F}(t-u)}\, du, \tag{3.22}$$

and the hazard rate is of the form

$$h(t) = \frac{1 - \psi'(t)}{\psi(t)}. \tag{3.23}$$

In the remainder of the present section, some new properties of $\psi(t)$ are investigated. From (3.20), we observe that the density function of $a(t)$ is

$$f_1(u) = \begin{cases} \frac{\bar{F}(t) f(t-u)}{\bar{F}^2(t-u)}, & 0 < u < 1 \\ \bar{F}(t) & u = t. \end{cases} \tag{3.24}$$

Further, (3.24) can be written as

$$\begin{aligned} f_1(u) &= \frac{\bar{F}(t)}{\bar{F}(t-u)} h(t-u) \\ &= \bar{F}_1(u) h(t-u), \end{aligned}$$

leading to the identity

$$h_1(t) = \begin{cases} h(t-u) & 0 \leq u < t \\ 1 & u = t, \end{cases} \tag{3.25}$$

between the hazard rate $h_1(t)$ of $a(t)$ and $h(t)$ of X_1, the time to the first minimal repair. In the next proposition it is shown that there is a one-to-one correspondence between $\psi(t)$ and $\bar{F}(t)$ which can be used to identify the life distribution that generates the NHPP. It enhances the merit of $\psi(t)$ on its own in defining the process, since $\{N(t),\, t \geq 0\}$ itself can be represented uniquely in terms of $\psi(t)$.

Proposition 3.6. The expected age function $\psi(t)$ can be written in terms of $\bar{F}(t)$ as

$$\psi(t) = \bar{F}(t) \int_0^t \frac{1}{\bar{F}(u)}\, du, \tag{3.26}$$

and conversely

$$\bar{F}(t) = \exp\left(- \int_0^t \frac{1 - \psi'(u)}{\psi(u)}\, du \right), \tag{3.27}$$

Proof. Starting from (3.23),

$$\psi'(t) + h(t)\psi(t) = 1.$$

Multiplying by $\frac{1}{\bar{F}(t)}$ and noting that $h(t) = \frac{f(t)}{\bar{F}(t)}$, we have

$$\frac{d}{dt}\left(\frac{\psi(t)}{\bar{F}(t)}\right) = \frac{1}{\bar{F}(t)}. \tag{3.28}$$

Integrating from 0 to t, we have (3.26). The formula (3.27) is obtained directly from (3.23) and $\bar{F}(t) = \exp\left(-\int_0^t h(u)\, du\right)$. □

Remark 3.1. From the identity (3.23), we have

$$\begin{aligned} H(t) &= \int_0^t \frac{1 - \psi'(u)}{\psi(u)}\, du \\ &= \int_0^t \frac{1}{\psi(u)}\, du - \log \psi(t). \end{aligned} \tag{3.29}$$

Thus the NHPP generated by $\bar{F}(t)$ or $H(t)$ is

$$P(N(t) = n) = \psi(t) \exp\left(- \int_0^t \frac{1}{\psi(u)}\, du \right) \frac{\left(\int_0^t \frac{1}{\psi(u)}\, du - \log \psi(t) \right)^n}{n!}, \quad n = 0, 1, 2, \ldots \tag{3.30}$$

The NHPP is characterized by the expected aging function corresponding to a given intensity function. Literature is abundant with intensity functions $H(t)$ that generated NHPP associated with different practical situations and the table given below provides the expressions of $\psi(t)$ of some models for easy reference. Other distributions than those given in Table 3.1 used are the Weibull, log Poisson, log normal, gamma, Makeham, etc., see McCollin (2008).

Table 3.1: Models for NHPP and their expected aging.

Model	$\bar{F}(t)$	$\psi(t)$
Gompertz	$\exp\left(-\frac{a}{\log b}(b^t-1)\right)$	$(\log b)^{-1}\int_0^{b^t-1}\frac{\mathrm{e}^{-\frac{ay}{\log b}}}{1+y}\,dy$
Pareto	$(1+bt)^{-a}$	$\frac{(1+bt)-(1+bt)^{-a}}{(a+1)b}$
Burr	$(1+\frac{t^b}{c})^{-a}$	$(1+\frac{t^b}{c})^{-a}\int_0^t(1+\frac{y^b}{c})^{-a}y^{\frac{1}{b}}\,dy$
Inverse exponential	$\exp\left(-a\mathrm{e}^{-\frac{b}{t}}\right)$	$\mathrm{e}^{a\mathrm{e}^{\frac{b}{t}}}\int_0^{\mathrm{e}^{-\frac{b}{t}}}\frac{\mathrm{e}^{ay}}{y(\log y)}\,dy$
Dhillon (1981)	$-\frac{1}{b}\left(\log(1+bt)\right)^{a+1}$	$\frac{1}{b^2}\int_{\log(1+bt)}^1\mathrm{e}^y y^{a+1}\,dy$

It is sometimes useful to write $\psi(t)$ as an expected value with respect to the distribution F. For this purpose, on integration by parts (3.26), we obtain

$$\begin{aligned}\psi(t) &= t-\bar{F}(t)\int_0^t\frac{uf(u)}{\bar{F}^2(u)}\,du\\ &= t-\bar{F}(t)(1-\bar{F}(t))E\left(\frac{X}{\bar{F}^2(X)}\middle|X\le t\right).\end{aligned}$$

We now move on to some characterization results of NHPP based on some widely used probability distributions.

3.6 Models characterized by special properties

In this section we attempt to establish some characterization theorems associated with the NHPP that enable the identification of the process through the properties of the functions associated with it. Although the general relationship between $\psi(t)$ and the hazard rate is given by (3.23), there are further simplified relationships between the two that are unique to certain life

distributions associated with NHPP. In the following propositions we identify such properties. The practical utility of this investigation is two fold. First it enables the identification of the model corresponding to a given set of observations. If the physical properties of the process supports our relationships then the model established in the proposition is confirmed. When no such situation is available, the sample analogues of the functions can be used to verify whether they satisfy the proposition to confirm the model. The second application comes in black box modeling where more than one distribution may pass the goodness of fit test. The correct model for the data is the one that satisfies the characteristic property.

Proposition 3.7. The stochastic process $\{N(t), t \geq 0\}$ is a NHPP with reciprocal linear intensity rate $h(t) = (at + b)^{-1}$, $b > 0$ if and only if $\psi(t)$ is inversely proportional to $h(t)$ for all $t > 0$.

Proof. Assume that $N(t)$ is a NHPP with intensity rate $h(t) = (at + b)^{-1}$. Then

$$\begin{aligned} \bar{F}(t) &= \exp\left(-\int_0^t h(u)\,du\right) \\ &= \left(1 + \frac{a\,t}{b}\right)^{-\frac{1}{a}}, \quad t > 0. \end{aligned}$$

Hence from (3.26), $\psi(t) = \frac{a\,t+b}{a+1}$ showing that $\psi(t)$ and $h(t)$ are inversely proportional.

Conversely, if $\psi(t)\,h(t) = c$, then by inverse proportionality, from (3.23) we obtain $1 - \psi'(t) = c$, which gives

$$\psi(t) = (1 - c)\,t + b',$$

and $h(t) = \frac{c}{(1-c)\,t+b'}$, which is of the required form of NHPP. □

We have several practical implications of the above proposition regarding the properties of the models involved.

(i) When $c = 1$, $\psi(t) = b'$ so that the expected age at each phase is the

same constant and $h(t) = \frac{1}{b'}$, giving the distribution of X as exponential with parameter b'. The distribution of X_n, the lifetime of n^{th} phase is gamma with density

$$f_n(t) = \frac{t^{\,n-1}}{(b')^n \Gamma(n)}\, \mathrm{e}^{-t/b'}, \quad t > 0,\ n = 1, 2, \ldots,$$

with $E(X_n^s) = (b')^s \frac{\Gamma(n+s)}{\Gamma(n)}$, $s = 1, 2, \ldots$, and $E(X_n) = nb'$. Finally, $Y_n = X_n - X_{n-1}$ has survival function $\bar{G}_n(t) = \mathrm{e}^{-\frac{t}{b'}}$, $t > 0$, so that $E(Y_n) = b'$, the expected time between the $(n-1)^{\text{th}}$ and n^{th} failures.

(ii) When $c > 1$, we get

$$\bar{F}(t) = \left(1 - \frac{t}{R}\right)^{\alpha}, \quad 0 \le t \le R,\ R, \alpha > 0, \tag{3.31}$$

where $R = \frac{b}{c-1}$ and $\alpha = \frac{c}{c-1}$. We note that (3.31) is a beta distribution rescaled by R. The intensity rate is $h(t) = \frac{\alpha}{R-t}$ and $H(t) = -\alpha \log\left(\frac{R-t}{R}\right)$ to give the distribution of X_n with density

$$f_n(t) = \frac{\alpha}{R\,(n-1)!} \left(-\alpha \log\left(1 - \frac{t}{R}\right)\right)^{n-1} \left(1 - \frac{t}{R}\right)^{\alpha-1}, \quad 0 \le t \le R, \tag{3.32}$$

with hazard rate

$$h_n(t) = \frac{\alpha}{R-t}\left(1 - \frac{S_{n-1}(t)}{S_n(t)}\right),$$

where

$$S_n(t) = \sum_{r=0}^{n-1} \frac{\left(-\alpha \log\left(1 - \frac{t}{R}\right)\right)^r}{r!}.$$

The m^{th} moment of X_n is

$$E(X_n^m) = \frac{\alpha^n\, R^m}{(n-1)!} \int_0^{\infty} \mathrm{e}^{-\alpha\, y} \left(1 - \mathrm{e}^{-y}\right)^m y^{n-1}\, dy.$$

In particular

$$E(X_n) = \frac{\alpha^n\, R\, \Gamma(n)}{(n-1)!} \left(\left(\frac{1}{\alpha}\right)^n - \left(\frac{1}{\alpha+1}\right)^n\right) = R\left(1 - \left(\frac{\alpha}{\alpha+1}\right)^n\right). \tag{3.33}$$

We interpret (3.33) as the average total lifetime of the process since it has started

at $t = 0$. Further, Y_n has survival function

$$\bar{G}(t) = \int_0^R \frac{\left(-\alpha \log\left(1 - \frac{u}{R}\right)\right)^{n-1}}{(n-1)!} f_n(t+u)\, du,$$

where $f_n(t)$ is as in (3.32). After some algebra, we find

$$\begin{aligned} E(Y_n) &= R\left(1 - \left(\frac{\alpha}{\alpha+1}\right)^n\right) - R\left(1 - \left(\frac{\alpha}{\alpha+1}\right)^{n-1}\right) \\ &= \frac{R}{\alpha}\left(\frac{\alpha}{\alpha+1}\right)^n. \end{aligned}$$

(iii) When $c < 1$, we have

$$\bar{F}(t) = \left(1 + \frac{t}{\alpha}\right)^{-\beta}, \quad t > 0,\ \alpha = \frac{b}{1-c} > 0,\ \beta = \frac{c}{1-c} > 0. \tag{3.34}$$

Following similar steps as in the case of $c > 1$, the intensity rate $h(t) = \frac{\beta}{\alpha+t}$ and $H(t) = \beta \log\left(1 + \frac{t}{\alpha}\right)$, which gives the distribution of X_n with density function

$$f_n(t) = \frac{\beta}{\alpha(n-1)!}\left(1 + \frac{t}{\alpha}\right)^{-\beta-1}\left(\beta \log\left(1 + \frac{t}{\alpha}\right)\right)^{n-1}, \quad x > 0, \tag{3.35}$$

which gives

$$h_n(t) = \frac{\beta}{\alpha+t}\left(1 - \frac{S_{n-1}(t)}{S_n(t)}\right), \quad \text{with} \quad S(t) = \sum_{r=0}^{n-1} \frac{\left(\beta \log\left(1 + \frac{t}{\alpha}\right)\right)^r}{r!}.$$

The corresponding m^{th} moment of X_n is obtained as

$$E(X_n^m) = \frac{\beta^n\, \alpha^m}{(n-1)!} \int_0^\infty \mathrm{e}^{-\beta y}\, (\mathrm{e}^y - 1)^m\, y^{n-1}\, dy.$$

For $m = 1$, we get

$$E(X_n) = \alpha\left(\left(\frac{\beta}{\beta-1}\right)^n - 1\right), \quad \beta > 1.$$

Now, the survival function of Y_n has the form

$$\bar{G}(t) = \int_0^R \frac{\left(\beta \log\left(1+\frac{t}{\alpha}\right)\right)^{n-1}}{(n-1)!} f_n(t+u)\, du,$$

which gives

$$E(Y_n) = \frac{\alpha}{\beta(\beta-1)} \left(\frac{\beta}{\beta-1}\right)^n (\beta(\beta-1)-1)\,.$$

One important feature observed from the above analysis is that the expected age can be increasing, decreasing or constant. A necessary and sufficient condition is that if $h(t)\psi(t) = c$, then expected age is decreasing (increasing) if $c > 1\,(c < 1)$. The result holds even if c is a non-negative function of t; by virtue of the identity $h(t)\psi(t) = 1 - \psi'(t)$, it is enough that $c'(t) > (<)\, 1$ for $\psi(t)$ to be decreasing (increasing).

Proposition 3.8. The stochastic process $\{N(t),\, t \geq 0\}$ is NHPP with intensity rate $h(t) = \alpha + \mathrm{e}^{\alpha t+\beta}$, $\alpha,\, \beta > 0$ if and only if

$$\psi(t)(h(t) - \alpha) = 1, \tag{3.36}$$

for all $t > 0$.

Proof. First assume that $N(t)$ is NHPP with $h(t)$ as in the proposition. Then

$$\begin{aligned} \bar{F}(t) &= \exp\left(-\int_0^t h(x)\, dx\right) \\ &= \exp\left(-\left(\frac{\mathrm{e}^{\alpha t+\beta}}{\alpha} + \alpha t - \frac{\mathrm{e}^{\beta}}{\alpha}\right)\right). \end{aligned} \tag{3.37}$$

Using this in (3.26) we have $\psi(t) = \mathrm{e}^{-(\alpha+\beta t)}$ and the identity (3.36). Conversely if (3.36) holds for all $t > 0$, equation (3.26) gives

$$\frac{\psi'(t)}{\psi(t)} = \alpha,$$

which is equivalent to writing $\psi(t) = \mathrm{e}^{-(\alpha t+\beta t)}$, for some $\beta > 0$. Then $h(t) = \alpha + \mathrm{e}^{\alpha t+\beta}$ and our theorem is proved. □

The distribution encountered in (3.37) is the Makeham distribution proposed to model human mortality in classical literature. We have the exponential law derived from it as a limiting case. Its density is log-concave and can be re-parameterized to form models with hazard rates $h_1(t) = \alpha + \mathrm{e}^{-(\alpha\, t+\beta)}$ and $h_2(t) = \alpha - \mathrm{e}^{-(\alpha\, t+\beta)}$. The mean residual life function has a closed form $m(t) = \mathrm{e}^{-(\alpha+\beta\, t)}$. This means that the residual life is rapidly decreasing over time, as so does the expected age. Since $H(t) = \alpha\, t + \frac{\mathrm{e}^{\beta}}{\alpha}\,(\mathrm{e}^{\alpha\, t} - 1)$, the distributions of X_n and Y_n are easily derived as

$$\bar{F}_n(t) = \exp\left(-\frac{\mathrm{e}^{\alpha\, t+\beta}}{\alpha} - \alpha\, t + \frac{\mathrm{e}^{-\beta}}{\alpha}\right)\left(\frac{\alpha\, t + \frac{\mathrm{e}^{\beta}}{\alpha}\,(\mathrm{e}^{\alpha\, t} - 1)}{(n-1)!}\right)^{n-1},$$

and

$$\bar{G}_n(t) = \int_0^{\infty}\left(\frac{\alpha\, u + \frac{\mathrm{e}^{\beta}}{\alpha}\,(\mathrm{e}^{\alpha\, u} - 1)}{(n-1)!}\right).$$

Although the r^{th} moments exist for X, X_n and Y_n, they cannot be obtained in closed form and have to be evaluated numerically.

Proposition 3.9. The stochastic process $\{N(t),\, t \geq 0\}$ is NHPP with intensity rate $h(t) = \frac{\lambda}{1-p\,\mathrm{e}^{-\lambda\, t}}$, $0 < p < 1$, $\lambda > 0$ if and only if

$$\psi(t) = \frac{\mathrm{e}^{\lambda\, t} - \lambda\, p\, t - 1}{\lambda\,(\mathrm{e}^{\lambda\, t} - p)}.$$

Proof. Assuming that $\{N(t),\, t \geq 0\}$ is NHPP with intensity rate $h(t) = \frac{\lambda}{1-p\,\mathrm{e}^{-\lambda\, t}}$, we get the distribution of lifetimes as

$$\bar{F}(t) = \frac{(1-p)\mathrm{e}^{-\lambda\, t}}{1 - p\,\mathrm{e}^{-\lambda\, t}}, \quad 0 < p < 1,\, \lambda > 0,\, t > 0.$$

In that case by direct calculation

$$\psi(t) = \frac{\mathrm{e}^{\lambda\, t} - \lambda\, p\, t - 1}{\lambda\,(\mathrm{e}^{\lambda\, t} - p)}. \tag{3.38}$$

Conversely if $\psi(t)$ is as in (3.38), we have

$$\begin{aligned}\psi'(t) &= 1 - \frac{\lambda^2 \, \mathrm{e}^{\lambda t\left(\mathrm{e}^{\lambda t} - \lambda p t - 1\right)}}{\lambda^2 \left(\mathrm{e}^{\lambda t} - p\right)^2} \\ &= 1 - \psi(t) \left(\frac{\lambda \, \mathrm{e}^{\lambda t}}{\mathrm{e}^{\lambda t} - p}\right),\end{aligned}$$

or

$$h(t) = \frac{1 - \psi'(t)}{\psi(t)} = \frac{\lambda \, \mathrm{e}^{\lambda t}}{\mathrm{e}^{\lambda t} - p},$$

as required. □

Remark 3.2. The above property of the NHPP can also be written as

$$\psi(t) = \frac{1}{\lambda^2} + (\beta + \delta \, t)(\lambda - h(t)),$$

with $\beta = \frac{1}{\lambda^2 p}$ and $\delta = \frac{1}{\lambda}$.

The distribution obtained in this proposition is the exponential geometric model discussed in Adamidis and Loukas (1998). It has a decreasing hazard rate with initial hazard rate $\lambda(1-p)^{-1}$ and long term hazard rate $h(\infty) = \lambda$, both of which are finite. The model can also be obtained by compounding exponential distribution with geometric.

Proposition 3.10. The stochastic process $\{N(t),\, t \geq 0\}$ is NHPP with intensity rate $h(t) = \frac{\mathrm{e}^{\frac{t}{\sigma}}}{\sigma(1+\mathrm{e}^{\frac{t}{\sigma}})}$, $\sigma > 0$, $t > 0$ if and only if

$$\psi(t) = \sigma + \frac{t - 2\sigma}{1 + \mathrm{e}^{\frac{t}{\sigma}}}.$$

Proof. Assuming that $\{N(t),\, t \geq 0\}$ is NHPP with intensity rate $h(t) = \frac{\mathrm{e}^{\frac{t}{\sigma}}}{\sigma(1+\mathrm{e}^{\frac{t}{\sigma}})}$, we get the corresponding survival function as

$$\bar{F}(t) = \frac{2}{1 + \mathrm{e}^{\frac{t}{\sigma}}}, \quad \sigma > 0 \, t > 0.$$

This gives

$$\psi(t) = \sigma + \frac{t - 2\sigma}{1 + \mathrm{e}^{\frac{t}{\sigma}}}. \tag{3.39}$$

Conversely if $\psi(t)$ has the form (3.39), we have

$$\begin{aligned}\psi'(t) &= \frac{1}{1+\mathrm{e}^{\frac{t}{\sigma}}} - \frac{\mathrm{e}^{\frac{t}{\sigma}}(t-2\sigma)}{\sigma\left(1+\mathrm{e}^{\frac{t}{\sigma}}\right)^2} \\ &= \frac{\sigma - \mathrm{e}^{\frac{t}{\sigma}}(t-3\sigma)}{\sigma\left(1+\mathrm{e}^{\frac{t}{\sigma}}\right)^2}.\end{aligned}$$

Thus

$$h(t) = \frac{1-\psi'(t)}{\psi(t)} = \frac{\mathrm{e}^{\frac{t}{\sigma}}}{\sigma + \sigma\mathrm{e}^{\frac{t}{\sigma}}},$$

which completes the proof. □

The model obtained in the above proposition is the half logistic model studied by Balakrishnan (1985). It can be defined as a continuous probability distribution obtained by taking the absolute value of a random variable that follows a logistic distribution.

3.7 Summary of the chapter

This chapter provides a systematic analysis of the multi-phase ART and its reliability implications. Key results on the preservation of aging properties and stochastic ordering relationships between the multi-phase model and the baseline distribution are established. The extension to NHPP offers a broader stochastic interpretation and highlights potential applications. The characterization results further demonstrate the theoretical relevance and usefulness of the multi-phase ART in reliability theory.

Chapter 4

Auto-relevated log-logistic distribution: Properties and applications

4.1 Introduction

As discussed in Chapter 3, the ART is a parsimonious transformation that enhances model flexibility without introducing additional parameters. Another key theoretical feature of ART is the preservation of important tail properties of the baseline distribution. In particular, Dileepkumar and Sankaran (2021) showed that the $\mathcal{L}$-class property is retained under ART. Furthermore, if the baseline distribution is heavy-tailed or belongs to classes such as regularly varying, dominated variation, or sub-exponential distributions, these characteristics are preserved after transformation. These properties are especially useful in extreme value modeling, as they allow the construction of flexible models while maintaining the essential tail behavior of the baseline distribution. Motivated by this, we construct a new model by considering the classical log-logistic (LL) distribution as the baseline.

[0]Results presented in this chapter are published in the article entitled *"Reliability Properties and Applications of Auto-Relevated Log-Logistic Model"*, published in the journal *Journal of Statistical Theory and Practice* (Anand et al. (2026)).

The remainder of this chapter is organized as follows: A brief overview of the log-logistic distribution is presented in Section 4.2. Section 4.3 introduces the auto-relevated log-logistic (ARLL) model and examines its structural properties. Reliability characteristics are studied in Section 4.4. Parameter estimation methods are discussed in Section 4.5, followed by a Monte Carlo simulation study in Section 4.6. The tail behavior of the ARLL model is analyzed in Section 4.7 along with the risk assessment measures in Section 4.8. A real data application is provided in Section 4.9, along with an extreme risk analysis. Finally, concluding remarks are given in Section 4.10.

4.2 Log-logistic distribution

The log-logistic distribution, initially proposed by Verhulst (1838), is an important heavy-tailed continuous probability model particularly used to model extreme situations characterized by one scale and one shape parameter. The corresponding CDF is

$$F_X(x) = 1 - \frac{1}{1 + (\alpha\, x)^{\beta}}, \quad x > 0,\, \alpha > 0,\, \beta > 0. \tag{4.1}$$

The survival function is obtained as

$$\bar{F}_X(x) = \frac{1}{1 + (\alpha\, x)^{\beta}}, \quad x > 0,\, \alpha > 0,\, \beta > 0.$$

A notable feature of this model is that the logarithm of a log-logistic random variable follows the logistic distribution, which enables closed form expressions for the CDF, density function, survival function and hazard rate, thereby providing analytical advantages when dealing with censored or truncated lifetime data. Further, the log-logistic model can accommodate both monotone and non-monotone hazard rate behavior; in particular, the hazard rate becomes UBT when the shape parameter exceeds unity, making it suitable for modeling practical time-to-event data wherein failure risk increases initially and decreases

afterward.

Due to this flexibility and mathematical tractability, the log-logistic distribution has been widely employed in modeling extreme and heavy-tailed data across several domains because of its analytical simplicity and strong tail behavior. In hydrology, it has been used effectively for flood frequency analysis and hydrological extremes, demonstrating good fit for peak-flow series and informing design-level flood estimation (Ahmad et al. (1988), Rowsiński et al. (2002), Almuhayfith et al. (2025)). Similar success has been reported by Fitzgerald (2005) and Hussain and Abbas (2019) in the rainfall extreme modeling, where the log-logistic distribution provides competitive performance in estimating high quantiles of annual and seasonal rainfall maxima. Beyond environmental applications, the distribution and its extended variants have gained prominence in industrial statistics, wherein log-logistic based methods have been used for analyzing extreme order statistics in quality control, including the development of extreme-value control charts, whose details are available in Rao and Kushary (2012). It has also been applied in the field of actuarial science for modeling large insurance and reinsurance losses, owing to their flexible heavy tails and suitability for tail-risk measures such as value at risk and tail value at risk (Alfaer et al. (2021), Teamah et al. (2021), Ranjbar et al. (2024)). Together, these studies highlight the suitability of the log-logistic family for modeling data in which extreme values play a dominant role. These desirable properties have motivated the development of numerous extensions of the baseline log-logistic model in recent literature to provide greater adaptability and model complex lifetime data more efficiently. A comprehensive review on this can be seen in Muse et al. (2021). Building on these foundations, we intend to apply the proposed ARLL model in extreme risk analysis based on the various risk assessment measures, which is discussed in the next section.

4.3 Auto-relevated log-logistic model

The ARLL distribution is obtained by considering the survival function of the LL distribution as the baseline model in the auto-relevation transform (3.1) of Chapter 3. Let $X\nu X$ denote the ARLL random variable. Then the survival function of ARLL model is obtained as

$$\bar{F}_{X\nu X}(x) = \frac{1 + \log\left(1 + (\alpha\, x)^{\beta}\right)}{1 + (\alpha\, x)^{\beta}}, \quad x > 0,\ \alpha > 0,\ \beta > 0. \tag{4.2}$$

The above equation can be written as

$$\bar{F}_{X\nu X}(x) = q(\bar{F}_X(x)), \quad \text{where } q(u) = u\,(1 - \log u),$$

where $q(u)$ is the associated distortion function. The corresponding density function is obtained as

$$f_{X\nu X}(x) = \frac{\alpha^{\beta}\beta\, x^{\beta-1} \log\left(1 + (\alpha\, x)^{\beta}\right)}{\left(1 + (\alpha\, x)^{\beta}\right)^2}. \tag{4.3}$$

The flexibility of the proposed distribution is illustrated in Figure 4.1, which plots the density function for different parameter values. As shown, the class of distributions accommodates various skewed shapes and near-symmetric shapes. We now formalize this behavior by presenting a theorem that characterizes the density function over the complete parameter space.

Proposition 4.1. Let X follow ARLL distribution with density function $f_{X\nu X}(\cdot)$ given in (4.3), then the following properties hold.

(i) $\lim\limits_{x\to\infty} f_{X\nu X}(x) = 0 \quad \text{for } \alpha > 0,\ \beta > 0.$

(ii) $\lim\limits_{x\to 0} f_{X\nu X}(x) = \begin{cases} 0, & \beta > \frac{1}{2} \\ \frac{\alpha}{2}, & \beta = \frac{1}{2} \\ \infty, & \beta < \frac{1}{2}. \end{cases}$

(iii) $f_{X\nu X}(x)$ is monotonically decreasing for $0 < \beta \leq \frac{1}{2}$.

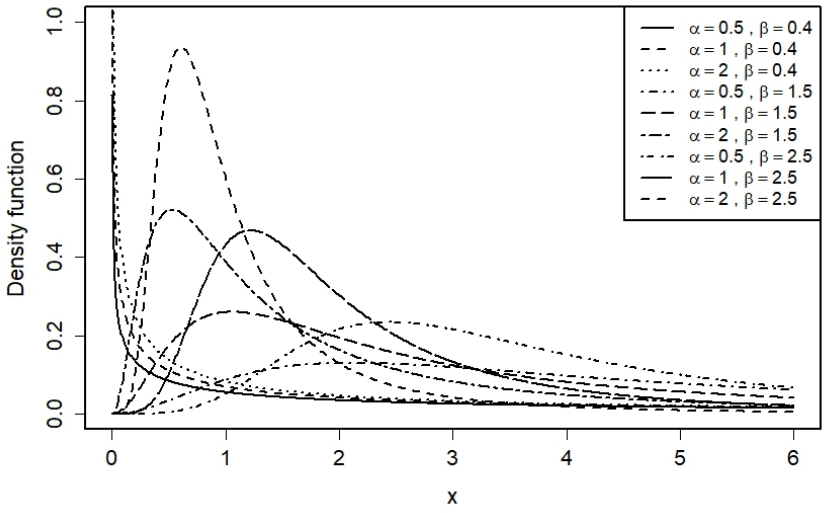

Figure 4.1: Density plots of ARLL for various parameter combinations.

Proof.

(i) We observe that the function given in (4.3) results in an indeterminate form as $x \to \infty$. By applying the L'Hôpital's rule, we have $\lim_{x\to\infty} f_{X\nu X}(x) = 0, \quad \text{for } \alpha > 0,\ \beta > 0.$

(ii) From (4.3), when $\beta > \frac{1}{2}$ and for $\beta < \frac{1}{2}$, $\lim_{x\to 0} f_{X\nu X}(x)$ tends to 0 and ∞ respectively, which is directly obtained by applying the L'Hôpital's rule. For the case when $\beta = \frac{1}{2}$, we obtain $f_{X\nu X}(x) = \frac{\alpha \log\left(\sqrt{\alpha x}+1\right)}{2\sqrt{\alpha x}\left(\sqrt{\alpha x}+1\right)^2}$, and when $x \to 0$ the result follows directly.

(iii) Again, from the first derivative of the density function given in (4.3), we have the sign determining term $\beta(\alpha x)^\beta - \left(1-\beta+(\beta+1)(\alpha x)^\beta\right) \log\left(1+(\alpha x)^\beta\right) < 0$ for $\beta \leq \frac{1}{2}$.

□

The density function of the ARLL distribution can be expressed in the form of a series expansion. From (4.3), we have

$$f_{X\nu X}(x) = \alpha\beta \sum_{n=1}^{\infty} \frac{(-1)^n (\alpha\, x)^{\beta(n+1)-1}}{2\,(1+(\alpha\, x)^\beta)^{n+2}}, \tag{4.4}$$

since $\log(1+x) = (-1)^{n+1} \sum_{n=1}^{\infty} \frac{x^n}{n}$, for $\mid x \mid \leq 1$. This can be used to derive several useful measures such as incomplete and complete moments, moment generating function, characteristic function, etc. For instance, the r^{th} moment of the ARLL model can be obtained from (4.4) as

$$E((X\nu X)^r) = \alpha\beta \sum_{n=1}^{\infty} \int_0^{\infty} x^r \frac{(-1)^n (\alpha\, x)^{\beta(n+1)-1}}{2\left(1+(\alpha\, x)^{\beta}\right)^{n+2}}\, dx.$$

For $r < \beta$, we have the closed form expression for $E(X^r)$ from Gradshteyn and Ryzhik (1994) (3.251 (11)) as

$$E((X\nu X)^r) = \sum_{n=1}^{\infty} \frac{(-1)^n}{2n} B\left(\beta(n+1)+r+1, n-\beta(n+1)-r+1\right) \alpha^{\beta(n+1)+r+1}, \tag{4.5}$$

where $B(a,b)$ is the beta function. We now present some interesting connections of the ARLL distribution with Gamma and Pareto models. These relationships provide useful transformations for generating random observations for the ARLL model.

Proposition 4.2. Let X follow ARLL (α, β) distribution, then $Y = \log(1 + (\alpha\, X)^{\beta})$, α, $\beta > 0$ follows Gamma $(2, 1)$ distribution.

Proof. Consider the density function of ARLL model given in (4.3). Now, the distribution of $Y = \log(1 + (\alpha\, X)^{\beta})$ using the Jacobian transformation method can be obtained as

$$f_Y(y) = y\, \mathrm{e}^{-y}, \quad y > 0,$$

which is the density function of Gamma $(2, 1)$ distribution. □

Proposition 4.3. If X follows ARLL (α, β) distribution, then $Y = (\alpha\, X)^{\beta}$, α, $\beta > 0$ follows auto-relevated Pareto type-II distribution.

Proof. Let $Y = (\alpha X)^{\beta}$ with α, $\beta > 0$. Then from (4.3), the density function of Y is obtained as

$$f_Y(y) = \frac{\log(1+y)}{(1+y)^2}, \quad y > 0.$$

The corresponding survival function is

$$\bar{F}_Y(y) = \frac{1 + \log(1+y)}{1+y}, \quad y > 0,$$

which is the survival function of auto-relevated Pareto type-II random variable. The baseline Pareto type-II distribution has the survival function $\bar{F}(x) = \frac{1}{1+x}$, $x > 0$. □

Remark 4.1. If X follows the ARLL model, then the transformed variable $Y = 1 + (\alpha X)^\beta$, where α, $\beta > 0$, follows an auto-relevated Pareto type-I distribution. The survival function of the baseline Pareto type-I distribution is given by $\bar{F}(x) = \frac{1}{x}$, $x > 1$.

To characterize the shape of a probability distribution, two fundamental measures are commonly employed: skewness and kurtosis. Skewness quantifies the degree of asymmetry of a distribution about its center, while kurtosis measures the heaviness of its tails relative to the central part of the distribution. Several approaches have been proposed in the literature to assess these characteristics. Among them, quantile-based methods provide robust and distribution-free measures of skewness and kurtosis. In particular, Galton's measure of skewness, introduced by Galton (1883), and Moors' measure of kurtosis, proposed by Moors (1988), are defined in terms of the quantile function $Q(\cdot)$ as

$$S = \frac{Q(6/8) - 2Q(4/8) + Q(2/8)}{Q(6/8) - Q(2/8)},$$
$$K = \frac{Q(7/8) - Q(5/8) + Q(3/8) - Q(1/8)}{Q(6/8) - Q(2/8)}.$$

Figure 4.2 displays the three-dimensional plots of Galton's skewness and Moors' kurtosis for the proposed model. Since the quantile function does not admit a closed-form expression, these measures are evaluated numerically. It is observed that both skewness and kurtosis depend solely on the parameter β, remaining invariant with respect to α. The skewness remains positive for all values of β, indicating persistent right-skewness of the distribution. As β increases, the magnitude of skewness decreases steadily. A similar pattern is observed for

Moors' kurtosis. For smaller values of β, the distribution exhibits higher kurtosis, indicating stronger tail heaviness and peakedness. As β increases, the kurtosis decreases and stabilizes, reflecting a transition toward lighter tails and a more moderate shape. Table 4.1 reports selected numerical values of Galton's skewness and Moors' kurtosis for varying β, illustrating the monotonic decline of both measures with increasing β.

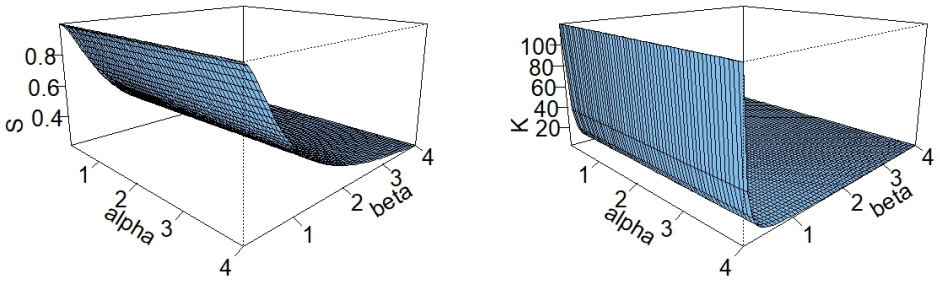

(a) Galton's skewness plot **(b)** Moor's kurtosis plot

Figure 4.2: Plots of Galton's skewness and Moor's kurtosis

Table 4.1: Values of S and K for varying β.

β	S	K
0.50	0.8249	6.6233
1.56	0.3973	1.8272
2.61	0.2733	1.5187
3.67	0.2171	1.4252
4.72	0.1857	1.3833
5.78	0.1654	1.3597
6.83	0.1515	1.3450
7.89	0.1411	1.3349
8.94	0.1333	1.3277
10.00	0.1270	1.3222

4.4 Reliability properties

The behavior of the hazard rate plays a central role in describing the aging properties of a lifetime model. For the proposed ARLL model, from (4.2) and (4.3), the hazard rate can be obtained as

$$\begin{aligned} h_{X\nu X}(x) &= \frac{\alpha\beta(\alpha\, x)^{\beta-1}\log\left(1+(\alpha x)^{\beta}\right)}{(1+(\alpha x)^{\beta})\,(1+\log\,(1+(\alpha x)^{\beta}))} \\ &= h_X(x)\left(\frac{\log\left(1+(\alpha x)^{\beta}\right)}{1+\log\,(1+(\alpha x)^{\beta})}\right), \end{aligned} \tag{4.6}$$

where $h_X(x) = \frac{\alpha\beta(\alpha\, x)^{\beta-1}}{1+(\alpha x)^{\beta}}$ is the hazard rate of the LL distribution. To analyze the aging behavior of $h_{X\nu X}(x)$, it is sufficient to analyze the term in the bracket of (4.6) since the behavior of $h_X(x)$ is known. Dileepkumar and Sankaran (2021) showed that the DHR property is generally not preserved under the ART formulation. The ART model corresponding to a DHR baseline can exhibit non-monotonic shapes for its hazard rate. Note that

$$\frac{d}{dx}\left(\frac{\log\left(1+(\alpha x)^{\beta}\right)}{1+\log\,(1+(\alpha x)^{\beta})}\right) = \frac{\beta(\alpha x)^{\beta}}{x\,(1+(\alpha x)^{\beta})\,(1+\log\,(1+(\alpha x)^{\beta}))^{2}} > 0, \tag{4.7}$$

for x, α, $\beta > 0$. Since the LL model has DHR property for $\beta \leq 1$, from (4.7) it follows that the ARLL model can have non-monotonic shapes for its hazard rate. This can be seen in the hazard plots given in Figure 4.3. We can also observe that the ARLL model incorporates the increasing, decreasing and UBT shapes for different values of the parameters α and β. The corresponding reversed hazard rate can be obtained as

$$\lambda_{X\nu X}(x) = \frac{f_{X\nu X}(x)}{F_{X\nu X}(x)} = \frac{\beta(\alpha x)^{\beta}\log\left(1+(\alpha x)^{\beta}\right)}{x\,(1+(\alpha x)^{\beta})\,((\alpha x)^{\beta}+\log\,(1+(\alpha x)^{\beta}))}. \tag{4.8}$$

Dileepkumar and Sankaran (2021) proved that the ART in general preserves the DRHR property. Since LL is DRHR, it follows that the ARLL model is also DRHR.

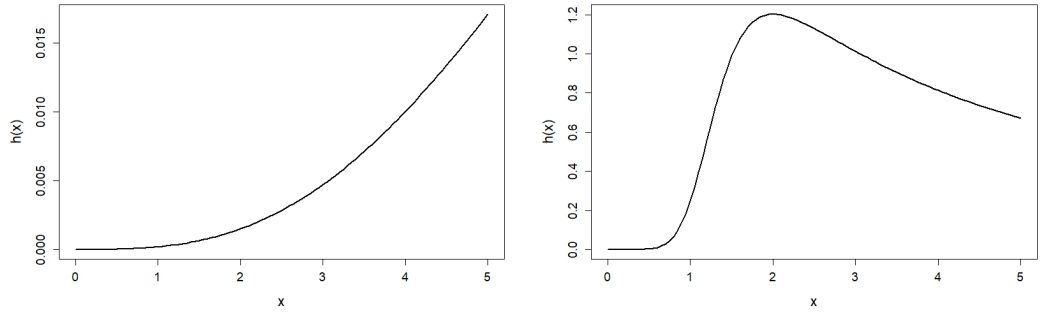

(a) $\alpha = 0.1$, $\beta = 2$ **(b)** $\alpha = 2$, $\beta = 1$

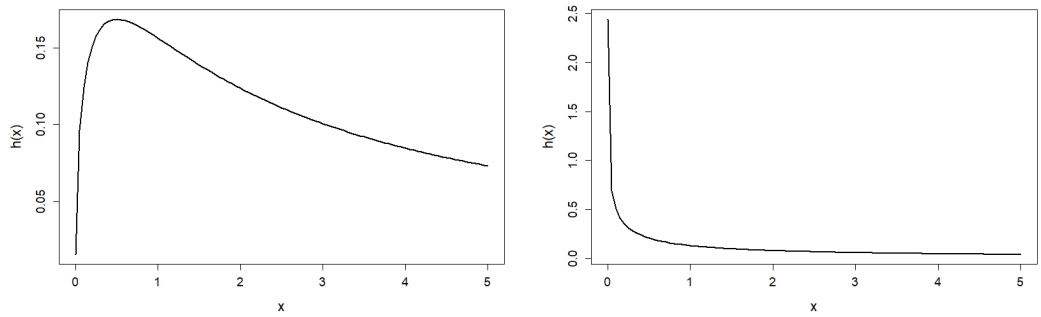

(c) $\alpha = 0.75$, $\beta = 0.75$ **(d)** $\alpha = 2$, $\beta = 0.4$

Figure 4.3: Hazard plots of ARLL for different parameters

The odds function of ARLL model is obtained as

$$\phi_{X\nu X}(x) = \frac{F_{X\nu X}(x)}{\bar{F}_{X\nu X}(x)} = \frac{(\alpha x)^{\beta} - \log\left(1 + (\alpha x)^{\beta}\right)}{1 + \log\left(1 + (\alpha x)^{\beta}\right)} \tag{4.9}$$

Figure 4.4 illustrates the odds functions of the ARLL and LL models for different parameter values. It is observed that the ARLL odds function increases more slowly compared to the LL model. This indicates the moderating effect of the ART transformation on the growth of the odds function.

A related aging concept is based on the odds rate. The odds rate of the ARLL model is

$$\theta'_{X\nu X}(x) = \frac{f_{X\nu X}(x)}{(\bar{F}_{X\nu X}(x))^2} = \frac{\alpha\beta(\alpha\, x)^{\beta-1} \log\left(1 + (\alpha\, x)^{\beta}\right)}{(1 + \log(1 + (\alpha\, x)^{\beta}))^2}. \tag{4.10}$$

Lando et al. (2022) showed that the odds rate is constant only for the standard LL distribution with survival function $\bar{F}_X(x) = \frac{1}{1+x}$, $x > 0$. When $\alpha = \beta = 1$,

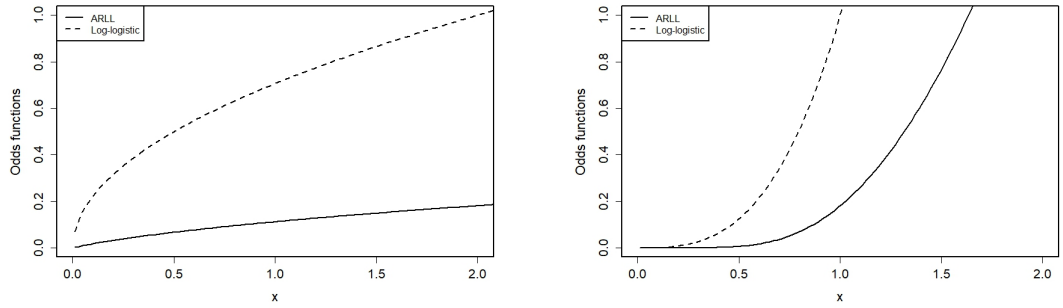

(a) $\alpha = 0.5,\ \beta = 0.5$ **(b)** $\alpha = 1,\ \beta = 3$

Figure 4.4: Odds function plots of ARLL and LL model

from (4.10), we obtain the odds rate of the ARLL model as

$$\theta'_{X\nu X}(x) = \frac{\log(1+x)}{(1+\log(1+x))^2},$$

which is monotonically decreasing in x. This suggests that the ARLL model has decreasing odds rate whereas the baseline LL has constant odds rate.

Another measure of aging is the log-odds rate (LOR), proposed by Zimmer et al. (1998). The log-odds rate of ARLL model is

$$LOR_{X\nu X}(x) = \frac{f_{X\nu X}(x)}{F_{X\nu X}(x)\bar{F}_{X\nu X}(x)} = \frac{\alpha\beta(\alpha\,x)^{\beta-1}\log\left(1+(\alpha\,x)^{\beta}\right)}{(1+\log(1+(\alpha\,x)^{\beta}))\,(\log(1+(\alpha\,x)^{\beta})-(\alpha\,x)^{\beta})}. \tag{4.11}$$

It has been shown in Wang et al. (2003) that the standard LL distribution has a constant log-odds rate with respect to $\log x$. Hence, the role of the LL distribution with respect to the log-odds rate in $\log x$, is analogous to the role of the exponential distribution with respect to the hazard rate. When $\alpha = \beta = 1$, the LOR of the ARLL model, obtained from (4.11), is given by

$$LOR_{X\nu X}(x) = \frac{x\log(1+x)}{(x-\log(1+x))\,\log\big(1+(1+x)\big)}.$$

It can be shown that this function is decreasing in $\log x$, implying that the ARLL model possesses the DLOR property. Using this result, and the bounds established by Zimmer et al. (1998) for distributions with ILOR or DLOR properties, we obtain the following bounds for the survival function of the ARLL

model (see Theorem 3 in Zimmer et al. (1998)).

Proposition 4.4. Let F satisfy $\bar{F}(x_i) = 1 - k_i$, $0 < k_i < 1$, for $i = 1, 2$, with $x_1 < x_2$. Then

$$\bar{F}_{X\nu X}(x) \begin{cases} < \dfrac{1}{1 + m^c \mathrm{e}^{cx}}, & x_1 < x < x_2 \\ = \dfrac{1}{1 + m^c \mathrm{e}^{cx}}, & x = x_1 \text{ or } x = x_2 \\ > \dfrac{1}{1 + m^c \mathrm{e}^{cx}}, & x > x_2 \text{ or } x < x_1, \end{cases}$$

where $(mx_i)^c = \frac{k_i}{1-k_i}$, $i = 1, 2$, and

$$c = \frac{\log\left(\dfrac{k_1(1-k_2)}{k_2(1-k_1)}\right)}{\ln\left(\dfrac{x_1}{x_2}\right)},$$

and

$$m = \frac{1}{x_i} \exp\left\{\frac{1}{c} \log\left(\frac{k_i}{1-k_i}\right)\right\}, \qquad i = 1 \text{ or } 2.$$

Proof. Proof follows directly from Zimmer et al. (1998) (Theorem 3). □

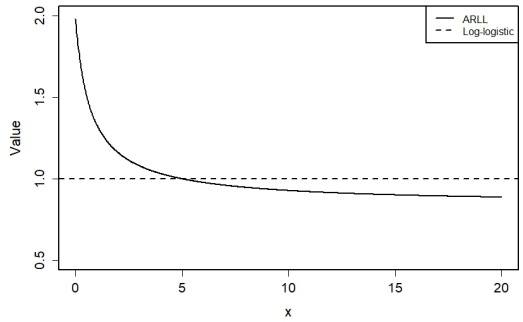

Figure 4.5: *LOR* plots of ARLL and LL models

Figure 4.5 displays the log-odds rates of the ARLL and LL models when $\alpha = \beta = 1$. The log-odds rate of the ARLL model decreases with x, confirming the DLOR property in $\log x$, whereas the LL model exhibits a constant log-odds rate. This graphical behavior supports the theoretical result and justifies the application of the bounds given in Proposition 4.4 based on the DLOR property.

Psarrakos and Navarro (2013) and Dileepkumar and Sankaran (2021) have derived various stochastic ordering results for the ART leveraging the distortion function. If X follows LL and Y is the corresponding ARLL model, then from Dileepkumar and Sankaran (2021), we have $X \leq_{lr} Y$. Now, from Shaked and Shanthikumar (2007), we have the following implications.

$$X \leq_{lr} Y \implies X \leq_{hr} Y \implies X \leq_{st} Y.$$

It is known that if $X_1 \sim \text{LL}(\alpha_1, \beta)$ and $X_2 \sim \text{LL}(\alpha_2, \beta)$, then $X_1 \leq_{st} X_2$, $X_1 \leq_{hr} X_2$, and $X_1 \leq_{icx} X_2$ whenever $\alpha_1 \geq \alpha_2$. Now, we have the following results for the corresponding ARLL models.

Proposition 4.5. Let Y_1 and Y_2 denote the ARLL models corresponding to X_1 and X_2, respectively. If $X_1 \sim \text{LL}(\alpha_1, \beta)$ and $X_2 \sim \text{LL}(\alpha_2, \beta)$ with $\alpha_1 > \alpha_2$, then $Y_1 \leq_{st} Y_2$, $Y_1 \leq_{hr} Y_2$, and $Y_1 \leq_{icx} Y_2$.

Proof. Since $X_1 \leq_{st} X_2$, $X_1 \leq_{hr} X_2$, and $X_1 \leq_{icx} X_2$ holds whenever $\alpha_1 \geq \alpha_2$, from Proposition 7 in Dileepkumar and Sankaran (2021), all three assertions follow directly. □

4.5 Parameter estimation

In this section, we discuss the parameter estimation of the ARLL model using the method of maximum likelihood estimation. Let $X_1, X_2, \ldots, X_n$ be a random sample of size n from the ARLL distribution with parameters (α, β), and $\underline{x} = (x_1, x_2, \ldots, x_n)$ denote the corresponding observed values. Then, the log-likelihood can be obtained from (4.3) as

$$\begin{aligned} L(\alpha, \beta \mid \underline{x}) = \sum_{i=1}^{n} \Big(& \beta \log(\alpha) + \log(\beta) + (\beta - 1)\log(x_i) \\ & + \log\big(\log\big(1 + (\alpha x_i)^{\beta}\big)\big) - 2\log\big(1 + (\alpha x_i)^{\beta}\big) \Big). \end{aligned} \tag{4.12}$$

The score functions of the likelihood are

$$\frac{\partial}{\partial\alpha}(L(\alpha,\beta \mid \underline{x})) = \sum_{i=1}^{n}\left(\frac{\beta}{\alpha} - \frac{2\beta x_i(\alpha x_i)^{\beta-1}}{1+(\alpha x_i)^{\beta}} + \frac{\beta x_i(\alpha x_i)^{\beta-1}}{(1+(\alpha x_i)^{\beta})\log(1+(\alpha x_i)^{\beta})}\right), \tag{4.13}$$

and

$$\tfrac{\partial}{\partial\beta}(L(\alpha,\beta \mid x)) = \sum_{i=1}^{n}\left(\log(\alpha) + \tfrac{1}{\beta} - \tfrac{2(\alpha x_i)^{\beta}\log(\alpha x_i)}{1+(\alpha x_i)^{\beta}} + \tfrac{(\alpha x_i)^{\beta}\log(\alpha x_i)}{(1+(\alpha x_i)^{\beta})\log(1+(\alpha x_i)^{\beta})} + \log(x_i)\right). \tag{4.14}$$

The MLE of the parameters α and β can be obtained by solving the likelihood equations $\frac{\partial}{\partial\alpha}(L(\alpha,\beta \mid x)) = 0$ and $\frac{\partial}{\partial\beta}(L(\alpha,\beta \mid x)) = 0$. However, since these equations do not admit closed-form solutions, numerical iterative procedures are employed to obtain the parameter estimates. As discussed in Chapter 1, the asymptotic distribution of MLE can be used to derive confidence intervals for the estimates.

4.6 Simulation study

A Monte Carlo simulation study was carried out to assess the performance of the proposed ARLL model. Since the quantile function does not exist in a closed form, random samples were generated via the acceptance-rejection sampling technique. For each simulated dataset, the parameters were estimated using the method of maximum likelihood. To evaluate the accuracy and stability of the estimators, the bias and MSE were computed. The simulation was conducted for four different sample sizes 50, 100, 250, and 500 to investigate the impact of sample size on the estimation efficiency. Each scenario was replicated 1000 times, and all computations were performed using the R statistical software.
From Table 4.2, it is evident that both the bias and MSE of the estimators decrease notably as the sample size increases, confirming the consistency of the proposed estimators. Furthermore, the model exhibits good computational efficiency and is straightforward to implement, highlighting its suitability for practical applications.

Table 4.2: Bias and MSE of the estimators of the ARLL model parameters.

Original values	Sample size	α		β	
		Bias	MSE	Bias	MSE
	50	-0.07066	0.03009	-0.02151	0.00939
$\alpha = 0.5$	100	-0.00458	0.01419	-0.00925	0.00392
$\beta = 0.75$	250	0.00366	0.00556	0.00355	0.00153
	500	0.00136	0.00302	0.00177	0.00079
	50	0.00591	0.05449	-0.10881	0.15254
$\alpha = 3$	100	0.00187	0.03277	-0.03571	0.06471
$\beta = 3$	250	-0.00122	0.01208	0.01042	0.02205
	500	-0.00022	0.00016	-0.00869	0.01143
	50	0.00170	0.02298	-0.04745	0.09096
$\alpha = 1.5$	100	0.00145	0.01153	-0.04046	0.04743
$\beta = 2.5$	250	-0.00107	0.00413	0.00327	0.01641
	500	-0.00077	0.00224	0.00028	0.00782
	50	-0.02314	0.12464	-0.04988	0.03503
$\alpha = 2$	100	0.01547	0.05125	-0.01485	0.01621
$\beta = 1.5$	250	0.00219	0.02146	0.00947	0.00592
	500	-0.00108	0.00996	0.00347	0.00297

4.7 Tail behavior

Analyzing the tail behavior of a statistical model is essential for understanding the probability and impact of extreme outcomes that may not be captured by central tendencies alone. In particular, heavy-tailed distributions are useful for modeling phenomena where extreme observations occur with non-negligible probability. In this section, we examine the tail properties of the proposed ARLL distribution. First, we present the definitions of heavy-tailed distributions and regularly varying tails, and then establish the corresponding results for the proposed model.

Definition 4.1. Let X be a random variable with CDF $F(\cdot)$. Then

(i) X is said to be heavy tailed if, for $s > 0$

$$\lim_{x\to\infty} \mathrm{e}^{sx}\bar{F}(x) = \infty.$$

(ii) X is said to have a regularly varying tail, if

$$\lim_{x\to\infty}\frac{\bar{F}(tx)}{\bar{F}(x)}=t^{-\eta},\quad t>0,$$

where $\eta>0$ is the tail index.

Proposition 4.6. Let X be the ARLL random variable. Then

(i) X is heavy tailed. (ii) X has regularly varying tails.

Proof.

(i) From (4.2), we have

$$\lim_{x\to\infty}\mathrm{e}^{sx}\bar{F}_{X\nu X}(x)=\mathrm{e}^{sx}\left(\frac{1+\log\left(1+(\alpha\,x)^{\beta}\right)}{1+(\alpha\,x)^{\beta}}\right)=\infty,\quad s>0,$$

which shows that X is heavy tailed.

(ii) Similarly, we have

$$\lim_{x\to\infty}\frac{\bar{F}_{X\nu X}(tx)}{\bar{F}_{X\nu X}(x)}=\lim_{x\to\infty}\left(\frac{\frac{1+\log\left(1+(\alpha tx)^{\beta}\right)}{1+(\alpha tx)^{\beta}}}{\frac{1+\log\left(1+(\alpha\,x)^{\beta}\right)}{1+(\alpha\,x)^{\beta}}}\right)=t^{-\beta},\quad t>0.,$$

which shows that X has regularly varying tails.

□

For a deeper understanding of the tail behavior of the proposed distribution, we analyze their classification within certain important classes of distribution. One such class is the class of long-tailed distributions, class $\mathcal{L}$, introduced by Chistyakov (1964) is a foundational subclass of heavy-tailed distributions. Another important class is the class $\mathcal{D}$ of dominated variation, a subclass of heavy-tailed distribution discussed in Feller (1968) and Feller (1971). It is also a generalization of regularly varying tails. A further subclass of heavy-tailed distributions is class $\mathcal{S}$ of sub-exponential distribution characterized by the property $\bar{F}(x)*\bar{F}(x)=\sim 2\bar{F}(x)$ as $x\to\infty$, where '$*$' denotes convolution. This

is an important feature in the modeling of various stochastic models, including ruin theory, random walks, branching processes, and classical renewal theory as discussed in Embrechts et al. (1997). Belonging to classes $\mathcal{L}, \mathcal{D}, \mathcal{S}$ ensures that distributions exhibit robust tail properties, making them suitable for applications in the field of reliability theory, extreme value theory, risk analysis, finance, etc. For more details, see Embrechts et al. (1997), Foss et al. (2011), Leipus et al. (2023). The formal definitions of these classes are given below.

Definition 4.2. (Klüppelberg (1988)) A distribution $F(\cdot)$ belongs to class $\mathcal{L}$ if

$$\lim_{x\to\infty} \frac{\bar{F}(x-y)}{\bar{F}(x)} = 1, \quad \forall\ y \in \mathbb{R}.$$

In addition, Klüppelberg (1988) showed that a distribution $F(\cdot)$ belongs to class $\mathcal{L}$ if and only if its hazard rate, $h(x)$, tends to zero as x approaches ∞.

Definition 4.3. (Klüppelberg (1988)) A distribution $F(\cdot)$ belongs to the class $\mathcal{D}$ of dominated-variation distributions if

$$\lim_{x\to\infty} \sup \frac{\bar{F}(x)}{\bar{F}(2x)} < \infty.$$

Definition 4.4. A distribution $F(\cdot)$ belongs to the class of sub-exponential distributions if

$$\lim_{x\to\infty} \frac{1 - F(x) * F(x)}{1 - F(x)} = 2.$$

where $'*'$ denotes the convolution operation.

Now we have the following proposition.

Proposition 4.7. The ARLL model belongs to the following class of distributions:

(i) Class $\mathcal{L}$.

(ii) Class $\mathcal{D}$ of dominated variation.

(iii) Class $\mathcal{S}$ of sub-exponential distributions.

Proof. (i) From the survival function given in 4.2 and Definition 4.2, we have

$$\frac{\bar{F}_{X\nu X}(x-y)}{\bar{F}_{X\nu X}(x)} = \left(\frac{\frac{1+\log\left(1+(\alpha(x-y)^{\beta}\right)}{1+(\alpha(x-y)^{\beta}}}{\frac{1+\log\left(1+(\alpha\, x)^{\beta}\right)}{1+(\alpha\, x)^{\beta}}} \right)$$

Applying limit $x \to \infty$ and simplifying gives

$$\lim_{x\to\infty} \frac{\bar{F}_{X\nu X}(x-y)}{\bar{F}_{X\nu X}(x)} = 1, \quad \forall\, y \in \mathbb{R}, \tag{4.15}$$

which shows that ARLL belongs to the class $\mathcal{L}$.

(ii) From the survival function given in 4.2 and Definition 4.3, we have

$$\lim_{x\to\infty} \frac{\bar{F}_{X\nu X}(x)}{\bar{F}_{X\nu X}(2x)} = 2^{\beta} < \infty.$$

Since the above limit is finite, ARLL belongs to the class $\mathcal{D}$ of dominated variation.

(iii) From Klüppelberg (1988), a distribution $F(\cdot)$ belongs to $\mathcal{D} \cap \mathcal{L}$, then it belongs to the sub-exponential class. Since (i) and (ii) holds true, ARLL belongs to $\mathcal{D} \cap \mathcal{L} \subset \mathcal{S}$. This completes the proof. □

The above results show that the proposed ARLL model preserves the heavy–tailed characteristics of the baseline LL distribution, including regularly varying tails and membership in the classes $\mathcal{L}$, $\mathcal{D}$, and $\mathcal{S}$. In addition, the analysis of Galton's skewness and Moors' kurtosis suggests a comparatively stronger tail heaviness for certain parameter regions, indicating that the transformation may produce slightly heavier right–tail behavior than the baseline model. In the following theorem, we show that the ARLL model has heavier tail when compared to the LL model.

Theorem 4.1. Let X and $X\nu X$ be random variables following the LL and ARLL distributions, respectively, with parameters $\alpha > 0$ and $\beta > 0$. Then the ARLL distribution has a heavier tail than the LL distribution.

Proof. The survival functions of the LL and ARLL distributions are

$$\bar{F}_X(x) = \frac{1}{1+(\alpha x)^\beta}, \qquad \bar{F}_{X\nu X}(x) = \frac{1+\log\big(1+(\alpha x)^\beta\big)}{1+(\alpha x)^\beta}.$$

Then, we have

$$\frac{\bar{F}_{X\nu X}(x)}{\bar{F}_X(x)} = 1+\log\big(1+(\alpha x)^\beta\big)\,.$$

Taking limits as $x \to \infty$ gives

$$\lim_{x\to\infty} \frac{\bar{F}_{X\nu X}(x)}{\bar{F}_X(x)} = \lim_{x\to\infty} \big(1+\log\big(1+(\alpha x)^\beta\big)\big) = \infty.$$

which shows that the ARLL distribution has a heavier tail than the LL distribution. □

Since the ARLL survival function decays more slowly in the tail, it assigns higher probability to large values of x, making it more suitable for modeling datasets exhibiting pronounced extreme behavior when compared to the LL model. This can be verified from the survival function plots of the ARLL and the LL model given in Figure 4.6. Consequently, the auto-relevation transformation enhances the tail heaviness of the baseline distribution, improving its ability to model heavy-tailed phenomena that commonly arise in fields such as reliability analysis, risk assessment, and extreme value theory.

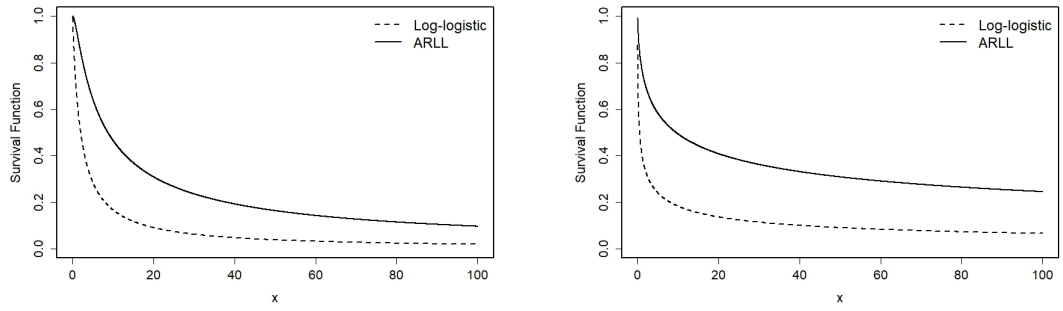

(a) $\alpha = 0.5$, $\beta = 1$ **(b)** $\alpha = 2$, $\beta = 0.5$

Figure 4.6: Survival function plots of ARLL and LL model

4.8 Risk assessment measures of the ARLL distribution

The probability distribution provides an effective framework for describing risk exposure in various domains, including finance and insurance. The level of risk exposure can be quantified using key risk indicators (KRI), which are numerical measures derived from the underlying model. These KRI help quantify and monitor the degree of exposure to specific risks. In this section, we discuss the theoretical and computational aspects of some important risk measures, including value at risk, tail value at risk, mean of order P analysis, and peak over random threshold value at risk analysis for the ARLL model.

4.8.1 Value at Risk

Value at risk (VaR), also known as the quantile risk measure or quantile premium principle, represents the q^{th} quantile of the aggregate loss distribution at a specified confidence level (e.g., 90%, 95%, or 99%). It measures the chance of adverse outcomes and helps determine the capital needed to handle such risks. VaR is especially important for investors, regulators, and rating agencies to assess how well an entity can handle extreme events. Mathematically, for a random variable X, VaR_q is defined as $Q(q)$, where $Q(\cdot)$ denotes the corresponding quantile function (refer Artzner (1999)). If X follows ARLL distribution, then its VaR_q is derived as

$$VaR_q = Q_{X\nu X}\left(\frac{(\alpha\, q)^{\beta} - \log\left(1 + (\alpha\, q)^{\beta}\right)}{1 + (\alpha\, q)^{\beta}}\right).$$

Since the quantile function of the ARLL model does not have a closed-form expression, the value of VaR_q is computed numerically.

4.8.2 Tail Value at Risk

The tail value-at-risk (TVaR), also known as conditional tail expectation (CTE) or tail conditional expectation (TCE), quantifies the expected loss given that a loss exceeds a specified probability level. Mathematically, it is defined as:

$$\begin{aligned} TVaR_q &= \frac{1}{q-1}\int_{VaR_q}^{\infty} x f_{X\nu X}(x)\,dx. \\ &= \frac{1}{q-1}\int_{VaR_q}^{\infty} \frac{\beta(\alpha\,x)^{\beta}\log\left(1+(\alpha\,x)^{\beta}\right)}{\left(1+(\alpha\,x)^{\beta}\right)^{2}}\,dx. \end{aligned}$$

Since this integral does not have a closed form, we evaluate $TVaR_q$ numerically. For further theoretical and practical discussions on such computations, one may refer to Landsman (2010).

Mean of order P analysis

The mean of order P (MOOP) provides a flexible tool for analyzing datasets by examining different statistical moments. As emphasized in Aljadani et al. (2024) and Alizadeh et al. (2025), varying the value of P allows analysts to explore how different moments capture distinct aspects of the data distribution. This is particularly useful in fields such as finance and reliability engineering, where understanding both average behavior and extreme observations is essential. For a dataset $\{x_1, x_2, \ldots, x_n\}$, the MOOP is defined as

$$\text{MOOP} = \left(\frac{1}{n}\sum_{i=1}^{n} x_i^P\right)^{\frac{1}{P}}, \quad P \in \mathbb{R},\ P \neq 0,$$

where x_i represents the i^{th} observation, n denotes the sample size, and P is the order of the moment. When $P = 1$, the MOOP reduces to the arithmetic mean, while for $P = 2$ it corresponds to the quadratic mean, which assigns greater weight to larger observations. In the case $P = 0$, it yields the geometric mean, provided that all $x_i > 0$. As the value of P increases, the measure becomes increasingly sensitive to extreme observations. This sensitivity makes the MOOP

particularly useful for identifying the influence of large observations and outliers in a dataset.

PORT-VaR analysis

The peak over random threshold value-at-risk (PORT-VaR) method provides a framework for analyzing extreme losses by combining parametric modeling with exceedance-based diagnostics. Unlike classical peak-over-threshold approaches, the threshold in PORT-VaR is defined endogenously through the fitted distribution. The implementation involves the following steps:

- **Model fitting:** A suitable heavy-tailed distribution is fitted to the observed loss data.
- **VaR estimation:** The value-at-risk at confidence level u is obtained from the fitted model as the quantile $Q_X(u)$.
- **Threshold definition:** The estimated VaR is treated as a random threshold.
- **Identification of exceedances:** Observations exceeding the VaR are extracted.
- **Frequency and severity analysis:** The number of exceedances and their empirical characteristics (such as mean excess loss and quantiles) are analyzed.

This approach enables a detailed assessment of tail behavior by linking model-based risk measures with empirical properties of extreme observations. Beyond risk quantification, this framework is also valuable for regulatory and capital adequacy purposes, as it supports the estimation of reserves required to withstand extreme loss scenarios, as discussed in Aljadani et al. (2024) and Alizadeh et al. (2025). By offering improved estimation of the risk associated with severe claims, PORT-VaR strengthens risk management decisions, helps determine adequate capital reserves, and enhances the accuracy of pricing

strategies and future exposure forecasting. Additionally, since insurers are required by regulatory authorities to assess and report their vulnerability to extreme events, PORT-VaR provides a transparent and quantitative framework for evaluating catastrophic risk, thereby supporting regulatory compliance and clearer communication with stakeholders, including policyholders and governing bodies.

4.9 Real data analysis

To analyze the applicability of the proposed model, we perform a real data analysis using two datasets. To evaluate the goodness of fit of the ARLL model, we employ the KS test. In addition, to visually assess the closeness between the empirical data and the fitted distribution, we present the Q-Q plot along with the histogram overlaid with the fitted density function. We fit the data using the proposed ARLL model and compare it with some existing generalizations of LL distribution; generalized log-logistic (GLL) (Rosaiah et al. (2006)), Marshall-Olkin log-logistic (MOLL) (Gui (2013)), and extended log-logistic (ELL) (Lima and Cordeiro (2017)). The CDF of the competing distributions are given as follows:

$$\text{(i) GLL: } F(x) = \left(\frac{(x/\alpha)^{\beta}}{1+(x/\alpha)^{\beta}}\right)^{\theta}, \;\; x \geq 0,\; \alpha,\; \beta,\; \theta > 0.$$

$$\text{(ii) MOLL : } F(x) = 1 - \frac{\gamma\,\alpha^{\beta}}{x^{\beta} + \gamma\,\alpha^{\beta}}, \;\; x \geq 0,\; \alpha,\; \beta,\; \gamma > 0.$$

$$\text{(iii) ELL: } F(x) = \left(1 - \left(1 - \frac{x^{\beta}}{\alpha^{\beta}+x^{\beta}}\right)^{a}\right)^{b}, \;\; x \geq 0,\; a,\; b,\; \alpha,\; \beta > 0.$$

The first dataset comprises the annual flood discharges from the North Saskatchewan river in Edmonton, expressed in units of 1000 ft^3/s. The record spans 48 years and was originally reported by Van Montfort (1970). The second dataset consists of travel insurance claim amounts obtained from the `travel_insurance` dataset in the `ExamPAData` package in R. For the present

analysis, we consider the subset of claims corresponding to individuals who traveled by car and whose trip duration was 12 days or more. The summary of both the datasets is provided in Table 4.3.

Table 4.3: Summary statistics of the datasets

Dataset	Sample size	Minimum	1st quartile	Median	Mean	3rd quartile	Maximum
Dataset I	48	19.89	30.34	40.40	51.50	61.34	185.56
Dataset II	46	135	711.5	1294.5	2250.6	3409.8	10620

Table 4.4: Goodness of fit measures for dataset I.

Model	Parameter estimates	KS statistic	p-value
ARLL	$\alpha = 0.0367$ $\beta = 3.4250$	0.0700	0.9730
GLL	$\alpha = 9.725$ $\beta = 2.4959$ $\gamma = 25.559$	0.0706	0.9700
ELL	$\alpha = 8.8640$ $\beta = 9.5696$ $a = 0.2510$ $b = 26.753$	0.0704	0.9680
LL	$\alpha = 0.0233$ $\beta = 3.4616$	0.0723	0.9670
MOLL	$\alpha = 14.279$ $\beta = 3.4614$ $\gamma = 45.182$	0.0733	0.9490

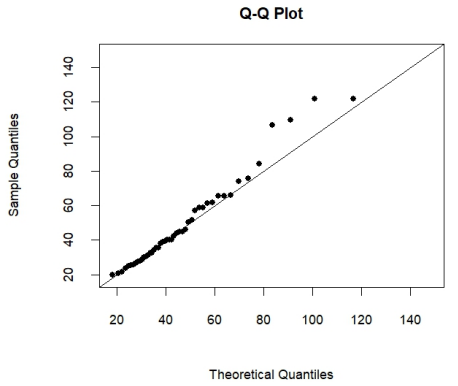

(a) Q-Q plot

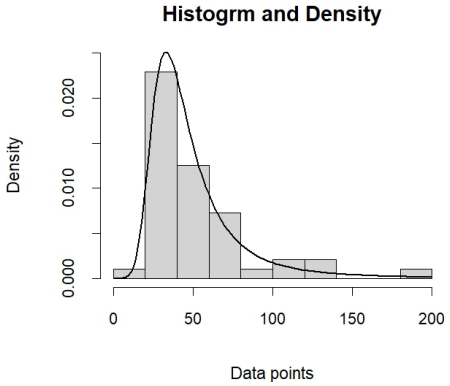

(b) Histogram and fitted density plot

Figure 4.7: Q-Q plot and histogram and density plot for dataset I.

Table 4.4 and Table 4.5 present the goodness of fit measures of the ARLL model along with competing models for datasets I and II, respectively. The results show that the ARLL model consistently provides better fit compared to the alternatives, indicating its suitability for both datasets. This observation is further supported by the histogram and Q–Q plots displayed in Figures 4.7 and 4.8.

Table 4.5: Goodness of fit measures for dataset II.

Model	Parameter estimates				KS statistic	p-value
ARLL	$\alpha = 0.0029$	$\beta = 1.2755$			0.0931	0.9700
LL	$\alpha = 0.0007$	$\beta = 1.5009$			0.0937	0.8720
MOLL	$\alpha = 18.2368$	$\beta = 1.5007$	$\gamma = 648.5055$		0.0936	0.8610
ELL	$\alpha = 0.1541$	$\beta = 28.9362$	$a = 10.3288$	$b = 5.1994$	0.1451	0.6820
GLL	$\alpha = 14.5651$	$\beta = 74.4893$	$\gamma = 1.1278$		0.5034	0.4420

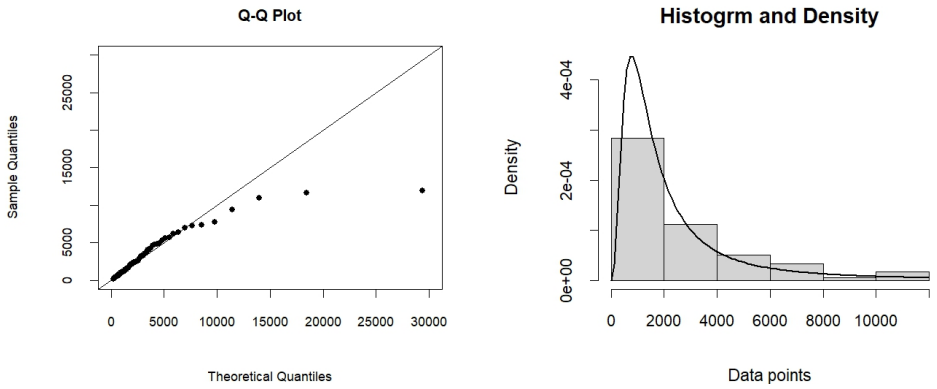

(a) Q-Q plot **(b)** Histogram and fitted density plot

Figure 4.8: Q-Q plot and histogram and density plot for dataset II.

4.9.1 Risk analysis

To demonstrate the applicability of the proposed model in risk analysis, we consider dataset II introduced earlier. Using this dataset, a comprehensive risk assessment is performed based on VaR, TVaR, MOOP, and PORT-VaR measures. The results of the MOOP analysis are summarized in Table 4.6, which reports the order P, the corresponding MOOP estimates, along with the associated bias and MSE for each $P = 1, \ldots, 10$. This facilitates a comparison between the true mean value (TMV) and MOOP estimates across different orders. The PORT-VaR analysis results are presented in Table 4.7, which includes the confidence levels (CL), the corresponding VaR and TVaR values, and the number of exceedances (N_{PORT}) above the VaR threshold. The table also provides descriptive statistics of the exceedances, including the minimum (Min_L), first quartile (Q1_L), median, expected value of losses above VaR

(EVL), third quartile (Q3_L), and maximum (Max_L) losses for each confidence level.

The TMV of the data is evaluated to be 7516.625. The MOOP values for $P = 1, \ldots, 10$ are reported in Table 4.6. It is observed that MOOP increases monotonically with P, indicating that higher-order moments place greater emphasis on large claim values. For all P, the bias remains negative, implying that MOOP underestimates the TMV; however, the magnitude of the bias decreases steadily as P increases, showing improved approximation at higher orders. A similar decreasing pattern is seen in the MSE, reflecting enhanced accuracy and stability of the estimator for larger P. These findings suggest that lower-order MOOP is influenced mainly by moderate claims, whereas higher-order MOOP effectively captures the contribution of extreme observations. This behavior is consistent with the heavy-tailed nature of the data and is further illustrated in Figure 4.9. Table 4.7 presents the model-based

Table 4.6: MOOP Analysis for different orders P

P	1	2	3	4	5
MOOP	2250.609	3201.920	4035.973	4747.958	5353.290
MSE	27730931.08	18616682.45	12114943.22	7665518.77	4680021.15
Bias	-5266.0166	-4314.7054	-3480.6527	-2768.6673	-2163.3357

P	6	7	8	9	10
MOOP	5867.920	6306.330	6681.218	7003.360	7281.708
MSE	2718228.87	1464814.22	697905.60	263441.26	55186.06
Bias	-1648.7052	-1210.2951	-835.4074	-513.2653	-234.9171

VaR and TVaR together with the empirical characteristics of exceedances across different confidence levels. Both measures increase monotonically with the confidence level, with TVaR growing more rapidly, highlighting pronounced tail risk. The N_{PORT} decreases steadily, indicating a gradual focus on more extreme observations as the threshold rises. The minimum exceedances remains close to the corresponding VaR, while the quartiles and median shift upward, reflecting increasing loss severity beyond the threshold. The maximum loss remains unchanged across all levels, as the largest observation consistently exceeds the VaR. The EVL shows noticeable variation, suggesting fluctuations

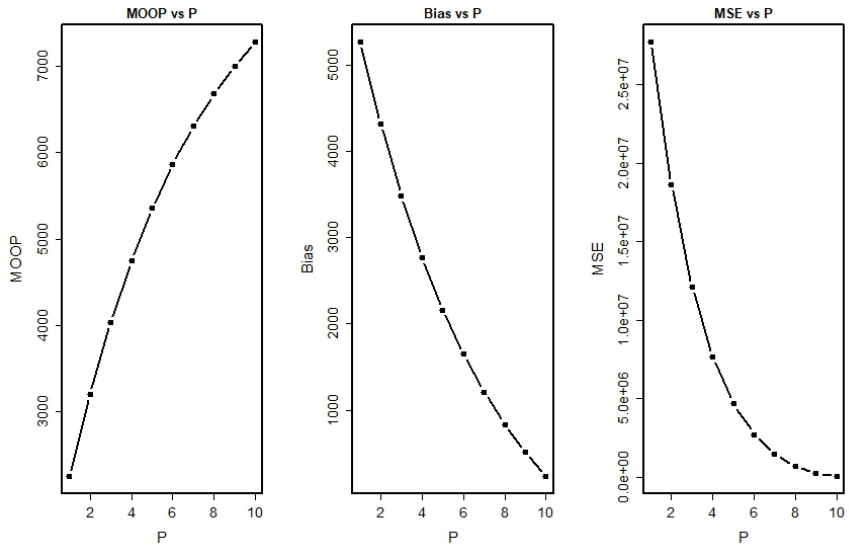

Figure 4.9: The plots of MOOP, Bias, and MSE for different orders P.

Table 4.7: Model based VaR, TVaR, N_{PORT} and empirical characteristics of peaks over VaR.

CL	VaR	TVaR	N_{PORT}	Min_L	Q1_L	Median	EVL	Q3_L	Max_L
0.50	1499.52	14285.24	20	1700	2775.0	3624.5	2714.18	5040.0	10620
0.55	1740.35	15692.91	19	1900	2840.0	3729.0	2605.65	5180.0	10620
0.60	2034.19	17419.26	16	2710	3306.5	3957.5	2762.31	5995.0	10620
0.65	2403.20	19591.84	16	2710	3306.5	3957.5	2393.30	5995.0	10620
0.70	2883.63	22418.47	14	3007	3520.0	4294.0	2201.65	6810.0	10620
0.75	3539.43	26263.55	10	3729	4125.0	5040.0	2265.97	7050.0	10620
0.80	4495.50	31833.35	6	4900	5180.0	6930.0	2495.67	7387.0	10620
0.85	6034.84	40712.32	4	6810	6930.0	7218.5	1931.91	9003.5	10620

in tail intensity while still indicating persistent heavy-tailed behavior. The graphical results in Figure 4.11 reinforce these findings. The density plots exhibit a right-skewed, heavy-tailed pattern with a visible shift toward higher values at larger confidence levels. The histograms reveal that exceedances are concentrated near the threshold, with relatively few extreme observations. The VaR-TVaR plot further illustrates an increasing gap between the two measures, emphasizing the impact of extreme losses. Overall, the PORT-VaR framework effectively captures both the frequency and severity of tail events, providing a coherent basis for assessing and managing extreme risk.

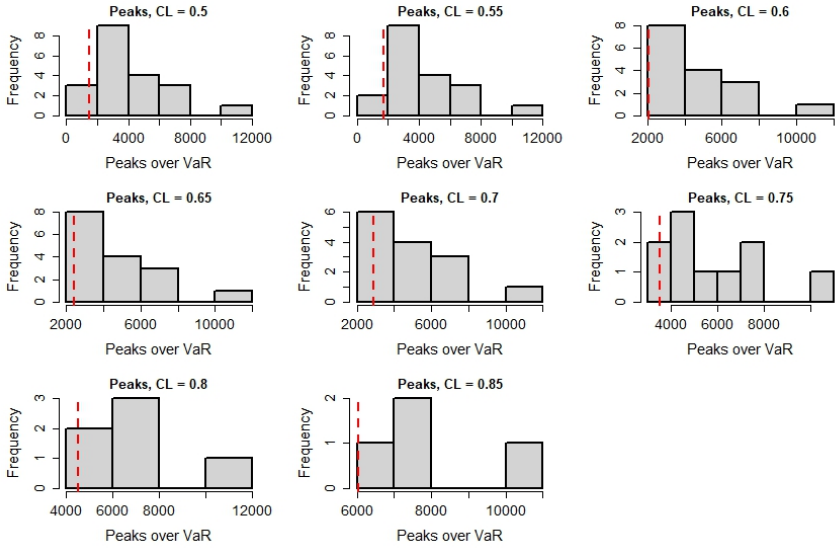

Figure 4.10: Histograms of peaks over VaR for different confidence levels.

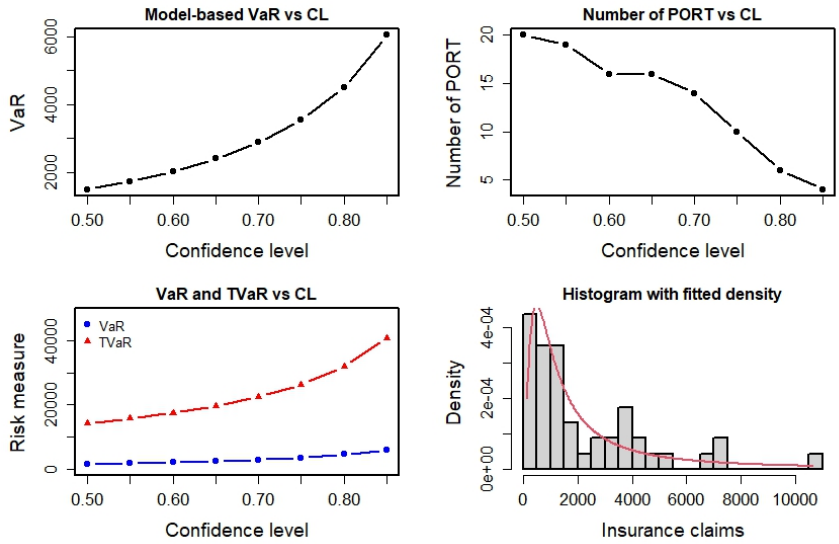

Figure 4.11: Model based VaR versus CL (top left), number of peaks over VaR versus CL (top right), VaR and TVaR versus CL (bottom left), and histogram of claims with fitted density (bottom right).

4.10 Summary of the chapter

This chapter introduced the ARLL distribution by applying the auto-relevation transform to the classical LL model. Several structural and reliability properties of the proposed distribution were derived, and the model was shown

to be heavy-tailed and to belong to several important classes of distributions. A Monte Carlo simulation study demonstrated the satisfactory performance of the maximum likelihood estimators. The practical applicability of the ARLL model was illustrated through real data analyses, where it provided a better fit compared with several existing extensions of the distribution. In addition, its usefulness in risk analysis was examined using real data and yielded satisfactory results. Overall, the ARLL distribution provided a flexible framework for modeling heavy-tailed phenomena and for conducting reliability and risk analyses involving extreme observations.

Chapter 5

Proportional reversed hazards reversed relevation transform

5.1 Introduction

In the previous chapters, we discussed a special cases of the relevation transform and their applications in reliability and extreme value modeling. In this chapter, we consider another important concept, called the reversed relevation transform, which represents the dual of the relevation transform. We now recall the CDF of the reversed relevation transform discussed in Chapter 1, given by

$$F_{X[Y]}(x) = F_Y(x) + F_X(x) \int_x^\infty \frac{1}{F_X(t)}\, dF_Y(t), \quad x \geq 0,\ \theta > 0. \tag{5.1}$$

In the above equation, by assuming Y as the proportional reversed hazards model of X, we obtain a special case called the proportional reversed hazards reversed relevation transform (PRHRRT). The objective of this chapter is to investigate the structural and reliability properties of the proposed model and illustrate its

Results presented in this chapter are published in the article entitled *"Reliability Properties and Applications of Proportional Reversed Hazards in Reversed Relevation Transform"*, published in the journal *Statistics in Transition new series* (Dileepkumar et al. (2025)).

applications using extreme value distributions.

The chapter is organized as follows. Section 5.2 provides a brief overview of the proportional reversed hazards model. In Section 5.3, the concept of the PRHRRT model is introduced and its structural properties are studied. Reliability related results are presented in Section 5.4. The aging properties and stochastic orders of PRHRRT are investigated in Sections 5.5 and 5.6, respectively. Information measures associated with PRHRRT are discussed in Section 5.7. Section 5.8 presents the quantile-based definition and properties of PRHRRT. In Section 5.9, a new generalization of the Fréchet distribution based on PRHRRT is introduced, along with its distributional properties and applications. Finally, Section 5.10 concludes the chapter.

5.2 Proportional reversed hazards model

In contrast to the PHM discussed in Chapter 2, Gupta et al. (1998) introduced the concept of proportional reversed hazards model (PRHM) which has wide range of applications in the field of reliability theory and survival analysis. Let $\lambda_X(\cdot)$ and $\lambda_Y(\cdot)$ be the reversed hazard rates of X and Y respectively. Then Y is said to be the PRHM of X with proportionality constant θ, if

$$\lambda_Y(x) = \theta\lambda_X(x), \quad \theta > 0. \tag{5.2}$$

An equivalent form of (5.2) is

$$F_Y(x) = \big(F_X(x)\big)^\theta, \quad \theta > 0. \tag{5.3}$$

In the context of lifetime studies, the reversed hazard rate has a crucial role when time elapsed since failure is a quantity of interest in order to predict the actual time of failure. PRHM can accommodate non-monotonic hazard rates even though the baseline hazard rate is monotonic. Gupta and Kundu (1999, 2001, 2002, 2007), Sarhan and Kundu (2009), Mahmoud and Alam (2010),

Popović et al. (2022) and several other authors have studied the importance of PRHM model in various lifetime contexts. Moreover, certain characterization results, aging properties and stochastic orders of the PRHM can be seen in Di Crescenzo (2000), Gupta and Wu (2001), Kundu and Gupta (2004), Gupta and Kundu (2007) and Shojaee and Babanezhad (2023). For a parallel system of independent and identically distributed components, the reversed hazard rate of the system lifetime is proportional to that of each component. Under the assumption of PRHM between X and Y in the reversed relevation setup, we obtain the proposed PRHRRT.

5.3 Proportional reversed hazard reversed relevation transform

Let X and Y be two non-negative random variables with absolutely continuous CDF $F_X(\cdot)$ and $F_Y(\cdot)$ respectively. Suppose Y is the PRHM of X as defined in (5.3). Then the reversed relevation random variable $X[Y]$ has the CDF of the form

$$F_{X[Y]}(x) = \big(F_X(x)\big)^\theta + F_X(x) \int_x^\infty \frac{1}{F_X(t)}\, d\big(F_X(t)\big)^\theta, \quad x \geq 0,\ \theta > 0,\ \theta \neq 1. \tag{5.4}$$

The model defined in (5.4) is referred to as the PRHRRT. Di Crescenzo and Toomaj (2015) have showed that the reversed relevation transform is commutative under the assumption of PRHM between the components. We now establish an identity connecting the CDF of $X[Y]$ and the baseline random variable X.

Proposition 5.1. Let X and Y be two non-negative random variables with absolutely continuous CDF $F_X(\cdot)$ and $F_Y(\cdot)$ respectively. Then Y is the PRHM

of X if and only if $F_{X[Y]}(x)$ satisfies

$$F_{X[Y]}(x) = \frac{\theta F_X(x) - \big(F_X(x)\big)^\theta}{\theta - 1}, \quad \theta > 0. \tag{5.5}$$

Proof. Let Y be the PRHM of X. Then from Di Crescenzo and Toomaj (2015) (Proposition 2), the identity (5.5) follows. Now, to prove the converse part, assume that

$$F_Y(x) + F_X(x) \int_x^\infty \frac{1}{F_X(t)} dF_Y(t) = \frac{\theta F_X(x) - \big(F_X(x)\big)^\theta}{\theta - 1}.$$

Rearranging and taking the first derivative with respect to x on both sides gives

$$\begin{aligned} \frac{-f_Y(x)}{F_X(x)} &= \frac{1}{(\theta-1)^2\big(F_X(x)\big)^2}\Big[(\theta-1)F_X(x)\Big(\theta f_X(x) - \theta\big(F_X(x)\big)^{\theta-1} f_X(x) - \\ &\quad (\theta-1)f_Y(x)\Big) - \Big(\theta F_X(x) - \big(F_X(x)\big)^\theta - (\theta-1)F_Y(x)\Big)(\theta-1)f_X(x)\Big]. \end{aligned}$$

Upon simplification, we get

$$\frac{f_X(x)\big(F_X(x)\big)^\theta}{\big(F_X(x)\big)^2} = \frac{f_X(x)F_Y(x)}{\big(F_X(x)\big)^2}$$

$$\implies F_Y(x) = \big(F_X(x)\big)^\theta, \quad \text{for all } x \geq 0,\ \theta > 0. \tag{5.6}$$

This completes the proof. □

Remark 5.1. The CDF of $X[Y]$ given in (5.5) can be represented in a mixture form as

$$\begin{aligned} F_{X[Y]}(x) &= \phi F_X(x) + (1-\phi)\big(F_X(x)\big)^\theta \\ &= \phi F_X(x) + (1-\phi)F_Y(x), \end{aligned} \tag{5.7}$$

where $\phi = \frac{\theta}{\theta-1}$ and one of the weights is negative depending on the value of ϕ.

Let $f_{X[Y]}(x)$ denote the density function of the random variable $X[Y]$. Then

from (5.5), we get

$$f_{X[Y]}(x) = f_X(x)\bigg(\frac{\theta}{\theta-1}\Big(1-\big(F_X(x)\big)^{\theta-1}\Big)\bigg), \tag{5.8}$$

where $f_X(x\cdot)$ is the density function of X. An equivalent representation of (5.5) is given by

$$\bar{F}_{X[Y]}(x) = \frac{\theta\bar{F}_X(x) - \bar{F}_Y(x)}{\theta-1}. \tag{5.9}$$

Example 5.1. Let X be an exponential random variable with density function $f_X(x) = \sigma\,\mathrm{e}^{-\sigma x},\ x > 0,\ \sigma > 0$. Then the CDF of PRHRRT-exponential distribution has the form

$$F_{X[Y]}(x) = \frac{\theta\ \big(1-\mathrm{e}^{-\sigma x}\big) - \big(1-\mathrm{e}^{-\sigma x}\big)^{\theta}}{\theta-1}, \quad x,\ \sigma,\ \theta > 0.$$

The corresponding density function is

$$f_{X[Y]}(x) = \sigma\ \mathrm{e}^{-\sigma x}\bigg(\frac{\theta}{\theta-1}\big(1-(1-\mathrm{e}^{-\sigma x})^{\theta-1}\big)\bigg).$$

Now, in the next proposition, we provide an interesting characterization of PRHRRT.

Proposition 5.2. Let X and Y be two lifetime random variables. Then, Y is the PRHM of X with proportionality constant $\theta = 2$ if and only if $X[Y]$ is the PHM of X with the same proportionality constant.

Proof. Suppose $F_Y(x) = \big(F_X(x)\big)^2$. Then from (5.5), we have

$$\begin{aligned} F_{X[Y]}(x) &= 2F_X(x) - \big(F_X(x)\big)^2 \\ \iff \bar{F}_{X[Y]}(x) &= 1 - 2F_X(x) + \big(F_X(x)\big)^2 \\ \iff \bar{F}_{X[Y]}(x) &= \big(\bar{F}_X(x)\big)^2. \end{aligned}$$

Thus $X[Y]$ is the PHM of X with proportionality constant 2, which completes the proof. □

Remark 5.2. Suppose that the family of distributions of X is invariant under

PHM (*i.e.*, X and the corresponding PHM random variable belongs to the same family of distributions) and Y is the PRHM of X with proportionality constant $\theta = 2$. Then X is invariant under PRHRRT. For example, under the aforementioned setup, X is exponential with mean λ if and only if $X[Y]$ is exponential with mean $\frac{\lambda}{2}$.

5.4 Reliability properties

In this section we delve into certain important reliability properties of the PRHRRT. The hazard rate of the random variable $X[Y]$ under the assumption of PRHM has the form

$$\begin{aligned} h_{X[Y]}(x) &= \frac{f_{X[Y]}(x)}{1 - F_{X[Y]}(x)} \\ &= h_X(x)\left(\frac{\theta(1 - F_X(x))\big(1 - \big(F_X(x)\big)^{\theta-1}\big)}{\theta(1 - F_X(x)) - \big(1 - \big(F_X(x)\big)^{\theta}\big)}\right) \\ &= h_X(x)\left(\frac{1 - \frac{F_Y(x)}{F_X(x)}}{1 - \frac{\bar{F}_Y(x)}{\theta \bar{F}_X(x)}}\right), \end{aligned} \tag{5.10}$$

where $h_X(\cdot)$ is the hazard rate of X.

Let $m_{X[Y]}(\cdot)$ denote the mean residual life of the random variable $X[Y]$, defined by

$$m_{X[Y]}(x) = \frac{1}{\bar{F}_{X[Y]}(x)} \int_x^\infty \bar{F}_{X[Y]}(t)\ dt, \quad x > 0. \tag{5.11}$$

On integrating (5.9) over the interval (x, ∞), we get

$$\int_x^\infty \bar{F}_{X[Y]}(t)\ dt = \frac{\theta}{\theta - 1} \int_x^\infty \bar{F}_X(t)\ dt - \frac{1}{\theta - 1} \int_x^\infty \bar{F}_Y(t)\ dt, \quad x > 0. \tag{5.12}$$

This gives

$$m_{X[Y]}(x)\bar{F}_{X[Y]}(x) = \frac{\theta}{\theta - 1} m_X(x)\bar{F}_X(x) - \frac{1}{\theta - 1} m_Y(x)\bar{F}_Y(x),$$

$$\implies m_{X[Y]}(x) = \frac{\theta\, m_X(x)\bar{F}_X(x) - m_Y(x)\bar{F}_Y(x)}{\theta\bar{F}_X(x) - \bar{F}_Y(x)}, \tag{5.13}$$

where $m_X(\cdot)$ and $m_Y(\cdot)$ are the mean residual life functions of X and Y respectively. The mean inactivity time of $X[Y]$ has the form

$$\begin{aligned}\mu_{X[Y]}(x) &= E(x - X[Y] \mid X[Y] \leq x) \\ &= \frac{1}{F_{X[Y]}(x)} \int_0^x F_{X[Y]}(t)\, dt \\ &= \frac{\theta\, \mu_X(x) - \big(F_X(x)\big)^{\theta-1}\mu_Y(x)}{\theta - \big(F_X(x)\big)^{\theta-1}},\end{aligned} \tag{5.14}$$

where $\mu_X(\cdot)$ and $\mu_Y(\cdot)$ are the mean inactivity times of X and Y respectively. Glaser's function of a random variable X with density function $f_X(\cdot)$ is defined as $\eta_X(x) = -\frac{f'_X(x)}{f_X(x)}$ (Glaser (1980)), where prime denotes the first derivative. It is used as an alternative for the hazard rate in lifetime studies. Under the PRHM assumption between X and Y, the Glaser's function of $X[Y]$ satisfies the identity

$$\eta_{X[Y]}(x) = \eta_X(x)\left(\frac{\big(F_X(x)\big)^{\theta}\big((\theta-1)\big(F_X(x)\big)^2\big) - \big(F_X(x)\big)^2 f'_X(x)}{F_X(x) f_X(x) f'_X(x)\big(F_X(x) - \big(F_X(x)\big)^{\theta}\big)}\right). \tag{5.15}$$

The reversed hazard rate of $X[Y]$ is given by

$$\begin{aligned}\lambda_{X[Y]}(x) = \frac{f_{X[Y]}(x)}{F_{X[Y]}(x)} &= \theta\lambda_X(x)\left(\frac{F_X(x) - F_Y(x)}{\theta F_X(x) - F_Y(x)}\right) \\ &= \lambda_Y(x)\left(\frac{F_X(x) - F_Y(x)}{\theta F_X(x) - F_Y(x)}\right).\end{aligned} \tag{5.16}$$

Now, consider following result based on odds function.

Proposition 5.3. Let $\phi_X(\cdot)$, $\phi_Y(\cdot)$ and $\phi_{X[Y]}(\cdot)$ denote the odds functions of X, Y and $X[Y]$ respectively. Then Y is the PRHM of X if and only if

$$\phi_{X[Y]}(x) = \frac{\theta\,\phi_X(x) - \phi_Y(x)\big(F_X(x)\big)^{\theta-1}}{\theta - \big(F_X(x)\big)^{\theta-1}}. \tag{5.17}$$

Proof. Under the assumption of PRHM, we have

$$\begin{aligned} \phi_{X[Y]}(x) &= \frac{\bar{F}_{X[Y]}(x)}{F_{X[Y]}(x)} \\ \iff \phi_{X[Y]}(x) &= \frac{\theta\bar{F}_X(x) - (1 - \big(F_X(x)\big)^\theta)}{\theta F_X(x) - \big(F_X(x)\big)^\theta} \\ \iff \phi_{X[Y]}(x) &= \frac{\theta\,\phi_X(x) - \phi_Y(x)\big(F_X(x)\big)^{\theta-1}}{\theta - \big(F_X(x)\big)^{\theta-1}}, \end{aligned}$$

where $\phi_Y(x) = \frac{1-\big(F_X(x)\big)^\theta}{\big(F_X(x)\big)^\theta} = \frac{\bar{F}_Y(x)}{F_Y(x)}$. □

The identities (5.9) to (5.17) are useful for obtaining the aforementioned reliability measures of $X[Y]$ from those of the baseline random variables X and Y. Moreover, we can make use of these identities to establish various aging and ordering properties of $X[Y]$ without knowing the distribution of $X[Y]$. In the following proposition, we have the distortion function connecting the random variables X and $X[Y]$.

Proposition 5.4. If Y is the PRHM of X, then $X[Y]$ is a distorted random variable of X with distortion function

$$q(u) = \frac{1}{\theta - 1}(\theta u - (1 - (1 - u)^\theta)). \tag{5.18}$$

Proof. Since Y is the PRHM of X, from (5.9), the survival function $\bar{F}_{X[Y]}(x)$ can be expressed as

$$\bar{F}_{X[Y]}(x) = q(\bar{F}_X(x)), \quad \text{where } q(u) = \frac{1}{\theta - 1}(\theta u - (1 - (1 - u)^\theta)),\ u \in (0, 1).$$

We can easily verify that $q(u)$ given in (5.18) is a distortion function. Thus, $X[Y]$ is a distorted random variable of X with distortion function $q(u)$. □

Note that the distortion function defined in (5.18) is convex. Representing $X[Y]$ as a distorted form of X facilitates the analysis of the preservation of various aging properties from X to $X[Y]$, as well as the establishment of stochastic order relations. These aspects are examined in upcoming sections.

5.5 Aging properties

In this section, we discuss some of the aging properties of $X[Y]$ in connection with the baseline random variable X. Since $X[Y]$ is a distorted random variable of X, in the next proposition we present conditions for the preservation of reliability classes under the formation of PRHRRT by adopting the results presented in Section 1.6.4 of Chapter 1.

Proposition 5.5. Let X and Y be two lifetime random variables, with CDF $F_X(\cdot)$ and $F_Y(\cdot)$ respectively. Let $X[Y]$ be the reversed relevation of X and Y. Assume that Y is the PRHM of X. Then we have the following;

(i) For $\theta \geq 2$, if X is IHR then $X[Y]$ is IHR.

(ii) For $0 < \theta \leq 2$, if X is DHR then $X[Y]$ is DHR.

(iii) For $\theta > 0$, if X is DRHR then $X[Y]$ is DRHR.

(iv) For $0 < \theta \leq 2$, if X is DLR then $X[Y]$ is DLR.

(v) For $\theta > 0$, if X is NWU then $X[Y]$ is NWU.

(vi) For $\theta > 0$, if X is DHRA then $X[Y]$ is DHRA.

Proof. From (5.18), we have the distortion function connecting X and $X[Y]$. By recalling Result 1, we have, if $l_1(u) = \frac{uq'(u)}{q(u)}$ is decreasing (increasing) in $(0,1)$ then the IHR (DHR) property will be preserved with respect to the distortion function $q(u)$. Thus, for proving (i) and (ii), we have to examine the monotonicity of $l_1(u) = \frac{uq'(u)}{q(u)} = \frac{u\left(\theta-\theta\ (1-u)^{\theta-1}\right)}{(1-u)^{\theta}+\theta\ u-1}$. For this, we have

$$l_1'(u) = \frac{\theta\left(u\left(((\theta-1)^2u-2)\,(1-u)^{\theta}-u+2\right)-\left((1-u)^{\theta}-1\right)^2\right)}{(u-1)^2\left((1-u)^{\theta}+\theta u-1\right)^2}. \tag{5.19}$$

The denominator of (5.19) is always non-negative, and by analyzing the numerator, we observe that the right hand side is strictly positive for $0 < \theta < 2$,

strictly negative for $\theta > 2$ and zero for $\theta = 2$. This completes the proof for (i) and (ii).

Again, from Result 2, if $l_2(u) = \frac{uq'(1-u)}{1-q(1-u)}$ is decreasing in $(0,1)$ then the DRHR property will be preserved from X to $X[Y]$. We have $l_2(u) = \frac{uq'(1-u)}{1-q(1-u)} = \frac{\theta\ \left(u^\theta - u\right)}{u^\theta - \theta\ u}$. On differentiating $l_2(u)$ with respect to u, we get

$$l_2'(u) = -\frac{(\theta-1)^2\theta u^\theta}{\left(u^\theta - \theta u\right)^2} \leq 0, \quad \text{for all } \theta > 0 \text{ and } u \in (0,1).$$

Thus $l_2(u)$ is decreasing in u and hence the proof of (iii) follows.

Let $l_3(u) = \frac{uq''(u)}{q'(u)} = -\frac{(\theta-1)u(1-u)^{\theta-1}}{(1-u)^\theta + u - 1}$.

$$l_3'(u) = -\frac{(\theta-1)(1-u)^{\theta-2}\left((1-u)^\theta + u(\theta - \theta u + u) - 1\right)}{\left((1-u)^\theta + u - 1\right)^2},$$

which is non-negative when $0 < \theta \leq 2$ for all $u \in (0,1)$. Now from Result 3, proof of (iv) follows.

It is easy to verify that the distortion function $q(u)$ is super-multiplicative (*i.e.* $q(u\ v) \geq q(u)\ q(v)$, for all $0 \leq u,\ v \leq 1$). Thus, from Result 4, assertion (v) holds true.

Similarly $q(u)$ satisfies the inequality $q(u^a) \geq \left(q(u)\right)^a$ for $0 < a < 1$. Now proof of (vi) follows from Result 5. □

These results are summarized in Table 5.1. We consider the following examples to illustrate the above results.

Example 5.2. Let X be a uniform random variable defined over the interval $(0, c)$. The hazard rate of X is $h_X(x) = \frac{1}{c-x}$, $0 < x < c$. Then, from (5.10) the hazard rate of $X[Y]$ has the form

$$h_{X[Y]}(x) = \left(\frac{1}{c-x}\right)\left(\frac{\theta(x-c)\left(x - c\left(\frac{x}{c}\right)^\theta\right)}{x\left(\theta x - c\left(\left(\frac{x}{c}\right)^\theta + \theta - 1\right)\right)}\right), \quad \text{for } 0 < x < c.$$

Plots of $h_{X[Y]}(x)$ for two different parameter combinations are presented in Figure 5.1. We can observe that $h_{X[Y]}(x)$ accommodates increasing and bathtub shapes,

Table 5.1: Aging classes preserved under PRHRRT

Aging classes	Parameter range
IHR	$\theta \geq 2$
DHR	$0 < \theta \leq 2$
DRHR	$\theta > 0$
DLR	$0 < \theta \leq 2$
NWU	$\theta > 0$
DHRA	$\theta > 0$

while the baseline has only increasing behavior for its hazard rate. From Figure 5.1 a, we can observe that the IHR property is preserved when $\theta > 2$, and has non-monotonic shapes when $0 < \theta < 2$ as shown in Figure 5.1 b.

Example 5.3. Let X be a random variable having a Burr type-XII distribution, with CDF $F_X(x) = 1 - \left(\frac{1}{1+x}\right)^c,\ x > 0,\ c > 0$. Then the hazard rate of X is $h_X(x) = \frac{c}{1+x}$, which is decreasing for all parameter values. Suppose Y is the PRHM of X, then the hazard rate of $X[Y]$ has the form

$$h_{X[Y]}(x) = \frac{c\,\theta\left(\frac{1}{x+1}\right)^{c+1}\left(\left(1-\left(\frac{1}{x+1}\right)^c\right)^\theta + \left(\frac{1}{x+1}\right)^c - 1\right)}{\left(\left(\frac{1}{x+1}\right)^c - 1\right)\left(\theta\left(\frac{1}{x+1}\right)^c + \left(1-\left(\frac{1}{x+1}\right)^c\right)^\theta - 1\right)}.$$

Figure 5.2 a illustrates the preservation of DHR property when $0 < \theta \leq 2$. For $\theta > 2$, the DHR property is not preserved, as illustrated in Figure 5.2 b. It can be observed that $X[Y]$ exhibits DHR and UBT-shaped hazard rates for different parameter combinations, whereas the baseline distribution remains DHR.

5.6 Stochastic orders

In this section, we explore various stochastic orderings of $X[Y]$ in relation to the baseline random variable X. In the coming propositions, we establish interesting stochastic orders between $X[Y]$, X and Y under the PRHM assumption between X and Y, based on the distortion relation given in (5.18).

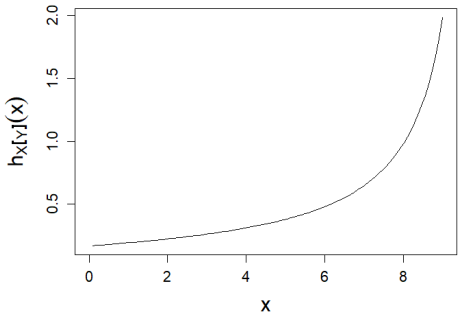

(a) $\theta = 2.5$ and $c = 10$

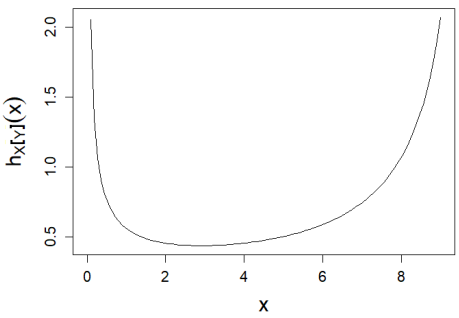

(b) $\theta = 0.2$ and $c = 10$

Figure 5.1: Plots of $h_{X[Y]}(x)$ for two parameter values.

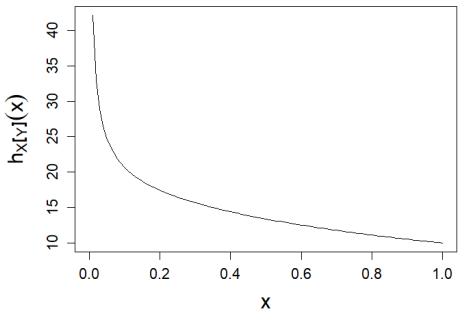

(a) $\theta = 0.5$ and $c = 10$

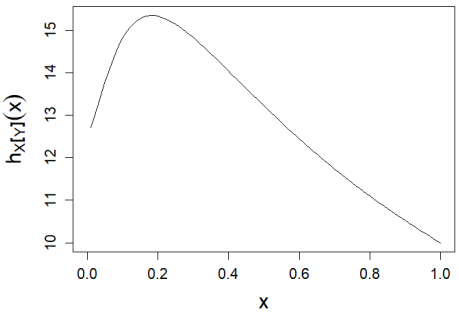

(b) $\theta = 5$ and $c = 10$

Figure 5.2: Plots of $h_{X[Y]}(x)$ for two parameter values.

Proposition 5.6. Let Y be the PRHM of X and $X[Y]$ is the corresponding reversed relevation random variable. Then $X[Y] \leq_{lr} \min\{X, Y\}$.

Proof. To prove this, it is enough to show that $X[Y] \leq_{lr} X$ and $X[Y] \leq_{lr} Y$. By recalling Result 8, we have

$$\frac{q'(u)}{q_1'(u)} = \frac{\theta - \theta(1-u)^{\theta-1}}{\theta - 1}.$$

Differentiating with respect to u, we have

$$\frac{d}{du}\left(\frac{q'(u)}{q_1'(u)}\right) = \frac{d}{du}\left(\frac{\theta - \theta(1-u)^{\theta-1}}{\theta - 1}\right) = \theta(1-u)^{\theta-2} > 0, \text{ for all } \theta > 0 \text{ and } u \in (0,1).$$

Thus $\frac{q'(u)}{q_!'(u)}$ is increasing in $u \in (0,1)$ and thus we have $X[Y] \leq_{lr} X$.

In similar lines, we can write the distortion function connecting $X[Y]$ and Y as

$r_1(u) = \frac{\theta\left(1-(1-u)^{\frac{1}{\theta}}\right)-u}{\theta-1}$ and $r_2(u) = u$ respectively. In similar lines, from Result 8

$$\frac{r_1'(u)}{r_2'(u)} = \frac{(1-u)^{\frac{1}{\theta}-1}-1}{\theta-1}.$$

Note that $\frac{d}{du}\left(\frac{r_1'(u)}{r_2'(u)}\right) = \frac{(1-u)^{\frac{1}{\theta}-2}}{\theta} > 0$, for all $\theta > 0$ and $u \in (0,1)$, and thus we have $X[Y] \leq_{lr} Y$. Now, from Shaked and Shanthikumar (2007), we get $X[Y] \leq_{lr} \min\{X, Y\}$. This completes the proof. □

From Shaked and Shanthikumar (2007) and Proposition (5.6), we have the following implications.

$$X[Y] \leq_{lr} \min\{X, Y\} \implies X[Y] \leq_{hr} \min\{X, Y\} \implies X[Y] \leq_{st} \min\{X, Y\}.$$

Now, we derive stochastic ordering relations between two PRHRRT random variables in the upcoming proposition.

Proposition 5.7. Let X_1 and X_2 be two lifetime random variables with distribution functions $F_1(\cdot)$ and $F_2(\cdot)$ respectively. Suppose Y_1 and Y_2 are the PRHM of X_1 and X_2 respectively with same proportionality constant. Then the following properties hold;

(i) If $X_1 \leq_{st} X_2$, then $X_1[Y_1] \leq_{st} X_2[Y_2]$.

(ii) If $X_1 \leq_{hr} X_2$, then $X_1[Y_1] \leq_{hr} X_2[Y_2]$.

(iii) If $X_1 \leq_{icx} X_2$, then $X_1[Y_1] \leq_{icx} X_2[Y_2]$.

(iv) If $X_1 \leq_{lr} X_2$, then $X_1[Y_1] \leq_{lr} X_2[Y_2]$, for $\theta > 2$.

(v) If $X_1 \leq_{rhr} X_2$, then $X_1[Y_1] \leq_{rhr} X_2[Y_2]$.

Proof. The proof of (i) follows directly from Result 9.

To prove (ii), from Result 10 we need to show that $\frac{u\ q'(u)}{q(u)}$ is decreasing in u. We have

$$\frac{d}{du}\left(\frac{uq'(u)}{q(u)}\right) = \frac{\theta\left(u\left(((\theta-1)^2u-2)(1-u)^\theta - u + 2\right) - \left((1-u)^\theta - 1\right)^2\right)}{(u-1)^2\left((1-u)^\theta + \theta u - 1\right)^2} \leq 0, \quad \text{for all } \theta > 0,$$

which proves assertion (ii).

Similarly (iii) follows from Result 13, since $q(u)$ is a convex function in $(0,1)$.

Again, from Result 12 we only need to prove that $\frac{u\ q''(u)}{q'(u)}$ is non-negative and decreasing in u. We have

$$\frac{d}{du}\left(\frac{u\ q''(u)}{q'(u)}\right) = -\frac{(\theta-1)(1-u)^{\theta-2}\left((1-u)^{\theta}+u(\theta-\theta u+u)-1\right)}{\left((1-u)^{\theta}+u-1\right)^2} \leq 0, \quad \text{for all } \theta \geq 2,$$

which proves (iv).

Similarly to prove (v), using Result 11 it is enough to show that $\frac{(1-u)\ q'(u)}{1-q(u)}$ is increasing in u. For this, consider

$$\frac{d}{du}\left(\frac{(1-u)\ q'(u)}{1-q(u)}\right) = \frac{\theta\left((1-u)^{\theta}+u-1\right)}{(1-u)^{\theta}+\theta(u-1)} > 0, \quad \text{for all } \theta > 0.$$

Thus, assertion (v) follows. □

Proposition 5.8. Let X and Y be two lifetime random variables with distribution functions $F_X(\cdot)$ and $F_Y(\cdot)$ respectively. If Y is the PRHM of X, then:

(i) $X[Y] \leq_c X$ for $\theta \geq 2$.

(ii) $X \leq_c X[Y]$ for $0 < \theta \leq 2$.

Proof. Sengupta and Deshpande (1994) showed that, for two non-negative random variables X and Y with hazard rates $h_X(x)$ and $h_Y(x)$ respectively, $X \leq_c Y$ if and only if $\frac{h_X(x)}{h_Y(x)}$ is non-decreasing in x, provided $h_Y(x) \neq 0$.
To prove (i) we consider the ratio of hazard rates of $X[Y]$ and X.

$$s_1(x) = \frac{h_{X[Y]}(x)}{h_X(x)} = \frac{\theta(F_X(x)-1)\left(F_X(x)-\left(F_X(x)\right)^{\theta}\right)}{F_X(x)\left(\theta F_X(x)-\left(F_X(x)\right)^{\theta}-\theta+1\right)}.$$

On differentiating with respect to x, we get

$$\frac{d}{dx}\left(s_1(x)\right) = \frac{\theta\left(-\left((\theta-1)^2(F_X(x))^2-2(\theta-2)\theta F_X(x)+(\theta-1)^2\right)(F_X(x))^{\theta}+F_X(x)^{2\theta}+(F_X(x))^2\right)f_X(x)}{(F_X(x))^2\left((F_X(x))^{\theta}-\theta F_X(x)+\theta-1\right)^2},$$

which is non-negative for $\theta \geq 2$. Thus $X[Y] \leq_c X$ for $\theta \geq 2$.

Similarly, to prove (ii) we analyze the monotonicity of the function $s_2(x)$ defined by

$$s_2(x) = \frac{h_X(x)}{h_{X[Y]}(x)} = \frac{F_X(x)\left(-F_X(x)^\theta + \theta F_X(x) - \theta - 1\right)}{\theta(F_X(x)-1)\left(F_X(x) - F_X(x)^\theta\right)}.$$

On differentiating with respect to x, we get

$$\frac{d}{dx}\big(s_2(x)\big) = \frac{\left((\theta-1)(F_X(x)-1)((\theta-1)F_X(x)-\theta-1)F_X(x)^\theta - F_X(x)^{2\theta} + F_X(x)^2\right) f_X(x)}{\theta(F_X(x)-1)^2\left(F_X(x)-F_X(x)^\theta\right)^2},$$

which is non-negative for $0 < \theta \leq 2$. Thus $X \leq_c X[Y]$ for $0 < \theta \leq 2$. □

5.7 Information measures

Measuring uncertainty associated with random variables is very important in many real-life situations. These uncertainties can be calculated using information measures. We now turn our focus to some important information measures concerning PRHRRT. Consider the cumulative Tsallis past entropy (CTE) introduced by Calì et al. (2017), which has the form

$$T_X(\alpha) = \frac{1}{\alpha - 1}\int_0^\infty \left(F_X(x) - \big(F_X(x)\big)^\alpha\right) dx, \quad \alpha > 0,\ \alpha \neq 1. \tag{5.20}$$

Now, we have the following proposition.

Proposition 5.9. Let Y be the PRHM of X with proportionality constant θ. Then

$$T_X(\theta) = E(X) - E(X[Y]), \tag{5.21}$$

where $T_X(\theta)$ is the CTE of X.

Proof. From (5.20), we have

$$\begin{aligned} T_X(\theta) &= \frac{1}{\theta - 1}\int_0^\infty \left(F_X(x) - \theta F_X(x) + \theta F_X(x) - \big(F_X(x)\big)^\theta\right) dx \\ &= \int_0^\infty \left(F_{X[Y]}(x) - F_X(x)\right) dx \end{aligned}$$

$$
\begin{aligned}
&= \int_0^\infty \big(\bar{F}_X(x) - \bar{F}_{X[Y]}(x)\big)\, dx \\
&= E(X) - E(X[Y]),
\end{aligned}
$$

which completes the proof. □

Remark 5.3. When Y is the PRHM of X with proportionality constant θ; from (5.20), we get

$$T_X(\theta) = \frac{1}{\theta - 1}\big(E(Y) - E(X)\big). \tag{5.22}$$

Now (5.21) and (5.22) together gives

$$E(X[Y]) = \frac{\theta E(X) - E(Y)}{\theta - 1}.$$

Remark 5.4. The identity (5.21) can be used for constructing simple non-parametric estimator for $T_X(\theta)$ by using the estimators of $E(X)$ and $E(X[Y])$.

Inaccuracy measures are used to measure the deviation of a distribution of interest from a reference distribution. It was first introduced by Kerridge (1961) in the discrete scenario and later developed for the continuous case by Nath (1968). If X and Y are two absolutely continuous random variables, then the inaccuracy measure or the cross entropy between X and Y is given by

$$\xi_{X,Y} = E_X(-\log f_Y(x)) = -\int_0^\infty f_X(x) \log f_Y(x)\, dx. \tag{5.23}$$

From (5.8) and (5.23), we get

$$
\begin{aligned}
\xi_{X,X[Y]} &= -\int_0^\infty f_X(x) \log\left(f_X(x)\frac{\theta}{\theta-1}\Big(\theta - \big(F_X(x)\big)^{\theta-1}\Big)\right) dx \\
&= H_X - \log\frac{\theta}{\theta-1} - \int_0^\infty f_X(x)\log\Big(\theta - \big(F_X(x)\big)^{\theta-1}\Big)\, dx \\
&= H_X - \int_0^1 \log\left(\frac{\theta(\theta - u^{\theta-1})}{\theta-1}\right) du,
\end{aligned}
$$

where H_X is the Shannon entropy of X.

Taneja et al. (2009) proposed the cumulative past inaccuracy measure (δ) as

$$\delta_{X,Y} = -\int_0^\infty F_X(x) \log F_Y(x)\ dx.$$

Consider the cumulative entropy ζ, discussed in Section 1.6.5 of Chapter 1. Now, we obtain an interesting identity connecting $\delta_{X[Y],X}$ with ζ_X and ζ_Y as

$$\delta_{X[Y],X} = \frac{\theta^2\zeta_X - \zeta_Y}{\theta(\theta-1)}.$$

Di Crescenzo et al. (2018) derived an inaccuracy measure based on the reversed relevation transform, denoted by $\tilde{R}_{X,Y}(x)$, given by

$$\tilde{R}_{X,Y}(x) = \frac{1}{F_Y(x)}\int_0^x \mu_X(u) f_Y(u)\ du + \mu_Y(x) - \mu_X(x), \quad x > 0.$$

Under the proportional reversed hazards assumption, $\tilde{R}_{X,Y}(x)$ becomes

$$\tilde{R}_{X,Y}(x) = \frac{1}{\theta-1}\big(\mu_X(x) - \mu_Y(x)\big).$$

Moreover, Di Crescenzo et al. (2018) introduced a reversed relevation inaccuracy ratio as follows

$$R^*_{X,Y}(x) = \frac{\zeta_X(x)}{R_{X,Y}(x)}.$$

In particular, when Y is the PRHM of X, we get

$$R^*_{X,Y}(x) = (1 - \log F_X(x))(\theta-1)\left(\frac{\mu_{X[X]}(x) - \mu_X(x)}{\mu_X(x) - \mu_Y(x)}\right). \tag{5.24}$$

Proposition 5.10. If Y is the PRHM of X with proportionality constant θ, then

$$R^*_{X,X[Y]}(x) = (\theta-1)(1 - \log F_X(x))\left(\frac{(\mu_{X[X]}(x) - \mu_X(x))(\theta - \big(F_X(x)\big)^{\theta-1})}{(\mu_X(x) - \mu_Y(x))\big(F_X(x)\big)^{\theta-1}}\right).$$

This can be easily verified from (5.24), so the proof is omitted.

5.8 Quantile based representation

Let $Q_X(\cdot)$ and $Q_Y(\cdot)$ be the quantile functions of two non-negative random variables X and Y respectively. Now by taking $x = Q_X(u)$, from equation (1.2) in Chapter 1, we get

$$\begin{aligned} F_{X[Y]}(Q_X(u)) &= F_Y(Q_X(u)) + u\int_u^1 \frac{1}{p}\, d(F_Y(Q_X(u))) \\ &= Q_Y^{-1}(Q_X(u)) + u\int_u^1 \frac{1}{p}\; d(Q_Y^{-1}(Q_X(u))) \\ \implies T^*(u) &= Q_1(u) + u\int_u^1 \frac{1}{p}\, d(Q_1(p)), \end{aligned} \tag{5.25}$$

where $Q_1(u) = Q_Y^{-1}(Q_X(u))$ and $T^*(u) = F_{X[Y]}(Q_X(u))$. From Gilchrist (2000), if $Q(u)$ is a quantile function and $\eta(x)$ is a non-decreasing function of x, then $\eta(Q(u))$ is also a quantile function. Since $F_{X[Y]}(\cdot)$ and $F_Y(\cdot)$ are non-decreasing functions, it follows that $T^*(\cdot)$ and $Q_1(\cdot)$ are the quantile functions corresponding to $F_X\Big(F_{X[Y]}^{-1}(x)\Big)$ and $F_X\big(F_Y^{-1}(x)\big)$, respectively. We may interpret $T^*(u)$ as the total lifetime of the system up to the $(100 \times u)\%$ quantile of X, given that the lifetime is less than a random time Y. From (5.25), we have

$$\begin{aligned} T^*(u) &= F_{X[Y]}(Q_X(u)) \\ \implies Q_{X[Y]}(T^*(u)) &= Q_X(u) \\ \implies Q_{X[Y]}(u) &= Q_X(T^{*-1}(u)). \end{aligned} \tag{5.26}$$

The identity (5.26) enable us to form the quantile function of $X[Y]$ from $T^*(u)$ and $Q_X(u)$. Nair and Sankaran (2009) defined various reliability measures using quantile functions such as the hazard quantile function, the mean residual quantile function, etc. These measures are useful in situations where we lack a closed-form expression for the distribution function. Moreover, quantile functions have several interesting properties that are not true in the case of distribution functions; for example, the sum of two quantile functions is again a quantile function. The relationship between the random variable X and $X[Y]$ based on

various quantile based reliability measures can be established using the identity (5.25). When Y follows the PRHM of X, we obtain $Q_1(u) = u^\theta$. Consequently, (5.25) reduces to

$$\begin{aligned} T^*_{RH}(u) &= u^\theta + u\int_u^1 \frac{1}{p}\, dp^\theta \\ &= \frac{\theta u - u^\theta}{\theta - 1}, \quad \theta > 0,\ 0 \le u \le 1. \end{aligned} \tag{5.27}$$

We refer to $T^*_{RH}(u)$ as the proportional reversed hazards reversed relevation quantile function (PRHRRQ). Note that $T^*_{RH}(u)$ is a quantile function with unit support. Several quantile-based properties of the PRHRRT can be studied using (5.27).

5.9 Applications based on Fréchet model

In this section, as an application of the PRHRRT in extreme value modeling, we propose a new form of the Fréchet distribution. Let X follow the two-parameter Fréchet distribution with CDF

$$F_X(x) = \mathrm{e}^{-(\frac{\sigma}{x})^\alpha},\ x > 0,\ \sigma > 0,\ \alpha > 0.$$

Then the distribution function of the corresponding PRHRRT random variable $W = X[Y]$ is obtained as

$$T_W(x) = \frac{\theta\, \mathrm{e}^{-(\frac{\sigma}{x})^\alpha} - \left(\mathrm{e}^{-(\frac{\sigma}{x})^\alpha}\right)^\theta}{\theta - 1}, \quad x > 0,\ \sigma,\ \alpha > 0,\ \theta > 0. \tag{5.28}$$

We denote the model (5.28) as the proportional reversed hazards reversed relevated Fréchet (PRHRR-F) distribution. The r^{th} raw moment of PRHRR-F denoted by μ'_r is of the form

$$\mu'_r = \frac{\sigma^r \left(\theta - \theta^{\frac{r}{\alpha}}\right) \Gamma\left(1 - \frac{r}{\alpha}\right)}{\theta - 1}, \quad \alpha > r,\ r = 0, 1, 2, \ldots. \tag{5.29}$$

The moment generating function of Z is obtained as

$$M_W(t) = \sum_{r=0}^{\infty} \mu'_r \frac{t^r}{r!}, \quad \alpha > r.$$

The corresponding hazard rate has the form

$$h_W(x) = -\frac{\alpha\,\theta\left(\frac{\sigma}{x}\right)^{\alpha}\left(\left(\mathrm{e}^{-\left(\frac{\sigma}{x}\right)^{\alpha}}\right)^{\theta-1}-1\right)}{x\,\mathrm{e}^{\left(\frac{\sigma}{x}\right)^{\alpha}}\left(\theta+\left(\mathrm{e}^{-\left(\frac{\sigma}{x}\right)^{\alpha}}\right)^{\theta}-1\right)-\theta\,x}.$$

From Figure 5.3, we can observe that $h_W(x)$ incorporates IHR, DHR and UBT shapes for various parameter combinations.

5.9.1 Parameter estimation

The estimation of unknown parameters ar evaluated using the method of maximum likelihood. Let $X_1, X_2, \ldots, X_n$ be a random sample of size n from the PRHRR-F $(\sigma,\ \alpha,\ \theta)$ distribution, and $\underline{x} = (x_1, x_2, \ldots, x_n)$ denote the corresponding observed values. Then, the log-likelihood function can be obtained as

$$L(\sigma, \alpha, \theta \mid \underline{x}) = \sum_{i=1}^{n} \log\left(\frac{\alpha\ \theta\ \mathrm{e}^{-\left(\frac{\sigma}{x_i}\right)^{\alpha}}\left(\frac{\sigma}{x_i}\right)^{\alpha}\left(\left(\mathrm{e}^{-\left(\frac{\sigma}{x_i}\right)^{\alpha}}\right)^{\theta-1}-1\right)}{(1-\theta)x_i}\right).$$

The MLE of the parameters, denoted by $\hat{\sigma}$, $\hat{\alpha}$, and $\hat{\theta}$, can be obtained by solving the equations $\frac{\partial L}{\partial \sigma} = 0$, $\frac{\partial L}{\partial \alpha} = 0$, and $\frac{\partial L}{\partial \theta} = 0$ simultaneously. Since this system of equations is nonlinear and does not admit closed-form solutions, we employ numerical methods. As discussed in the previous chapters, the confidence intervals of the estimates can be constructed using the asymptotic distribution of MLE.

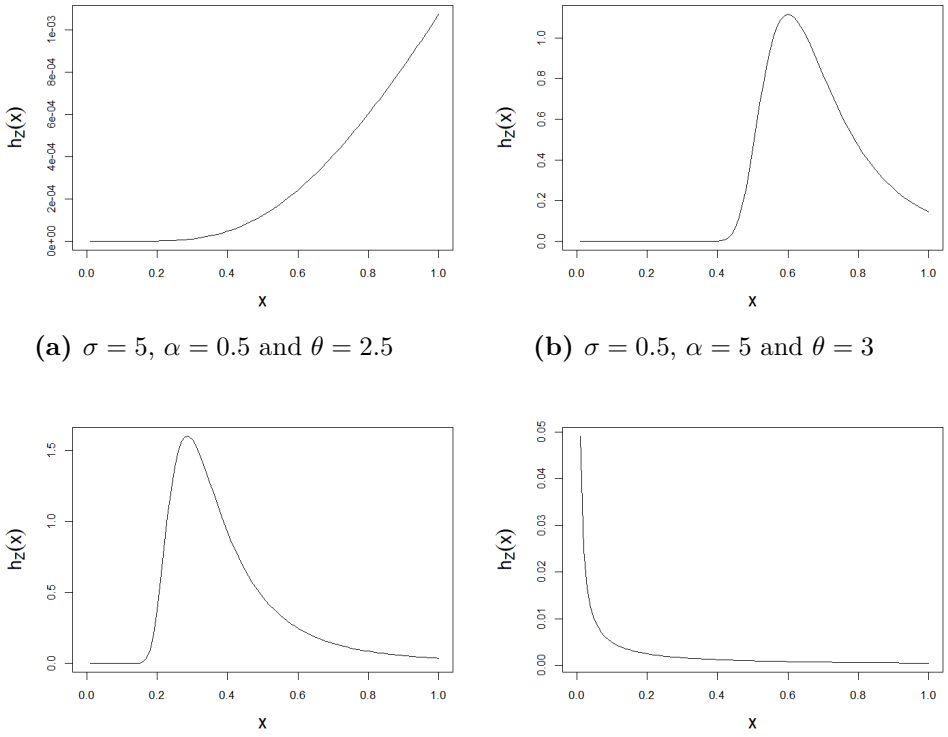

(a) $\sigma = 5$, $\alpha = 0.5$ and $\theta = 2.5$ **(b)** $\sigma = 0.5$, $\alpha = 5$ and $\theta = 3$

(c) $\sigma = 0.2$, $\alpha = 3$ and $\theta = 4$ **(d)** $\sigma = 0.01$, $\alpha = 0.01$ and $\theta = 1.5$

Figure 5.3: Plots of $h_W(x)$ for various parameter combinations.

5.9.2 Real data analysis

To illustrate the practical applicability of the proposed model, we consider real-life datasets and compare the model with several competing distributions, namely the generalized Fréchet (GF), Marshall-Olkin Fréchet (MOF), exponential Fréchet (EF), Weibull Fréchet (WF), and the classical Fréchet distribution. The parameters are estimated using the maximum likelihood method, and the adequacy of fit is assessed using the KS test.

The dataset I, taken from Smith and Naylor (1987), consists of 63 observations on the strengths of glass fibers, originally collected by staff members at the UK national physical laboratory. From Table 5.2, the PRHRR-F model provides the best fit, as it yields the smallest KS statistic and the largest p-value among the competing models. The standard errors of $\hat{\sigma}$, $\hat{\alpha}$, and $\hat{\theta}$ are 0.0569, 0.0438, and 0.2359, respectively. The 95% confidence intervals for the parameter

estimates $\hat{\sigma}$, $\hat{\alpha}$, and $\hat{\theta}$ are (1.6411, 1.8644), (3.5736, 3.7453), and (0.5382, 1.4631), respectively. The observed histogram along with the fitted density functions is presented in Figure 5.4 and the corresponding Q-Q plot is displayed in Figure 5.6 a. These plots indicate that the PRHRR-F distribution provides a good fit to the data.

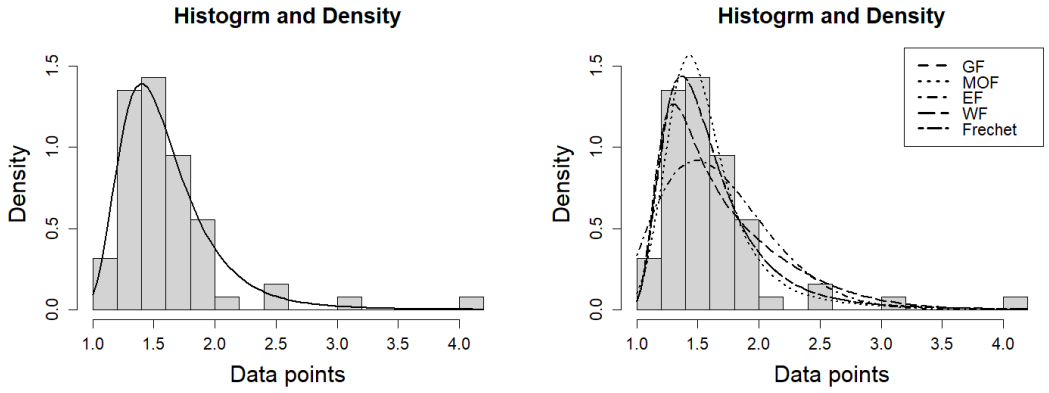

(a) PRHRR-F distribution **(b)** Other competing models

Figure 5.4: Histogram and density plots for the dataset I.

Table 5.2: Estimates, KS statistics and p-values for the dataset I.

Distributions	Estimates			KS statistics	p-value
PRHRR-F (σ, α, θ)	$\hat{\sigma} = 1.7527$	$\hat{\alpha} = 3.6595$	$\hat{\theta} = 0.9995$	0.0683	0.9114
GF (λ, α, β)	$\hat{\lambda} = 1.6737$	$\hat{\alpha} = 5.4376$	$\hat{\beta} = 0.3948$	0.0772	0.8185
Fréchet (σ, α)		$\hat{\sigma} = 1.4108$	$\hat{\alpha} = 5.4377$	0.0772	0.8185
MOF (α, β, λ)	$\hat{\alpha} = 1.4559$	$\hat{\beta} = 5.2227$	$\hat{\lambda} = 0.0023$	0.0813	0.7686
WF (α, β, λ)	$\hat{\alpha} = 1.6248$	$\hat{\beta} = 5.9372$	$\hat{\lambda} = 0.3750$	0.1659	0.0551
EF (α, β, λ)	$\hat{\alpha} = 1.7936$	$\hat{\beta} = 2.3223$	$\hat{\lambda} = 0.3016$	0.1739	0.0389

To demonstrate the applicability of the proposed model beyond reliability contexts, we consider another dataset reported in Hand et al. (1994). The dataset II consist of the prices of 31 different children's wooden toys sold in a Suffolk craft shop in April 1991. To evaluate the performance of the proposed model relative to other competing alternatives, the KS goodness of fit test is employed. The parameter estimates and the corresponding goodness of fit test results are presented in Table 5.3. From Table 5.3, it is evident that the PRHRR-F model provides a better fit than the competing alternatives.

The standard errors and 95% confidence intervals of $\hat{\sigma}$, $\hat{\alpha}$, and $\hat{\theta}$ are 0.0868, 0.0372, and 2.7654 and (1.9347, 2.2751), (1.0177, 1.1636), and (6.6134, 17.4540), respectively. Figure 5.5 shows the observed histogram along with the fitted density functions, and the Q-Q plot is presented in Figure 5.6 b. These plots further confirm the adequacy of the proposed model for the data.

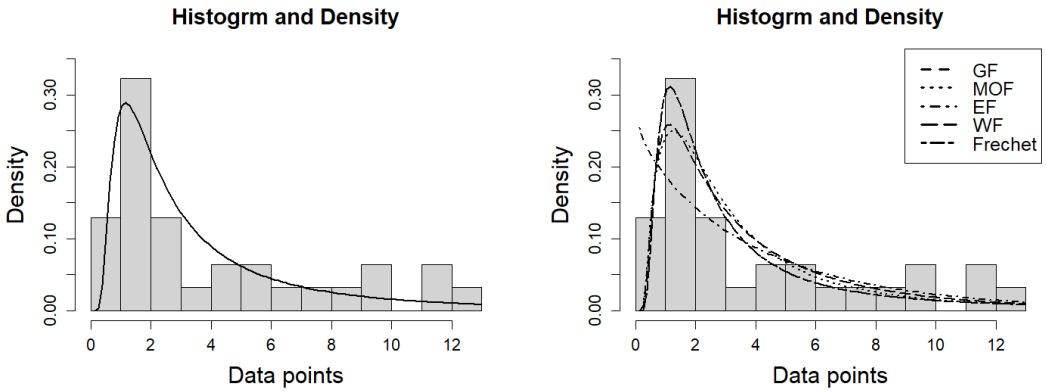

(a) PRHRR-F distribution **(b)** Other competing models

Figure 5.5: Histogram and density plots for the dataset II.

Table 5.3: Estimates, KS statistics and p-values for the dataset II.

Distributions	Estimates		KS statistics	p-value
PRHRR-F (σ, α, θ)	$\hat{\sigma} = 2.1045$	$\hat{\alpha} = 1.0906$ $\hat{\theta} = 12.0434$	0.0821	0.9851
GF (λ, α, β)	$\hat{\lambda} = 1.2321$	$\hat{\alpha} = 1.2147$ $\hat{\beta} = 1.6709$	0.0980	0.9271
Fréchet (σ, α)		$\hat{\sigma} = 1.8802$ $\hat{\alpha} = 1.2148$	0.0979	0.9271
WF (α, β, λ)	$\hat{\alpha} = 2.7451$	$\hat{\beta} = 1.0389$ $\hat{\lambda} = 0.7502$	0.1000	0.9156
MOF (α, β, λ)	$\hat{\alpha} = 1.6728$	$\hat{\beta} = 0.8776$ $\hat{\lambda} = 6.4507$	0.1014	0.9074
EF (α, β, λ)	$\hat{\alpha} = 2.6055 \times 10^{-14}$	$\hat{\beta} = 0.9559$ $\hat{\lambda} = 3.9062$	0.1392	0.5848

5.10 Summary of the chapter

In this chapter, we introduced the PRHRRT as a special case of the reversed relevation transform and discussed its reliability properties in detail. The aging and stochastic ordering properties of the model were also established. An alternative representation of the PRHRRT model based on quantile functions was presented. In addition, certain information measures associated with the

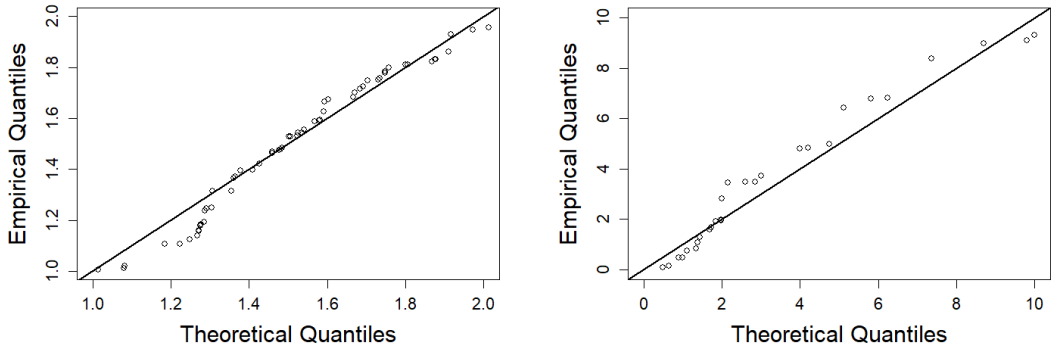

(a) Dataset I **(b)** Dataset II

Figure 5.6: Q-Q plots for both datasets.

proposed model were derived. Finally, we introduced the PRHRR-F (σ, α, θ) distribution, investigated its important characteristics, and demonstrated its practical applicability using two real-life datasets.

Chapter 6

The reversed auto-relevation transform

6.1 Introduction

In this chapter, we consider another special case of the reversed relevation transform, called the reversed auto-relevation transform (RART), which arises when the random inspection time and the failure time are identically distributed. This setting provides a natural framework for modeling systems operating under inspection-based replacement or maintenance policies. The reliability aspects of the proposed model are initially studied to establish its fundamental properties. Subsequently, adopting a statistical perspective, the chapter focuses on information-theoretic and quantile-based characteristics, which provide deeper insight into the behavior of the RART model beyond the reliability framework considered earlier.

The chapter is organized as follows. Section 6.2 provides a detailed description of the RART, along with characterization results based on certain reliability measures. The preservation of various aging classes under the formation of the RART is studied in Section 6.3, together with illustrations of its practical relevance. In Section 6.4, several stochastic ordering relations are derived. The stress–strength reliability expression based on the RART model is derived in Section 6.5. Quantile-based properties and applications of the

RART model are discussed in Section 6.6. Section 6.7 develops results based on entropy, extropy, inaccuracy, and divergence measures. In Section 6.8, a new RART Gumbel model is proposed and its practical utility is explored. Finally, Section 6.9 concludes the chapter.

6.2 Reversed auto-relevation transform

Recall the definition of the reversed relevation transform given in (1.2) in Chapter 1. By assuming that the random variables X and Y are identically distributed with CDF $F_X(\cdot)$, the RART model is obtained as

$$F_{X[X]}(x) = F_X(x)(1 - \log F_X(x)) = F_X(x)\left(1 + \Lambda_X(x)\right), \tag{6.1}$$

where $\Lambda_X(\cdot)$ is the cumulative reversed hazard rate of X. The random variable corresponding to the CDF given in (6.1) is denoted by $X[X]$. The corresponding survival function has the form

$$\bar{F}_{X[X]}(x) = \bar{F}_X(x) + F_X(x)\log F_X(x), \tag{6.2}$$

where $\bar{F}_X(\cdot)$ is the baseline survival function. The corresponding density function is given by

$$f_{X[X]}(x) = -f_X(x)\log F_X(x). \tag{6.3}$$

Alternatively, $f_{X[X]}(x)$ can be expressed as a weighted form of $f_X(x)$ as

$$f_{X[X]}(x) = \frac{w(x)}{E(w(X))}\ f_X(x), \tag{6.4}$$

where $w(x) = -\log F_X(x)$ is the weight function and $E\left(-\log F_X(X)\right) = 1$. While examining the hazard rate of $X[X]$, we obtain an interesting identity relating $h_{X[X]}(x)$ and $h_X(x)$, which is presented in the following proposition.

Proposition 6.1. Let X be a non-negative continuous random variable. Then,

$X[X]$ is the RART random variable of X if and only if

$$h_{X[X]}(x) = h_X(x)\left(\frac{\phi_X(x)\Lambda_X(x)}{\phi_X(x) - \Lambda_X(x)}\right), \tag{6.5}$$

where $\phi_X(\cdot)$ and $\Lambda_X(\cdot)$ are the odds function and cumulative reversed hazard rate of X respectively.

Proof. Assume that $X[X]$ is the RART random variable of X. Then

$$\begin{aligned}
& h_{X[X]}(x) = \frac{f_{X[X]}(x)}{\bar{F}_{X[X]}(x)} \\
\iff \quad & h_{X[X]}(x) = \frac{-f_X(x)\log F_X(x)}{\bar{F}_X(x) + F_X(x)\log F_X(x)} \\
\iff \quad & h_{X[X]}(x) = h_X(x)\left(\frac{-\bar{F}_X(x)\log F_X(x)}{\bar{F}_X(x) + F_X(x)\log F_X(x)}\right) \qquad (6.6) \\
\iff \quad & h_{X[X]}(x) = h_X(x)\left(\frac{\phi_X(x)\Lambda_X(x)}{\phi_X(x) - \Lambda_X(x)}\right),
\end{aligned}$$

which completes the proof. □

From (6.6), we observe that, since $\frac{-\bar{F}_X(x)\log F_X(x)}{\bar{F}_X(x)+F_X(x)\log F_X(x)} > 1$, for all $x > 0$, $h_{X[X]}(x) > h_X(x)$. Thus, RART model accelerates the hazard rate of the device by $\frac{-\bar{F}_X(x)\log F_X(x)}{\bar{F}_X(x)+F_X(x)\log F_X(x)}$. This indicates that the RART model is suitable for situations where the hazard rate of a component needs to be accelerated. The reversed hazard rate of the random variable $X[X]$, denoted by $\lambda_{X[X]}(\cdot)$, is given by

$$\begin{aligned}
\lambda_{X[X]}(x) &= \frac{f_{X[X]}(x)}{F_{X[X]}(x)} \\
&= \frac{f_X(x)\big(-\log F_X(x)\big)}{F_X(x)\big(1-\log F_X(x)\big)} \\
&= \lambda_X(x)\left(\frac{-\log F_X(x)}{1-\log F_X(x)}\right) \\
&= \lambda_X(x)\left(\frac{\Lambda_X(x)}{1+\Lambda_X(x)}\right), \qquad (6.7)
\end{aligned}$$

where $\lambda_X(\cdot)$ denotes the reversed hazard rate of X. Some useful implications of the relation in (6.7) are presented below in the form of characterization results for certain distributions.

Theorem 6.1. The random variable X has inverse Weibull distribution with CDF $F_X(x) = \mathrm{e}^{-\left(\alpha x^{-\beta}\right)},\ x > 0,\ \alpha > 0,\ \beta > 0$ if and only if

$$\lambda_{X[X]}(x) = \lambda_X(x)\left(\frac{\alpha}{\alpha + x^{\beta}}\right). \tag{6.8}$$

Proof. Assuming X follows inverse Weibull distribution, by direct calculations we obtain the required identity (6.8). Conversely, (6.7) gives

$$\frac{\lambda_{X[X]}(x)}{\lambda_X(x)} = \frac{\Lambda_X(x)}{1 + \Lambda_X(x)} = \frac{\alpha}{\alpha + x^{\beta}},$$

which corresponds to the inverse Weibull distribution with CDF $F_X(x) = \mathrm{e}^{-\left(\alpha x^{-\beta}\right)}$. □

Remark 6.1. As a special case of the inverse Weibull distribution, we note that X follows the inverse exponential distribution with CDF $F_X(x) = \mathrm{e}^{-\left(\frac{\alpha}{x}\right)},\ x > 0,\ \alpha > 0$, if and only if

$$\frac{\Lambda_X(x)}{1 + \Lambda_X(x)} = \lambda_X(x)\left(\frac{\alpha}{\alpha + x}\right).$$

Remark 6.2. Similarly, another special case of inverse Weibull distribution is the inverse Rayleigh distribution. We observe that X follows inverse Rayleigh distribution with CDF $F_X(x) = \mathrm{e}^{\left(-\frac{\alpha}{x}\right)^2}$, $x > 0,\ \alpha > 0$ if and only if

$$\lambda_{X[X]}(x) = \lambda_X(x)\left(\frac{\alpha^2}{\alpha^2 + x^2}\right).$$

Table 6.1 presents similar characterizations for certain lifetime distributions. The relationship between odds ratios of the baseline random variable X and the RART random variable $X[X]$ is presented in the following proposition.

Proposition 6.2. Let X be a non-negative random variable. Then $X[X]$ is the

Table 6.1: Characterizations based on reversed hazard rate.

Distribution	$F_X(x)$	$\lambda_X(x)$	$\lambda_{X[X]}(x)$
Power	$\left(\frac{x}{\alpha}\right)^{\beta}$, $0 \leq x \leq \alpha$, $\beta > 0$	$\frac{\beta}{x}$	$\lambda_X(x)\left(\frac{1}{1-\left(\beta \log\left(\frac{x}{\alpha}\right)\right)^{-1}}\right)$
Dagum	$\left(1+\frac{1}{\alpha x}\right)^{-\beta}$, $x > 0$, $\alpha > 0$, $\beta > 0$	$\frac{\beta}{\alpha x + x^2}$	$\lambda_X(x)\left(\frac{1}{1+\left(\beta \log\left(1+\frac{1}{\alpha x}\right)\right)^{-1}}\right)$
Inverse Pareto	$\left(\frac{x}{\alpha+x}\right)^{\beta}$, $x > 0$, $\alpha > 0$, $\beta > 0$	$\frac{\alpha\beta}{\alpha x + x^2}$	$\lambda_X(x)\left(\frac{1}{1-\left(\beta \log\left(\frac{x}{\alpha+x}\right)\right)^{-1}}\right)$
Log-logistic	$\frac{(\alpha x)^{\beta}}{1+(\alpha x)^{\beta}}$, $x > 0$, $\alpha > 0$, $\beta > 0$	$\frac{\beta}{x\left(1+(\alpha x)^{\beta}\right)}$	$\lambda_X(x)\left(\frac{1}{1-\left(\log\left(\frac{(\alpha x)^{\beta}}{1+(\alpha x)^{\beta}}\right)\right)^{-1}}\right)$
Burr XII	$1-(1+x)^{-k}$, $x > 0$, $k > 0$	$\frac{k}{(1+x)\left((1+x)^{k}-1\right)}$	$\lambda_X(x)\left(\frac{1}{1-\left(\log\left(1-(1+x)^{-k}\right)\right)^{-1}}\right)$

RART random variable of X if and only if

$$\text{(i)} \quad \phi_{X[X]}(x) = \frac{\phi_X(x) - \log\left(1+\phi_X(x)\right)}{1+\log\left(1+\phi_X(x)\right)} \tag{6.9}$$

$$\text{(ii)} \quad \theta_{X[X]}(x) = \frac{\theta_X(x)\left(1-\log\left(\frac{\theta_X(x)}{1+\theta_X(x)}\right)\right)}{1+\theta_X(x)\log\left(\frac{\theta_X(x)}{1+\theta_X(x)}\right)}, \tag{6.10}$$

where $\theta_{X[X]}(x)$ and $\phi_{X[X]}(x)$ are the odds ratios of $X[X]$.

Proof. Suppose that $X[X]$ is the RART random variable of X. Then

$$\begin{aligned}
& \phi_{X[X]}(x) = \frac{\bar{F}_{X[X]}(x)}{F_{X[X]}(x)} \\
\iff \quad & \phi_{X[X]}(x) = \frac{\bar{F}_X(x) + F_X(x)\log F_X(x)}{F_X(x)(1-\log F_X(x))} \\
\iff \quad & \phi_{X[X]}(x) = \frac{\phi_X(x) - \log\left(1+\phi_X(x)\right)}{1+\log\left(1+\phi_X(x)\right)},
\end{aligned}$$

which proves (i). Now, to prove (ii), we have

$$\begin{aligned}
& \theta_{X[X]}(x) = \frac{F_{X[X]}(x)}{\bar{F}_{X[X]}(x)} \\
\iff \quad & \theta_{X[X]}(x) = \frac{F_X(x)(1-\log F_X(x))}{\bar{F}_X(x) + F_X(x)\log F_X(x)} \\
\iff \quad & \theta_{X[X]}(x) = \frac{\theta_X(x)\left(1-\log\left(\frac{\theta_X(x)}{1+\theta_X(x)}\right)\right)}{1+\theta_X(x)\log\left(\frac{\theta_X(x)}{1+\theta_X(x)}\right)},
\end{aligned}$$

which completes the proof. □

The odds rate of $X[X]$ in terms of the baseline odds rate is of the form

$$\theta'_{X[X]}(x) = \theta'_X(x)\left(-\frac{\left(\bar{F}_X(x)\right)^2 \log(F_X(x))}{(1+F_X(x)(\log(F_X(x))-1))^2}\right). \tag{6.11}$$

We now examine characterization of distributions using odds rate of RART.

Theorem 6.2. The random variable X has inverse exponential distribution with CDF $F_X(x) = \mathrm{e}^{-\left(\frac{\alpha}{x}\right)},\ x>0,\ \alpha>0$ if and only if

$$\theta'_{X[X]}(x) = \theta'_X(x)\left(\frac{\alpha\, x\left(1-\mathrm{e}^{-\frac{\alpha}{x}}\right)^2}{x^2+\mathrm{e}^{-\frac{\alpha}{x}}(\alpha+x)^2}\right). \tag{6.12}$$

Proof. Since the proof of sufficient part is straightforward, we proceed to prove the necessary part. Assuming (6.12), from (6.11) we have

$$\frac{\theta'_{X[X]}(x)}{\theta'_X(x)} = -\frac{\left(\bar{F}_X(x)\right)^2 \log(F_X(x))}{(1+F_X(x)(\log(F_X(x))-1))^2} = \frac{\alpha\, x\left(1-\mathrm{e}^{-\frac{\alpha}{x}}\right)^2}{x^2+\mathrm{e}^{-\frac{\alpha}{x}}(\alpha+x)^2}$$

$$\implies F_X(x) = \mathrm{e}^{-\frac{\alpha}{x}}, \quad x>0,\ \alpha>0,$$

which completes the proof. □

Lando et al. (2022) observed that the odds rate of X is constant (*i.e.*, no aging), when X follows the log-logistic distribution. If we assume $X[X]$ has constant odds rate, then

$$F_{X[X]}(x) = \frac{x}{1+x} \implies F_X(x)\,(1-\log F_X(x)) = \frac{x}{1+x}. \tag{6.13}$$

Note that, the distribution of the baseline X cannot be determined explicitly from the above equation. But, we can easily generate values of X from (6.13) using numerical techniques. On the other hand, if we assume the baseline X has constant odds rate, *i.e.*, log-logistic distribution, then the distribution of $X[X]$ is obtained as

$$F_{X[X]}(x) = \frac{x\left(1-\log\left(\frac{x}{1+x}\right)\right)}{1+x}, \quad x>0. \tag{6.14}$$

The corresponding odds rate is

$$\theta'_{X[X]}(x) = \frac{\log(\frac{1+x}{x})}{x^2(1+\log(\frac{1+x}{x}))^2}. \tag{6.15}$$

We observe that the above function is decreasing for $x > 0$ which highlights the flexibility of RART transformation in constructing models having more flexible odds rate function. The following proposition elucidates the relationship between log-odds rate (LOR) of the baseline random variable X and the RART random variable $X[X]$.

Proposition 6.3. Let X be a non-negative random variable. Then $X[X]$ is the RART of X if and only if

$$LOR_{X[X]}(x) = LOR_X(x)\left(\frac{\bar{F}_X(x)\Lambda_X(x)}{\bar{F}_X(x)+\Lambda_X(x)}\right). \tag{6.16}$$

Proof. Let $X[X]$ be the RART random variable of X. Then from (1.16) we have

$$\begin{aligned}
& LOR_{X[X]}(x) &=& \frac{f_{X[X]}(x)}{F_{X[X]}(x)\bar{F}_{X[X]}(x)} \\
\iff & LOR_{X[X]}(x) &=& \frac{-f_X(x)\log F_X(x)}{F_X(x)(1-\log F_X(x))(\bar{F}_X(x)+F_X(x)\log F_X(x))} \\
\iff & LOR_{X[X]}(x) &=& \frac{-LOR_X(x)\bar{F}_X(x)\log F_X(x)}{\bar{F}_X(x)-\log F_X(x)(\bar{F}_X(x)+F_X(x))} \\
\iff & LOR_{X[X]}(x) &=& LOR_X(x)\left(\frac{\bar{F}_X(x)\Lambda_X(x)}{\bar{F}_X(x)+\Lambda_X(x)}\right),
\end{aligned}$$

which completes the proof. □

Chistyakov (1964) initially introduced the concept of $\mathcal{L}$-class of distributions, which are widely applied in the areas of branching process, queuing theory, renewal theory and risk modeling. A characterization for the $\mathcal{L}$-class using hazard rate was derived by Klüppelberg (1988), which states that

$$F_X(\cdot) \in \mathcal{L} \text{ if and only if } \lim_{x\to\infty} h_X(x) = 0, \tag{6.17}$$

where $h_X(\cdot)$ is the hazard rate of X with CDF $F_X(\cdot)$. We next prove the

preservation of the $\mathcal{L}$-class property under RART.

Proposition 6.4. Let X be an absolutely continuous non-negative random variable. Then, $X \in \mathcal{L}$-class if $X[X] \in \mathcal{L}$-class of distributions.

Proof. From (6.5) we have

$$\lim_{x\to\infty} h_{X[X]}(x) = \lim_{x\to\infty} h_X(x) \times \lim_{x\to\infty} \left(\frac{-\bar{F}_X(x) \log F_X(x)}{\bar{F}_X(x) + F_X(x) \log F_X(x)} \right). \tag{6.18}$$

By applying L'Hopithal's rule, we obtain

$$\lim_{x\to\infty} \left(\frac{-\bar{F}_X(x) \log F_X(x)}{\bar{F}_X(x) + F_X(x) \log F_X(x)} \right) = \lim_{x\to\infty} \left(1 + \frac{1}{F_X(x)} \right) = 2.$$

Now, from (6.18), we have $\lim_{x\to\infty} h_{X[X]}(x) = 0$ if and only if $\lim_{x\to\infty} h_X(x) = 0$, which completes the proof. □

The following example illustrates the findings in Proposition 6.4.

Example 6.1. Let X be a Burr type-XII random variable with CDF $F_X(x) = 1 - \frac{1}{(1+x^c)^k},\ x > 0,\ k > 0,\ c > 0$ and $h_X(x) = \frac{c\,k\,x^{c-1}}{1+x^c}$. Observe that $\lim_{x\to\infty} h_X(x) = 0$ and hence $X \in \mathcal{L}$-class family. Thus, from Proposition 6.4, we can directly conclude that the corresponding RART random variable $X[X]$ is also a member of $\mathcal{L}$-class family. To verify this, we have the CDF and hazard rate of $X[X]$ as

$$F_{X[X]}(x) = \left(1 - (1+x^c)^{-k}\right)\left(1 - \log\left(1 - (1+x^c)^{-k}\right)\right), \quad x > 0,\, k > 0,\, c > 0$$

$$h_{X[X]}(x) = \frac{c\,k\,x^{c-1} \log\left(1 - (1+x^c)^{-k}\right)}{(1+x^c)\left(\left(1 - (1+x^c)^{k}\right)\log\left(1 - (1+x^c)^{-k}\right) - 1\right)},$$

which gives $\lim_{x\to\infty} h_{X[X]}(x) = 0$. This validates the result.

Example 6.2. Let X be a Weibull random variable with CDF $F_X(x) = 1 - \mathrm{e}^{-(x/\sigma)^\alpha},\ x > 0,\ \alpha > 0,\ \sigma > 0$, and hazard rate $h_X(x) = \frac{\alpha x^{\alpha-1}}{\sigma^\alpha}$. Then the RART Weibull random variable $X[X]$ has the CDF $F_{X[X]}(x) =$

$\left(1-\mathrm{e}^{-(x/\sigma)^{\alpha}}\right)\left(1-\log\left(1-\mathrm{e}^{-(x/\sigma)^{\alpha}}\right)\right)$, and hazard rate

$$h_{X[X]}=\frac{\alpha\left(\frac{x}{\sigma}\right)^{\alpha}\log\left(1-\mathrm{e}^{-\left(\frac{x}{\sigma}\right)^{\alpha}}\right)}{x\left(1-\mathrm{e}^{\left(\frac{x}{\sigma}\right)^{\alpha}}\right)\log\left(1-\mathrm{e}^{-\left(\frac{x}{\sigma}\right)^{\alpha}}\right)-x},\quad x>0,\,\alpha>0,\,\sigma>0. \tag{6.19}$$

Further, consider the following two cases;

Case 1: $0<\alpha<1$**.**

For $0<\alpha\leq 1$, we have $\lim_{x\to\infty} h_X(x)=0$, *i.e.*, $X\in\mathcal{L}$-class of distributions. This directly gives $\lim_{x\to\infty} h_{X[X]}(x)=0$, and hence $X[X]\in\mathcal{L}$-class of distributions.

Case 2: $\alpha\geq 1$**.**

When $\alpha=1$, $\lim_{x\to\infty} h_{X[X]}(x)=\frac{1}{\sigma}$, indicating a constant limiting hazard and hence $X\notin\mathcal{L}$; whereas for $\alpha>1$, $\lim_{x\to\infty} h_X(x)=\infty$, showing an unbounded hazard rate, and therefore $X[X]\in\mathcal{L}$ only if $X\in\mathcal{L}$.

6.2.1 Characterization based on truncated moments

As noted earlier, the RART model can be expressed as a weighted distribution (see (6.4)). Treating it as a family of probability distributions, we employ a classical characterization based on the ratio of two truncated moments. This result is derived using the following theorem due to Glänzel (1987).

Theorem 6.3. Let $(\Omega,\mathcal{F},\mathbf{P})$ be a given probability space and let $I=[a,b]$ be an interval for some $a<b$ ($a=-\infty, b=\infty$ might as well be allowed). Let $X:\Omega\to I$ be a continuous random variable with CDF $F_X(\cdot)$, and let $p_1(x)$ and $p_2(x)$ be two real function defined on I such that

$$E(p_1(X)\mid X\geq x)=E(p_2(X)\mid X\geq x)\,\epsilon(x),\quad x\in I, \tag{6.20}$$

is defined for some real function $\epsilon(x)$, where $E(\cdot)$ denotes the expectation. Assume that $p_1(\cdot)$, $p_2(\cdot)\in C^1(I)$, $\epsilon(\cdot)\in C^2(I)$, and $F_X(\cdot)$ is twice continuously differentiable and strictly monotone on I. Finally, assume that the equation $\epsilon(x)\,p_1(x)=p_2(x)$ has no real solution in the interior of I. Then $F_X(\cdot)$ is uniquely

determined by the functions $p_1(\cdot)$, $p_2(\cdot)$, and $\epsilon(\cdot)$, given as

$$F_X(x) = \int_a^x C \left| \frac{\epsilon'(u)}{\epsilon(u)p_1(u) - p_2(u)} \right| \exp(-s(u))\, du,$$

where the function s is a solution of the differential equation $s'(x) = \frac{\epsilon'(x)\, p_1(x)}{\epsilon'(x)\, p_1(x) - p_2(x)}$, and C is the normalizing constant, such that $\int_I dF = 1$.

Using Theorem 6.3, we now establish the following characterization result for the RART.

Proposition 6.5. Let X be a continuous random variable with CDF $F_X(\cdot)$ and let $X[X]$ be the corresponding RART form. Let $p_1(x) = \frac{1}{F_X(x)}$ and $p_2(x) = p_1(x)(-\log F_X(x))$, for $x > 0$. Then, $X[X]$ is a RART random variable if and only if $\epsilon(\cdot)$ defined in Theorem 6.3 has the form

$$\epsilon(x) = -\frac{2}{3} \log F_X(x).$$

Proof. Let $X[X]$ be a random variable with CDF $F_{X[X]}(x)$, then

$$E(p_1(X) \mid X[X] \geq x) = \frac{1}{2}(\log F_X(x))^2$$
$$E(p_2(X) \mid X[X] \geq x) = -\frac{1}{3}(\log F_X(x))^3.$$

Then, from (6.20) we have

$$\epsilon(x) = -\frac{2}{3} \log F_X(x).$$

This gives

$$\epsilon(x)p_1(x) - p_2(x) = \frac{1}{3}\left(\frac{\log F_X(x)}{F_X(x)}\right) < 0, \text{ for all } x > 0.$$

Which proves the sufficient part. Conversely suppose that $\epsilon(x)$ takes the above form. Then

$$s'(x) = \frac{\epsilon'(x)p_1(x)}{\epsilon(x)p_1(x) - p_2(x)} = -\frac{2f_X(x)}{F_X(x)\log F_X(x)}.$$

Upon integration we obtain $s(x) = -2\ \log(-\log F_X(x))$. In view of Theorem 6.3, $X[X]$ has CDF (6.1), which completes the proof. □

Corollary 6.4. Let $X : \Omega \to (0, \infty)$ be a continuous random variable and let $p_1(x)$ be a function as defined in Theorem 6.3. Then, $X[X]$ is a RART random variable if and only if there exist functions $p_2(x)$ and $\epsilon(x)$ defined in Theorem 6.3 satisfying the differential equation

$$\frac{\epsilon'(x)p_1(x)}{\epsilon(x)p_1(x) - p_2(x)} = -\frac{2f_X(x)}{F_X(x)\log F_X(x)}, \quad x > 0.$$

The general solution of the above differential equation is

$$\epsilon(x) = -\frac{2}{(\log F_X(x))^2}\int\left(\frac{f_X(x)(-\log F_X(x))}{F_X(x)}\right)p_2(x)(p_1(x))^{-1}dx + C, \quad (6.21)$$

where C is a constant.

Remark 6.3. The sets of functions $(q_1(x), q_2(x), \epsilon(x))$ specified in Theorem 6.3 adhere to (6.21) with the constant $C = 1$. It is pertinent to mention that alternative functions for the triplets $(q_1(x), q_2(x), \epsilon(x))$ can also be selected, provided they meet the criteria laid out in Theorem 6.3.

6.2.2 Distorted representation

Next, we present the distorted representation of RART. Expressing RART in this form enables the study of the preservation of various aging and stochastic ordering properties from those of the baseline distribution. In the following proposition, we derive the distortion function connecting the baseline distribution and RART.

Proposition 6.6. Let X be a non-negative continuous random variable and $X[X]$ be the corresponding RART form. Then, $X[X]$ admits a distortion representation, with distortion function

$$q(u) = u + (1-u)\log(1-u), \quad u \in (0, 1). \quad (6.22)$$

Proof. From (6.2), we have

$$\bar{F}_{X[X]}(x) = \bar{F}_X(x) + (1 - \bar{F}_X(x)) \log(1 - \bar{F}_X(x)) = q(\bar{F}_X(x)),$$

where $q(u) = u + (1 - u) \log(1 - u)$ is the distortion function connecting X and $X[X]$. □

Note that, the distortion function given in (6.22) is a convex function in u. Next, we analyze the aging properties of RART.

6.3 Aging properties

We explore the aging characteristics of RART, based on the aging patterns exhibited by the corresponding baseline random variable X. Different categories of aging, along with their characteristics and practical uses, are discussed in Barlow and Proschan (1975) and Lai et al. (2003). In the forthcoming proposition, we present the preservation of certain important aging classes under RART, based on the results listed in Section 1.6.4 of Chapter 1.

Proposition 6.7. Let $X[X]$ be the reversed auto-relevation random variable of X with distortion function $q(u)$, given in (6.22). Then, the following properties hold.

(a) If X is DHR, then $X[X]$ is also DHR.

(b) If X is DRHR, then $X[X]$ is also DRHR.

(c) If X is DLR, then $X[X]$ is also DLR.

(d) If X is NWU, then $X[X]$ is also NWU.

(e) If X is DHRA, then $X[X]$ is also DHRA.

(f) If X is DLOR, then $X[X]$ is also DLOR.

Proof. For proving (a), by Result 1, it is sufficient to show that $l_1(u)$ is increasing on $(0,1)$. We have

$$l_1(u) = -\frac{u\log(1-u)}{u+(1-u)\log(1-u)}, \quad l_1'(u) = \frac{u^2-(1-u)\{\log(1-u)\}^2}{(1-u)\big(u+(1-u)\log(1-u)\big)^2}.$$

Since $l_1'(u) > 0$ for all $u \in (0,1)$, it follows that $l_1(u)$ is increasing, thereby establishing part (a).

To prove (b), from Result 2 we have

$$l_2(u) = -\frac{u\log u}{u-u\log u} \quad \text{and} \quad l_2'(u) = -\frac{1}{u(\log u-1)^2} < 0, \quad \text{for } u \in (0,1).$$

Thus $l_2(u)$ is decreasing, which completes the proof of (b).

By recalling Result 3, to prove (c) it suffices to examine the monotonicity of $l_3(u)$. We have

$$l_3(u) = -\frac{u}{(1-u)\log(1-u)}, \quad l_3'(u) = -\frac{u+\log(1-u)}{(u-1)^2\{\log(1-u)\}^2}.$$

Since $l_3'(u) > 0$ for all $u \in (0,1)$, it follows that $l_3(u)$ is increasing, which establishes part (c).

For the distortion function $q(u)$ given in (6.22), it can be verified that the inequalities $q(uv) \geq q(u)\,q(v)$ for $u, v \in (0,1)$ and $q(u^a) \geq \big(q(u)\big)^a$ for $u \in (0,1)$ and $0 < a < 1$ hold. These results establish parts (d) and (e) in view of Result 4 and Result 5.

Similarly, for proving (f), from Result 6, we have

$$l_4(u) = -\frac{u\log(1-u)}{(\log(1-u)-1)((u-1)\log(1-u)-u)}.$$

Similar to the proofs of (a), (b) and (c) we can show that $l_4(u)$ is a decreasing function in u. This completes the proof. □

Remark 6.4. Lai and Xie (2006) established that, NWU property implies the NWUHR property. This implies that NWUHR is preserved under RART.

We present the following examples to illustrate the results established in the above proposition.

Example 6.3. Let X be a Pareto type-I random variable with CDF $F_X(x) = 1-x^{-\alpha}$, $x > 1, \alpha > 0$, and hazard rate $h_X(x) = \frac{\alpha}{x}$. The respective RART random variable $X[X]$ has survival and hazard rates of the form

$$\bar{F}_{X[X]}(x) = x^{-\alpha}\left((x^{\alpha}-1)\log\left(1-x^{-\alpha}\right)+1\right), \quad x > 1,\ \alpha > 0,$$

$$h_{X[X]}(x) = \frac{\alpha}{x}\left(\frac{-\log\left(1-x^{-\alpha}\right)}{1+(x^{\alpha}-1)\log\left(1-x^{-\alpha}\right)}\right).$$

It can be readily verified that $h_{X[X]}(x)$ exhibits DHR behavior for all parameter values. Plots of $h_{X[X]}(x)$ for two parameter choices are displayed in Figure 6.1. Since the baseline random variable also possesses the DHR property, this example illustrates the preservation of the DHR class under the RART model.

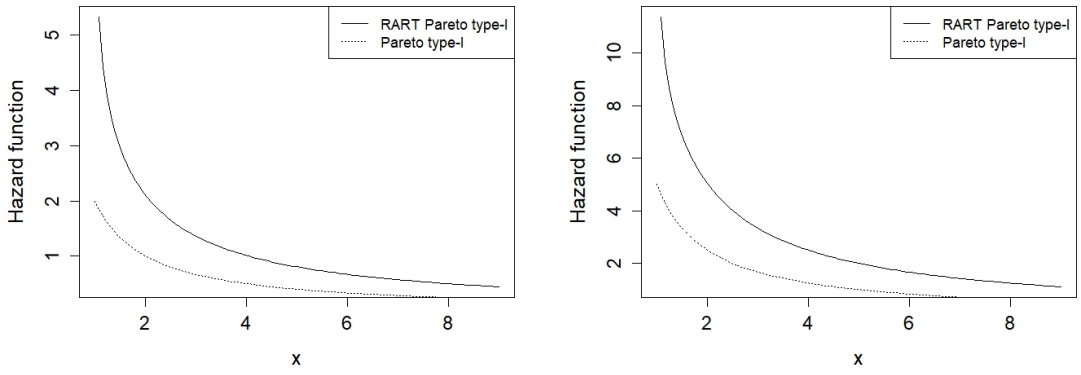

(a) $\alpha = 1$ **(b)** $\alpha = 5$

Figure 6.1: Hazard plots of Pareto type-I and RART Pareto type-I.

Note that, in general IHR property is not preserved under RART. To illustrate this, we present the following two examples.

Example 6.4. Let X be a Weibull random variable with CDF $F_X(x) = 1 - \mathrm{e}^{-(\frac{x}{\sigma})^{\alpha}}$, $x > 0$, $\alpha, \sigma > 0$. For illustration purpose, we assume without loss of generality that $\sigma = 1$. Then, the RART random variable $X[X]$ has CDF $F_{X[X]}(x) = (1-\mathrm{e}^{-x^{\alpha}})\left(1-\log\left(1-\mathrm{e}^{-x^{\alpha}}\right)\right)$, $x > 0$, $\alpha > 0$. Now, the hazard rate

of the RART Weibull distribution is given as

$$h_{X[X]}(x) = \alpha x^{\alpha-1}\left(\frac{-\log\left(1-\mathrm{e}^{-x^{\alpha}}\right)}{(\mathrm{e}^{x^{\alpha}}-1)\log\left(1-\mathrm{e}^{-x^{\alpha}}\right)+1}\right).$$

Plots of $h_{X[X]}(x)$ for various values of $\alpha \geq 1$ are provided in Figure 6.2. It is evident that $h_{X[X]}(x)$ can exhibit IHR, DHR, and UBT shapes for different choices of α, indicating that the IHR property is not preserved under the RART transformation. Although the baseline model has an IHR behavior, the RART model introduces greater flexibility in the hazard rate. Hence, the RART model serves as a parsimonious mechanism for extending classical models to achieve more flexible hazard rate behavior.

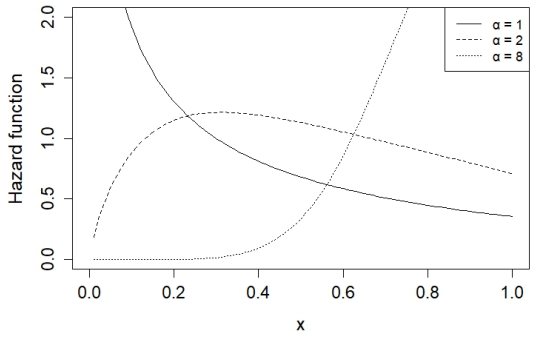

Figure 6.2: Plots of hazard rates RART Weibull for different values of α.

Example 6.5. Let X be a half-logistic (HL) random variable with CDF $F_X(x) = 1-\frac{2}{\mathrm{e}^{\frac{x}{\sigma}}+1}$, $x \geq 0$, $\sigma > 0$. Then, the corresponding RART random variable has CDF $F_{X[X]}(x) = \left(1-\frac{2}{\mathrm{e}^{\frac{x}{\sigma}}+1}\right)\left(1-\log\left(1-\frac{2}{\mathrm{e}^{\frac{x}{\sigma}}+1}\right)\right)$. Now, the hazard rate of RART-HL distribution is obtained as

$$h_{X[X]}(x) = \frac{2\,\mathrm{e}^{\frac{x}{\sigma}}\log\left(\frac{\mathrm{e}^{\frac{x}{\sigma}}-1}{\mathrm{e}^{\frac{x}{\sigma}}+1}\right)}{\sigma\left(\mathrm{e}^{\frac{x}{\sigma}}+1\right)\left(\left(1-\mathrm{e}^{\frac{x}{\sigma}}\right)\log\left(\frac{\mathrm{e}^{\frac{x}{\sigma}}-1}{\mathrm{e}^{\frac{x}{\sigma}}+1}\right)+2\right)}, \quad x \geq 0,\ \sigma > 0.$$

The hazard rate plots of the HL and RART-HL models, shown in Figure 6.3, indicate that the RART-HL distribution accommodates both decreasing and bathtub-shaped behaviors for different values of σ, whereas the baseline model

exhibits an IHR pattern throughout.

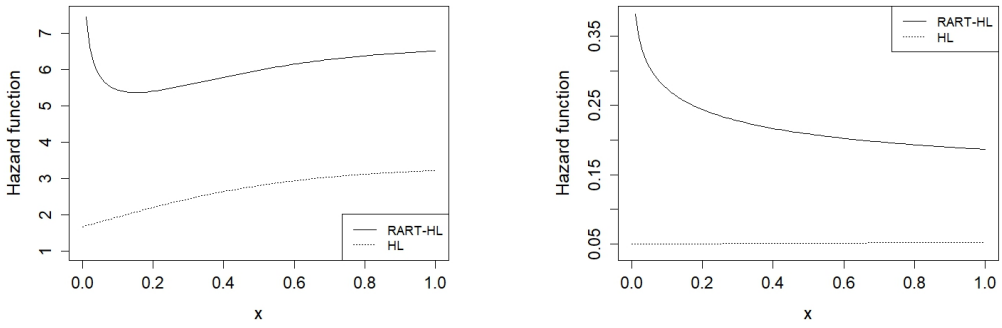

(a) $\sigma = 0.3$ **(b)** $\sigma = 5$

Figure 6.3: Plots of hazard rates of HL and RART-HL distribution.

In the next proposition, we establish an identity connecting the RAI functions of $X[X]$ and X.

Proposition 6.8. Let X be a non-negative continuous random variable. Then, $X[X]$ is the RART random variable of X if and only if

$$\tilde{L}_{X[X]}(x) = \tilde{L}_X(x)\left(\frac{(\Lambda_X(x))^2}{(1+\Lambda_X(x))\,(\Lambda_X(x)-\log(1+\Lambda_X(x)))}\right). \tag{6.23}$$

Proof. Since $X[X]$ is the RART of X, from the definition of RAI given in (1.18), we have

$$\begin{aligned} \tilde{L}_{X[X]}(x) &= \frac{x\lambda_X(x)\left(\frac{\Lambda_X(x)}{1+\Lambda_X(x)}\right)}{-\log\Big(F_X(x)\,(1+\Lambda_X(x))\Big)} \\ \iff \tilde{L}_{X[X]}(x) &= \tilde{L}_X(x)\left(\frac{(\Lambda_X(x))^2}{(1+\Lambda_X(x))\,(\Lambda_X(x)-\log(1+\Lambda_X(x)))}\right), \end{aligned}$$

which completes the proof. □

We next establish an identity connecting the Glaser's functions of X and $X[X]$.

Proposition 6.9. $X[X]$ is the RART random variable of X if and only if

$$\eta_{X[X]}(x) = \eta_X(x) + \frac{\lambda_X(x)}{\Lambda_X(x)}, \tag{6.24}$$

where $\eta_{X[X]}(\cdot)$ is the Glaser's function of $X[X]$.

Proof. Assume that $X[X]$ is the RART random variable of X. Then

$$\begin{aligned} & \eta_{X[X]}(x) = -\frac{f'_{X[X]}(x)}{f_{X[X]}(x)} \\ \iff \quad & \eta_{X[X]}(x) = -\frac{f_X(x)}{F_X(x)\log F_X(x)} - \frac{f'_X(x)}{f_X(x)} \\ \iff \quad & \eta_{X[X]}(x) = \eta_X(x) + \frac{\lambda_X(x)}{\Lambda_X(x)}, \end{aligned}$$

which completes the proof. □

Remark 6.5. From the definition of RAI function given in (1.18) and from (6.24), we obtain

$$\tilde{L}_X(x) = x\left(\eta_{X[X]}(x) - \eta_X(x)\right). \tag{6.25}$$

The relation (6.25) connects the additional gain in the Glaser's function under RART transformation with the reversed aging intensity function of X.

6.4 Stochastic orders

We investigate the stochastic ordering properties of the RART random variable $X[X]$ in comparison with its baseline counterpart X. The following proposition establishes the corresponding ordering relationships by invoking the results listed in Section 1.6.4 of Chapter 1 together with the distortion representation in (6.22).

Proposition 6.10. Let X be a non-negative continuous random variable and $X[X]$ be the corresponding RART random variable. Then $X[X] \leq_{lr} X$.

Proof. From (6.22), the function $q(u) = u + (1-u)\log(1-u)$ serves as the distortion connecting X and $X[X]$, and $q_1(u) = u$ is the identity distortion function. From Result 8, it suffices to show that $\frac{q'(u)}{q'_1(u)}$ is increasing for $u \in (0,1)$.

We have

$$\frac{d}{du}\left(\frac{q'(u)}{q_1'(u)}\right) = \frac{d}{du}\big(-\log(1-u)\big) = \frac{1}{1-u} > 0, \quad u \in (0,1).$$

Hence, $\frac{q'(u)}{q_1'(u)}$ is increasing on $(0,1)$, which completes the proof. □

Based on the findings outlined in Shaked and Shanthikumar (2007) and Navarro et al. (2013), we have the following implications:

$$\begin{array}{ccccccccc} & & X[X] \leq_{mrl} X & & & & X[X] \leq_{ew} X & & \\ & & \Uparrow & & & & \Uparrow & & \\ X[X] \leq_{lr} X & \Longrightarrow & X[X] \leq_{hr} X & \Longrightarrow & X[X] \leq_{or} X & \Longrightarrow & X[X] \leq_{st} X & \Longrightarrow & X[X] \leq_{icx} X \\ \Downarrow & & & & & & & & \Downarrow \\ X[X] \leq_{rhr} X & \Longrightarrow & X[X] \leq_{mit} X & & & & X[X] \leq_{su} X & \Longleftarrow & X[X] \leq_{*} X \end{array}$$

We consider an example to illustrate the above proposition.

Example 6.6. Let X have CDF $F_X(x) = x^2$, $0 < x < 1$. Then, the density function is $f_X(x) = 2\,x$. The corresponding RART random variable has CDF and density function given by

$$F_{X[X]}(x) = x^2\,(1 - 2\,\log x) \quad \text{and} \quad f_{X[X]}(x) = -2\,\log x, \quad 0 < x < 1.$$

Now, from the definition of likelihood ratio ordering, we have

$$\begin{aligned} \frac{f_X(x)}{f_{X[X]}(x)} &= -\frac{x}{\log x} \\ \Longrightarrow \frac{d}{dx}\left(\frac{f_X(x)}{f_{X[X]}(x)}\right) &= \frac{1-\log x}{(\log x)^2} > 0, \end{aligned}$$

we have $X[X] \leq_{lr} X$.

We now present the following results establishing stochastic ordering relations between two RART models.

Proposition 6.11. Let $X[X]$ and $Y[Y]$ be the RART random variables corresponding to the baseline random variables X and Y respectively. Then the following results hold:

(i) If $X \leq_{st} Y$ then $X[X] \leq_{st} Y[Y]$.

(ii) If $X \leq_{rhr} Y$ then $X[X] \leq_{rhr} Y[Y]$.

(iii) If $X \leq_{icx} Y$ then $X[X] \leq_{icx} Y[Y]$.

(iv) If $X[X] \leq_{ttt} Y[Y]$ then $X \leq_{ttt} Y$.

(v) If $X \leq_{ew} Y$ then $X[X] \leq_{ew} Y[Y]$.

(vi) If $X \leq_{hr} Y$ and $X \leq_{rrh} Y$ then $X[X] \leq_{rrh} Y[Y]$.

Proof. The proof of (i) is straightforward from Result 9.

Now, for proving (ii), we consider the following function:

$$k(u) = \frac{(1-u)q'(u)}{1-q(u)} = -\frac{(1-u)\log(1-u)}{1-u-(1-u)\log(1-u)} = \frac{1}{\log(1-u)-1} + 1.$$

According to Result 11, to prove (ii), it is sufficient to show that $k(u)$ is non-negative and increasing in $(0,1)$. Since $\log(1-u) < 0$ for $u \in (0,1)$, we have $k(u) \geq 0$ for $u \in (0,1)$. By differentiating $k(u)$ with respect to u, we get

$$k'(u) = \frac{1}{(1-u)(\log(1-u)-1)^2} > 0, \quad \text{for all } u \in (0,1).$$

Thus $k(u)$ is increasing for $u \in (0,1)$. This completes the proof of (ii).

Revisiting Result 13, Result 14, and Result 16 we can observe that (iii), (iv), and (v) holds true due to the concave property of $q(u)$.

To prove (vi), it suffices to show that $l_5(u) = \frac{w(u)}{u\,w'(u)}$ and $\frac{-u\,\log(u)\,l_5'(u)}{l_5(u)}$ are non-decreasing in u, where $w(u) = 1 - q(1-u)$. From Result 17 and the distortion representation given in (6.22), it follows that

$$l_5(u) = 1 - \frac{1}{\log u} \quad \text{and} \quad \frac{-u\,\log u\,l_5'(u)}{l_5(u)} = \frac{1}{1-\log u}.$$

Then

$$l_5'(u) = \frac{1}{u(\log u)^2} > 0, \quad \text{for } 0 < u < 1,$$

and

$$\frac{d}{du}\left(\frac{-u\,\log u\, l_5'(u)}{l_5(u)}\right) = \frac{1}{u(\log u - 1)^2} > 0, \quad \text{for } 0 < u < 1.$$

Thus $l_5(u)$ and $\frac{-u\,\log(u)\, l_5'(u)}{l_5(u)}$ are non-decreasing in u. Hence the result. □

The following example illustrates stochastic ordering relation between two RART models.

Example 6.7. Let X and Y have CDFs $F_X(x) = \mathrm{e}^{-\frac{1}{x}}$ and $F_Y(x) = \mathrm{e}^{-\frac{2}{x}}$ respectively, where $x > 0$. Here $X \leq_{st} Y$, since $F_X(x) \geq F_Y(x)$, for all $x > 0$. Now, the CDFs of corresponding RART random variables can be respectively obtained as

$$F_{X[X]}(x) = \mathrm{e}^{-\frac{1}{x}}\left(1 + \frac{1}{x}\right) \quad \text{and} \quad F_{Y[Y]}(x) = \mathrm{e}^{-\frac{2}{x}}\left(1 + \frac{2}{x}\right), \quad x > 0.$$

Then, we have

$$\frac{F_{Y[Y]}(x)}{F_{X[X]}(x)} = \frac{\mathrm{e}^{-\frac{2}{x}}\left(\frac{2}{x} + 1\right)}{\mathrm{e}^{-\frac{1}{x}}\left(\frac{1}{x} + 1\right)} \leq 1 \quad \text{for all } x > 0,$$

which confirms the result in Proposition 6.11. For the choices of $F_X(x)$ and $F_Y(x)$, the corresponding hazard rate ordering result also holds, *i.e.*, $X \leq_{hr} Y \implies X[X] \leq_{hr} Y[Y]$, which is illustrated in Figure 6.4.

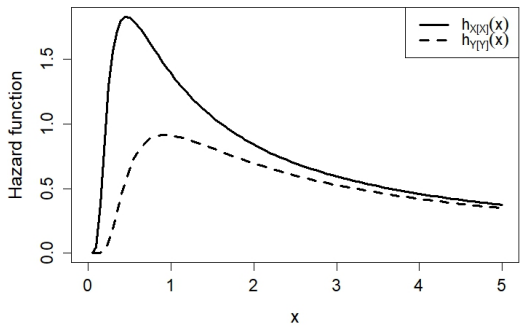

Figure 6.4: Hazard plots of $X[X]$ and $Y[Y]$

Another concept of importance is the odds rate order, which was introduced and studied by Lando et al. (2022) and further developed by Zardasht V (2024).

Motivated from these works, we derive the odds rate ordering between X and $X[X]$ in the following proposition.

Proposition 6.12. Let $X[X]$ be the RART random variable of X. Then $X[X] \leq_{or} X$.

Proof. We only need to show that the ratio $\frac{\theta'_{X[X]}(x)}{\theta'_X(x)} \leq 1$, for all $x > 0$. From (1.15), we have

$$\frac{\theta'_X(x)}{\theta'_{X[X]}(x)} = -\frac{(1 + F_X(x)(\log(F_X(x)) - 1))^2}{\left(\bar{F}_X(x)\right)^2 \log(F_X(x))} \leq 1, \text{ for all } x > 0.$$

Taking $u = F_X(x)$, the above equation can be rewritten as

$$p(u) = -\frac{(1-u)^2 \log u}{(1 - u(1 - \log(u)))^2} \leq 1, \text{ for all } 0 < u < 1.$$

This is illustrated in Figure 6.5.

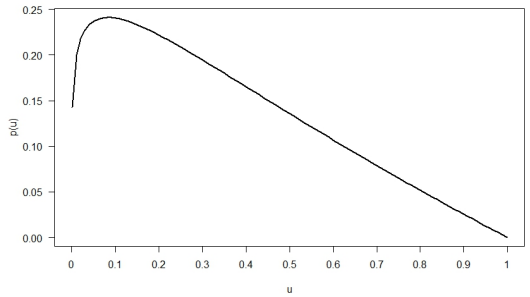

Figure 6.5: Plot of $p(u)$.

□

As discussed in Chapter 1, the *LOR* and RAI orders provide effective frameworks for comparing lifetime distributions through their respective aging measures. Building on these concepts, we analyze the corresponding stochastic ordering properties for the RART random variable. The following propositions establish the associated ordering relationships between X and $X[X]$.

Proposition 6.13. Let $X[X]$ be the RART random variable of X. Then $X \leq_{LOR} X[X]$.

Proof. Since $f_{X[X]}(x)$ is a weighted density, according to Proposition 4.1 in Navarro et al. (2008), it is sufficient to demonstrate that the weight function satisfies the condition:

$$w(x)\ E(w(X)) \leq E(w(X) \mid X \geq x)\ E(w(X) \mid X \leq x). \tag{6.26}$$

In our context, from (6.4) we can see that the weight function $w(x) = -\log F_X(x)$. Then, the following conditional expectations can be easily obtained as

$$E(w(X) \mid X \geq x) = 1 - \log F_X(x) \quad E(w(X) \mid X \leq x) = 1 - \left(\frac{F_X(x)}{\bar{F}_X(x)}\right) \log F_X(x).$$

Now, the condition (6.26) becomes

$$-\log F_X(x) \leq 1 - \frac{\log F_X(x)}{\bar{F}_X(x)},$$

which is true for all $x > 0$. This completes the proof. □

Proposition 6.14. Let $X[X]$ and $Y[Y]$ be the RART random variables corresponding to the baseline random variables X and Y respectively. Then

$$X \leq_{LOR} Y \implies X[X] \leq_{LOR} Y[Y].$$

Proof. The proof is straight forward from Proposition 4.3 in Navarro et al. (2008). □

Proposition 6.15. Let $X[X]$ be the RART random variable of X. Then $X[X] \leq_{RAI} X$.

Proof. Consider the function

$$s(x) = \frac{\log F_X(x)}{\log F_{X[X]}(x)} = \frac{\log F_X(x)}{\log\big(F_X(x)(1 - \log F_X(x))\big)}.$$

Letting $u = F_X(x)$, we obtain

$$s(u) = \frac{\log(u)}{\log(u(1-\log(u)))}.$$

On differentiating, we get

$$s'(u) = \frac{\frac{(\log(u))^2}{1-\log(u)} + \log(u - u\log(u))}{u(\log(u - u\log(u)))^2} > 0, \quad \text{for } 0 < u < 1.$$

Thus, $s(u)$ is increasing in u, which completes the proof. □

6.5 Stress-strength reliability

The seminal work of Birnbaum (1956) introduced stress-strength models, forming a fundamental framework for inference in reliability analysis. This measure quantifies the probability that the stress acting on a system (X) exceeds its strength (Y), thereby providing important insights into system reliability. Let $F_X(\cdot)$ and $f_X(\cdot)$ denote the CDF and density function of X, respectively, and let $F_Y(\cdot)$ and $f_Y(\cdot)$ denote the corresponding functions of Y. Then, the stress–strength reliability $\mathrm{R}_{X,Y}$ is defined as

$$\mathrm{R}_{X,Y} = P(Y < X) = \int_x f_Y(x)F_X(x)\,dx. \tag{6.27}$$

We now assess the stress-strength reliability of a system by considering the stress and strength random variables as X and $X[X]$, respectively.

Proposition 6.16. Let X be a lifetime random variable and $X[X]$ be its reversed auto-relevation form. Then $\mathrm{R}_{X,X[X]} = \frac{1}{4}$.

Proof. Suppose that $X[X]$ is the reversed auto-relevation random variable of X. Then from (6.3) and (6.27), we have

$$\mathrm{R}_{X,X[X]} \;=\; P(X[X] < X) = \int_0^\infty f_{X[X]}(x)F_X(x)\,dx$$

$$
\begin{aligned}
&= -\int_0^{\infty} f_X(x) \log F_X(x) F_X(x)\, dx \\
&= -\int_{-\infty}^{0} u\, \mathrm{e}^{2u}\, du = \frac{1}{4},
\end{aligned}
$$

which completes the proof. □

Remark 6.6. Following the same steps of Proposition 6.18, we can prove that $\mathrm{R}_{X[X],X} = \frac{3}{4}$.

The concept of stress-strength reliability for a multi-component (s-out-of-n) system was introduced by Bhattacharyya and Johnson (1974). In this setup, consider a system consisting of n independent and identically distributed components $(X_1, \ldots, X_n)$ with CDF $F_X(\cdot)$. The system remains operational provided that at least s out of the n components function. The system is subjected to a common stress Y with density function $f_Y(\cdot)$. The corresponding multi-component stress-strength reliability is given by

$$
\begin{aligned}
R_{X,Y}^{s,n} &= P(\text{at least } s \text{ of } (X_1, \ldots, X_n) \text{ exceeds } Y) \\
&= \sum_{i=s}^{n} \binom{n}{i} \int_{-\infty}^{\infty} \big(1 - F_X(x)\big)^i \big(F_X(x)\big)^{k-i} f_Y(x)\, dx, \qquad (6.28)
\end{aligned}
$$

where s and n are positive integers. In the coming proposition, we derive an expression for the multi-component stress-strength reliability connecting the random variables X and $X[X]$.

Proposition 6.17. Let $X[X]$ be the RART random variable of X. Then

$$
R_{X,X[X]}^{s,n} = \sum_{i=s}^{n} \binom{n}{i} \frac{i\,!(n-i)\,!}{(n+1)\,!} \Big(H(n+1) - H(n-i) \Big), \qquad (6.29)
$$

where $H(n) = \sum_{j=1}^{n} \frac{1}{j}$ is the sum of first n terms in a harmonic progression.

Proof. Suppose that $X[X]$ is the RART random variable of X. Then from (6.3)

and (6.28), we have

$$R^{s,n}_{X,X[X]} = -\sum_{i=s}^{n}\binom{n}{i}\int_{-\infty}^{\infty}\big(1-F_X(x)\big)^i\big(F_X(x)\big)^{k-i}f_X(x)\log F_X(x)\,dx.$$

Letting $u = F_X(x)$, we obtain

$$R^{s,n}_{X,X[X]} = -\sum_{i=s}^{n}\binom{n}{i}\int_{0}^{1}(1-u)^i\ u^{n-i}\ \log u\,du.$$

Using integration by parts, we have

$$R^{s,n}_{X,X[X]} = \sum_{i=s}^{n}\binom{n}{i}\frac{i\ !(n-i)\ !}{(n+1)\ !}\Big(\sum_{j=1}^{n+1}\frac{1}{j}-\sum_{j=1}^{n-i}\frac{1}{j}\Big),$$

which completes the proof. □

6.6 Quantile based properties

As discussed in Chapter 1, a probability distribution can be uniquely characterized either by its CDF or by its quantile function. In many cases, distributions are defined directly through their quantile functions, even when the corresponding CDF does not admit a closed-form expression. Notable examples include the Govindarajulu distribution (Govindarajulu (1977)), the Tukey lambda distribution (Tukey (1962)), and the power-Pareto distribution (Gilchrist (2000)). Quantile functions possess several interesting properties such as, sum of two quantile functions is again a quantile function and product of two positive quantile functions is again a quantile function etc. Note that these are not true for distribution functions. This makes quantile based models and methods more attractive than the traditional distribution function approach. We now propose a quantile based definition of RART and examine its properties based on various quantile based measures. Let $Q_X(\cdot)$ and $Q_Y(\cdot)$ be the quantile functions of X and Y respectively. From the definition of RART given in (6.1) of Chapter 6,

by taking $x = Q_X(u)$, we get

$$\begin{aligned} F_{X[X]}(Q_X(u)) &= u(1 - \log u) \\ \implies Q_X(u) &= Q_{X[X]}(\xi(u)), \end{aligned} \tag{6.30}$$

where $\xi(u) = u(1 - \log u)$ and $Q_{X[X]}(u)$ is the quantile function of $X[X]$. This can be equally represented as

$$Q_{X[X]}(u) = Q_X(\xi^{-1}(u)). \tag{6.31}$$

Thus, the quantile function of $X[X]$ can be derived from (6.31), which also enables the generation of random samples of $X[X]$ using those of X. The quantile density can be obtained as

$$q_X(u) = \xi'(u)\, q_{X[X]}(\xi(u)) = -\log(u)\, q_{X[X]}(\xi(u)). \tag{6.32}$$

We now present some quantile based reliability properties of $X[X]$ in connection with that of X.

(i) Nair et al. (2013) defined the hazard quantile function of X, denoted by $qh_X(u)$ as $qh_X(u) = ((1-u)q_X(u))^{-1}$. From (6.32), we get

$$\begin{aligned} qh_X(u) &= \left((1-u)\left(-\log(u)\, q_{X[X]}(\xi(u))\right)\right)^{-1} \\ &= qh_{X[X]}(\xi(u)) \left(\frac{\xi(u) - 1}{(1-u)\log(u)}\right). \end{aligned} \tag{6.33}$$

(i) The quantile alternative of the reversed hazard rate called the reversed hazard quantile function, denoted by $qrh_X(\cdot)$ is given by

$$\begin{aligned} qrh_X(u) &= \lambda_X(Q_X(u)) = (u\, q_X(u))^{-1} \\ &= qrh_{X[X]}(\xi(u)) \left(-\frac{\xi(u)}{u \log u}\right). \end{aligned} \tag{6.34}$$

(iii) Since $u \in (0,1)$, we can use the first order approximation of $\log u$ as $u - 1$, and $\xi(u)$ can be approximated to $2\,u - u^2$. The corresponding

approximate form of (6.30) is $Q_X(u) = Q_{X[X]}(2u - u^2)$. Note that $\xi(u) = 2\,u - u^2$ is a quantile function and it is a special case of the well-known Govindarajulu quantile function (Govindarajulu (1977)) defined by $Q^*(u) = \theta + \sigma\left((\beta+1)u^\beta - \beta u^{\beta+1}\right)$, with $\theta = 0$, $\sigma = 1$ and $\beta = 1$.

There are several advantages arising from the quantile based approach of RART model, of which some illustrations are given below.

(i) For the affine transformation $Y = A\,X + B$, the quantile function of Y becomes $Q_Y(u) = A\,Q_X(u) + B$, where $Q_X(\cdot)$ is the quantile function of X. With (6.31), we can establish the same identity for the respective RART variable $X[X]$ and $Y[Y]$ as $Q_{Y[Y]}(u) = A\,Q_{X[X]}(u) + B$. The corresponding quantile density has the form $q_{Y[Y]}(u) = A\,q_{X[X]}(u)$. Thus, the addition or subtraction of a quantity does not alter the quantile density of the RART random variable.

(ii) Given two quantile functions $Q_X(\cdot)$ and $Q_Y(\cdot)$, we have $Q_Z(u) = Q_X(u) + Q_Y(u)$, is also a quantile function of a random variable Z. This leads to

$$Q_{Z[Z]}(u) = Q_{X[X]}(u) + Q_{Y[Y]}(u).$$

Thus the additive identity connecting X, Y and Z is preserved for the respective RART random variables $X[X]$, $Y[Y]$ and $Z[Z]$.

(iii) For two non-negative quantile functions $Q_X(\cdot)$ and $Q_Y(\cdot)$, their product $Q_Z(u) = Q_X(u)Q_Y(u)$ is again a quantile function. From (6.30), following similar steps as in (i), we get $Q_{Z[Z]}(u) = Q_{X[X]}(u)Q_{Y[Y]}(u)$. Thus, the quantile function of the RART random variable $Z[Z]$ is the product of the quantile functions of the RART random variables $X[X]$ and $Y[Y]$.

(iv) If X has quantile function $Q_X(\cdot)$, then the quantile function of $T(X)$ is $T(Q_X(u))$, provided $T(\cdot)$ is a non-decreasing function. This is known as the $Q-$transformation of quantile functions (Gilchrist (2000)). Let $Y = T(X)$,

then from (6.30) we have

$$\begin{aligned} Q_{Y[Y]}(\xi(u)) &= Q_Y(u) \\ &= T(Q_X(u)) \\ &= T(Q_{X[X]}(\xi(u))). \end{aligned}$$

$$\implies Q_{Y[Y]}(u) = T(Q_{X[X]}(u)), \quad \text{for all } u \in (0,1).$$

Thus, the $Q-$transformation identity between X and Y is preserved under RART.

(v) If $T(\cdot)$ is a non-decreasing function and satisfies the boundary conditions $T(0) = 0$ and $T(1) = 1$, then $Q_Y(u) = Q_X(T(u))$ is a quantile function (Gilchrist (2000)). Using the same approach as in (iv), we can show that the identity between X and Y is preserved under RART, *i.e.*, $Q_{Y[Y](u)} = Q_{X[X]}(T(u))$.

Since $\xi(u) = u(1 - \log u)$ is monotonically increasing for $u \in (0,1)$ and satisfies the condition $\xi(0) = 0$ and $\xi(1) = 1$, the RART identity (6.30) can be employed to construct new quantile based models with more flexible reliability properties. To illustrate this, take X as the baseline random variable and Y as the RART form, *i.e.*, $Q_Y(u) = Q_X(\xi(u))$. Now by properly choosing a baseline X, we can construct new models through this identity. For example, let X be the random variable corresponding to the class of distributions with linear mean residual quantile (LMRQ) function having quantile function of the form

$$Q_X(u) = (c + \mu)\log(1 - u) - c\,u, \quad 0 < u < 1,\ \mu > 0,\ -\mu < c < \mu. \tag{6.35}$$

The corresponding hazard quantile function is given by

$$qh_X(u) = \frac{1}{\mu + c\,(2u - 1)}. \tag{6.36}$$

Further details on the LMRQ class can be found in Midhu et al. (2013). Hence, from (6.30), the corresponding quantile-based RART-LMRQ model has quantile

function

$$Q_Y(u) = Q_X(\xi(u)) = 2\,c\,u(\log u - 1) - (c+\mu)\log(1 + u(\log u - 1)), \quad (6.37)$$

where Y is the corresponding random variable of quantile-based RART-LMRQ model. Then, the hazard quantile function of Y has the form

$$\begin{aligned} qh_Y(u) &= qh_X(\xi(u)) \left(\frac{\xi(u) - 1}{(1-u)\log u} \right) \\ &= \frac{u(1 - \log u) - 1}{(u-1)(2\,c\,u\log u - 2\,c\,u + c - \mu)\log u}. \end{aligned} \quad (6.38)$$

Plots of $qh_X(u)$ and $qh_Y(u)$ for various parameter values are shown in Figure 6.6. It is observed that $qh_Y(u)$ exhibits increasing, decreasing, and UBT shapes, whereas the baseline model allows only increasing, decreasing, or constant hazard quantile behavior.

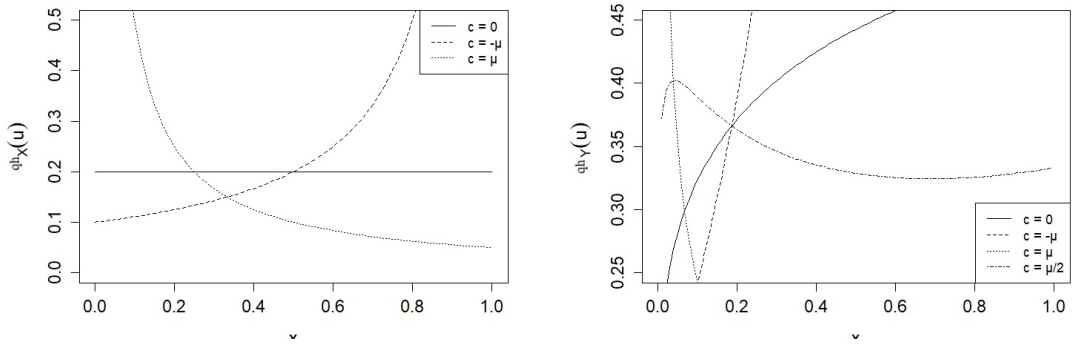

Figure 6.6: Plots of $qh_X(u)$ and $qh_Y(u)$ for different parameters.

Another concept of interest is the hazard quantile ordering, introduced by Vineshkumar et al. (2015). Let X and Y be two random variables with hazard quantile functions $qh_X(\cdot)$ and $qh_Y(\cdot)$. Then X is said to be smaller than Y in the hazard quantile order, denoted by $X \leq_{hq} Y$, if $qh_X(u) \geq qh_Y(u)$ for all $u \in (0,1)$. A related notion is the mean residual quantile ordering, also proposed by Vineshkumar et al. (2015), under which $X \leq_{mrq} Y$ if the corresponding mean residual quantile functions satisfy $qm_X(u) \leq qm_Y(u)$ for all $u \in (0,1)$. In the following propositions, we investigate these quantile-based stochastic ordering

relations between X and $X[X]$.

Proposition 6.18. If $X[X]$ is the RART random variable of X and X or $X[X]$ is DHR, then $X[X] \leq_{hq} X$.

Proof. Assume that X is DHR. Since $X[X] \leq_{hr} X$, from Remark 3.1 of Vineshkumar et al. (2015), the result follows. Similarly we can prove by assuming $X[X]$ is DHR. □

Proposition 6.19. If $X[X]$ is the RART random variable of X, then $X[X] \leq_{mrq} X$.

Proof. From Proposition 4.1 in Vineshkumar et al. (2015), the result directly follows. □

6.7 Entropy and inaccuracy measures

In this section, we examine entropy and inaccuracy measures for the reversed auto-relevation random variable $X[X]$ in relation to those of the baseline random variable X. Among the various measures of uncertainty, the cumulative residual entropy (CRE), introduced by Wang et al. (2003), has received considerable attention. For a non-negative random variable X with absolutely continuous CDF $F_X(\cdot)$, the CRE is defined as

$$C_X = -\int_0^\infty \bar{F}_X(x) \log \bar{F}_X(x)\, dx.$$

Later, Asadi and Zohrevand (2007) studied the dynamic version of CRE called the dynamic cumulative residual entropy (DCRE), given by

$$C_X(x) = -\int_x^\infty \frac{\bar{F}_X(t)}{\bar{F}_X(x)} \log \frac{\bar{F}_X(t)}{\bar{F}_X(x)}\, dt.$$

Di Crescenzo and Longobardi (2009) introduced the cumulative entropy and its dynamic version. The cumulative entropy of a random variable X is defined as

$$\mathscr{CE}_X(x) = -\int_0^\infty F_X(x) \log F_X(x)\, dx. \tag{6.39}$$

Also, the dynamic cumulative entropy of a random variable X denoted by $\tilde{C}_X(\cdot)$ is defined as

$$\tilde{C}_X(x) = -\int_0^x \frac{F_X(t)}{F_X(x)} \log \frac{F_X(t)}{F_X(x)}\, dt, \quad x > 0. \tag{6.40}$$

This can also be expressed as

$$\tilde{C}_X(x) = -\frac{1}{F_X(x)} \left(\int_0^x F_X(t) \log F_X(t)\, dt - \mu_X(x) F_X(x) \log F_X(x) \right), \tag{6.41}$$

where $\mu_X(x)$ is the mean inactivity time of X. Using (6.41), the mean inactivity time of $X[X]$ was expressed in terms of $\tilde{C}_X(\cdot)$ by Di Crescenzo et al. (2018) as

$$\mu_{X[X]}(x) = \mu_X(x) + \frac{\tilde{C}_X(x)}{1 + \Lambda_X(x)}. \tag{6.42}$$

Example 6.8. Let X follow power distribution with CDF $F(x) = x^\beta,\ 0 \le x \le 1,\ \beta > 0$ and $\mu_X(x) = \frac{x}{\beta+1}$. Now, from (6.41), we have

$$\tilde{C}_X(x) = -\frac{\beta}{x^\beta} \int_0^x \left(t^\beta \log t - t^\beta \log x \right)\, dt = \frac{\beta\, x}{(\beta+1)^2}.$$

Then from (6.42), we have

$$\mu_{X[X]}(x) = \frac{x}{\beta+1} + \frac{\frac{\beta\, x}{(\beta+1)^2}}{1 - \beta \log x} = \frac{x\left(\beta + \frac{\beta}{1-\beta\log(x)} + 1\right)}{(\beta+1)^2}. \tag{6.43}$$

We note that in Example 6.8, when $\beta = 1$, X reduces to a uniform random variable and $\mu_{X[X]}(x)$ in (6.43) becomes

$$\mu_{X[X]}(x) = \frac{x}{4}\left(2 + \frac{1}{1 - \log x}\right).$$

An inaccuracy measure between two random variables X and Y based on the reversed relevation transform called the reversed relevation inaccuracy measure, was proposed by Di Crescenzo et al. (2018). Given the existence of $E(X)$, Di Crescenzo et al. (2018) developed the reversed relevation inaccuracy measure between X and $X[X]$ as

$$\tilde{R}_{X,X[X]}(x) = (\mu_{X[X]} - \mu_X)(1 + \Lambda_X(x)) = \tilde{C}_X(x). \tag{6.44}$$

The KL divergence, also known as relative entropy, is a fundamental concept in information theory that measures the difference or divergence between two probability distributions. It is used to quantify how one probability distribution differs from another, in terms of information content or structure. The KL divergence D, between two random variables X and Y is given by

$$D_{X,Y} = \int_0^\infty f_X(x) \log \frac{f_X(x)}{f_Y(x)}\, dx. \tag{6.45}$$

By letting $Y = X[X]$ in (6.45), we obtain

$$\begin{aligned} D_{X,X[X]} &= \int_0^\infty f_X(x) \log \frac{f_X(x)}{f_{X[X]}(x)}\, dx \\ &= -\int_0^\infty \log\left(-\log F_X(x)\right) f_X(x)\, dx \\ &= -\int_0^1 \log\left(-\log u\right)\, du \quad = \quad \gamma, \end{aligned} \tag{6.46}$$

where $\gamma = 0.577216$ is the Euler's constant. In similar lines, we obtain $D_{X[X],X} = 1 - \gamma = 1 - D_{X,X[X]}$.

The Kerridge inaccuracy measure defined in (1.20), can be alternatively expressed using the Shannon entropy given in (1.19) as

$$H_{X,Y} = -\int_0^\infty f_X(x) \log f_X(x)\, dx + \int_0^\infty f_X(x) \log \frac{f_X(x)}{f_Y(x)}\, dx. \tag{6.47}$$

Then, from (6.46) we have $H_{X,X[X]} - H_X = \gamma$.

Another distance measure proposed by Rényi (1961), called the Rényi divergence measure of order α is defined as

$$D_{\alpha,X,Y} = \frac{1}{\alpha - 1} \log \left(\int_0^\infty \left(\frac{f_X(x)}{f_Y(x)} \right)^{\alpha-1} f_X(x)\, dx \right) \quad \alpha > 0,\ \alpha \neq 1. \tag{6.48}$$

Now, the Rényi divergence between $X[X]$ and X has the form

$$\begin{aligned} D_{\alpha,X[X],X} &= \frac{1}{\alpha - 1} \log \left(\int_0^\infty \left(\frac{-f_X(x) \log F_X(x)}{f_X(x)} \right)^{\alpha-1} (-f_X(x) \log F_X(x))\ dx \right) \\ &= \frac{1}{\alpha - 1} \log \left(\int_0^\infty (-\log F_X(x))^\alpha\, f_X(x)\, dx \right). \end{aligned} \tag{6.49}$$

Substituting $u = F_X(x)$, we get

$$\begin{aligned} D_{\alpha,X[X],X} &= \frac{1}{\alpha - 1} \log \left(\int_0^1 (-\log u)^\alpha\, du \right), \\ &= \frac{\log \Gamma(1+\alpha)}{\alpha - 1}, \quad \alpha > 0,\ \alpha \neq 1. \end{aligned} \tag{6.50}$$

Following the same steps, we obtain

$$D_{\alpha,X,X[X]} = \frac{\log \Gamma(2-\alpha)}{1-\alpha}, \quad \text{for } \alpha < 2 \text{ and } \alpha \neq 1.$$

Another point of interest lies in the examination of Tsallis divergence of order α, discussed in Kayal and Tripathy (2018). The Tsallis divergence between two random variables X and Y is defined as

$$\mathbb{T}_{X,Y} = \frac{1}{\alpha - 1} \int_0^\infty f_X^\alpha(x)\, f_Y^{1-\alpha}(x)\, dx - 1, \quad \alpha > 0,\ \alpha \neq 1. \tag{6.51}$$

When $X = X[X]$ and $Y = X$, (6.51) becomes

$$\begin{aligned}\mathbb{T}_{X[X],X} &= \frac{1}{\alpha-1}\int_0^\infty \left(\frac{f_{X[X]}(x)}{f_X(x)}\right)^\alpha f_X(x)\,dx - 1 \\ &= \frac{1}{\alpha-1}\int_0^\infty (-\log F_X(x))^\alpha\, f_X(x)\,dx - 1. \qquad (6.52)\end{aligned}$$

Using the substitution $u = F_X(x)$, (6.51) can be written as

$$\mathbb{T}_{X[X],X} = \frac{1}{\alpha-1}\int_0^1 (-\log u)^\alpha\, du - 1 = \frac{\Gamma(1+\alpha)}{\alpha-1} - 1, \quad \alpha > 0,\ \alpha \neq 1.$$

Following the same steps, we get

$$\mathbb{T}_{X,X[X]} = \frac{\Gamma(2-\alpha)}{\alpha-1} - 1, \quad \text{for } \alpha < 2 \text{ and } \alpha \neq 1.$$

In numerous real-world scenarios, the uncertainty of a system may not necessarily be linked to its future but rather to its past. For example, if a system undergoes random inspection at a specific time t, and is discovered to have deteriorated, the level of uncertainty is contingent on past occurrences. In these contexts, the past lifetime random variable is appropriate for characterizing the time interval between a system's failure and the moment it is identified as non-functional. Along similar lines, Kundu (2023) introduced the cumulative past extropy as

$$J_X = -\frac{1}{2}\int_0^\infty F_X^2(x)\,dx.$$

A weighted cumulative past extropy with general weight function was introduced by Chaudhary and Gupta (2023) as

$$J_X^w = -\frac{1}{2}\int_0^\infty F_X^2(x)\,w(x)\,dx, \qquad (6.53)$$

where $w(x)$ is the weight function. Another measure of distance is the Gini's mean difference (GMD) which was introduced by Gini (1912). Let X_1 and X_2

be two independent random variables with common CDF. Then, the GMD is defined as

$$\mathrm{GMD}_{X_1,X_2} = E\,|X_1 - X_2|\,.$$

GMD is a measure of variability and is widely used in the field of statistics and economics. Yitzhaki (2003) showed that the GMD can be used as an alternative for variance when the underlying distribution is far from normal. A thorough review on GMD was done by Yitzhaki and Schechtman (2013) wherein a compare and contrast of the properties of GMD and variance is also available. Recently, Kattumannil et al. (2024) studied the relationships between certain entropy measures and GMD. An expression for the GMD of a random variable X and the corresponding distortion random variable X_q, was derived in Capaldo et al. (2024), which is given as

$$\mathrm{GMD}_{X,X_q} = E\,|X - X_q| = \int_0^\infty \big(\bar{F}_X(x) + q(\bar{F}_X(x))\big)\,\big(1 - 2\,\bar{F}_X(x)\big)\,dx, \tag{6.54}$$

where $q(\cdot)$ is the underlying distortion function. In the next proposition we derive an expression for the GMD of X and $X[X]$.

Proposition 6.20. Let X be a non-negative random variable and $X[X]$ be the corresponding RART form. Then the GMD between X and $X[X]$ is

$$\mathrm{GMD}_{X,X[X]} = 2\,E(X) + 8\,S_X + \xi_X + 4\,J_X^w, \tag{6.55}$$

where $w(x) = -\log F_X(x)$ is the weight function.

Proof. From the distortion relation (6.22) and (6.54), we have

$$\begin{aligned}
\mathrm{GMD}_{X,X[X]} &= \int_0^\infty \big(2\,\bar{F}_X(x) + F_X(x)\log F_X(x)\big)\,\big(1 - 2\,\bar{F}_X(x)\big)\,dx \\
&= 2\int_0^\infty \bar{F}_X(x)\,dx - 4\int_0^\infty \bar{F}_X^2(x)\,dx + \int_0^\infty \big(F_X(x)(1 - 2\,\bar{F}_X(x))\big)\log F_X(x)\,dx \\
&= 2\,E(X) + 8\,S_X + \xi_X + 2\int_0^\infty F_X^2(x)\log F_X(x)\,dx
\end{aligned}$$

$$= 2\,E(X) + 8\,S_X + \xi_X + 4\,J_X^w,$$

which completes the proof. □

From (6.1) and (6.39), we obtain

$$E(X[X]) = \int_0^\infty \bar{F}_{X[X]}(x)\,dx = E(X) + \xi_X. \tag{6.56}$$

Thus, expected value of $X[X]$ can be found from the baseline measures such as $E(X)$ and ξ_X. We can rewrite (6.56) as $\xi_X = E(X[X] - X)$, which will be useful in constructing simple non-parametric estimator for ξ_X.

Example 6.9. Let X be a random variable with CDF $F_X(x) = \mathrm{e}^{-\left(\frac{\sigma}{x}\right)^\alpha}$, $x > 0,\ \sigma,\ \alpha > 0$ and $E(X) = \sigma\,\Gamma(1 - \frac{1}{\alpha}),$ for $\alpha > 1$. Then from (6.56) we have

$$\begin{aligned} E(X[X]) &= E(X) + \xi_X \\ &= \sigma\,\Gamma\left(1 - \frac{1}{\alpha}\right) - \int_0^\infty \mathrm{e}^{-\left(\frac{\sigma}{x}\right)^\alpha} \left(\frac{\sigma}{x}\right)^\alpha dx \\ &= \sigma\,\Gamma\left(1 - \frac{1}{\alpha}\right) - \frac{\sigma}{\alpha}\,\Gamma\left(1 - \frac{1}{\alpha}\right) \\ E(X[X]) &= \sigma\,\Gamma\left(2 - \frac{1}{\alpha}\right). \end{aligned}$$

Di Crescenzo and Longobardi (2004) proposed a discrimination measure based on the KL divergence between two past lifetime random variables X and Y with CDFs $F_X(\cdot)$ and $F_Y(\cdot)$ respectively, which is given by

$$I_{X,Y}(x) = -\int_0^x \frac{f_X(t)}{F_X(x)} \log\left(\frac{f_X(t)/F_X(x)}{f_Y(t)/F_Y(x)}\right) dt. \tag{6.57}$$

Proposition 6.21. Let $X[X]$ be the RART random variable of X. Then

$$I_{X,X[X]}(x) = \frac{\mathrm{Li}(F_X(x))}{F_X(x)} - \log\left(1 - \Lambda_X(x)\right), \tag{6.58}$$

where $\mathrm{Li}(x) = \int_0^x \frac{1}{\log t}\, dt$ for $x \neq 1$, is the logarithmic integral function.

Proof. From (6.57), we have

$$\begin{aligned}
I_{X,X[X]}(x) &= -\int_0^x \frac{f_X(t)}{F_X(x)} \log\left(\frac{f_X(t)/F_X(x)}{f_{X[X]}(t)/F_{X[X]}(x)}\right) dt \\
&= \int_0^x \frac{f_X(t)}{F_X(x)} \log\left(\frac{-\log F_X(t)}{1-\log F_X(x)}\right) dt \\
&= \frac{1}{F_X(x)} \int_0^x f_X(t) \log\left(-\log F_X(t)\right)\, dt - \log\left(1-\log F_X(x)\right) \\
&= \frac{1}{F_X(x)} \int_0^{F_X(x)} \log\left(-\log u\right)\, du - \log\left(1-\log F_X(x)\right) \\
&= \frac{\mathrm{Li}(F_X(x))}{F_X(x)} - \log\left(1-\log F_X(x)\right),
\end{aligned}$$

which completes the proof. □

6.8 Applications based on truncated Gumbel model

To illustrate the applicability of the RART framework, we consider the left-truncated Gumbel (TG) distribution truncated at 0. This model was introduced and studied by Neamah and Qasim (2021) in a reliability context. We assume that the baseline random variable X follows the TG distribution. The CDF of X is given by

$$F_X(x) = \frac{\mathrm{e}^{\mathrm{e}^{\frac{a}{b}\left(1-\mathrm{e}^{-\frac{x}{b}}\right)}} - 1}{\mathrm{e}^{\mathrm{e}^{\frac{a}{b}}} - 1}, \quad x > 0,\ -\infty < a < \infty,\ b > 0. \tag{6.59}$$

The corresponding density function and hazard rate are

$$f_X(x) = \frac{\mathrm{e}^{\frac{-b\ \mathrm{e}^{\frac{a-x}{b}}+a-x}{b}}}{b\ (1-\mathrm{e}^{-\mathrm{e}^{\frac{a}{b}}})}, \quad x>0,\ -\infty<a<\infty,\ b>0,$$

and

$$h_X(x) = \frac{\mathrm{e}^{\frac{a-x}{b}}}{b\left(\mathrm{e}^{\mathrm{e}^{\frac{a-x}{b}}}-1\right)},$$

respectively. Note that $h_X(x)$ is strictly increasing. By substituting (6.59) into (6.1), we obtain a new distribution, referred to as the reversed auto-relevated truncated Gumbel (RARTG). The corresponding RARTG random variable $X[X]$ has CDF $F_{X[X]}(\cdot)$ given by

$$F_{X[X]}(x) = \frac{\left(\mathrm{e}^{\mathrm{e}^{\frac{a}{b}}\left(1-\mathrm{e}^{-\frac{x}{b}}\right)}-1\right)\left(1-\log\left(\frac{\mathrm{e}^{\mathrm{e}^{\frac{a}{b}}\left(1-\mathrm{e}^{-\frac{x}{b}}\right)}-1}{\mathrm{e}^{\mathrm{e}^{\frac{a}{b}}}-1}\right)\right)}{\mathrm{e}^{\mathrm{e}^{\frac{a}{b}}}-1}. \tag{6.60}$$

The corresponding density function and hazard rate are obtained as

$$f_{X[X]}(x) = \frac{\mathrm{e}^{\frac{b\ \mathrm{e}^{\frac{a}{b}}\left(1-\mathrm{e}^{-\frac{x}{b}}\right)+a-x}{b}}\log\left(\frac{\mathrm{e}^{\mathrm{e}^{\frac{a}{b}}\left(1-\mathrm{e}^{-\frac{x}{b}}\right)}-1}{\mathrm{e}^{\mathrm{e}^{\frac{a}{b}}}-1}\right)}{b\left(1-\mathrm{e}^{\mathrm{e}^{\frac{a}{b}}}\right)}, \tag{6.61}$$

and

$$h_{X[X]}(x) = \frac{\mathrm{e}^{\frac{b\ \mathrm{e}^{\frac{a}{b}}\left(1-\mathrm{e}^{-\frac{x}{b}}\right)+a-x}{b}}\log\left(\frac{\mathrm{e}^{\mathrm{e}^{\frac{a}{b}}\left(1-\mathrm{e}^{-\frac{x}{b}}\right)}-1}{\mathrm{e}^{\mathrm{e}^{\frac{a}{b}}}-1}\right)}{b\left(\mathrm{e}^{\mathrm{e}^{\frac{a}{b}}\left(1-\mathrm{e}^{-\frac{x}{b}}\right)}-\left(\mathrm{e}^{\mathrm{e}^{\frac{a}{b}}\left(1-\mathrm{e}^{-\frac{x}{b}}\right)}-1\right)\log\left(\frac{\mathrm{e}^{\mathrm{e}^{\frac{a}{b}}\left(1-\mathrm{e}^{-\frac{x}{b}}\right)}-1}{\mathrm{e}^{\mathrm{e}^{\frac{a}{b}}}-1}\right)+\mathrm{e}^{\mathrm{e}^{\frac{a}{b}}}\right)}. \tag{6.62}$$

From Figure 6.7, we can observe that $h_{X[X]}(x)$ exhibits both monotonic and non-monotonic shapes for various parameter values, whereas the baseline hazard $h_X(x)$ only has IHR. Furthermore, since $\lim_{x\to\infty} h_X(x) = \frac{1}{b}$ for $-\infty<a<\infty$ and $b>0$, it follows from Proposition 6.4 that the RARTG model belongs to the

$\mathcal{L}$-class.

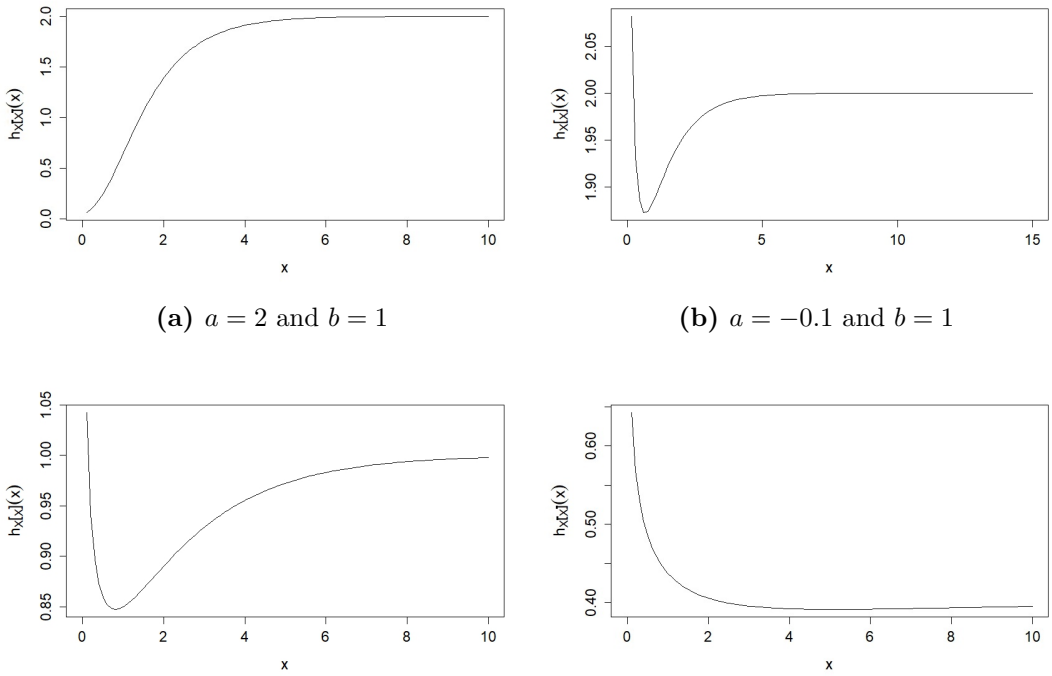

(a) $a = 2$ and $b = 1$ **(b)** $a = -0.1$ and $b = 1$

(c) $a = 0.5$ and $b = 2$ **(d)** $a = -2$ and $b = 5$

Figure 6.7: Plots of $h_X(x)$ and $h_{X[X]}(x)$ for various parameter combinations.

6.8.1 Estimation of parameters

Let $X_1, X_2, \ldots, X_n$ be a random sample of size n from the RARTG distribution with parameters (a, b), and $\underline{x} = (x_1, x_2, \ldots, x_n)$ denote the corresponding observed values. Then, the log-likelihood function can be obtained from (6.61) as

$$L(a,b) = \sum_{i=1}^{n} \left[\frac{b\,\mathrm{e}^{\frac{a}{b}} \left(1 - \mathrm{e}^{-\frac{x_i}{b}}\right) + a - x_i}{b} - \log b - \log\left(1 - \mathrm{e}^{\mathrm{e}^{\frac{a}{b}}}\right) + \log\left(\log\left(\frac{\mathrm{e}^{\mathrm{e}^{\frac{a}{b}}(1-\mathrm{e}^{-\frac{x_i}{b}})} - 1}{\mathrm{e}^{\mathrm{e}^{\frac{a}{b}}} - 1}\right)\right)\right]. \tag{6.63}$$

The MLE of the parameters can be obtained by solving the equations $\frac{\partial L}{\partial a} = 0$, and $\frac{\partial L}{\partial b} = 0$ simultaneously. Since this system of equations is nonlinear and does

not admit closed-form solutions, we employ numerical methods.

6.8.2 Real data application

To demonstrate the practical applicability of the proposed RARTG model, we consider a real-life dataset reported in Clarke (2002). The data consist of mean daily discharge measurements obtained from readings taken at 7:00 and 19:00 hours at the Bela Vista and Espumoso gauging stations on the Jacuí River in southern Brazil. The model parameters are estimated using the method of maximum likelihood, and the goodness of fit is evaluated through Q-Q plot and the KS test statistic. We compare the goodness of fit of the proposed mode with the baseline TG distribution. Table 6.2 presents the goodness of fit measures for the considered models. The Q-Q plot is depicted in Figure 6.8. We can infer that for both datasets, the proposed RARTG model performs better when compared with baseline TG distribution.

Table 6.2: Fit measures and goodness of fit for floods data.

Model	Gauging Station	Parameter Estimates	KS statistic	P-value
TG (a, b)	Bela Vista	$\hat{a} = 725.7088$, $\hat{b} = 378.1960$	0.0703	0.9540
	Espumoso	$\hat{a} = 459.0344$, $\hat{b} = 310.8924$	0.1002	0.6660
RARTG (a, b)	Bela Vista	$\hat{a} = 1175.648$, $\hat{b} = 564.6551$	0.0614	0.9870
	Espumoso	$\hat{a} = 834.6292$, $\hat{b} = 471.7457$	0.0855	0.8430

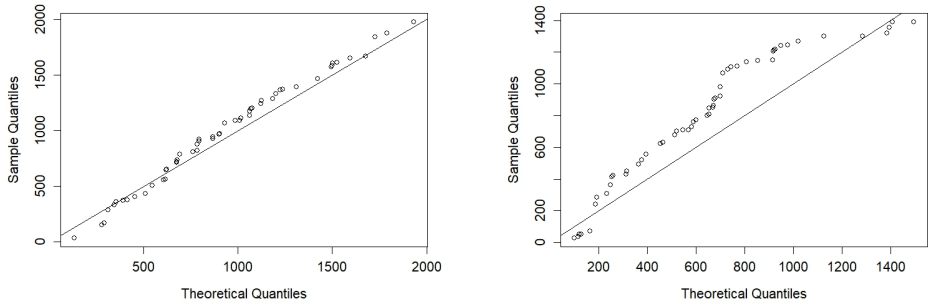

(a) Q-Q plot of Bela Vista data **(b)** Q-Q plot of Espumoso data

Figure 6.8: Q-Q plots for the dataset

6.9 Summary of the chapter

This chapter examined the reversed auto-relevation transform as an effective tool for reliability and lifetime analysis. Key properties and characterizations of RART, based on various reliability measures, were developed. The preservation of important aging classes and stochastic orders under RART was established with supporting illustrations. Closed-form expressions for stress–strength reliability in both single and multi-component settings were obtained. Quantile-based features highlighted the flexibility and practical relevance of the RART framework. In addition, measures based on entropy, extropy, inaccuracy, and divergence were derived to provide information-theoretic insights. Finally, a new model based on the truncated Gumbel distribution was introduced and its applicability demonstrated using real data.

Chapter 7

Multi-phase reversed auto-relevation transform

7.1 Introduction

In Chapter 6 several structural and reliability properties of the RART model were developed and analyzed. The present chapter extends the RART framework to a multi-phase setting and investigates the reliability characteristics of the corresponding lifetime distribution at the n^{th} phase. Particular attention is given to the evolution of key aging measures, including the hazard rate and mean residual life, across successive phases. When the baseline distribution associated with the initial phase is specified, the proposed framework provides insight into the progressive changes in system reliability under imperfect repair conditions. Since such repairs do not restore the system to its original state, the lifetime distribution deteriorates over successive phases. To capture this effect, we examine the underlying reliability properties and study their behavior under various stochastic orderings.

The remainder of the chapter is structured as follows: Section 7.2 introduces the multi-phase RART framework and analyzes important reliability measures. Building on this, Section 7.3 investigates how key aging characteristics evolve from one phase to the next. The preservation of important aging properties

are also investigated. In Section 7.4, we analyze the preservation of various stochastic ordering relationships from the baseline to the multi-phase RART. The conclusions are provided in Section 7.5.

7.2 Multi-phase RART

The RART model can be interpreted in terms of real-world degradation mechanisms, particularly in imperfect repair settings where repairs do not fully restore the system to its original condition. As a result, successive lifetimes become stochastically shorter, reflecting gradual deterioration. Motivated by such scenarios, Lu (2025) highlighted the relevance of recursive reversed auto-relevation models in systems undergoing repeated repairs or replacements. This leads naturally to a multi-phase RART framework, where each phase represents a further decline in system reliability due to cumulative degradation.

Let $F(\cdot)$ denote the CDF of a random variable. Applying the RART, yields a new CDF, $F_2^*(\cdot)$. By iteratively applying this transformation, a sequence of CDFs emerges, representing each step of the iteration. Consequently, after the n^{th} phase, the CDF can be expressed as

$$F_n^*(x) = \begin{cases} F(x), & n = 1 \\ F_{n-1}^*(x) \# F(x), & n \geq 2. \end{cases} \tag{7.1}$$

For $n \geq 2$, (7.1) can be expressed as

$$F_n^*(x) = F(x) \sum_{r=0}^{n-1} \frac{(-\log F(x))^r}{r!}, \quad x > 0,\ n = 1, 2, \ldots. \tag{7.2}$$

Let $\tilde{X}_n$ denote the random variable with survival function given in (7.2), with density function $f_n^*(\cdot)$. Let $f(\cdot)$ and $F(\cdot)$ denote the density and CDF of X, respectively. The reversed hazard rates of X and $\tilde{X}_n$ are given by $\lambda(x) = \frac{f(x)}{F(x)}$ and $\lambda_n^*(x) = \frac{f_n^*(x)}{F_n^*(x)}$, respectively. The corresponding cumulative reversed hazard rates are $\Lambda(x) = \int_x^\infty \lambda(t)\, dt = -\log F(x)$ and $\Lambda_n^*(x) = -\log F_n^*(x)$. Hence, (7.2)

can be expressed as

$$F_n^*(x) = F(x)\sum_{r=0}^{n-1}\frac{\Lambda^r(x)}{r!} \quad \text{and} \quad f_n^*(x) = \frac{\Lambda^{n-1}(x)f(x)}{(n-1)!}.$$

Note that $f_n^*(x)$ can be expressed in the form of a weighted distribution, *i.e.*,

$$f_n^*(x) = \frac{w(x)f(x)}{E(w(X))}, \tag{7.3}$$

where $w(x) = \frac{\Lambda^{n-1}(x)}{(n-1)!}$ is the corresponding weight function with $E\big(w(X)\big) = 1$. A more compact representation is obtained by defining $D_n(x) = \sum_{r=0}^{n-1}\frac{\Lambda^r(x)}{r!}$, $n = 1, 2, \ldots$, so that $D_1(x) = 1$, $D_2(x) = 1 + \Lambda(x)$, and

$$F_n^*(x) = F(x)D_n(x) \tag{7.4}$$

$$f_n^*(x) = (D_n(x) - D_{n-1}(x))f(x). \tag{7.5}$$

Observe that $F_n^*(\cdot)$ is itself a valid life distribution and hence inherits reliability properties related to those of X. The identities and relationships connecting the reliability measures of $F(x)$ and $F_n^*(x)$ often aid in analyzing the characteristics of $F_n^*(x)$, particularly in situations where its explicit form is not readily tractable. Furthermore, such relationships can also be utilized to characterize life distributions.

Proposition 7.1. A continuous random variable X has inverse exponential distribution with CDF $F(x) = \exp\left(-\frac{\sigma}{x}\right)$, $x > 0\, \sigma > 0$. Then, we have

$$f_n^*(x) = \frac{\mathrm{e}^{-\frac{\sigma}{x}}\left(\frac{\sigma}{x}\right)^{n-1}}{(n-1)!}, \tag{7.6}$$

which is the density function of the inverse gamma distribution.

Proof. Proof is straightforward from (7.5). □

Similarly, Table 7.1 presents the expressions for the distribution function $F(x)$ and the transformed density $f_n^*(x)$ for selected lifetime models.

Table 7.1: Some lifetime models and their n^{th} stage RART form

Model	$F(x)$	$\Lambda(x)$	$f_n^*(x)$
Fréchet	$\mathrm{e}^{-\left(\frac{\sigma}{x}\right)^{\alpha}}$, x, σ, $\alpha > 0$	$\left(\frac{\sigma}{x}\right)^{\alpha}$	$\frac{\alpha \mathrm{e}^{-\left(\frac{\sigma}{x}\right)^{\alpha}}\left(\left(\frac{\sigma}{x}\right)^{\alpha}\right)^{n}}{x(n-1)!}$
Power	$\left(\frac{x}{\sigma}\right)^{\alpha}$, $0 < x < \sigma$, σ, $\alpha > 0$	$-\alpha \log(\frac{x}{\sigma})$	$\frac{\alpha\left(\frac{\sigma}{x}\right)^{-\alpha}\left(\alpha \log\left(\frac{\sigma}{x}\right)\right)^{n-1}}{x(n-1)!}$
Beta type-II	$(1+\frac{1}{x})^{-\alpha}$, x, $\alpha > 0$	$\alpha \log\left(1+\frac{1}{x}\right)$	$\frac{\alpha\left(1+\frac{1}{x}\right)^{-\alpha-1}\left(\alpha \log\left(1+\frac{1}{x}\right)\right)^{n-1}}{x^2(n-1)!}$
Log-logistic	$\frac{x^{\alpha}}{1+x^{\alpha}}$, x, $\alpha > 0$	$\log\left(\frac{1+x^{\alpha}}{x^{\alpha}}\right)$	$\frac{\Gamma\left(n, \log\left(\frac{1+x^{\alpha}}{x^{\alpha}}\right)\right)}{\Gamma(n)}$
Dagum	$(1+x^{-\sigma})^{-\alpha}$, x, σ, $\alpha > 0$	$\alpha\left(\log\left(\frac{1+x^{\sigma}}{x^{\sigma}}\right)\right)$	$\frac{\Gamma\left(n, \alpha\left(\log\left(\frac{1+x^{\sigma}}{x^{\sigma}}\right)\right)\right)}{\Gamma(n)}$

The hazard rate of the n^{th} phase RART can be obtained from (7.4) and (7.5) as

$$\begin{aligned} h_n^*(x) &= \frac{(D_n(x) - D_{n-1}(x))f(x)}{1 - F(x)D_n(x)} \\ &= \frac{(D_n(x) - D_{n-1}(x))\bar{F}(x)}{1 - F(x)D_n(x)} h(x) \\ &= \left(\frac{\bar{F}(x)(\Lambda(x))^{n-1}}{\Gamma(n) - \Gamma(n, \Lambda(x))}\right) h(x), \end{aligned} \tag{7.7}$$

where $\Gamma(a, z) = \int_z^{\infty} t^{a-1}\mathrm{e}^{-t}\, dt$ is the incomplete gamma function. If n belongs to the set of integers, $\Gamma(n, x) = \Gamma(n)\mathrm{e}^{-x} \sum_{k=0}^{n-1} \frac{x^k}{k!}$. As a special case, for $n = 2$, we get

$$F_2^*(x) = F(x)\left(1 + \Lambda_X(x)\right),\ h_1^*(x) = h(x),\ h_2^*(x) = \left(\frac{-\bar{F}(x)\log F(x)}{\bar{F}(x) + F(x)\log F(x)}\right) h(x). \tag{7.8}$$

Observe that for any fixed $x > 0$, the sequence $\{h_n^*(x),\, n = 1, 2 \ldots\}$ is increasing in n. This can be illustrated through of an example.

Example 7.1. Suppose X is a standard exponential random variable with CDF $F(x) = 1 - \exp(-x)$, $x > 0$. Then, from (7.2) we have the CDF of the n^{th} phase RART exponential distribution as

$$F_n^*(x) = \frac{\Gamma\left(n, -\log\left(1 - \mathrm{e}^{-x}\right)\right)}{\Gamma(n)}.$$

From (7.7), we have

$$h_n^*(x) = \frac{\mathrm{e}^{-x}\left(-\log\left(1 - \mathrm{e}^{-x}\right)\right)^{n-1}}{\Gamma(n) - \Gamma\left(n, -\log\left(1 - \mathrm{e}^{-x}\right)\right)}. \tag{7.9}$$

The plot of $h_n^*(x)$ for various values of n is presented in Figure 7.1, we can observe that $h_n^*(x)$ is constant for $n = 1$ and monotonically decreasing for $n > 1$. In addition, the hazard rate is increasing in n, *i.e.*, $h_n^*(x) \leq h_{n+1}^*(x)$ for all $x > 0$ and $n = 1, 2, \ldots$, substantiating our earlier statement.

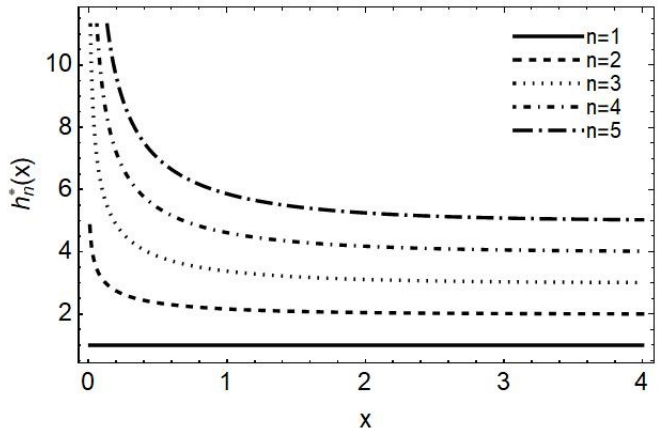

Figure 7.1: Hazard plots for different values of n.

This feature is a key aspect of the n^{th} phase RART models. The progressive increase in the hazard rate across phases leads to a corresponding reduction in the survival time of the equipment. Hence, when the lifetime of a device is characterized by the CDF $F_n^*(\cdot)$, it indicates a decline in reliability after each repair. Now, the reversed hazard rate of the n^{th} phase RART can be obtained as

$$\begin{aligned} \lambda_n^*(x) &= \frac{(D_n(x) - D_{n-1}(x))f(x)}{F(x)D_n(x)} \\ &= \left(1 - \frac{D_{n-1}(x)}{D_n(x)}\right)\lambda(x). \end{aligned} \tag{7.10}$$

Specializing for $n = 2$, we get

$$\lambda_1^*(x) = \lambda(x), \quad \text{and} \quad \lambda_2^*(x) = \left(\frac{D_2(x) - D_1(x)}{D_1(x)}\right)\lambda(x). \tag{7.11}$$

We now illustrate use of the above identities in characterizing life distributions.

Proposition 7.2. A continuous random variable X will follow the inverse exponential distribution with CDF $F(x) = \exp\left(-\frac{\sigma}{x}\right)$, $x > 0$, $\sigma > 0$ if and only

if

$$F_n^*(x) = \left(1 + a_1\left(\frac{x}{\sigma}\right) + a_2\left(\frac{x}{\sigma}\right)^2 + \ldots + a_{n-1}\left(\frac{x}{\sigma}\right)^{n-1}\right)\lambda_n^*(x),$$

where $a_r = \frac{(n-1)!}{r!}$.

Proof. When X has $F(x) = \mathrm{e}^{-\frac{\sigma}{x}}$, then the cumulative reversed hazard rate of X is $\Lambda(x) = \frac{\sigma}{x}$. Then, from (7.10), we have

$$\begin{aligned}
\lambda(x) &= \left(\frac{\sum_{r=0}^{n-1}\frac{(\frac{\sigma}{x})^r}{r!}}{\sum_{r=0}^{n-1}\frac{(\frac{\sigma}{x})^r}{r!} - \sum_{r=0}^{n-2}\frac{(\frac{\sigma}{x})^r}{r!}}\right)\lambda_n^*(x) \\
&= \left((n-1)!\sum_{r=0}^{n-1}\left(\frac{x}{\sigma}\right)^{n-r-1}\right)\lambda_n^*(x) \\
&= \left(1 + a_1\left(\frac{x}{\sigma}\right) + a_2\left(\frac{x}{\sigma}\right)^2 + \ldots + a_{n-1}\left(\frac{x}{\sigma}\right)^{n-1}\right)\lambda_n^*(x),
\end{aligned}$$

where $a_r = \frac{(n-1)!}{r!}$. This completes the proof. □

In a similar manner, Table 7.2 presents the expressions of the functions $F(x)$ and $\lambda(x)$ for a few selected lifetime distributions. Note that in Table 7.2, $a_r = \frac{(n-1)!}{r!}$.

Table 7.2: Some lifetime models and their n^{th} stage RART form

Model	$F(x)$	$\Lambda(x)$	$\lambda(x)$
Fréchet	$\mathrm{e}^{-\left(\frac{\sigma}{x}\right)^{\alpha}}$, x, λ, $\alpha > 0$	$\left(\frac{\sigma}{x}\right)^{\alpha}$	$\lambda_n^*(x)\left(\sum_{r=0}^{n-1} a_r\left(\frac{x}{\sigma}\right)^{\alpha(n-r+1)}\right)$
Power	$\left(\frac{x}{\sigma}\right)^{\alpha}$, x, λ, $\alpha > 0$	$-\alpha\log(\frac{x}{\sigma})$	$\lambda_n^*(x)\left(\sum_{r=0}^{n-1} a_r\left(-\alpha\log\left(\frac{x}{\sigma}\right)\right)^{r-n+1}\right)$
Beta type-II	$\left(1+\frac{1}{x}\right)^{-\alpha}$, x, σ, $\alpha > 0$	$\alpha\log\left(1+\frac{1}{x}\right)$	$\lambda_n^*(x)\left(\sum_{r=0}^{n-1} a_r\left(\alpha\log\left(1+\frac{1}{x}\right)\right)^{r}\right)$
Dagum	$(1+x^{-\sigma})^{-\alpha}$, x, σ, $\alpha > 0$	$\alpha\log(1+x^{-\sigma})$	$\lambda_n^*(x)\left(\sum_{r=0}^{n-1} a_r\left(\alpha\log(1+x^{-\sigma})\right)^{r}\right)$
Pareto	$1-(1+x)^{-\alpha}$, x, $\alpha > 0$	$-\log(1-(1+x)^{-\alpha})$	$\lambda_n^*(x)\left(\sum_{r=0}^{n-1} a_r\left(-\log(1-(1+x)^{-\alpha})\right)^{r}\right)$

We now provide some structural properties of the n^{th} phase RART based on those of the corresponding baseline.

(i) From (7.10), we have $\lim_{x\to 0}\left(1 - \frac{D_{n-1}(x)}{D_n(x)}\right) = 0$ and $\lim_{x\to\infty}\left(1 - \frac{D_{n-1}(x)}{D_n(x)}\right) = 1$.

(ii) Since $D_{n-1}(x) \leq D_n(x)$ for all $x > 0$, we have $\lambda_n^*(x) \in (0, \lambda(x))$, for all $x > 0$. This gives bound for n^{th} phase RART reversed hazard rate, in

terms of its baseline. Similarly, we can obtain the bounds of $h_n^*(x)$ as $h_n^*(x) \in \left(0, \left(\frac{\bar{F}(x)(\Lambda(x))^{n-1}}{\Gamma(n)-\Gamma(n,\Lambda(x))}\right) h(x)\right)$.

(iii) Consider the second phase RART given in (7.8). Since the first order approximation of $\log(1+x) = x$, we can write $F_2^*(x) = 1 - \bar{F}^2(x)$ or equivalently $\bar{F}_2^*(x) = \bar{F}^2(x)$, which is the survival function of minimum of two identically distributed random variables, having same survival functions $\bar{F}(x)$. This is consistent with the fact that $\tilde{X}_n$ is the proportional hazards model of X with proportionality constant 2. To illustrate this, consider two identical random variables following a Weibull distribution with survival function $\bar{F}(x) = \exp\left(-(\lambda x)^\beta\right)$, $x > 0$, $\lambda, \beta > 0$. Let Z denote the minimum of the two variables and let Y be the second phase RART random variable with baseline $\bar{F}(x)$. To examine the quality of the approximation, two independent Weibull random variables are generated with parameters $\lambda = 1$ and $\beta = 3$ and their minimum is recorded to obtain observations of Z. The density function of Y is then superimposed on histograms of the observed samples of Z for different sample sizes. Figure 7.2 presents these comparisons for $n = 10^2, 10^4, 10^5$, and 10^6, demonstrating that the histograms converge to the distribution of Y as the sample size increases.

7.3 Aging properties

From (7.7)-(7.11), it follows that the hazard and reversed hazard rates vary systematically across successive phases, capturing the cumulative effect of imperfect repairs. This highlights the importance of analyzing aging properties to understand the evolution of failure behavior over phases. In particular, examining how the aging characteristics of the baseline lifetime X are transmitted to $\tilde{X}_n$ provides insight into the long-term reliability of the system. We now present results describing hazard-based aging properties from X to $\tilde{X}_n$. From (7.7), $h_n^*(x)$ can be expressed as a multiplicative deformation of the baseline

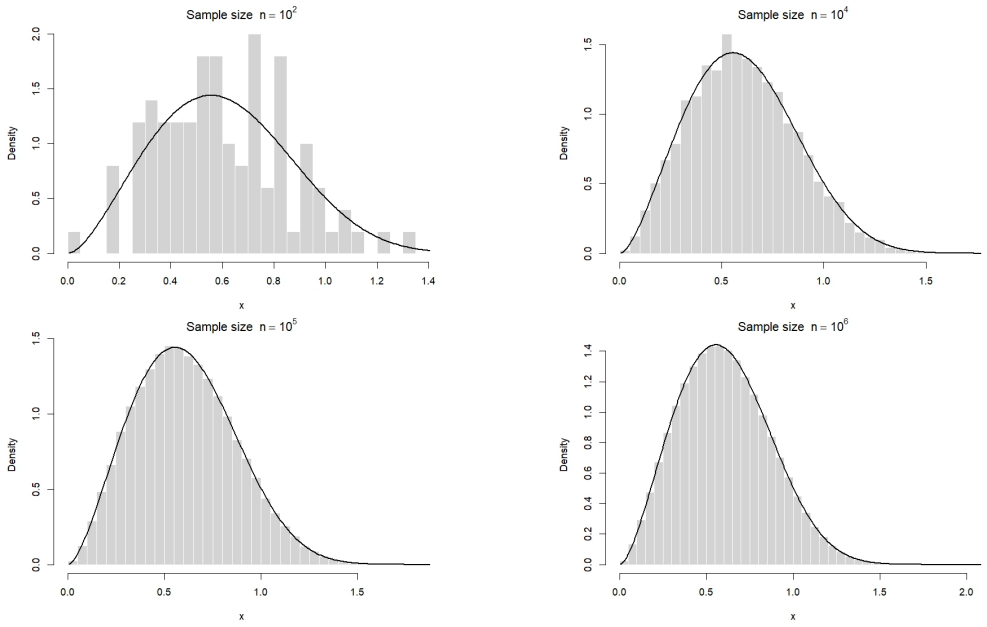

Figure 7.2: Plot of histogram of Z superimposed with the density curve of Y, for different sample sizes

hazard, given by

$$h_n^*(x) = B_n(x)\, h(x), \qquad \text{where } B_n(x) = \frac{\bar{F}(x)\,(\Lambda(x))^{n-1}}{\Gamma(n) - \Gamma\big(n, \Lambda(x)\big)}.$$

Consider

$$\frac{d}{dx} B_n(x) = \frac{(-\log F(x))^{n-2}\, \Delta_n(x)\, f(x)}{F(x)\,(\Gamma(n) - \Gamma(n, -\log F(x)))^2}, \tag{7.12}$$

where the sign-determining term $\Delta_n(x)$ is

$$\Delta_n(x) = -(1 - F(x))F(x)(-\log F(x))^n + \gamma(n, -\log F(x))\,((1-n) + F(x)(n - 1 + \log F(x)))\,.$$

Here, $\gamma(n, z) = \Gamma(n) - \Gamma(n, z)$ denotes the lower incomplete gamma function. Letting $u = F(x)$ and $v = -\log F(x)$, we have $u = \mathrm{e}^{-v}$, and $\Delta_n(x)$ becomes

$$\Delta_n(u) = u(1-u)v^n + \gamma(n, v)\,((1-n)(1-u) - uv)\,.$$

Now, for $n > 1$, we observe that $(1 - n)$ is negative. Since $F(x) \in (0, 1)$, the term $(1 - n)(1 - u) - uv$ is also negative. Comparing the growth rates of the power function v^n against the gamma integral $\gamma(n, v)$, we obtain the inequality:

$$u(1-u)v^n < \gamma(n, v)\,|(1-n)(1-u) - uv|\,.$$

This gives

$$\Delta_n(x) < 0, \quad \text{for all } x > 0 \text{ and } n > 1.$$

This shows that $B_n(x)$ is a decreasing function of x for all $n > 1$. This can again be verified using the plot of $\Delta_n(x)$ for different values of n, depicted in Figure 7.3. Now, from (7.7) we have the following immediate results:

(i) If X is DHR then $\tilde{X}_n$ is DHR.

(ii) If $\tilde{X}_n$ is IHR then X is IHR.

However, when X has IHR, the induced aging behavior of $h_n^*(x)$ may exhibit different patterns. The implications of these results are illustrated through the following examples.

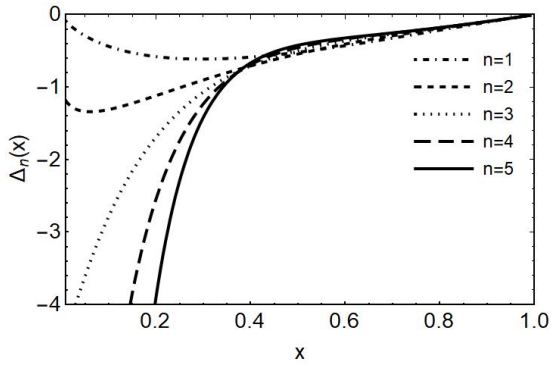

Figure 7.3: Plot of $\Delta_n(x)$ for different values of n

Example 7.2. Let X be a standard Burr type-XII random variable with CDF $F(x) = 1 - \left(\frac{1}{1+x}\right)^2$, $x > 0$. From (7.7), the hazard rate of the n^{th} phase RART can be obtained as

$$h_n^*(x) = \frac{2\left(-\log\left(\frac{x(2+x)}{(1+x)^2}\right)\right)^{n-1}}{(1+x)^3\left(\Gamma(n) - \Gamma\left(n, -\log\left(\frac{x(2+x)}{(1+x)^2}\right)\right)\right)}, \quad x > 0.$$

Figure 7.4 displays the plot of the above hazard rate corresponding to different values of n. In Figure 7.4, the curve corresponding to $n = 1$ represents the baseline Burr type-XII model. For higher values of n, the hazard rate shows a decreasing pattern similar to that of the baseline model. This observation is

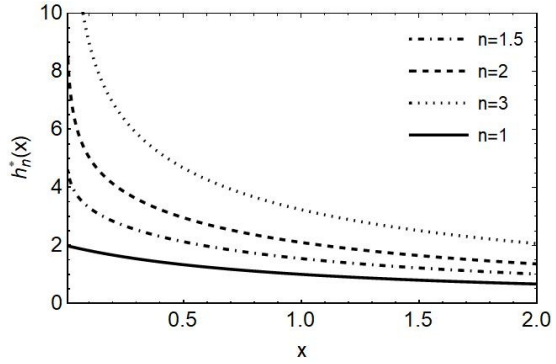

Figure 7.4: Plots of hazard rate for the n^{th} phase RART Burr type-XII model for various values of n

consistent with our earlier result that the DHR property is retained under the formation of the n^{th} phase RART.

Example 7.3. Let X be a half-logistic (HL) random variable with CDF $F(x) = 1 - \frac{2}{1+e^{\frac{x}{\sigma}}}$, $x > 0$, $\sigma > 0$ and hazard rate $h(x) = \frac{1}{\sigma\left(1+e^{-\frac{x}{\sigma}}\right)}$. Then, from (7.7), we have the hazard rate of the n^{th} phase reversed auto-relevated half-logistic (RART-HL) as

$$h_n^*(x) = \frac{2e^{\frac{x}{\sigma}}\left(-\log\left(1-\frac{2}{1+e^{\frac{x}{\sigma}}}\right)\right)^{n-1}}{\sigma\left(1+e^{\frac{x}{\sigma}}\right)^2\left(\Gamma(n)-\Gamma\left(n,-\log\left(1-\frac{2}{1+e^{\frac{x}{\sigma}}}\right)\right)\right)}. \tag{7.13}$$

It is well known that the half-logistic model exhibits the IHR property. To examine the behavior of the hazard rate of the n^{th} phase RART-HL model, we refer to (7.7). From the right hand side of (7.7), we have

$$B_n(x) = \frac{2\left(-\log\left(1-\frac{2}{1+e^{\frac{x}{\sigma}}}\right)\right)^{n-1}}{\left(1+e^{\frac{x}{\sigma}}\right)\left(\Gamma(n)-\Gamma\left(n,-\log\left(1-\frac{2}{1+e^{\frac{x}{\sigma}}}\right)\right)\right)}.$$

In Figure 7.5, we plot the hazard rate of baseline HL model and the function $B_n(x)$ for different values of n. It is observed that for $n = 1$, 2, 3, and 4, $B_n(x)$ is observed to be decreasing, as obtained in the theoretical result. Also, the baseline hazard rate $h(x)$ consistently lies below the corresponding curves of $B_n(x)$ throughout the considered range of x. Figure 7.6 compares the behavior of the above hazard rate across different values of n. For $n = 1$, expression (7.13)

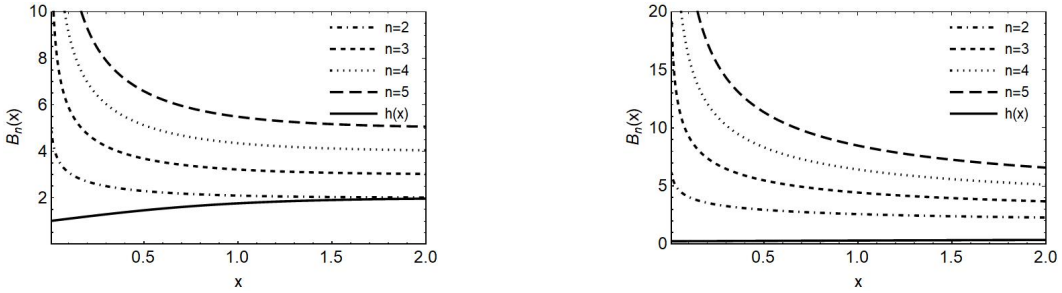

(a) $\sigma = 0.5$ **(b)** $\sigma = 3$

Figure 7.5: Plots of $h(x)$ and $B_n(x)$ for different values of n for the n^{th} phase RART-HL model

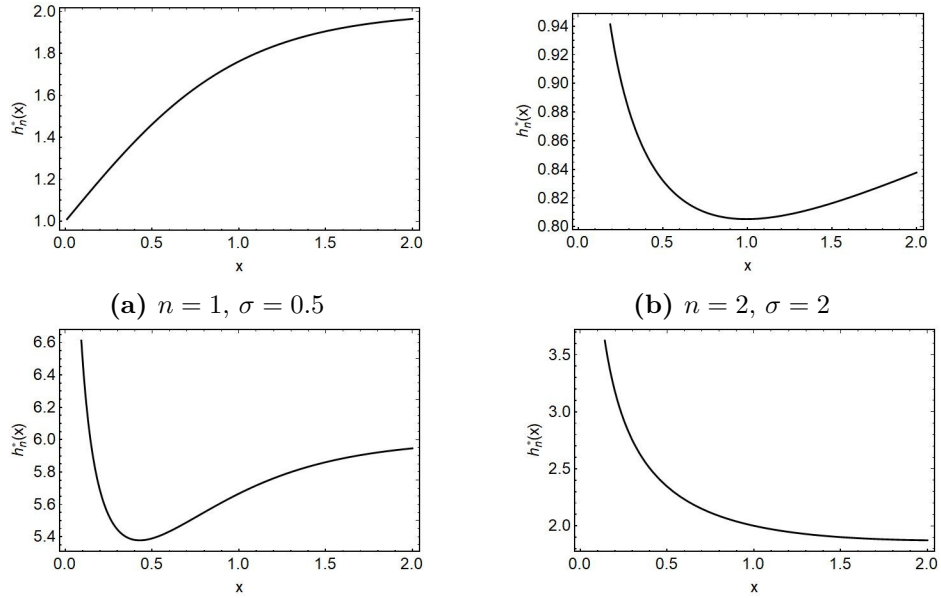

(a) $n = 1$, $\sigma = 0.5$ **(b)** $n = 2$, $\sigma = 2$

(c) $n = 3$, $\sigma = 0.5$ **(d)** $n = 4$, $\sigma = 0.5$

Figure 7.6: Hazard plots for different values of n for n^{th} phase RART-HL model

reduces to the baseline hazard rate, which, as expected, is IHR. When $n = 2$ and $n = 3$, the n^{th} phase RART-HL model displays a bathtub-shaped hazard rate, with change points occurring near $x = 1$ and $x = 0.5$ respectively. For $n = 4$, the shape changes again, and the curve is monotonically decreasing. This behavior reaffirms that the n^{th} phase RART transformation enhances the model's flexibility in capturing various hazard rate shapes, when the baseline is IHR.

From the above illustration, it is evident that as n increases, the survival probability decreases, indicating a higher likelihood of failure. This behavior confirms that, under the imperfect repair model, the system reliability deteriorates progressively with successive repairs, consistent with the increasing nature of the

hazard rate sequence. Note that for each value of n, we obtain a corresponding CDF. We now proceed to demonstrate the practical applicability of the proposed model using two real-life reliability datasets. For this, without loss of generality, we assume $n = 2$ and proceed with the data fitting. Thus we obtain the RART-HL model, whose CDF is given as

$$F_2^*(x) = \left(1 - \frac{2}{\mathrm{e}^{x/\sigma} + 1}\right)\left(1 - \log\left(1 - \frac{2}{\mathrm{e}^{\frac{x}{\sigma}} + 1}\right)\right). \tag{7.14}$$

Both datasets are sourced from Nigm et al. (2003). Dataset I and dataset II each consist of ordered failure times for 20 components. We model these datasets using the RART-HL distribution and evaluate its performance by comparing it with several competing models reported in the literature. The alternative models considered include the baseline half-logistic, odd Fréchet half-logistic (OFHL) (Bhat et al. (2024)), exponentiated generalized standard half-logistic (EGSHL) (Cordeiro (2017)), and half-logistic generalized Weibull (HLGW) (Anwar and Bibi (2018)) distributions.

(i) Half logistic: $F(x) = 1 - \dfrac{2}{\mathrm{e}^{\frac{x}{\sigma}} + 1}, \quad \sigma > 0,\ x > 0.$

(ii) OFHL: $F(x) = \exp\left(-\left(\dfrac{2\,\mathrm{e}^{-\beta x}}{1 - \mathrm{e}^{-\beta x}}\right)^{\sigma}\right), \quad \sigma > 0,\ \beta > 0,\ x > 0.$

(iii) EGSHL: $F(x) = \dfrac{((1 + \mathrm{e}^{-x})^{\sigma} - 2^{\sigma}\mathrm{e}^{-\sigma x})^{\beta}}{(1 + \mathrm{e}^{-x})^{\sigma\beta}}, \quad \sigma > 0,\ \beta > 0,\ x > 0.$

(iv) HLGW: $F(x) = \left(\dfrac{1 - \mathrm{e}^{-\gamma x^{\beta}}}{1 + \mathrm{e}^{-\gamma x^{\beta}}}\right)^{\sigma}, \quad \sigma > 0,\ \beta > 0,\ \gamma > 0,\ x > 0.$

The goodness of fit measures for dataset I and dataset II, obtained for the respective models, are summarized in Table 7.3 and Table 7.4. From Table 7.3 and Table 7.4 we can infer that the goodness of fit measures corresponding to the RART-HL model are better when compared to the competing alternatives, making it a better choice for the considered datasets. Moreover, the histogram and Q-Q plots given in Figure 7.7 also indicate that the proposed model fits both the datasets well.

Table 7.3: Goodness of fit measures for dataset I.

Model	Parameter estimates			KS statistic	p-value
RART-HL	$\sigma = 0.2819$			0.1073	0.9563
EGSHL	$\sigma = 9.6348$	$\beta = 0.7617$		0.1138	0.9321
OFHL	$\sigma = 0.3083$	$\beta = 21.135$		0.1336	0.8225
Half-logistic	$\sigma = 0.1201$			0.1556	0.6620
HLGW	$\sigma = 5.9559$	$\beta = 0.4865$	$\gamma = 6.2617$	0.2971	0.0463

Table 7.4: Goodness of fit measures for dataset II.

Model	Parameter estimates			KS statistic	p-value
RART-HL	$\sigma = 0.2658$			0.1022	0.9710
EGSHL	$\sigma = 10.082$	$\beta = 0.7401$		0.1058	0.9611
OFHL	$\sigma = 0.3401$	$\beta = 22.611$		0.1210	0.8978
Half-logistic	$\sigma = 0.1132$			0.1666	0.5785
HLGW	$\sigma = 6.0081$	$\beta = 0.4710$	$\gamma = 6.3340$	0.2979	0.0455

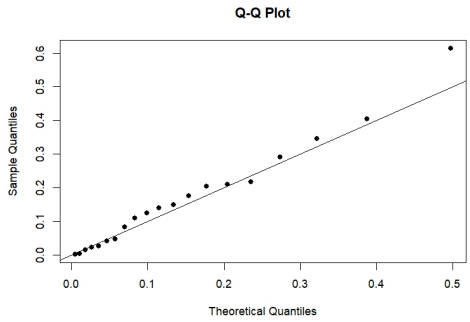

(a) Q-Q plot of dataset I

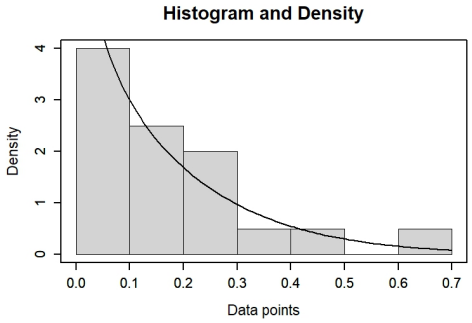

(b) Histogram and fitted density of dataset I

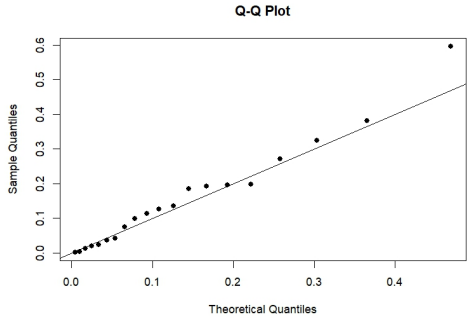

(c) Q-Q plot of dataset II

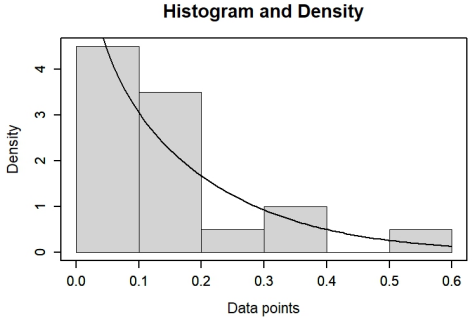

(d) Histogram and fitted density of dataset II

Figure 7.7: Q-Q plot and histogram of the RART-HL model for dataset I and dataset II.

To explore the aging properties further, as in the previous chapters we use the concept distortion function. The next proposition provides the distorted relation

between X and $\tilde{X}_n$.

Proposition 7.3. Let $\tilde{X}_n$ be the n^{th} phase RART random variable corresponding to X. Then $\tilde{X}_n$ is a distorted random variable of X with distortion function

$$q(u) = 1 - (1-u)\sum_{r=0}^{n-1} \frac{(-\log(1-u))^r}{r!}, \quad 0 < u < 1. \tag{7.15}$$

Proof. From (7.2), the survival function of $\tilde{X}_n$ is

$$\bar{F}_n^*(x) = 1 - (1-\bar{F}(x))\sum_{r=0}^{n-1} \frac{(-\log(1-\bar{F}(x)))^r}{r!} = q(\bar{F}(x)),$$

where $q(u) = 1 - (1-u)\sum\limits_{r=0}^{n-1} \frac{(-\log(1-u))^r}{r!}$, which completes the proof. □

The following proposition establishes sufficient conditions for the preservation of well-known aging classes for the n^{th} phase RART utilizing the results listed in Section 1.6.4 of Chapter 1.

Proposition 7.4. If $\tilde{X}_n$ is the n^{th} phase RART random variable of X, then for $n > 1$ the following results hold.

(i) If X is DRHR then $\tilde{X}_n$ is DRHR.

(ii) If X is DLR then $\tilde{X}_n$ is DLR.

(iii) If X is ILOR, then $\tilde{X}_n$ is ILOR.

(iv) If X is DHRA then $\tilde{X}_n$ is DHRA.

(v) If X is NWU then $\tilde{X}_n$ is NWU.

Proof. From Result 2 the monotonic increase of $l_2(u)$ is sufficient to establish (i). We have

$$l_2(u) = \frac{u(-\log u)^n}{\log(u)\Gamma(n, -\log u)}.$$

Let $-\log u = t$, then $u = \mathrm{e}^{-t}$. Now, we have

$$l_2(t) = -\frac{\mathrm{e}^{-t}t^{n-1}}{\Gamma(n,t)} = -\frac{t^{n-1}}{\Gamma(n)\sum\limits_{r=0}^{n-1}\frac{t^k}{k!}}.$$

Then

$$l_2'(t) = \frac{\mathrm{e}^{-2t} t^{n-2} \left(\mathrm{e}^t(-n+t+1)\Gamma(n,t) - t^n\right)}{\left(\Gamma(n,t)\right)^2}.$$

From the above equation, we infer that the term inside the bracket is negative. *i.e.*,

$$\mathrm{e}^t(t-n+1)\Gamma(n,t) - t^n < 0, \quad \text{for all } t > 0 \text{ and } n > 1.$$

This proves (i).

Again, from Result 3, to establish assertion (ii), it suffices to verify that $l_3(u)$ is an increasing function of u. We obtain

$$l_3(u) = \frac{-(n-1)u}{(1-u)\log(1-u)}.$$

Put $p = -\log(1-u)$ or $u = 1 - \mathrm{e}^{-p}$. Then, we have

$$l_3(p) = \frac{(n-1)(\mathrm{e}^p - 1)}{p} \quad \text{and} \quad l_3'(p) = \frac{(n-1)\left(\mathrm{e}^p(p-1)+1\right)}{p^2} > 0,$$

for all $p > 0$ and $n > 1$. This establishes (ii).

For proving (iii), from Result 6 it suffices to show that $l_4(u)$ decreases with u. After simplification, $l_4(u)$ reduces to

$$l_4(u) = \frac{(1-u)u\Gamma(n)(-\log(1-u))^{n-1}}{\Gamma(n,-\log(1-u))(\Gamma(n) - \Gamma(n,-\log(1-u)))},$$

which is a decreasing function for $u \in (0,1)$. Substituting $p = \log(1-u)$ and $u = 1 - \mathrm{e}^{-p}$ as earlier, we obtain

$$l_4(p) = \frac{(1-\mathrm{e}^{-p})\,\mathrm{e}^{-p}\,\Gamma(n)\,p^{n-1}}{\Gamma(n,p)\big(\Gamma(n) - \Gamma(n,p)\big)}.$$

In a manner similar to the proofs of (i) and (ii), it can be shown that $l_4(u)$ is a decreasing function of u for $n > 1$. To corroborate these results, we have the graphical illustration in Figure 7.8, which presents the plots of $l_2(u)$, $l_3(u)$, and $l_4(u)$ for various values of n.

For the distortion function $q(u)$ given in (7.15), it is evident that the inequalities

$q(u\,v) \geq q(u)\,q(v)$ for $u, v \in (0,1)$ and $q(u^a) \geq (q(u))^a$ for $u \in (0,1)$ and $0 < a < 1$, hold true. These confirmations serve to complete the proofs for both statements (iv) and (v), from Result 5 and Result 4 respectively. This completes the proof. □

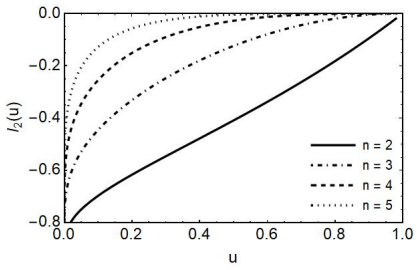

(a) Plot of $l_2(u)$ against u

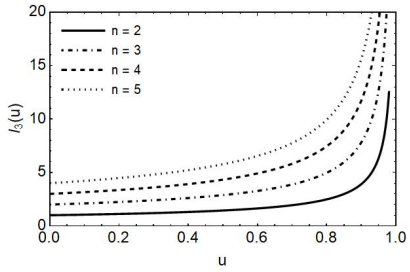

(b) Plot of $l_3(u)$ against u

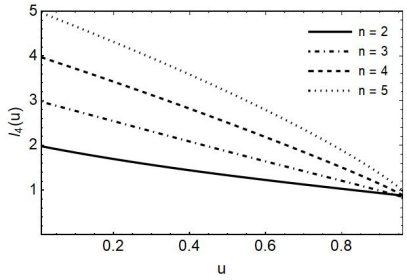

(c) Plot of $l_4(u)$ against u

Figure 7.8: Plots of $l_2(u)$, $l_3(u)$ and $l_4(u)$ for different values of n.

Remark 7.1. Lai and Xie (2006) established that, NWU property implies the NWUHR property. Consequently, this implies that NWUHR is preserved under RART.

7.4 Stochastic orders

In this section, we examine stochastic ordering relationships between X and $\tilde{X}_n$ using the distortion function. The following propositions establish these orders by invoking the results from Section 1.6.4 of Chapter 1.

Proposition 7.5. Let X be a non-negative continuous random variable and $\tilde{X}_n$ be the corresponding n^{th} phase RART random variable. Then $\tilde{X}_n \leq_{lr} X$, for $n \geq 1$.

Proof. Recalling Result 8, we have

$$\frac{q'(u)}{q'_1(u)} = \frac{(-\log(1-u))^{n-1}}{\Gamma(n)},$$

and

$$\frac{d}{du}\left(\frac{q'(u)}{q'_1(u)}\right) = \frac{(n-1)(-\log(1-u))^{n-2}}{(1-u)\Gamma(n)} > 0, \quad \text{for } n \geq 1,$$

which completes the proof. □

Based on the findings outlined in Shaked and Shanthikumar (2007), Navarro et al. (2013), we have the following implications in the case of n^{th} phase RART.

$$\begin{array}{ccccccc} & & \tilde{X}_n \leq_{mrl} X & & & & \tilde{X}_n \leq_{ew} X \\ & & \Uparrow & & & & \Uparrow \\ \tilde{X}_n \leq_{lr} X & \Longrightarrow & \tilde{X}_n \leq_{hr} X & \Longrightarrow & \tilde{X}_n \leq_{or} X & \Longrightarrow & \tilde{X}_n \leq_{st} X \Longrightarrow \tilde{X}_n \leq_{icx} X \\ \Downarrow & & & & & & \Downarrow \\ \tilde{X}_n \leq_{rhr} X & \Longrightarrow & \tilde{X}_n \leq_{mit} X & & & & \tilde{X}_n \leq_{su} X \Longleftarrow \tilde{X}_n \leq_{*} X \end{array}$$

Proposition 7.6. Let X and Y be two random variables with survival functions $\bar{F}_X(x)$ and $\bar{F}_Y(x)$. Suppose $\tilde{X}_n$ and $\tilde{Y}_n$ are the corresponding n^{th} phase RART random variables respectively. Then, for $n > 1$ the following properties hold:

(i) If $X \leq_{st} Y$, then $\tilde{X}_n \leq_{st} \tilde{Y}_n$.

(ii) If $X \leq_{rhr} Y$, then $\tilde{X}_n \leq_{rhr} \tilde{Y}_n$.

(iii) If $X \leq_{ttt} Y$, then $\tilde{X}_n \leq_{ttt} \tilde{Y}_n$.

(iv) If $X \leq_{disp} Y$, then $\tilde{X}_n \leq_{disp} \tilde{Y}_n$.

Proof. Proof of (i) is direct from Result 9.

To prove (ii), again from Result 11 we only need to show that $\frac{(1-u)q'(u)}{1-q(u)}$ is increasing in $(0,1)$. We have

$$\frac{(1-u)q'(u)}{1-q(u)} = \frac{(1-u)(-\log(1-u))^{n-1}}{\Gamma(n,-\log(1-u))},$$

whose first derivative is obtained as

$$\frac{(-\log(1-u))^{n-2}\left((n+\log(1-u)-1)\Gamma(n,-\log(1-u))-(u-1)(-\log(1-u))^{n}\right)}{\Gamma(n,-\log(1-u))^{2}}>0,$$

for $n>1$, which proves (ii).

The proof of (iii) is also direct due to Result 14, and the fact that the function $q(u)$ given in (7.15) is convex.

Proof of (iv) directly follows Result 15. □

Proposition 7.7. Let X be a non-negative continuous random variable, and $\tilde{X}_n$ denote its n^{th} phase RART random variable. Then, for all $n \geq 1$, $\tilde{X}_n \leq_{or} X$.

Proof. We only need to show that the ratio $\frac{\theta'(x)}{\theta_n'(x)} \leq 1$.

$$\frac{\theta'(x)}{\theta_n'(x)}=\frac{\Gamma(n)(-\log(1-\bar{F}(x)))^{1-n}\left(\frac{\Gamma(n,-\log(1-\bar{F}(x)))}{\Gamma(n)}-1\right)^{2}}{\left(\bar{F}(x)\right)^{2}}\leq 1,\ \text{for all } x>0,$$

which completes the proof. □

Proposition 7.8. Suppose that X and Y are independent random variables and that $X \leq_{hr} Y$. Then $X \leq_b Y$ implies $\tilde{X}_n \leq_b \tilde{Y}_n$ for $n \geq 2$.

Proof. From Theorem 18 of Kayid and Almohsen (2024), it suffices to verify that

$$l_5(u)=\frac{w(u)}{u\,w'(u)}\quad\text{and}\quad l_6(u)=\frac{-u\,\log(u)\,l_5'(u)}{l_5(u)},$$

are non-decreasing functions of $u \in (0,1)$, where $w(u) = 1 - q(1-u)$. From the distortion representation of n^{th} phase RART given in (7.15), we have

$$l_5(u)=\frac{(-\log(u))^{1-n}\Gamma(n,-\log(u))}{u},\quad\text{and}\quad l_6(u)=\frac{u(-\log(u))^{n}}{\Gamma(n,-\log(u))}+n+\log(u)-1.$$

Then

$$l_5'(u)=\frac{(n+\log(u)-1)(-\log(u))^{-n}\Gamma(n,-\log(u))+u}{u^{2}}>0,\quad\text{for } n\geq 2,$$

and

$$l_6'(u) = \frac{(n + \log(u))(-\log(u))^n}{\log(u)\Gamma(n, -\log(u))} + \frac{u(-\log(u))^{2n}}{\log(u)\Gamma(n, -\log(u))^2} + \frac{1}{u} > 0,$$

for $n \geq 2$. Thus $l_5(u)$ and $l_6(u)$ are non-decreasing in u, which completes the proof. □

7.5 Summary of the chapter

In this chapter, we extend the reversed auto-relevation transform to a multi-phase framework and explore its reliability implications. Key reliability measures are derived and used to characterize lifetime distributions using the proposed model. The aging patterns of the proposed model have been thoroughly investigated, and the necessary conditions for the preservation of key aging classes across successive phases of the RART model have been established. A new lifetime model has been constructed using the proposed transform by considering the baseline as half-logistic model.

Chapter 8

RART based GEVD and parameter estimation

In Chapters 2-7, relevation and reversed relevation based models were developed and analyzed, with emphasis on their reliability properties and links to extreme value distributions. Building on this foundation, in the present chapter we consider a left-truncated generalized extreme value distribution and studies its reliability and aging behavior. Since the standard GEVD is not directly suitable for lifetime modeling, truncation provides a natural framework for such analysis. As discussed in Chapter 1, the CDF of the GEVD is given by

$$G(x) = \exp\left[-\left(1 - \frac{\xi(x-\mu)}{\sigma}\right)^{\frac{1}{\xi}}\right]. \tag{8.1}$$

where $-\infty < \mu < \infty$ is the location parameter, $\sigma > 0$ is the scale parameter, and $-\infty < \xi < \infty$ is the shape parameter. Also, $x < \mu + \frac{\xi}{\sigma}$, when $\xi > 0$, $x > \mu + \frac{\xi}{\sigma}$, when $\xi < 0$, and $x \in \mathbb{R}$, when $\xi = 0$. Further, a RART-based extension of the truncated GEVD is proposed, and its reliability properties are examined. Despite the added flexibility of these models, their practical implementation depends

Results presented in this chapter are published in the article entitled *"A Regression Method of Estimation for Generalized Extreme Value Distribution"*, published in the journal *Kybernetika* (Anand and Chandran (2025)).

on stable and efficient parameter estimation. It is well known that classical estimation methods for the GEVD may face numerical difficulties, especially in truncated and more complex settings. To address this, the latter part of the chapter develops a regression-based estimation approach for the GEVD.

The remainder of the chapter is organized as follows: Section 8.1 analyzes the truncated GEVD and studies its associated reliability and aging properties. Section 8.2 introduces the RART of the truncated GEVD and investigates its aging behavior. A simulation study is also performed to analyze the performance of the model parameter estimates. Section 8.3 presents a comprehensive review of the existing literature on parameter estimation for the GEVD, highlighting the limitations of classical methods. A brief overview of commonly used estimation techniques is provided in Section 8.4, followed by the proposed regression-based estimation method in Section 8.5. Bootstrap confidence intervals for the regression estimates are derived in Section 8.6. Section 8.7 presents the results of a Monte Carlo simulation study, while Section 8.8 illustrates the practical performance of the proposed approach using real data. Finally, the chapter is summarized in Section 8.9.

8.1 Truncated GEVD

To apply the GEVD in reliability contexts, we consider its left-truncated version at zero, referred to as the TGEVD, introduced by Baran et al. (2021). This model has been used, for instance, in calibrating wind speed forecasts to avoid physically unrealistic negative values. The CDF of the TGEVD, denoted by $G_0(\cdot)$, is given in (8.2), where μ_0, σ_0, and ξ_0 represent the location, scale, and shape parameters, respectively.

$$G_0(x) = \begin{cases} 0, & x < 0 \\ \dfrac{\exp\left(-\left(1-\frac{\xi_0(x-\mu_0)}{\sigma_0}\right)^{\frac{1}{\xi_0}}\right) - \exp\left(-\left(1+\frac{\xi_0\mu_0}{\sigma_0}\right)^{\frac{1}{\xi_0}}\right)}{1-\exp\left(-\left(1+\frac{\xi_0\mu_0}{\sigma_0}\right)^{\frac{1}{\xi_0}}\right)}, & 0 < x < \frac{\sigma_0}{\xi_0} + \mu_0 \\ 1, & x > \frac{\sigma_0}{\xi_0} + \mu_0, \end{cases} \tag{8.2}$$

For reliability applications, we assume $\mu_0 + \frac{\sigma_0}{\xi_0} > 0$ to ensure a non-negative and bounded support, yielding a well-defined model within the reliability framework. Under these conditions, the CDF and corresponding density function simplify as follows:

$$G_0(x) = \frac{\mathrm{e}\left(\mathrm{e}^{-\left(1-\frac{x\xi_0}{\sigma_0}\right)^{\frac{1}{\xi_0}}} - \frac{1}{\mathrm{e}}\right)}{\mathrm{e}-1}, \quad 0 < x < \frac{\sigma_0}{\xi_0}\,\sigma_0,\ \xi_0 > 0, \tag{8.3}$$

$$g_0(x) = \frac{\mathrm{e}^{1-\left(1-\frac{x\xi_0}{\sigma_0}\right)^{\frac{1}{\xi_0}}}\left(1-\frac{x\xi_0}{\sigma_0}\right)^{\frac{1}{\xi_0}-1}}{(\mathrm{e}-1)\sigma_0}. \tag{8.4}$$

We now examine the aging property of the TGEVD model defined in (8.3). The hazard rate can be derived as

$$\begin{aligned} h(x) &= \frac{g_0(x)}{G_0(x)} \\ &= -\frac{\left(1-\frac{x\xi_0}{\sigma_0}\right)^{\frac{1}{\xi_0}}}{\left(\mathrm{e}^{\left(1-\frac{x\xi_0}{\sigma_0}\right)^{\frac{1}{\xi_0}}} - 1\right)(x\xi_0 - \sigma_0)}. \end{aligned} \tag{8.5}$$

The corresponding first derivative is given by

$$\frac{d}{dx}(h(x)) = -\frac{\left(\xi_0\left(\mathrm{e}^{\left(1-\frac{x\xi_0}{\sigma_0}\right)^{\frac{1}{\xi_0}}} - 1\right) + \mathrm{e}^{\left(1-\frac{x\xi_0}{\sigma_0}\right)^{\frac{1}{\xi_0}}}\left(\left(1-\frac{x\xi_0}{\sigma_0}\right)^{\frac{1}{\xi_0}} - 1\right) + 1\right)\left(1-\frac{x\xi_0}{\sigma_0}\right)^{\frac{1}{\xi_0}}}{\left(\mathrm{e}^{\left(1-\frac{x\xi_0}{\sigma_0}\right)^{\frac{1}{\xi_0}}} - 1\right)^2 (\sigma_0 - x\xi_0)^2}.$$

For $\xi_0 > 0$ and $0 < x < \frac{\sigma_0}{\xi_0}$, we have $\frac{d}{dx}(h(x)) > 0$, implying that $h(x)$ is an increasing function. Thus, the TGEVD exhibits the IHR property when $\xi_0 > 0$. As discussed in Chapter 6, the RART model serves as a parsimonious transformation that enhances flexibility in the hazard rate, particularly when the baseline distribution possesses the IHR property. Motivated by this observation, we introduce the RART-TGEVD model in the next section and examine its reliability and aging properties.

8.2 RART truncated GEVD

Consider the CDF of RART model discussed in Chapter 6, given as

$$F_{X[X]}(x) = F_X(x)(1 - \log F_X(x)), \tag{8.6}$$

where X is the baseline random variable and $X[X]$ is the corresponding RART model. Choosing $F_X(x) = G_0(x)$, we obtain the RART-TGEVD model with CDF

$$F_Z(x) = \frac{\mathrm{e}\left(\mathrm{e}^{-\left(1-\frac{x\xi_0}{\sigma_0}\right)^{\frac{1}{\xi_0}}} - \frac{1}{e}\right)\left(1 - \log\left(\frac{e\left(\mathrm{e}^{-\left(1-\frac{x\xi_0}{\sigma_0}\right)^{\frac{1}{\xi_0}}} - \frac{1}{\mathrm{e}}\right)}{\mathrm{e}-1}\right)\right)}{\mathrm{e}-1}, \quad 0 < x < \frac{\sigma_0}{\xi_0}, \tag{8.7}$$

where σ_0, $\xi_0 > 0$. Here, Z denotes the RART-TGEVD random variable. The corresponding density function and hazard rate are

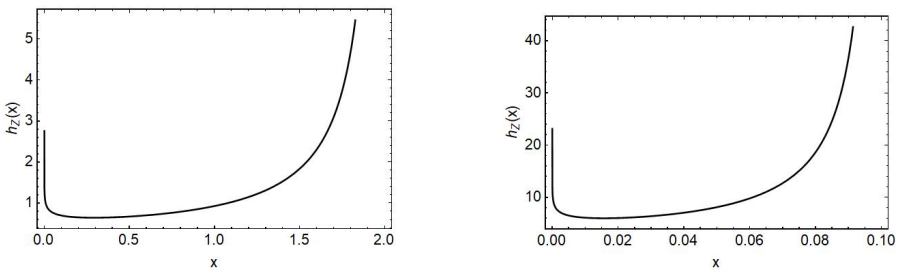

(a) $\xi = 2$, $\sigma = 4$ **(b)** $\xi = 5$, $\sigma = 0.5$

Figure 8.1: Hazard plot of RART-TGEVD

$$
\begin{aligned}
f_Z(x) &= \frac{\exp\left(1-\left(1-\frac{x\xi_0}{\sigma_0}\right)^{\frac{1}{\xi_0}}\right)\left(1-\frac{x\xi_0}{\sigma_0}\right)^{\frac{1}{\xi_0}}\log\left(\frac{\mathrm{e}\left(\mathrm{e}^{-\left(1-\frac{x\xi_0}{\sigma_0}\right)^{\frac{1}{\xi_0}}}-\frac{1}{\mathrm{e}}\right)}{\mathrm{e}-1}\right)}{(\mathrm{e}-1)(x\xi_0-\sigma_0)}, \\
h_Z(x) &= \frac{\mathrm{e}\left(1-\frac{x\xi_0}{\sigma_0}\right)^{\frac{1}{\xi_0}}\log\left(\frac{\mathrm{e}\left(\mathrm{e}^{-\left(1-\frac{x\xi_0}{\sigma_0}\right)^{\frac{1}{\xi_0}}}-\frac{1}{\mathrm{e}}\right)}{\mathrm{e}-1}\right)}{(x\xi_0-\sigma_0)\left[\mathrm{e}\left(\mathrm{e}^{\left(1-\frac{x\xi_0}{\sigma_0}\right)^{\frac{1}{\xi_0}}}-1\right)+\left(\mathrm{e}-\mathrm{e}^{\left(1-\frac{x\xi_0}{\sigma_0}\right)^{\frac{1}{\xi_0}}}\right)\log\left(\frac{\mathrm{e}\left(\mathrm{e}^{-\left(1-\frac{x\xi_0}{\sigma_0}\right)^{\frac{1}{\xi_0}}}-\frac{1}{\mathrm{e}}\right)}{\mathrm{e}-1}\right)\right]}.
\end{aligned}
\tag{8.8}
$$

From the hazard rate plot depicted in Figure 8.1, it is observed that the RART-TGEVD model incorporates a bathtub-shaped hazard rate. This highlight the increased flexibility introduced by the transformation. However, for practical applications, reliable parameter estimation is essential. Since the support of the model depends on the parameters, standard MLE method is not directly applicable. A closer examination reveals that inference fundamentally depends on the underlying GEVD, which forms the basis of both truncation and transformation. Consequently, challenges related to estimation accuracy, numerical stability, and theoretical validity can be traced back to the estimation of the GEVD parameters. Existing studies indicate that even classical inferential procedures for the GEVD face notable theoretical and computational difficulties, which are further exacerbated in the truncated and RART-TGEVD settings. This motivates a shift in focus toward developing robust estimation methods for the GEVD itself. Accordingly, a new estimation methodology is proposed and later examined in the context of the truncated model. Before introducing this approach, we review the existing literature on parameter estimation for the GEVD, highlighting the need for improved methods.

8.3 Review of literature on parameter estimation of GEVD

The parameter estimation of the model given in (8.1) has been studied by various authors. An initial attempt to find the MLE of GEVD can be seen in Prescott and Walden (1980), and it was later developed by Hosking (1985) and Smith (1985). The Fisher information matrix for MLE of GEVD was also derived in Prescott and Walden (1980). It was Smith (1985), who described the existence of MLE for the GEVD parameters in complete generality. Smith (1985) also showed that the regularity conditions for MLE holds only when the shape parameter ξ lies in the interval $\left(0, \frac{1}{2}\right)$. The asymptotic normality of MLE of the parameters of GEVD were established in Bücher and Segers (2017). Also, Martins and Stedinger (2000), using simulation studies showed that for small samples, MLE leads to absurd results. Stedinger et al. (1993) derived the method of moments (MOM) estimates for GEVD parameters. Hosking et al. (1985) gave a detailed note on how to calculate probability weighted moment (PWM) estimators of the parameters of GEVD. Similarly the l-moment (LM) estimates, which are equivalent to PWM estimates, were calculated by Hosking (1990). Moreover, in Hosking et al. (1985) it was shown that, for sample sizes from 15 to 100, the PWM or equivalent LM perform better in terms of bias and variance, than MLE. In Madsen et al. (1997), the MOM, PWM and MLE are compared for sample sizes 10 to 50 and for $-0.25 < \xi < 0.3$, and it was inferred that the MOM estimates perform better than the MLE and PWM estimates, in terms of root mean square error. Wong and Li (2006) derived the maximum product spacing (MPS) estimators for the parameters of GEVD in situations where the MLE breaks down. Moreover, they observed that the MPS estimates are more efficient than the MLE for the parameters of GEVD. Wong and Li (2006) also illustrated through simulation studies that for small samples, MPS technique provide more stable estimates than the MLE and PWM estimates for the parameters of GEVD, in terms of bias and MSE. Moreover, Bakar et al. (2022) compared the MPS

estimates of the parameters of GEVD with the corresponding LM estimates and it was observed that their efficiencies are relatively close. The above mentioned estimation techniques have certain flaws in them. One notable limitation is the absence of global MLE for the shape parameter of GEVD. Additionally, traditional methods such as MOM, PWM, LM, and MPS often yield absurd results, particularly when confronted with small sample sizes. Due to these drawbacks, researchers are trying to develop better procedures to estimate the parameters of GEVD.

This served as a motivation for us to find new estimation techniques for the parameters of GEVD which rectifies the above mentioned limitations. Van Zyl (2012) introduced one such technique called the regression method of estimation for the generalized Pareto distribution (GPD). Van Zyl (2012) showed through simulation studies that the parameter estimates of GPD derived using the regression method exists throughout the parameter space and that it works well for small samples. Pickands (1975) showed that for modeling extremes the GPD, is equivalent to the GEVD model whenever the maximum has a non-degenerate limit distribution $G(\cdot)$, as mentioned in equation (1.3). This connection is crucial for extreme value theory because it allows for modeling extremes using threshold exceedances (GPD) or block maxima (GEVD). Therefore, we examine the regression method for estimating the parameters of the GEVD.

8.4 Estimation techniques

In this section, we summarize the various estimators of the shape and scale parameters of GEVD model. For computational ease, we assume $\mu = 0$ without loss of generality. This includes MOM estimators, MLE, PWM estimators, LM estimators and the MPS estimators, that are available in the literature. Derivation of these estimators and other properties can be seen in Prescott and Walden (1980), Smith (1985), Hosking et al. (1985), Hosking (1990), Stedinger et al. (1993), Madsen et al. (1997), and Wong and Li (2006).

8.4.1 Method of moments

The MOM estimators of the two parameters of GEVD are obtained by equating the first two population raw moments to the corresponding sample raw moments. This leads to the following two equations.

$$\hat{\sigma}_{MOM} = \frac{\hat{\xi}_{MOM} \sum_{i=1}^{n} X_i}{1 - \Gamma(1 + \hat{\xi}_{MOM})}. \tag{8.9}$$

$$\sum_{i=1}^{n} X_i^2 = \frac{\big(\sum_{i=1}^{n} X_i\big)^2 \big(1 - 2\Gamma(1 + \hat{\xi}_{MOM}) + \Gamma(1 + 2\,\hat{\xi}_{MOM})\big)}{\big(1 - \Gamma(1 + \hat{\xi}_{MOM})\big)^2}. \tag{8.10}$$

For a given sample, solution of the above two equations yields the MOM estimators. Details are available in Stedinger et al. (1993) and Madsen et al. (1997).

8.4.2 Maximum likelihood

Even though the shape parameter ξ of GEVD takes values throughout the real line, the MLE of ξ exists only on the interval $(0, \frac{1}{2})$, since the regularity conditions for MLE does not hold outside the interval. That is, for the shape parameter of GEVD, only local MLE exists. Whereas in the case of the scale parameter σ, the MLE exists for the whole parameter space of σ. Let $(X_1, \ldots, X_n)$ be a random sample of size n from GEVD. Then the log likelihood function is

$$L(\sigma, \xi \mid X_1, \ldots X_n) = \sum_{i=1}^{n} \left[\log \sigma^{-1} + (\frac{1}{\xi} - 1) \log \big(1 - \xi\sigma^{-1}(x_i)\big) + \big(1 - \xi\sigma^{-1}(x_i)\big)^{\frac{1}{\xi}} \right].$$

Taking the first derivative of the above equation with respect to σ and ξ and equating to zero, two non-linear equations are obtained. They are

$$\sum_{i=1}^{n}\left[\frac{1}{\sigma}+\left(\frac{1}{\xi}-1\right)\frac{\xi x_i}{\sigma(\sigma-\xi x_i)}\frac{x_i}{\sigma^2}\left(1-\frac{\xi x_i}{\sigma}\right)^{(\frac{1}{\xi}-1)}\right]=0,$$

$$\sum_{i=1}^{n}\left(1-\frac{\xi x_i}{\sigma}\right)^{\frac{1}{\xi}}\left(\frac{x_i}{\sigma-\xi x_i}+\frac{\log(1-\frac{\xi x_i}{\sigma})}{\xi}\right)=0.$$

For a given data, the solution of these two equations yields the MLE of σ and ξ. One may refer Prescott and Walden (1980) and Smith (1985) for more details.

8.4.3 Probability weighted moments

The general form of PWM of a random variable X with distribution function $F(\cdot)$ is

$$M_{p,r,s}=E[X^p\{F(X)\}^r\{1-F(X)\}^s], \tag{8.11}$$

where p, r, s are real numbers. Let $x(u)$ be the quantile function of X defined by

$$x(u)=F^{-1}(x)=\inf\{x:F(x)\geq u\},\quad 0\leq u\leq 1.$$

If $x(u)$ is in a closed form, then the equation for probability weighted moments can be written as

$$M_{p,r,s}=\int_0^1\{x(F)\}^pF^r(1-F)^sdF. \tag{8.12}$$

The equation (8.12) is found to be easier to evaluate when compared to equation (8.11). Let $M_{0,r,1}=\beta_r$, $r=0,1,\ldots$. For the GEVD, $M_{0,r,1}=\beta_r$ can be evaluated as follows.

$$\beta_r=\frac{1}{r+1}\left[\frac{\sigma}{\xi}(1-(r+1)^{(-\xi)}\Gamma(1+\xi))\right]. \tag{8.13}$$

For $r=0$ and $r=1$, β_r is obtained as

$$\begin{aligned}\beta_0&=\frac{\sigma}{\xi}(1-\Gamma(1+\xi)),\\ \beta_1&=\frac{1}{2}\left[\frac{\sigma}{\xi}(1-2^{(-\xi)}\Gamma(1+\xi))\right].\end{aligned} \tag{8.14}$$

Let $(X_1, \ldots, X_n)$ be a random sample from GEVD, Landwehr et al. (1979) proposed an unbiased estimator of β_r, say b_r and is given as

$$b_r = \frac{1}{n}\sum_{j=1}^{n}\frac{(j-1)(j-2)\ldots(j-r)}{(n-1)(n-2)\ldots(n-r)}x_{(j)}, \tag{8.15}$$

where $x_{(1)}, \ldots, x_{(n)}$ are order statistics of the given sample. Equating β_0 to b_0 and β_1 to b_1, two new equations are obtained as

$$\frac{1}{n}\sum_{j=1}^{n}x_{(j)} = \frac{\sigma}{\xi}(1-\Gamma(1+\xi)),$$
$$\frac{1}{n}\sum_{j=1}^{n}\frac{j-1}{n-1}x_{(j)} = \frac{1}{2}\left[\frac{\sigma}{\xi}(1-2^{(-\xi)}\Gamma(1+\xi))\right].$$

For a given data, the solution of the above equations yields the PWM estimators of σ and ξ. More details can be viewed in Hosking et al. (1985).

8.4.4 L-Moments

L-Moments are expectations of certain linear combinations of ordered statistics, introduced by Hosking (1990). If mean of a distribution exists, then LM of all order exists. Let $(X_1, \ldots, X_n)$ be a random sample from a distribution, with CDF $F(x)$ and quantile function $x(u)$, and $x_{(1)}, \ldots, x_{(n)}$ be the corresponding order statistics. The r^{th} population LM, L_r is given as

$$L_r \equiv \frac{1}{r}\sum_{i=1}^{r-1}(-1)^i\binom{r-1}{i}E(x_{(r-i)}), \quad r = 1, 2, \ldots.$$

If the quantile function of X is available in closed form, the expression for population LM is

$$L_r = \int_0^1 x(F)P^*_{r-1}(F)dF, \quad r = 1, 2, \ldots,$$

where $P_r^*(F) = \sum_{i=0}^{r}(-1)^{r-i}\binom{r}{i}\binom{r+i}{i}F^i$. For a given sample $(X_1, \ldots, X_n)$ the sample LM, l_r is defined as

$$l_r = \binom{n}{r}^{-1}\sum_{1\le i_1\le i_2<\ldots<i_r\le n}\cdots\sum\frac{1}{r}\sum_{j=0}^{r-1}(-1)^j\binom{r-1}{j}x_{(i_{r-j})}, \quad r = 1, 2, \ldots, n,$$

where $X_{(i_{r-j})}$ is the $i_{(r-j)}{}^{th}$ order statistic of the sample $(X_1, \ldots, X_n)$. Parameter estimation using LM is done by equating the sample LM to the corresponding population LM. The first two population LM of GEVD are

$$L_1 = \frac{\sigma}{\xi}(1 - \Gamma(1+\xi)),$$
$$L_2 = \frac{\sigma}{\xi}\Gamma(1+\xi)(1-2^{-\xi}).$$

Equating the corresponding sample and population LM yields two non-linear equations. They are

$$\frac{1}{n}\sum_{i=1}^{n}x_{(i)} = \frac{\sigma}{\xi}(1 - \Gamma(1+\xi)),$$
$$\frac{1}{n}\binom{n}{2}^{-1}\sum_{i>j}\sum(x_{(i)} - x_{(j)}) = \frac{\sigma}{\xi}\Gamma(1+\xi)(1-2^{-\xi}).$$

The solution of these two equations gives the LM estimates of σ and ξ. One may refer Hosking (1990) for more details.

8.4.5 Method of maximum product spacing

Let $(X_1, \ldots, X_n)$ be a random sample from a distribution, with CDF $F(\cdot \mid \underline{\theta})$, where $\underline{\theta}$ is the vector of parameters. Let $x_{(1)}, \ldots, x_{(n)}$ be the corresponding order statistics. Define $Z_i(\underline{\theta})$ as

$$Z_i(\underline{\theta}) = F(x_{(i)} \mid \underline{\theta}) - F(x_{(i-1)} \mid \underline{\theta}), \quad i = 1, \ldots, n+1,$$

where $F(x_0 \mid \underline{\theta}) = 0$ and $F(x_{(n+1)} \mid \underline{\theta}) = 1$. Wong and Li (2006) derived the MPS estimators for the parameters of GEVD and GPD. For GEVD, $Z_i(\xi, \sigma)$ can be written as

$$Z_i(\xi, \sigma) = G(x_{(i)} \mid \xi, \sigma) - G(x_{(i-1)} \mid \xi, \sigma), \qquad i = 1, \ldots, n+1. \tag{8.16}$$

The MPS estimates of the parameters of GEVD are obtained by maximizing the geometric mean of the spacing given in (8.16), with respect to each parameter. The geometric mean, $P(\xi, \sigma)$ of this spacing can be written as

$$P(\xi, \sigma) = \left[\prod_{i=1}^{n+1} Z_i(\xi, \sigma)\right]^{\frac{1}{n+1}}. \tag{8.17}$$

Maximizing $P(\xi, \sigma)$ is equivalent to minimizing $\log P(\xi, \sigma) = R(\xi, \sigma)$, given by

$$R(\xi, \sigma) = \frac{1}{n+1} \sum_{i=1}^{n+1} \log Z_i(\xi, \sigma). \tag{8.18}$$

Hence, the MPS estimates can be obtained as the solutions of the non-linear equations

$$\frac{\partial R(\xi, \sigma)}{\partial \xi} = 0 \quad \text{and} \quad \frac{\partial R(\xi, \sigma)}{\partial \sigma} = 0. \tag{8.19}$$

A comparison between MPS estimators and the LM estimators of GEVD was carried out and the details can be seen in Bakar et al. (2022).

8.5 Regression method of estimation for GEVD

In this section a regression method of estimation for the parameters of GEVD is discussed. The procedure is analogous to the one proposed by Van Zyl (2012) to estimate the parameters of GPD. For computational ease, we assume $\mu = 0$. The method is not in general applicable to all models. However, if a linear regression equation can be obtained by inverting the CDF, then this method can be applied. Consider the CDF $G(\cdot)$ of GEVD given in (1.5). Now, by inverting

$G(\cdot)$ we get

$$\begin{aligned} \log G(x) &= -\left(1-\frac{\xi x}{\sigma}\right)^{\frac{1}{\xi}} \\ -1+(-\log G(x))^{\xi} &= -\frac{\xi x}{\sigma} \\ \frac{(-\log G(x))^{\xi}-1}{\xi} &= -\frac{x}{\sigma}, \end{aligned} \tag{8.20}$$

which can be written in the form of a regression equation as described below. Let $(X_1,\ldots,X_n)$ be a random sample of size n from GEVD and $\widehat{G}_n(\cdot)$ be the ECDF. Let $x_{(1)},\ldots,x_{(n)}$ be the ordered statistics corresponding to the given sample. Since the empirical distribution function $\widehat{G}_n(\cdot)$, is an estimate of the $G(\cdot)$, by substituting $\widehat{G}_n(\cdot)$ in equation (8.20), we obtain

$$\frac{(-\log \widehat{G}_n(x))^{\xi}-1}{\xi} = -\frac{x}{\sigma}+\epsilon_r. \tag{8.21}$$

For the given sample $x_{(1)},\ldots,x_{(n)}$, we can write (8.21) as

$$G_{\xi}(x_{(r)}) = -\frac{x_{(r)}}{\sigma}+\epsilon_r, \quad r=1,2,\ldots,n, \tag{8.22}$$

where $G_{\xi}(x_{(r)}) = \frac{(-\log \widehat{G}_n(x))^{\xi}-1}{\xi}$, and ϵ_r is the error term, resulting from substituting $G(\cdot)$ with its estimate $\widehat{G}_n(\cdot)$. Note that, (8.22) is in the form of a regression equation which can be written in vector form as follows:

$$\boldsymbol{G}_{\xi} = \boldsymbol{X}\beta+\boldsymbol{\epsilon}, \tag{8.23}$$

where $\boldsymbol{G}_{\xi} = (G_{\xi}(x_{(1)}),\ldots,G_{\xi}(x_{(n)}))$, is an $n\times 1$ vector, $\boldsymbol{X} = (x_{(1)},\ldots,x_{(n)})$, is an $n\times 1$ vector, $\beta = -\frac{1}{\sigma}$ and $\boldsymbol{\epsilon} = (\epsilon_1,\ldots,\epsilon_n)$ is an $n\times 1$ vector. Therefor, it is enough to estimate the parameters β and ξ of the regression equation (8.22). For this, we follow the Box-Cox procedure discussed in Zellner (1996) where a Laplace assumption profile likelihood is constructed for a series of ξ's. Then, ξ is estimated as the value which maximizes the profile likelihood and β is estimated using iterative weighted least squares technique. The Box-Cox

variance stabilizing transformation suggested by Box and Cox (1964), is define as follows.

Definition 8.1. (Box and Cox (1964)) Let $y = x\beta + \epsilon$ be a simple linear regression model with y, the dependent variable, x, the independent variable, β the regression coefficient and ϵ, the error term. Then a parametric transformation for the dependent variable $y > 0$, is given as

$$y^{(\lambda)} = \begin{cases} \frac{y^{\lambda}-1}{\lambda}, & \lambda \neq 0 \\ \log y, & \lambda = 0. \end{cases} \tag{8.24}$$

Box and Cox (1964) introduced this transformation as a solution for a linear model which fails to satisfy the regularity conditions of regression model such as, constancy of the error variance, normality and independence of observations. Since $-\log \widehat{G}_n(x) > 0$, $G_\xi(x_{(r)})$ can be written as

$$G_\xi(x_{(r)}) = \begin{cases} \frac{(-\log \widehat{G}_n(x))^{\xi}-1}{\xi}, & \xi \neq 0 \\ \log(-\log \widehat{G}_n(x)), & \xi = 0. \end{cases} \tag{8.25}$$

This shows that the left hand side of equation (8.22) is in the form of Box-Cox transformation. We now estimate the shape parameter ξ using profile likelihood method discussed in Zellner (1996). The profile likelihood is defined as follows:

Definition 8.2. (Barandoff (1983)) Let $F(x, \Theta^*)$ be a distribution function with Θ^*, the parametric space. Let $\Theta^* = (\theta, \eta)$ be a partition of the parametric space, where θ is the parameter of interest and η is a higher dimensional nuisance parameter. Let $(X_1, X_2, \ldots, X_n)$ be a random sample from $F(x, \Theta^*)$, then $L(\theta, \eta \mid X_1, X_2, \ldots, X_n)$ is the complete likelihood. Then the profile likelihood is

$$pL(\theta) = \sup_{\eta} L(\theta, \eta \mid X_1, X_2, \ldots, X_n). \tag{8.26}$$

We note that the MLE $\hat{\theta}$ for θ also maximizes the profile likelihood $pL(\theta)$. More details on profile likelihood can be seen in Murphy and Van der Vaart (2000).

We now estimate the shape parameter ξ using profile likelihood method discussed in Zellner (1996). For this, we construct a profile likelihood for G_ξ as a function of ξ and β and obtain the estimate of ξ by assuming β as the nuisance parameter. As the left hand side of equation (8.21) is a function involving ξ, a Jacobian needs to be evaluated in order to obtain the profile likelihood. The Jacobian $J(\xi)$ is obtained as

$$J(\xi) = \prod_{r=1}^{n} \frac{\big(-\log G_\xi(x_{(r)})\big)^{(\xi-1)}}{G_\xi(x_{(r)}}. \tag{8.27}$$

The Laplace probability density with mean zero is given by

$$f(x) = \frac{1}{2\,\phi} \exp(-\frac{\mid u \mid}{\phi}), \quad -\infty < x < \infty,\, \phi > 0. \tag{8.28}$$

The variance of the above Laplace distribution is $2\,\phi$. For a given sample $(X_1, X_2, \ldots, X_n)$ of size n, the MLE of ϕ is the mean absolute deviation about the median of, ,

$$\hat{\phi} = \frac{1}{n} \sum_{i=1}^{n} \left| \mathbf{y} - \mathbf{X}\hat{\beta} \right|. \tag{8.29}$$

Following the procedure of Zellner (1996), the Laplace profile likelihood for a given ξ denoted by $pL(\xi)$, is obtained as

$$pL(\xi) = C + \sum_{r=1}^{n} \log \left| \frac{\big(-\log G_\xi(x_{(r)})\big)^{(\xi-1)}}{G_\xi(x_{(r)}} \right| - n \log\left(\hat{\phi}(\xi)\right), \tag{8.30}$$

where C represents the proportionality constant. From (8.30), we derive the estimate $\hat{\xi}$ for ξ. Using $\hat{\xi}$, we evaluate the estimate $\hat{\beta}$ for β using the iterative weighted least squares technique. The iteration formula is given by

$$\hat{\beta}^{(j+1)} = (\mathbf{X}'W^{(j)}\mathbf{X})^{-1}\mathbf{X}'W^{(j)}G_\xi(x_{(r)}), \tag{8.31}$$

where $W^{(j)}$ is the diagonal matrix of weights with entries, $w_r^{(j)} =\mid G_\xi(x_{(r)}) - x_{(r)}\beta^{(j)} \mid^{-1}$, $r = 1, 2, \ldots, n$ and $j = 0, 1, \ldots$ denotes the number of iterations. For estimating the parameters β and ξ, we follow the method suggested by Zellner

(1996). That is, we apply iterative weighted least squares estimate $\hat{\beta}$ given in (8.31), to the profile likelihood equation (8.30). Thus, the profile likelihood equation becomes a function solely depending on ξ. From this, the estimate $\hat{\xi}$ is obtained as the value of ξ which maximizes the profile likelihood. Now, to find $\hat{\beta}$, an initial value $\beta^{(0)}$ of β, is arbitrarily chosen and substituted in (8.31) to evaluate $\beta^{(1)}$. Once $\beta^{(1)}$ is obtained, $\beta^{(0)}$ is replaced by $\beta^{(1)}$ to obtain $\beta^{(2)}$. This process is continued out until $\mid \beta^{(j+1)} - \beta^{(j)} \mid < \delta$, where δ is a small quantity.

We note that the closed form expression for the above estimates do not exist. So, further evaluation of the estimates are carried out using numerical techniques. In the next section, we consider a left truncated GEVD and its parameter estimation using the above method.

8.5.1 Regression method in truncated GEVD

Following a similar approach as in the case of the GEVD, we derive regression-based estimators for the parameters of the TGEVD model given in (8.3). Let $(X_1, \ldots, X_n)$ be a random sample from the truncated GEVD G_0 with $\mu_0 = 0$, and let $x_{(1)}, \ldots, x_{(n)}$ denote the corresponding order statistics. The empirical distribution function $G_{n_0}(x)$ is then substituted into (8.2), which yields

$$G_{\xi_0}(x_{(r)}) = -\frac{x_{(r)}}{\sigma_0} + \epsilon_{0_r}, \tag{8.32}$$

where

$$G_{\xi_0}(x) = \frac{\left(-\log\left(G_{n_0}(x)(1 - \mathrm{e}^{-1}) + \mathrm{e}^{-1}\right)\right)^{\xi_0} - 1}{\xi_0}, \tag{8.33}$$

and the error term ϵ_{0_r} is assumed to follow a normal distribution with mean 0 and variance ϕ_{0_r}, for $r = 1, 2, \ldots, n$. The resulting equation (8.32) takes the form of a simple linear regression model, with the left-hand side expressed in a variance-stabilizing Box-Cox form. Accordingly, the same procedure is employed to obtain the estimators of σ_0 and ξ_0. The final expressions for the estimators of

β_0 and ξ_0 are given below.

$$\hat{\beta_0}^{(j+1)} = (\mathbf{X}'W_0^{(j)}\mathbf{X})^{-1}\mathbf{X}'W_0^{(j)}G_{\xi_0}, \quad j = 0, 1, \ldots, \tag{8.34}$$

$$pL_0(\xi) = \mathrm{C} + (\xi_0 - 1)\sum_{r=1}^{n} \log\left[\frac{\Big(-\log G_{\xi_0}(x_{(r)})\Big)^{(\xi_0-1)}}{G_{\xi_0}(x_{(r)})}\right] - \frac{n}{2}\log(\hat{\phi}_0(\xi_0)), \tag{8.35}$$

where $pL_0(\cdot)$ is the profile likelihood of regression equation corresponding to the truncated GEVD, $W_0^{(j)}$ is the diagonal matrix of weights with entries $w_{r_0}^{(j)} = |G_{\xi_0}(x_{(r)}) - x_{(r)}\beta_0^{(j)}|^{-1}$, $r = 1, 2, \ldots, n$ and $\hat{\phi}_0(\xi_0)$ is the estimate of ϕ_0.

Moreover, for small sample sizes, it is noted that when $\xi = 0.1$ and 0.2, the MOM performs better than MLE, PWM, and L-moments, as reported in Stedinger et al. (1993). A brief discussion on the assumption of a general distribution for the error term is provided in the next subsection. For both GEVD and TGEVD, the regression-based estimation requires iterative procedures, which makes the direct construction of confidence intervals difficult. Therefore, bootstrap methods are employed to obtain confidence intervals for the parameter estimates.

8.6 Bootstrap confidence interval

The current section deals with the evaluation of bootstrap confidence intervals for the parameter estimates of GEVD and TGEVD using regression method. Bootstrap is a resampling technique introduced by Efron (1979), wherein the observed sample is considered as a finite population and random samples are generated with replacement from the observed sample. Here, the intervals are constructed using the bootstrap-p method, were p stands for percentile. Algorithm for evaluating the bootstrap confidence intervals for the parameters of GEVD is given below. Let $(X_1, \ldots, X_n)$ be a random sample from GEVD.

1. Generate a bootstrap sample $\{x_1^*, x_2^*, \ldots, x_n^*\}$ of size n from $(X_1, \ldots, X_n)$.

Using this sample, the bootstrap estimates $\hat{\sigma}^*$ and $\hat{\xi}^*$ are evaluated using regression method discussed in Section 8.5.

2. Step 1 is repeated B times.

3. Let $\widehat{F}_1(x)$ and $\widehat{F}_2(x)$ be the empirical distribution functions of bootstrap replicates for σ^* and ξ^* respectively. Define $\sigma^{*p}(x) = \widehat{F}_1^{-1}(x)$ and $\xi^{*p}(x) = \widehat{F}_2^{-1}(x)$. Then the approximate $100(1-\alpha)\%$ bootstrap-p asymptotic confidence intervals for $\hat{\sigma}^*$ and $\hat{\xi}^*$ are

$$\Big(\sigma^{*p}(\alpha/2)\ ,\ \sigma^{*p}(1-\alpha/2)\Big) \qquad \text{and} \qquad \Big(\xi^{*p}(\alpha/2)\ ,\ \xi^{*p}(1-\alpha/2)\Big),$$

respectively.

Similarly, the bootstrap confidence intervals for the parameter estimates of TGEVD can be obtained as

$$\Big(\sigma_0^{*p}(\alpha/2)\ ,\ \sigma_0^{*p}(1-\alpha/2)\Big) \qquad \text{and} \qquad \Big(\xi_0^{*p}(\alpha/2)\ ,\ \xi_0^{*p}(1-\alpha/2)\Big).$$

More details on bootstrap are available in Efron (1981) and Efron (1987), and Rizzo (2019).

8.7 Simulation study

In this section, a Monte Carlo simulation study is conducted to assess the efficiency of the proposed regression-based method in comparison with existing estimators for the parameters of the GEVD and TGEVD. The performance is evaluated in terms of mean squared error (MSE) and absolute bias. Five sample sizes, $n = 10, 20, 50, 100$, and 500, are considered. For the GEVD, the parameter settings $(\xi = 0.1, \sigma = 2)$, $(\xi = 0.2, \sigma = 2)$, $(\xi = -2, \sigma = 1)$, and $(\xi = 2, \sigma = 1)$ are used, while for the TGEVD, $(\xi = 0.1, \sigma = 2)$, $(\xi = 0.2, \sigma = 2)$, $(\xi = 1, \sigma = 1)$, and $(\xi = 2, \sigma = 1)$ are considered. All computations are performed in R based on 1000 simulation replications.

Table 8.1: MSEs of the estimates of GEVD

Sample Size	Scale Parameter σ						Shape Parameter ξ					
	Regression	MOM	MLE	PWM	L-Moment	MPS	Regression	MOM	MLE	PWM	L-Moment	MPS
$\xi = 0.1$, $\sigma = 2$												
10	0.0986	0.1368	0.4063	0.5141	0.4351	0.7325	0.0583	0.3496	0.3547	0.6213	0.4956	0.2260
20	0.0242	0.0739	0.2152	0.1616	0.1623	0.2468	0.0735	0.1317	0.2015	0.2344	0.2538	0.0506
50	0.0096	0.0455	0.1305	0.0934	0.1018	0.0661	0.0094	0.0507	0.1166	0.1228	0.1220	0.0109
100	0.0039	0.0340	0.0704	0.0619	0.0685	0.0284	0.0041	0.0356	0.0707	0.0752	0.0573	0.0049
500	0.0006	0.0178	0.0338	0.0086	0.0089	0.0053	0.0009	0.0142	0.0285	0.0110	0.0113	0.0007
$\xi = 0.2$, $\sigma = 2$												
10	0.0707	0.1261	0.3427	0.4539	0.2236	0.7393	0.0299	0.2926	0.3789	0.6000	0.4693	0.2288
20	0.0219	0.1096	0.2272	0.1591	0.1598	0.2452	0.0303	0.1271	0.2103	0.2531	0.1721	0.0536
50	0.0084	0.0411	0.1206	0.0961	0.0882	0.0531	0.0085	0.0625	0.1078	0.1335	0.0636	0.0105
100	0.0036	0.0335	0.0841	0.0462	0.0563	0.0324	0.0072	0.0402	0.0749	0.0627	0.0309	0.0039
500	0.0005	0.0168	0.0339	0.0072	0.0072	0.0051	0.0009	0.0156	0.0272	0.0106	0.0074	0.0006
$\xi = -2$, $\sigma = 1$												
10	0.1718	0.4200	0.3937	0.2360	0.1735	0.1905	0.0688	0.4215		0.6280	0.4985	0.2878
20	0.0596	0.1828	0.1930	0.1697	0.0857	0.0689	0.0651	0.2775		0.4990	0.2193	0.0888
50	0.0190	0.0429	0.1164	0.0253	0.0260	0.0200	0.0449	0.1725		0.1339	0.1162	0.0229
100	0.0075	0.0172	0.0795	0.0103	0.0107	0.0086	0.0231	0.0805		0.0576	0.0570	0.0094
500	0.0009	0.0018	0.0341	0.0016	0.0018	0.0012	0.0056	0.0115		0.0102	0.0112	0.0012
$\xi = 2$ and $\sigma = 1$												
10	0.2114	0.4560	0.3581	0.3144	0.2521	0.1656	0.3498	0.3733		0.7933	0.7388	0.7046
20	0.1755	0.2647	0.1875	0.2307	0.2210	0.0528	0.2678	0.3621		0.6758	0.5710	0.2164
50	0.0895	0.2182	0.1171	0.0342	0.0316	0.0153	0.1709	0.1557		0.2156	0.2142	0.0614
100	0.0206	0.2289	0.0783	0.0128	0.0124	0.0070	0.0928	0.0918		0.0992	0.0950	0.0280
500	0.0051	0.1397	0.0341	0.0022	0.0022	0.0013	0.0255	0.0509		0.0190	0.0184	0.0052

Table 8.2: Absolute biases of the estimates of GEVD

Sample Size	Scale Parameter σ						Shape Parameter ξ					
	Regression	MOM	MLE	PWM	L-Moment	MPS	Regression	MOM	MLE	PWM	L-Moment	MPS
$\xi = 0.1$, $\sigma = 2$												
10	0.2374	0.2651	0.6173	1.1570	0.7136	0.7325	0.2082	0.3695	0.5847	1.2447	0.9174	0.2260
20	0.1213	0.2191	0.4571	0.3252	0.3227	0.2468	0.2489	0.2656	0.4448	0.4032	0.4086	0.0506
50	0.0778	0.1765	0.3471	0.2302	0.2418	0.0661	0.0758	0.1875	0.3362	0.2773	0.2745	0.0109
100	0.0506	0.1594	0.2654	0.1830	0.1747	0.0284	0.0506	0.1622	0.2658	0.2084	0.1997	0.0049
500	0.0199	0.1137	0.1838	0.0718	0.0425	0.0053	0.0254	0.1029	0.1687	0.0809	0.0825	0.0007
$\xi = 0.2$ and $\sigma = 2$												
10	0.1805	0.2555	0.5710	0.9751	0.3875	0.7393	0.1530	0.3659	0.6052	1.1800	0.5027	0.2288
20	0.1193	0.2077	0.4647	0.3211	0.3181	0.2452	0.1334	0.2745	0.4484	0.4128	0.3163	0.0536
50	0.0740	0.1754	0.3456	0.2314	0.2222	0.0531	0.0736	0.2152	0.3272	0.2845	0.1954	0.0105
100	0.0483	0.1573	0.2877	0.1587	0.1718	0.0324	0.0666	0.1724	0.2714	0.1919	0.1350	0.0039
500	0.0177	0.1042	0.1841	0.0665	0.0651	0.0051	0.0248	0.1024	0.1649	0.0819	0.0672	0.0006
ξ = -2 and $\sigma = 1$												
10	0.3132	0.6604	0.5977	0.3846	0.3175	0.1905	0.2308	0.6890		0.8344	0.5021	0.2878
20	0.1898	0.4152	0.4329	0.2271	0.2115	0.0689	0.2179	0.5068		0.6262	0.3738	0.0888
50	0.1082	0.1544	0.3400	0.1183	0.1190	0.0200	0.1839	0.3073		0.2806	0.2696	0.0229
100	0.0665	0.0952	0.2818	0.0772	0.0787	0.0086	0.1205	0.2080		0.1885	0.1876	0.0094
500	0.0238	0.0338	0.1846	0.0316	0.0339	0.0012	0.0610	0.0866		0.0810	0.0838	0.0012
$\xi = 2$ and $\sigma = 1$												
10	0.3831	0.4797	0.5809	0.4085	0.4072	0.3124	0.5093	0.6220		1.0979	0.8745	0.6510
20	0.2411	0.3957	0.4641	0.2679	0.2461	0.177	0.4250	0.4626		0.8445	0.5895	0.3596
50	0.2329	0.3530	0.3407	0.1403	0.1366	0.0919	0.3361	0.3283		0.3458	0.3548	0.1845
100	0.1591	0.3415	0.2794	0.0900	0.0878	0.0623	0.2465	0.2669		0.2435	0.2402	0.1248
500	0.0551	0.2789	0.1847	0.0380	0.0377	0.0301	0.1271	0.2055		0.1093	0.1091	0.0603

Table 8.3: MSE and absolute biases of the estimates of TGEVD using regression method

Sample Size	Shape Parameter		Scale Parameter		Sample Size	Shape Parameter		Scale Parameter	
	MSE	Absolute bias	MSE	Absolute bias		MSE	Absolute bias	MSE	Absolute bias
$\xi_0 = 0.1$ and $\sigma_0 = 2$					$\xi_0 = 1$ and $\sigma_0 = 1$				
10	0.4215	0.6605	0.1790	0.2836	10	0.2943	0.5200	0.0150	0.1012
20	0.3343	0.4930	0.0992	0.2444	20	0.2636	0.4461	0.0055	0.0588
50	0.2564	0.4138	0.0252	0.1160	50	0.2499	0.4117	0.0012	0.0275
100	0.1943	0.3834	0.0090	0.0707	100	0.2048	0.3341	0.0006	0.0199
500	0.1852	0.3041	0.0015	0.0295	500	0.1168	0.2909	0.0002	0.0120
$\xi_0 = 0.2$ and $\sigma_0 = 2$					$\xi_0 = 2$ and $\sigma_0 = 1$				
	MSE	bias	MSE	bias		MSE	bias	MSE	bias
10	0.2674	0.4366	0.3723	0.5680	10	0.5771	0.7083	0.0931	0.2441
20	0.2012	0.3824	0.1073	0.2782	20	0.2562	0.4373	0.0223	0.1256
50	0.1747	0.3252	0.0714	0.2036	50	0.2045	0.3936	0.0113	0.0887
100	0.1139	0.2823	0.0205	0.1144	100	0.1772	0.3585	0.0067	0.0645
500	0.0290	0.1273	0.0043	0.0512	500	0.0883	0.2541	0.0050	0.0199

The MSE and absolute bias of estimates of GEVD evaluated using all the above mentioned techniques are tabulated in Table 8.1 and Table 8.2 respectively. Unlike MLE, the estimates obtained using regression method exists throughout the parameter space of GEVD. Also as sample size increases, the MSE and absolute bias decreases which indicates the efficiency of the regression method. We can infer that, for small samples the MSE and absolute bias of estimates evaluated using regression method are smaller when compared to that of other estimates, justifying that for small samples the regression method outperforms the other techniques. The PWM estimates and LM estimates are found to be least efficient for small samples. In the case of large samples, the estimates evaluated using regression method have smaller MSE and absolute bias than the other estimates.

The performance of various estimation methods for the TGEVD is also examined, yielding conclusions similar to those for the GEVD. Table 8.3 presents the MSE and absolute bias of the regression-based estimates for parameters of TGEVD. It is observed that both measures decrease as the sample size increases. Furthermore, the regression-based estimates exhibit better performance for the scale parameter than for the shape parameter.

8.8 Real data analysis

This section presents a real data application to illustrate the computational procedures discussed in this study. We analyze the international crude oil prices during the Ukrainian war, a period characterized by substantial economic disruption and pronounced price volatility. Owing to the extreme nature of these fluctuations, the daily maximum crude oil prices (in US dollars) are modeled using the GEVD. The dataset consists of 52 observations corresponding to trading days from January 1, 2022, to March 18, 2022 (excluding weekends), obtained from `https://in.investing.com/commodities/crude-oil-historical-data`. The summary statistics of the considered data is presented in the following Table 8.4. To assess the adequacy of the GEVD for the

Table 8.4: Descriptive statistics for the considered data.

Minimum	First Quartile	Median	Third	Maximum	Mean
76.46	86.46	92.17	101.04	129.79	95.14

given dataset, the KS goodness of fit test is performed. The resulting p-value and KS statistic are 0.9211 and 0.0736, respectively. In addition, Figure 8.2 displays the empirical and fitted CDFs along with the corresponding P-P plot. These results indicate that the GEVD provides an adequate fit to the data. The model parameters are estimated using the proposed regression method, and bootstrap confidence intervals are constructed for each parameter. For comparison, MLE are also obtained. The corresponding p-value and KS statistic for the MLE-based fit are 0.9086 and 0.0752, respectively. The slightly improved goodness of fit measures suggest that the proposed regression method yields a better fit for the dataset. A summary of these results is provided in Table 8.5. The TGEVD model is also fitted to the same dataset, yielding the parameter estimates $\hat{\xi} = -0.0649$, $\hat{\sigma} = 9.1977$, and $\hat{\mu} = 88.5821$. The corresponding p-value and KS statistic are 0.9726 and 0.0644, respectively. A comparison of the goodness of fit measures for the GEVD and TGEVD models indicates that the TGEVD provides a better fit to the crude oil price data. Figure 8.3 displays the empirical and fitted CDFs

Table 8.5: Estimates and confidence intervals using regression method and the MLE for the crude oil data for GEVD.

Regression method			MLE	
Parameters	Estimates	Bootstrap intervals	Parameters	Estimates
$\hat{\xi}$	-0.3002	$(-0.5210, -0.08016)$	$\hat{\xi}$	-0.1436
$\hat{\sigma}$	7.9853	$(5.8575, 9.0531)$	$\hat{\sigma}$	9.3690
$\hat{\mu}$	88.2761	$(86.3975, 89.7732)$	$\hat{\mu}$	88.6277

along with the corresponding P-P plot for the TGEVD model.

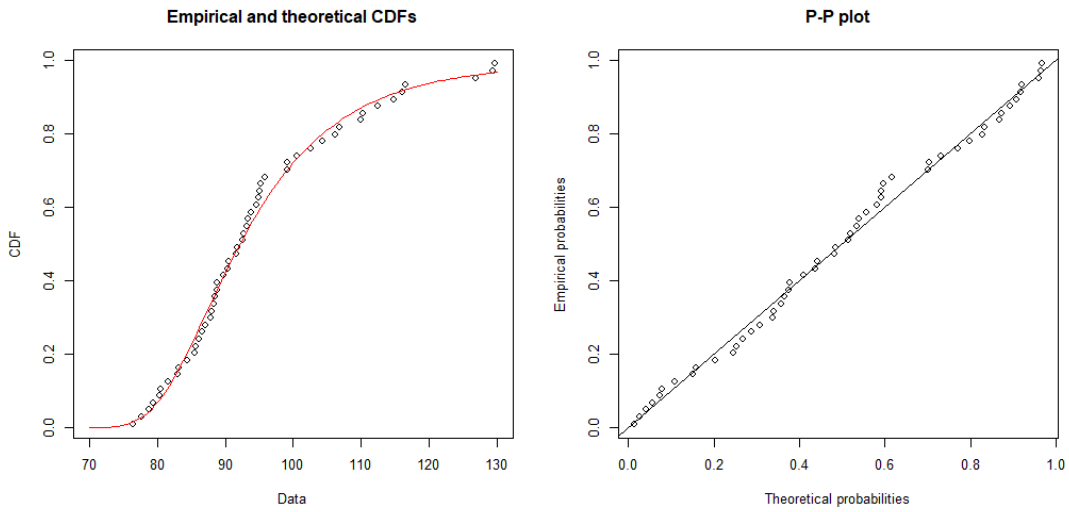

Figure 8.2: Goodness of fit plots for GEVD using regression estimates.

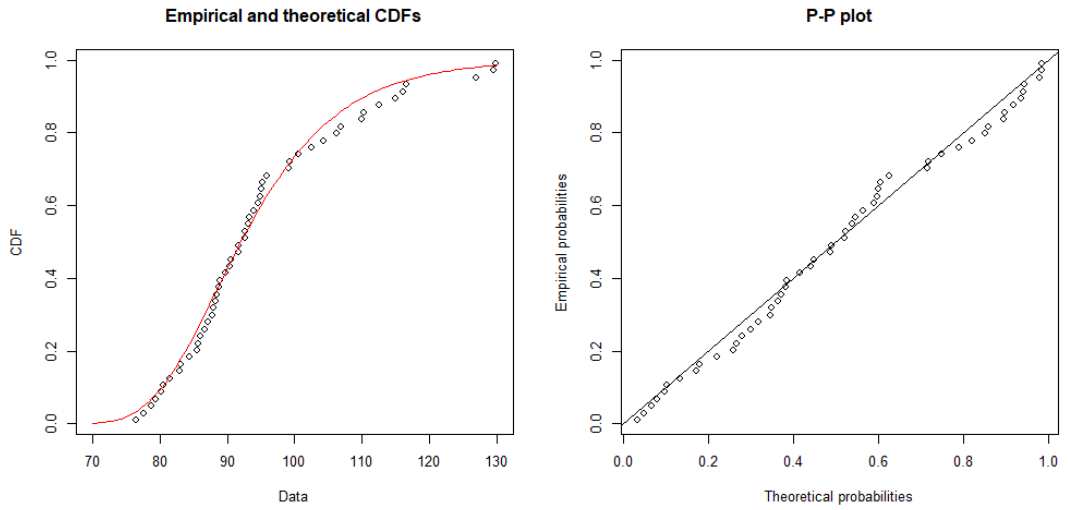

Figure 8.3: Goodness of fit plots for TGEVD using regression estimates.

8.9 Summary of the chapter

This chapter investigates the truncated GEVD and its extension through the RART, with particular emphasis on reliability, aging behavior, and parameter estimation. The structural and aging properties of the truncated model and its RART form are analyzed. A regression-based estimation procedure for GEVD is developed and its performance is assessed through a comprehensive simulation study. The results demonstrate that the proposed method yields reliable and efficient estimates, particularly in small samples, and performs competitively with existing techniques. Bootstrap confidence intervals further support the stability of the estimates. The practical applicability of the proposed approach is illustrated through a real data analysis, where the model provides an adequate fit. Also, the proposed method provided better estimates for the real data when compared to the MLE.

Chapter 9

Conclusions and recommendations for future research

This thesis presents a comprehensive study on the reliability aspects of the relevation and reversed relevation transforms along with their extensions, generalizations, and associated statistical properties. The central objective has been to explore various aging properties, establish stochastic ordering results, investigate information-theoretic relationships, and construct novel lifetime models using these transforms. In addition, emphasis has been placed on exploring the applicability of extreme value distributions through theoretical development, simulation experiments, and real data applications. The key findings and contributions of each chapter are summarized below.

9.1 Summary of the thesis

The introductory chapter outlined the essential concepts in reliability theory, lifetime distributions, stochastic ordering, and information measures, together with the motivation and objectives of the study. Chapter 2 examined the relevation transform within the modified proportional hazards framework, establishing key aging and stochastic ordering properties and introducing a flexible extension of the exponential distribution. Chapter 3 developed the

auto-relevation framework in a multi-phase setting, investigating its reliability aspects and its connections with stochastic processes, and deriving interesting characterization results. Chapter 4 presented the auto-relevated log-logistic distribution and studied its reliability features, including non-monotonic hazard behavior and tail properties, along with applications to risk measures and real datasets.

Chapter 5 analyzed the reversed relevation transform under the proportional reversed hazards framework, deriving results related to information measures, aging behavior, and stochastic ordering, and proposing a new extension of the Fréchet distribution. Chapter 6 investigated the reversed auto-relevation transform, establishing characterization results and examining the preservation of aging properties, supported by real data analysis. We further derived associated stochastic ordering results and information measure-based properties, highlighting the flexibility of the proposed model.

Chapter 7 considered the multi-phase reversed auto-relevation transform, exploring its reliability characteristics and deriving several characterization results. Finally, Chapter 8 proposed and analyzed a RART-based generalized extreme value distribution, and further focused on parameter estimation for the generalized extreme value distribution and its truncated variant using a regression-based methodology, supported by simulation studies and real data applications.

9.2 Future scope and recommendations

The present work has opened multiple avenues for further research in the domains of reliability theory, stochastic modeling, and lifetime data analysis. Based on the findings and developments presented throughout this thesis, several possible future directions are outlined below:

1. The newly developed lifetime models and generalizations can be further explored under different censoring schemes, such as hybrid censoring,

interval censoring, and progressive hybrid censoring.

2. Bayesian estimation techniques for the proposed models, along with the development of priors suitable for extreme value structures, would serve as an important extension. MCMC-based inference, prior sensitivity analysis, and posterior predictive checks could be studied.

3. Multivariate extensions of the relevation and reversed relevation transforms may be considered. Developing dependence structures through copula-based approaches or shared frailty models would broaden practical applicability.

4. The models introduced in this work can be extended to regression frameworks, including accelerated failure time and proportional hazards/reversed hazards models for co-variate dependent lifetime data.

5. Exploration of the proposed models in machine learning oriented survival frameworks, such as deep survival networks, software reliability models, reliability-based neural models, or non-parametric predictive techniques, may offer innovative applications.

6. Real world applications can be expanded to broader fields such as biomedical survival studies, actuarial risk modeling, climate extremes, and financial tail-risk evaluation, validating flexibility across diverse domains.

7. Goodness of fit tests and model discrimination criteria tailored for models constructed via relevation-based transformations can be developed to improve model selection accuracy.

8. Generalizing the multi-phase auto-relevation and reversed auto-relevation transforms to continuous-time stochastic processes and studying their long-term behavior may yield valuable theoretical insights.

9. A natural extension is to generalize the relevation and reversed relevation transforms by incorporating dependence between the random variables X and Y, thereby allowing for more flexible and realistic reliability models.

The above recommendations highlight potential directions towards expanding the theoretical depth and practical implementation of relevation-based reliability models. Continued research along these lines is expected to contribute substantially to lifetime modeling, stochastic processes, advanced survival data inference and extreme value applications.

Published Papers

1. Anand, R., & Chandran, C. (2025). A regression method of estimation for generalized extreme value distribution. *Kybernetika*, 61(4), 467–480. (SCI and Scopus indexed)

2. Dileepkumar, M., Anand, R., & Sankaran, P. G. (2025). Reliability properties and applications of proportional reversed hazards in reversed relevation transform. *Statistics in Transition New Series*, 26(1), 183–203. (SCI and Scopus indexed)

3. Anand, R., Dileepkumar, M., & Greeshma, Chandran. (2026). Reliability Properties and Applications of Auto-Relevated Log-Logistic Model. *Journal of Statistical Theory and Practice*, 20(3), 92. (SCI and Scopus indexed)

4. N, Unnikrishnan Nair., Dileepkumar, M., & Anand, R. Auto-relevation model and its implications to minimal repair. (Accepted for publication in *Journal of Mathematical Methods for Statistics*, Pleiades Publishing). (SCI and Scopus indexed)

Communicated Papers

5. Dileepkumar, M., Anand, R., & N, Unnikrishnan Nair. Reliability aspects of reversed auto-relevation transform and its applications. (Revision submitted to *Metrika*, Springer).

6. Anand, R., & Dileepkumar, M. Reliability aspects of modified proportional hazards relevation transform. (Under revision in *Communications in Statistics - Simulation and Computation*, Springer).

7. Anand, R., Dileepkumar, M., & N, Unnikrishnan Nair. Reliability aspects of multi-phase reversed auto-relevation transform. (Under revision in *International Journal of Reliability, Quality & Safety Engineering*).

Conference Proceedings

8. Anand, R., & Dileepkumar, M. Stochastic ordering and characterization results based on the reversed auto-relevation transform. (To appear in*Proceedings of International Conference on Recent Advances in Statistical Methods and Applications).*

Presentations

- The 41^{st} Annual Convention of (ISPS), "International Virtual Conference on Statistics And Data Science: Theory And Practice For Progress And Prosperity, (ICSDS) - 2021, organized jointly by the ISPS and the Department of Statistics, University College of Science, Osmania University, Hyderabad, during 11 - 13 March 2021.

- The 42^{nd} annual convention of ISPS,"International Conference on Statistics, Probability Data Science and Related Areas, (ICSPDS) - 2023", organised by ISPS and Department of Statistics CUSAT, during 3-5 January 2023.

- The "International Conference on Statistical Sciences & Stochastic Modeling (ICSSSM) - 2023" and Pre-conference workshop on "Computational techniques for Stochastic Modeling", organized by the Department of Statistics, University of Calicut during 14-17 February 2023.

- The 44^{th} annual convention of ISPS, "International Conference on Innovative Trends in Statistics, Optimization and Data Science (IC-ITSODS) - 2024", organised by ISPS and Department of Statistics Kurukshethra University, Haryana, during 21-23 December 2024.

- Annual Conference of International Indian Statistical Association (IISA 2024 Conference), held at Cochin University of Science and Technology, jointly organized by Department of Statistics, Cochin University of Science and Technology and International Indian Statistical Association, during 27 - 31 December 2024.

- The "International Seminar on Applied Statistics & Data Analytics (ISASDA) - 2025", organized by Department of Statistics, University of Calicut, during 04-06 March 2025.

- The 45^{th} annual convention of ISPS, "International Conference on Recent Advances and Innovative Statistics with Enhancing Data Science (IC-RAISE DS) - 2025" organised by ISPS and Department of Mathematics, VIT-AP University, Vijayawada, during 22-24 November 2025.

Bibliography

[1] Abdul Sathar, E. and N. Dhanya, R (2021). On dynamic survival extropy. *Communications in Statistics - Theory and Methods 50*(6), 1295–1313.

[2] Adamidis, K. and S. Loukas (1998). A lifetime distribution with decreasing failure rate. *Statistics & Probability Letters 39*(1), 35–42.

[3] Ahmad, M. I., C. D. Sinclair, and A. Werritty (1988). Log-logistic flood frequency analysis. *Journal of Hydrology 98*(3-4), 205–224.

[4] Alfaer, M., C. Chesneau, and F. Jamal (2021). The extended log-logistic distribution: Inference and actuarial applications. *Mathematics 9*(12), 1386.

[5] Alizadeh, M., M. Afshari, J. E. Contreras-Reyes, D. Mazarei, and H. M. Yousof (2025). The extended Gompertz model: applications, mean of order P assessment and statistical threshold risk analysis based on extreme stresses data. *IEEE Transactions on Reliability 74*(2), 2779–2791.

[6] Aljadani, A., M. M. Mansour, and H. M. Yousof (2024). A novel model for finance and reliability applications: theory, practices and financial peaks over a random threshold value-at-risk analysis. *Pakistan Journal of Statistics and Operation Research 20*(3), 489–515.

[7] Almuhayfith, F. E., M. Kachour, A. F. Daghestani, Z. U. Rehman, T. Hussain, and H. S. Bakouch (2025). A lower-bounded extreme value distribution for flood frequency analysis with applications. *Mathematics 13*(21), 3378.

[8] Amoroso, L. (1925). L'economia pura. *Giornale degli Economisti e Rivista di Statistica 66*(3), 116–122.

[9] Anand, R. and C. Chandran (2025). A regression method of estimation for generalized extreme value distribution. *Kybernetika 61*(4), 467–480.

[10] Anand, R., M. Dileepkumar, and C. Greeshma (2026). Reliability properties and applications of auto-relevated log-logistic model. *Journal of Statistical Theory and Practice 20*, 92.

[11] Anderson, T. W. and D. A. Darling (1952). Asymptotic theory of certain "goodness of fit" criteria based on stochastic processes. *The Annals of Mathematical Statistics 23*(2), 193–212.

[12] Anderson, T. W. and D. A. Darling (1954). A test of goodness of fit. *Journal of the American Statistical Association 49*(268), 765–769.

[13] Anwar, M. and A. Bibi (2018). The half-logistic generalized Weibull distribution. *Journal of probability and statistics 2018*(1), 8767826.

[14] Arriaza, A., J. Navarro, and A. Suárez-Llorens (2018). Stochastic comparisons of replacement policies in coherent systems under minimal repair. *Naval Research Logistics 65*(7), 550–565.

[15] Artzner, P. (1999). Application of coherent risk measures to capital requirements in insurance. *North American Actuarial Journal 3*(2), 11–25.

[16] Aryal, G. R. and C. P. Tsokos (2009). On the transmuted extreme value distribution with application. *Nonlinear Analysis: Theory, Methods & Applications 71*(12), e1401–e1407.

[17] Asadi, M. and Y. Zohrevand (2007). On the dynamic cumulative residual entropy. *Journal of Statistical Planning and Inference 137*(6), 1931–1941.

[18] Bakar, M. A. A., N. M. Ariff, and M. S. M. Nadzir (2022). Comparative analysis between L-moments and maximum product spacing method for extreme PM_{10} concentration. In *Proceedings of the International Conference on Mathematical Sciences and Statistics 2022 (ICMSS 2022)*, pp. 214–227. Atlantis Press.

[19] Balakrishnan, N. (1985). Order statistics from the half logistic distribution. *Journal of Statistical Computation and Simulation 20*(4), 287–309.

[20] Balakrishnan, N. and R. Aggarwala (2000). *Progressive Censoring: Theory, Methods, and Applications*. Springer Science & Business Media, New York.

[21] Balakrishnan, N., G. Barmalzan, and A. Haidari (2018). Modified proportional hazard rates and proportional reversed hazard rates models via Marshall-Olkin distribution and some stochastic comparisons. *Journal of the Korean Statistical Society 47*(1), 127–138.

[22] Balakrishnan, N. and E. Cramer (2014). *The Art of Progressive Censoring*. Birkhäuser, New York.

[23] Balakrishnan, N. and R. A. Sandhu (1995). A simple simulational algorithm for generating progressive type-II censored samples. *The American Statistician 49*(2), 229–230.

[24] Baran, S., P. Szokol, and M. Szabó (2021). Truncated generalized extreme value distribution based EMOS model for calibration of wind speed ensemble forecasts. *Environmetrics 32*(6), e2678.

[25] Barandoff, N. O. (1983). On a formula for the distribution of the maximum likelihood estimator. *Biometrika 70*(2), 343–365.

[26] Barlow, R. E. and R. Campo (1975). Total time on test processes and applications to failure data analysis. In *Barlow RE, Fussel R, Singpurwalla ND, editors. Reliability and Fault Tree Analysis. SIAM , Philadelphia, PA*, pp. 451–481. Society for Industrial and Applied Mathematics.

[27] Barlow, R. E. and F. Proschan (1975). *Statistical Theory of Reliability and Life Testing*. Holt, Rinehart and Winston, New York.

[28] Baxter, L. A. (1982). Reliability applications of the relevation transform. *Naval Research Logistics (NRL) 29*(2), 323–330.

[29] Beichelt, F. (1993). A unifying treatment of replacement policies with minimal repair. *Naval Research Logistics (NRL) 40*(1), 51–67.

[30] Beichelt, F. and P. Tittmann (1991). A generalized reduction method for the connectedness probability of stochastic networks. *IEEE Transactions on Reliability 40*(2), 198–204.

[31] Belzunce, F., R. E. Lillo, J.-M. Ruiz, and M. Shaked (2001). Stochastic comparisons of nonhomogeneous processes. *Probability in the Engineering and Informational Sciences 15*(2), 199–224.

[32] Belzunce, F., C. Martínez-Riquelme, J. A. Mercader, and J. M. Ruiz (2021). Comparisons of policies based on relevation and replacement by a new one unit in reliability. *Test 30*, 211–227.

[33] Belzunce, F., C. Martínez-Riquelme, and J. M. Ruiz (2019). Allocation of a relevation in redundancy problems. *Applied Stochastic Models in Business and Industry 35*(3), 492–503.

[34] Belzunce, F., C. M. Riquelme, and J. Mulero (2016). *An Introduction to Stochastic Orders*. Academic Press, London.

[35] Bennett, S. (1983). Analysis of survival data by the proportional odds model. *Statistics in Medicine 2*(2), 273–277.

[36] Bhat, A., S. Ahmad, A. M. Gemeay, A. H. Muse, M. Bakr, and O. S. Balogun (2024). A novel extension of half-logistic distribution with statistical inference, estimation and applications. *Scientific Reports 14*(1), 4326.

[37] Bhattacharyya, G. and R. A. Johnson (1974). Estimation of reliability in a multicomponent stress-strength model. *Journal of the American Statistical Association 69*(348), 966–970.

[38] Birnbaum, Z. W. (1956). On a use of the Mann-Whitney statistic. In *Proceedings of the Third Berkeley Symposium on Mathematical Statistics and Probability, Volume 1: Contributions to the Theory of Statistics*, Volume 3, pp. 13–18. University of California Press.

[39] Bondesson, L. (1992). *Generalized Gamma Convolutions and Related Classes of Distributions and Densities*, Volume 76. Springer, New York.

[40] Box, G. E. and D. R. Cox (1964). An analysis of transformations. *Journal of the Royal Statistical Society: Series B (Methodological) 26*(2), 211–243.

[41] Breneman, J. E., C. Sahay, and E. E. Lewis (2022). *Introduction to Reliability Engineering*. John Wiley & Sons, Hoboken, NJ, USA.

[42] Bryson, M. C. and M. Siddiqui (1969). Some criteria for aging. *Journal of the American Statistical Association 64*(328), 1472–1483.

[43] Bücher, A. and J. Segers (2017). On the maximum likelihood estimator for the generalized extreme-value distribution. *Extremes 20*(4), 839–872.

[44] Calì, C., M. Longobardi, and J. Ahmadi (2017). Some properties of cumulative Tsallis entropy. *Physica A: Statistical Mechanics and its Applications 486*(C), 1012–1021.

[45] Capaldo, M., A. Di Crescenzo, and F. Pellerey (2024). Generalized Gini's mean difference through distortions and copulas, and related minimizing problems. *Statistics & Probability Letters 206*, 109981.

[46] Chandra, N. K. and D. Roy (2001). Some results on reversed hazard rate. *Probability in the Engineering and informational Sciences 15*(1), 95–102.

[47] Chaudhary, S. K. and N. Gupta (2023). General weighted cumulative residual (past) extropy of minimum (maximum) ranked set sampling with unequal samples. *Communications in Statistics - Theory and Methods 53*(22), 8076–8096.

[48] Cheng, R. and N. Amin (1983). Estimating parameters in continuous univariate distributions with a shifted origin. *Journal of the Royal Statistical Society: Series B (Methodological) 45*(3), 394–403.

[49] Chistyakov, V. P. (1964). A theorem on sums of independent positive random variables and its applications to branching random processes. *Theory of Probability & Its Applications 9*(4), 640–648.

[50] Clarke, R. T. (2002). Estimating time trends in Gumbel-distributed data by means of generalized linear models. *Water Resources Jesearch 38*(7), 16–1–16–11.

[51] Coles, S., J. Bawa, L. Trenner, and P. Dorazio (2001). *An Introduction to Statistical Modeling of Extreme Values*. Springer, London.

[52] Collett, D. (2015). *Modelling Survival Data in Medical Research (3rd ed.)*. Chapman and Hall/CRC.

[53] Cordeiro, G. (2017). The exponentiated generalized standardized half-logistic distribution. *International Journal of Statistics and Probability 6*(24–42), 4326.

[54] Cox, D. R. and D. V. Hinkley (1974). *Theoretical statistics*. CRC Press, New York.

[55] Denneberg, D. (1990). Premium calculation: Why standard deviation should be replaced by absolute deviation1. *ASTIN Bulletin 20*(2), 181–190.

[56] Dhillon, B. S. (1981). Life distributions. *IEEE Transactions on Reliability 30*(5), 457–460.

[57] Di Crescenzo, A. (2000). Some results on the proportional reversed hazards model. *Statistics & Probability Letters 50*(4), 313–321.

[58] Di Crescenzo, A., S. Kayal, and A. Toomaj (2018). A past inaccuracy measure based on the reversed relevation transform. *Metrika 82*(5), 607–631.

[59] Di Crescenzo, A. and M. Longobardi (2004). A measure of discrimination between past lifetime distributions. *Statistics & Probability Letters 67*(2), 173–182.

[60] Di Crescenzo, A. and M. Longobardi (2009). On cumulative entropies. *Journal of Statistical Planning and Inference 139*(12), 4072–4087.

[61] Di Crescenzo, A. and A. Toomaj (2015). Extension of the past lifetime and its connection to the cumulative entropy. *Journal of Applied Probability 52*(4), 1156–1174.

[62] Di Crescenzo, A. and A. Toomaj (2017). Further results on the generalized cumulative entropy. *Kybernetika 53*(5), 959–982.

[63] Dileepkumar, M., R. Anand, and P. Sankaran (2025). Reliability properties and applications of proportional reversed hazards in reversed relevation transform. *Statistics in Transition new series 26*(1), 183–203.

[64] Dileepkumar, M. and P. Sankaran (2021). Some results of auto-relevation transform in reliability analysis. *Statistics and Applications 20*(2), 251–263.

[65] Dileepkumar, M. and P. Sankaran (2024). On proportional odds relevation transform and its applications. *Communications in Statistics - Theory and Methods 53*(7), 2369–2389.

[66] Dileepkumar, M., P. G. Sankaran, and N. U. Nair (2018). Quantile based relevation transform and its properties. *Statistica 78*(3), 197–214.

[67] Dimitrov, B., D. Green Jr, and S. Chukova (1997). Probability distributions in periodic random environment and their applications. *SIAM Journal on Applied Mathematics 57*(2), 501–517.

[68] Efron, B. (1979). Bootstrap methods: Another look at the jackknife. *The Annals of Statistics 1*(1), 1–26.

[69] Efron, B. (1981). Nonparametric standard errors and confidence intervals. *Canadian Journal of Statistics 9*(2), 139–158.

[70] Efron, B. (1987). Better bootstrap confidence intervals. *Journal of the American statistical Association 82*(397), 171–185.

[71] Embrechts, P., C. Klüppelberg, and T. Mikosch (1997). *Modelling Extremal Events for Insurance and Finance*. Springer, Berlin.

[72] Fang, R., C. Li, and X. Li (2023). On relevation transform involved with statistical dependence between two component lifetimes. *Applied Stochastic Models in Business and Industry 39*(4), 584–601.

[73] Feller, W. (1968). *An introduction to probability theory and its applications, Volume 1*, Volume 1. John Wiley & Sons.

[74] Feller, W. (1971). *An introduction to probability theory and its applications, Volume 2*, Volume 2. John Wiley & Sons.

[75] Fisher, R. A. (1912). On an absolute criterion for fitting frequency curves. *Messenger of Mathematics 41*, 155–156.

[76] Fisher, R. A. and L. H. C. Tippett (1928). Limiting forms of the frequency distribution of the largest or smallest member of a sample. *Mathematical Proceedings of the Cambridge Philosophical Society 24*(2), 180–190.

[77] Fitzgerald, D. L. (2005). Analysis of extreme rainfall using the log logistic distribution. *Stochastic Environmental Research and Risk Assessment 19*(4), 249–257.

[78] Foss, S., D. Korshunov, and S. Zachary (2011). *An Introduction to Heavy-Tailed and Subexponential Distributions*, Volume 6. Springer New York, NY.

[79] Fréchet, M. (1927). Sur la loi de probabilité de l'écart maximum. *Ann. Soc. Math. Polon. 6*, 93–116.

[80] Galton, F. (1883). *Inquires into Human Faculty and its Development*. London: Macmillan.

[81] Gilchrist, W. (2000). *Statistical Modelling with Quantile Functions*. CRC Press, Abingdon.

[82] Gini, C. (1912). *Variabilità e mutabilità: contributo allo studio delle distribuzioni e delle relazioni statistiche.[Fasc. I.]*. Tipogr. di P. Cuppini.

[83] Glänzel, W. (1987). *A Characterization Theorem Based on Truncated Moments and its Application to Some Distribution Families*, pp. 75–84. Dordrecht: Springer Netherlands.

[84] Glaser, R. E. (1980). Bathtub and related failure rate characterizations. *Journal of the American Statistical Association 75*(371), 667–672.

[85] Gnedenko, B. (1943). Sur La Distribution Limite Du Terme Maximum D'Une Serie Aleatoire. *Annals of Mathematics 44*(3), 423–453.

[86] Govindarajulu (1977). A class of distributions useful in life testing and reliability. *IEEE Transactions on Reliability 26*(1), 67–69.

[87] Gradshteyn, I. and I. Ryzhik (1994). *Table of Integrals, Series, and Products*. 6th edn New York: Academic Press.

[88] Grosswald, E., S. Kotz, and N. L. Johnson (1980). Characterizations of the exponential distribution by relevation-type equations. *Journal of Applied Probability 17*(3), 874–877.

[89] Gui, W. (2013). Marshall-olkin extended log-logistic distribution and its application in minification processes. *Applied Mathematical Sciences 7*(77-80), 3947–3961.

[90] Gupta, R. C., P. L. Gupta, and R. D. Gupta (1998). Modeling failure time data by Lehman alternatives. *Communications in Statistics - Theory and methods 27*(4), 887–904.

[91] Gupta, R. C. and S. Kirmani (1988). Closure and monotonicity properties of nonhomogeneous poisson processes and record values. *Probability in the Engineering and Informational Sciences 2*(4), 475–484.

[92] Gupta, R. C. and H. Wu (2001). Analyzing survival data by proportional reversed hazard model. *International Journal of Reliability and Applications 2*(1), 1–26.

[93] Gupta, R. D. and D. Kundu (1999). Theory & methods: Generalized exponential distributions. *Australian & New Zealand Journal of Statistics 41*(2), 173–188.

[94] Gupta, R. D. and D. Kundu (2001). Exponentiated exponential family: an alternative to gamma and Weibull distributions. *Biometrical Journal: Journal of Mathematical Methods in Biosciences 43*(1), 117–130.

[95] Gupta, R. D. and D. Kundu (2002). Generalized exponential distributions: statistical inferences. *Journal of Statistical theory and Applications 1*(1), 101–118.

[96] Gupta, R. D. and D. Kundu (2007). Generalized exponential distribution: Existing results and some recent developments. *Journal of Statistical planning and inference 137*(11), 3537–3547.

[97] Hand, D. J., F. Daly, K. McConway, D. Lunn, and E. Ostrowski (1994). *Handbook of small data sets*. Boca Raton, FL: Chapman & Hall/ CRC Press.

[98] Hosking, J. R. (1985). Algorithm as 215: Maximum-likelihood estimation of the parameters of the generalized extreme-value distribution. *Journal of the Royal Statistical Society: Series C (Applied Statistics) 34*(3), 301–310.

[99] Hosking, J. R. (1990). L-moments: Analysis and estimation of distributions using linear combinations of order statistics. *Journal of the Royal Statistical Society: Series B (Methodological) 52*(1), 105–124.

[100] Hosking, J. R. M., J. R. Wallis, and E. F. Wood (1985). Estimation of the generalized extreme-value distribution by the method of probability-weighted moments. *Technometrics 27*(3), 251–261.

[101] Huang, X., C. Xiong, T. Jiang, J. Lu, and J. Xu (2022). Efficient estimation and inference in the proportional odds model for survival data. *Mathematics 10*(18), 3362.

[102] Hussain, Z. and K. Abbas (2019). Rainfall frequency analysis using frechet and log-logistic distributions of sites of azad jammu and kashmir, pakistan. *Applied Ecology & Environmental Research 17*(6), 13607–13623.

[103] Jahanshahi, S., H. Zarei, and A. Khammar (2020). On cumulative residual extropy. *Probability in the Engineering and Informational Sciences 34*(4), 605–625.

[104] Jenkinson, A. F. (1955). The frequency distribution of the annual maximum (or minimum) values of meteorological elements. *Quarterly Journal of the Royal Meteorological Society 81*(348), 158–171.

[105] Jiang, R., P. Ji, and X. Xiao (2003). Aging property of unimodal failure rate models. *Reliability Engineering & System Safety 79*(1), 113–116.

[106] Johnson, N. L. and S. Kotz (1981). Dependent relevations: time-to-failure under dependence. *American Journal of Mathematical and Management Sciences 1*(2), 155–165.

[107] Jokiel-Rokita, A. and P. Skoliński (2021). Maximum likelihood estimation for an inhomogeneous Gamma process with a log-linear rate function. *Journal of Statistical Theory and Practice 15*(4), 1–27.

[108] Kalbfleisch, J. D. and R. L. Prentice (2011). *The statistical analysis of failure time data*, Volume 360. John Wiley & Sons, New York.

[109] Kapodistria, S. and G. Psarrakos (2012). Some extensions of the residual lifetime and its connection to the cumulative residual entropy. *Probability in the Engineering and Informational Sciences 26*(1), 129–146.

[110] Kattumannil, S. K., E. Sreedevi, and N. Balakrishnan (2024). Relationships between cumulative entropy/extropy, gini mean difference and probability weighted moments. *Probability in the Engineering and Informational Sciences 38*(1), 28–38.

[111] Kayal, S. (2016). On generalized cumulative entropies. *Probability in the Engineering and Informational Sciences 30*(4), 640–662.

[112] Kayal, S. and R. Tripathy, Manas (2018). A quantile-based tsallis-α divergence. *Physica A: Statistical Mechanics and its Applications 492*, 496–505.

[113] Kayid, M. and R. A. Almohsen (2024). Preservation of relative hazard rate and relative reversed hazard rate orders by distorted distributions. *Acta Applicandae Mathematicae 194*(1), 14.

[114] Kerridge, D. F. (1961). Inaccuracy and inference. *Journal of the Royal Statistical Society. Series B (Methodological) 23*(1), 184–194.

[115] Kinnison, R. (1983). Applied extreme-value statistics. Technical report, Pacific Northwest National Lab.(PNNL), Richland, WA (United States).

[116] Kirmani, S. and R. C. Gupta (1989). On repair age residual repair life in the minimal repair process. *Probability in the Engineering and Informational Sciences 3*(3), 381–391.

[117] Kirmani, S. and R. C. Gupta (2001). On the proportional odds model in survival analysis. *Annals of the Institute of Statistical Mathematics 53*(2), 203–216.

[118] Klüppelberg, C. (1988). Subexponential distributions and integrated tails. *Journal of Applied Probability 25*(1), 132–141.

[119] Kochar, S. C. (2022). *Stochastic Comparisons with Applications: In Order Statistics and Spacings*. Springer Nature, Switzerland.

[120] Krakowski, M. (1973). The relevation transform and a generalization of the gamma distribution function. *Revue française d'automatique, informatique, recherche opérationnelle. Recherche opérationnelle 7*(V2), 107–120.

[121] Kumar, R., T. Sahoo, and S. Naqvi (2026). Optimal allocation policies for relevations in coherent systems. *Advances in Applied Probability*, 1–39.

[122] Kundu, C. (2023). On cumulative residual (past) extropy of extreme order statistics. *Communications in Statistics - Theory and Methods 52*(16), 5848–5865.

[123] Kundu, D. and R. D. Gupta (2004). Characterizations of the Proportional (Reversed) Hazard Model. *Communications in Statistics - Theory and Methods 33*(12), 3095–3102.

[124] Lad, F., G. Sanfilippo, and G. Agrò (2015). Extropy: Complementary dual of entropy. *Statistical Science 30*(1), 40–58.

[125] Lai, C., M. Xie, and D. Murthy (2003). A modified Weibull distribution. *IEEE Transactions on Reliability 52*(1), 33–37.

[126] Lai, C. D. and M. Xie (2006). *Stochastic Ageing and Dependence for Reliability*. Springer, New York.

[127] Lando, T., I. Arab, and P. E. Oliveira (2022). Properties of increasing odds rate distributions with a statistical application. *Journal of Statistical Planning and Inference 221*(4), 313–325.

[128] Landsman, Z. (2010). On the tail mean–variance optimal portfolio selection. *Insurance: Mathematics and Economics 46*(3), 547–553.

[129] Landwehr, J. M., N. Matalas, and J. Wallis (1979). Probability weighted moments compared with some traditional techniques in estimating gumbel parameters and quantiles. *Water Resources Research 15*(5), 1055–1064.

[130] Lau, K. S. and B. P. Rao (1990). Characterization of the exponential distribution by the relevation transform. *Journal of Applied Probability 27*(3), 726–729.

[131] Lawless, J. F. (2003). *Statistical Models and Methods for Lifetime Data*. John Wiley & Sons, Inc. Hoboken, New Jersy.

[132] Leadbetter, M. R., G. Lindgren, and H. Rootzén (1983). *Extremes and Related Properties of Random Sequences and Processes*. Springer, New York.

[133] Leipus, R., J. Siaulys, and D. Konstantinides (2023). *Closure Properties for Heavy-Tailed and Related Distributions*. Springer Nature, Cham.

[134] Lewis, P. A. and G. S. Shedler (1976). Analysis and modelling of point processes in computer systems. *Bull. ISI* ***XLVII*** *3*, 193–210.

[135] Li, C. and X. Li (2024). On relevation redundancy to coherent systems at component and system levels. *Journal of Applied Probability 61*(1), 104–120.

[136] Lima, S. R. and G. M. Cordeiro (2017). The extended log-logistic distribution: properties and application. *Anais da Academia Brasileira de Ciências 89*(01), 03–17.

[137] Lu, B. (2025). On variability of the mean inactivity time at random time. *Statistical Papers 66*(4), 94.

[138] Macdonald, P. D. M. (1971). Comments and queries: Comment on "an estimation procedure for mixtures of distributions" by choi and bulgren. *Journal of the Royal Statistical Society: Series B (Methodological) 33*(2), 326–329.

[139] Madsen, H., P. F. Rasmussen, and D. Rosbjerg (1997). Comparison of annual maximum series and partial duration series methods for modeling extreme hydrologic events: 1. At-site modeling. *Water Resources Research 33*(4), 747–757.

[140] Mahmoud, M. A. and F. M. A. Alam (2010). The generalized linear exponential distribution. *Statistics & probability letters 80*(11-12), 1005–1014.

[141] Martins, E. S. and J. R. Stedinger (2000). Generalized maximum-likelihood generalized extreme-value quantile estimators for hydrologic data. *Water Resources Research 36*(3), 737–744.

[142] McCollin, C. (2008). *Intensity Functions for Nonhomogeneous Poisson Processes*. John Wiley & Sons, Ltd.

[143] McCullagh, P. (1977). A logistic model for paired comparisons with ordered categorical data. *Biometrika 64*(3), 449–453.

[144] Midhu, N. N., P. G. Sankaran, and N. U. Nair (2013). A class of distributions with the linear mean residual quantile function and it's generalizations. *Statistical Methodology 15*, 1–24.

[145] Moors, J. (1988). A quantile alternative for kurtosis. *Journal of the Royal Statistical Society: Series D (The Statistician) 37*(1), 25–32.

[146] Murphy, S. A. and A. W. Van der Vaart (2000). On profile likelihood. *Journal of the American Statistical Association 95*(450), 449–465.

[147] Murthy, D. P., M. Xie, and R. Jiang (2004). *Weibull models*. John Wiley, New York.

[148] Muse, A. H., S. M. Mwalili, and O. Ngesa (2021). On the log-logistic distribution and its generalizations: A survey. *International Journal of Statistics and Probability 10*(3), 93–113.

[149] Muth, E. J. (1977). Reliability models with positive memory derived from the mean residual life function. *The Theory and Applications of Reliability 2*, 401–434.

[150] Nair, N. U. and P. G. Sankaran (2009). Quantile-based reliability analysis. *Communications in Statistics - Theory and Methods 38*(2), 222–232.

[151] Nair, N. U., P. G. Sankaran, and N. Balakrishnan (2013). *Quantile-Based Reliability Analysis*. Springer, Birkhauser, New York.

[152] Nair, N. U., P. G. Sankaran, and S. M. Sunoj (2019). Some properties of proportional reversed hazards model based on quantile functions. *International Journal of Reliability, Quality and Safety Engineering 26*(03), 1950011.

[153] Nath, P. (1968). Inaccuracy and coding theory. *Metrika 13*(1), 123–135.

[154] Navarro, J. (2022). *Introduction to System Reliability Theory*. Springer, Berlin.

[155] Navarro, J., Y. Águila, M. A. Sordo, and A. Suárez-Llorens (2013). Stochastic ordering properties for systems with dependent identically distributed components. *Applied Stochastic Models in Business and Industry 29*(3), 264–278.

[156] Navarro, J., Y. Águila, M. A. Sordo, and A. Suárez-Llorens (2014). Preservation of reliability classes under the formation of coherent systems. *Applied Stochastic Models in Business and Industry 30*(4), 444–454.

[157] Navarro, J., A. Arriaza, and A. Suárez-Llorens (2019). Minimal repair of failed components in coherent systems. *European Journal of Operational Research 279*(3), 951–964.

[158] Navarro, J., Y. Del Águila, M. A. Sordo, and A. Suárez-Llorens (2016). Preservation of stochastic orders under the formation of generalized distorted distributions. applications to coherent systems. *Methodology and Computing in Applied Probability 18*(2), 529–545.

[159] Navarro, J., M. R. Jose, and D. A. Yolanda (2008). Characterizations and ordering properties based on log-odds functions. *Statistics 42*(4), 313–328.

[160] Navarro, J., T. Rychlik, and M. Szymkowiak (2025). Key distributions in the preservation of aging classes under the construction of systems. *Journal of Computational and Applied Mathematics 469*, 116650.

[161] Neamah, M. W. and B. A. Qasim (2021). A new left truncated Gumbel distribution: Properties and estimation. *Journal of Physics: Conference Series 1897*(1), 012015.

[162] Nigm, A., E. K. Al-Hussaini, and Z. F. Jaheen (2003). Bayesian one-sample prediction of future observations under pareto distribution. *Statistics 37*(6), 527–536.

[163] Oguntunde, P., O. Balogun, H. Okagbue, and S. Bishop (2015). The Weibull-exponential distribution: Its properties and applications. *Journal of Applied Sciences 15*(11), 1305–1311.

[164] Otiniano, C. E., B. S. De Paiva, and D. S. Neto (2019). The transmuted GEV distribution: properties and application. *Communications for Statistical Applications and Methods 26*(3), 239–259.

[165] Pellerey, F., M. Shaked, and J. Zinn (2000). Nonhomogeneous Poisson processes and logconcavity. *Probability in the Engineering and Informational Sciences 14*(3), 353–373.

[166] Pettitt, A. N. (1984). Proportional odds models for survival data and estimates using ranks. *Journal of the Royal Statistical Society: Series C (Applied Statistics) 33*(2), 169–175.

[167] Pickands, J. (1975). Statistical inference using extreme order statistics. *Annals of Statistics 3*(1), 119–131.

[168] Popović, B. V., A. İ. Genç, and F. Domma (2022). Generalized proportional reversed hazard rate distributions with application in medicine. *Statistical Methods & Applications 31*(3), 459–480.

[169] Prescott, P. and A. Walden (1980). Maximum likelihood estimation of the parameters of the generalized extreme-value distribution. *Biometrika 67*(3), 723–724.

[170] Provost, S. B., A. Saboor, G. M. Cordeiro, and M. Mansoor (2018). On the q-generalized extreme value distribution. *REVSTAT-Statistical Journal 16*(1), 45–70.

[171] Psarrakos, G. and J. Navarro (2013). Generalized cumulative residual entropy and record values. *Metrika 76*(5), 623–640.

[172] Ranjbar, V., M. Alizadeh, M. Afshari, and H. M. Yousof (2024). Odd log-logistic xgamma model: Bayesian and classical estimation with risk analysis utilizing reinsurance revenues data. *Journal of Statistical Theory and Applications 23*(3), 329–362.

[173] Ranneby, B. (1984). The maximum spacing method. an estimation method related to the maximum likelihood method. *Scandinavian Journal of Statistics 11*(2), 93–112.

[174] Rao, R. S. and D. Kushary (2012). Extreme value charts and anom based on log logistic distribution. *Journal of Modern Applied Statistical Methods 11*(2), 413–421.

[175] Rényi, A. (1961). On measures of entropy and information. In *Proceedings of the Fourth Berkeley Symposium on Mathematical Statistics and Probability, Volume 1: Contributions to the Theory of Statistics*, Volume 4, pp. 547–562. University of California Press.

[176] Resnick, S. I. (1987). *Extreme Values, Regular Variation, and Point Processes.* Springer, New York.

[177] Rezaei, M. and V. Khalaf, Ahrari (2014). On the reversed average intensity order. *Journal of Statistical Research of Iran JSRI 11*(1), 25–39.

[178] Rizzo, M. L. (2019). *Statistical Computing with R.* Chapman and Hall/CRC, New York.

[179] Rosaiah, K., R. Kantam, and S. Kumar (2006). Reliability test plans for exponentiated log-logistic distribution. In *Walter de Gruyter GmbH & Co. KG*, Volume 21, pp. 165–175.

[180] Rossini, A. J. and A. A. Tsiatis (1996). A semiparametric proportional odds regression model for the analysis of current status data. *Journal of the American Statistical Association 91*(434), 713–721.

[181] Rowsiński, J., W. G. Strupczewski, and V. P. Singh (2002). A note on the applicability of log-Gumbel and log-logistic probability distributions in hydrological analyses: I. Known pdf. *Hydrological Sciences Journal 47*(1), 107–122.

[182] Ruiz, J. and N. Jorge (1996). Characterizations based on conditional expectations of the doubled truncated distribution. *Annals of the Institute of Statistical Mathematics 48*(3), 563–572.

[183] Sankaran, P. G. and M. Dileepkumar (2019). Reliability properties of proportional hazards relevation transform. *Metrika 82*(4), 441–456.

[184] Sarhan, A. M. and D. Kundu (2009). Generalized linear failure rate distribution. *Communications in Statistics - Theory and Methods 38*(5), 642–660.

[185] Sengupta, D. and J. V. Deshpande (1994). Some results on the relative ageing of two life distributions. *Journal of Applied Probability 31*(4), 991–1003.

[186] Shaked, M. and J. G. Shanthikumar (2007). *Stochastic Orders*. Springer, New York.

[187] Shannon, C. E. (1948). A mathematical theory of communication. *The Bell System Technical Journal 27*(3), 379–423.

[188] Shanthikumar, J. and L. A. Baxter (1985). Closure properties of the relevation transform. *Naval Research Logistics (NRL) 32*(1), 185–189.

[189] Shojaee, O. and M. Babanezhad (2023). On some stochastic comparisons of arithmetic and geometric mixture models. *Metrika 86*(5), 499–515.

[190] Smith, R. L. (1985). Maximum likelihood estimation in a class of nonregular cases. *Biometrika 72*(1), 67–90.

[191] Smith, R. L. and J. Naylor (1987). A comparison of maximum likelihood and Bayesian estimators for the three-parameter Weibull distribution. *Journal of the Royal Statistical Society Series C: Applied Statistics 36*(3), 358–369.

[192] Sordo, M. A. and G. Psarrakos (2017). Stochastic comparisons of interfailure times under a relevation replacement policy. *Journal of Applied Probability 54*(1), 134–145.

[193] Sordo, M. A. and A. Suárez-Llorens (2011). Stochastic comparisons of distorted variability measures. *Insurance: Mathematics and Economics 49*(1), 11–17.

[194] Sordo, M. A., A. Suárez-Llorens, and A. J. Bello (2015). Comparison of conditional distributions in portfolios of dependent risks. *Insurance: Mathematics and Economics 61*, 62–69.

[195] Stedinger, J. R., R. M. Vogel, and E. Foufoula-Georgiou (1993). Frequency analysis of extreme events. In D. R. Maidment (Ed.), *Handbook of Hydrology*, pp. 18.1–18.66. McGraw-Hill.

[196] Taneja, H., V. Kumar, and R. Srivastava (2009). A dynamic measure of inaccuracy between two residual lifetime distributions. In *International Mathematical Forum*, Volume 4, no. 5, pp. 1213–1220.

[197] Teamah, A.-E. A., A. A. Elbanna, and A. M. Gemeay (2021). Heavy-tailed log-logistic distribution: properties, risk measures and applications. *Statistics, Optimization & Information Computing 9*(4), 910–941.

[198] Tukey, J. W. (1962). The future of data analysis. *The Annals of Mathematical Statistics 33*(1), 1–67.

[199] Van Montfort, M. (1970). On testing that the distribution of extremes is of type I when type II is the alternative. *Journal of Hydrology 11*(4), 421–427.

[200] Van Zyl, J. M. (2012). A median regression model to estimate the parameters of the three-parameter generalized Pareto distribution. *Communications in Statistics - Simulation and Computation 41*(4), 544–553.

[201] Verhulst, P.-F. (1838). Notice sur la loi que la population suit dans son accroissement. *Correspondence Mathematique et Physique 10*(1838), 113–129.

[202] Vineshkumar, B., N. U. Nair, and P. Sankaran (2015). Stochastic orders using quantile-based reliability functions. *Journal of the Korean Statistical Society 44*(2), 221–231.

[203] Von Mises, R. (1936). La distribution de la plus grande de n valuers. *Rev. math. Union Interbalcanique 1*, 141–160.

[204] Wang, Vemuri, Rao, and Chen (2003). Cumulative residual entropy, a new measure of information & its application to image alignment. In *Proceedings Ninth IEEE International Conference on Computer Vision*, pp. 548–553. IEEE.

[205] Wang, F.-K. (2000). A new model with bathtub-shaped failure rate using an additive burr xii distribution. *Reliability Engineering & System Safety 70*(3), 305–312.

[206] Wang, S. (1996). Premium calculation by transforming the layer premium density. *ASTIN Bulletin 26*(1), 71–92.

[207] Wang, Y., M. H. Anwar, and J. W. Zimmer (2003). Monotone log-odds rate distributions in reliability analysis. *Communications in Statistics - Theory and Methods 32*(11), 2227–2244.

[208] Wong, T. and W. Li (2006). A note on the estimation of extreme value distributions using maximum product of spacings. *Institute of Mathematical Statistics Lecture Notes-Monograph Series 55*, 272–283.

[209] Wu, J., W. Ding, Y. Zhang, and P. Zhao (2022). On reliability improvement for coherent systems with a relevation. *Naval Research Logistics (NRL) 69*(4), 654–666.

[210] Yarmohammadi, M., A. Afshar, R. Mahmoudvand, and P. Nasiri (2022). Predicting intensity function of nonhomogeneous Poisson process. *Journal of Statistical Modelling: Theory and Applications 3*(2), 39–50.

[211] Yitzhaki, S. (2003). Gini's mean difference: A superior measure of variability for non-normal distributions. *Metron 61*(2), 285–316.

[212] Yitzhaki, S. and E. Schechtman (2013). *The Gini Methodology: A Primer on a Statistical Methodology*, Volume 272. Springer, Berlin.

[213] Zaid, E. O. A., A. E. W. Attwa, Rasha, and T. Radwan (2022). Some measures information for generalized and q-generalized extreme values and its properties. *Fractals 30*(10), 2240246.

[214] Zardasht V (2024). Some results on the odds rate order along with its statistical testing. *ESAIM: PS 28*, 274–291.

[215] Zellner, A. (1996). *An Introduction to Bayesian Inference in Econometrics*. Wiley, New York.

[216] Zhang, J. and Y. Zhang (2023). Stochastic comparisons of relevation allocation policies in coherent systems. *Test 32*(3), 865–907.

[217] Zhang, Y. and P. Zhao (2019). Optimal allocation of minimal repairs in parallel and series systems. *Naval Research Logistics 66*(6), 517–526.

[218] Zimmer, J. W., W. Yao, and K. P. Pramod (1998). Log-odds rate and monotone log-odds rate distributions. *Journal of Quality Technology 30*(4), 376–385.